Titre: Title:	Hydrodynamics of Bubble Column Reactors Operating with Non-Newtonian Liquids
Auteur: Author:	Amin Esmaeili Khalil Saraei
Date:	2015
Type:	Mémoire ou thèse / Dissertation or Thesis
Référence: Citation:	Esmaeili Khalil Saraei, A. (2015). Hydrodynamics of Bubble Column Reactors Operating with Non-Newtonian Liquids [Ph.D. thesis, École Polytechnique de Montréal]. PolyPublie. https://publications.polymtl.ca/1726/

UNIVERSITÉ DE MONTRÉAL

HYDRODYNAMICS OF BUBBLE COLUMN REACTORS OPERATING WITH NON-NEWTONIAN LIQUIDS

AMIN ESMAEILI KHALIL SARAEI

DÉPARTEMENT DE GÉNIE CHIMIQUE

ÉCOLE POLYTECHNIQUE DE MONTRÉAL

THÉSE PRÉSENTÉE EN VUE DE L'OBTENTION

DU DIPLÔME DE PHILOSOPHIAE DOCTOR

(GÉNIE CHIMIQUE)

AVRIL 2015

UNIVERSITÉ DE MONTRÉAL

ÉCOLE POLYTECHNIQUE DE MONTRÉAL

Cette thèse intitulée:

HYDRODYNAMICS OF BUBBLE COLUMN REACTORS OPERATING WITH NON-NEWTONIAN LIQUIDS

présentée par: ESMAEILI KHALIL SARAEI Amin

en vue de l'obtention du diplôme de : Philosophiae Doctor

a été dûment acceptée par le jury d'examen constitué de :

M. BERTRAND François, Ph.D., président

M. CHAOUKI Jamal, Ph.D., membre et directeur de recherche

M. GUY Christophe, Ph.D., membre et codirecteur de recherche

M. LEGROS Robert, Ph.D., membre

M. AL-DAHHAN Muthanna H., Ph.D., membre

DEDICATION

- To My Beloved Family

ACKNOWLEDGEMENTS

This is the opportune moment to acknowledge all who in one way or another contributed to the completion of this thesis. First and foremost, I wish to express my deep and sincere gratitude to my advisors Prof. Jamal Chaouki and Prof. Christophe Guy for their solid support, motivation, caring and patience, as well as providing me with an excellent atmosphere for conducting my research. Their vast knowledge and logical way of thinking helped me throughout this process. It was a pleasure to work with them; the lessons they taught me go beyond what is written in this thesis and will help me in all aspects of my life.

I would like to acknowledge the members of my committee, Prof. Muthanna H. Al-Dahhan, Prof. Robert Legros, Prof. François Bertrand for taking interest in my work, examining my thesis and providing insightful comments.

I am deeply thankful to Mr. Jaber Shabanian and Dr. Amirhossein Manni, whose friendly attitude and collaboration in making the optical probes and performing rheological measurements were incredibly valuable. I am grateful to Dr. Sherif Farag for his assistance in conducting a part of the experimental work in the HP-HT multiphase reactors unit. I would also like to thank Ms. Soumaya Benzennou and Ms. Odile Vekemans for kindly translating the abstract of this thesis into French.

In my daily work I have been blessed with a supportive and cheerful group of fellow students. I am very grateful to all my colleagues in our research group and my fellow labmates for their cooperative manner and friendly support. I would like to offer my special thanks to Dr. Mohammad Latifi, Dr. Jean-Philippe Laviolette, Dr. Rouzbeh Jafari, and Dr. Pierre Sauriol for their help and transparency during my research.

One of the most beautiful qualities of true friendship is understanding and being there for one another. This journey would not have been possible without the constant support of my great friends Majid, Milad, Jaber, Omid, Hamed, Ata, Monica, Moe, Ebrahim, Olivier, Samira, Sepehr, Ali, Philippe, Navid, Said, and all those whose company made my stay in Montreal a pleasant and memorable one.

During the course of my studies, numerous devices and pieces of equipment needed to be designed and machined. My deepest appreciation goes to the technicians in the Department of Chemical

Engineering, particularly Robert, Yazid, Tristan, Sylvain, and Melina for their excellent technical assistance, and whose great experience that helped me to effectively solve various technical issues. In addition, I wish to thank the secretaries of the Department of Chemical Engineering for helping us and providing us with an ideal atmosphere in which to advance our projects.

I also wish to gratefully acknowledge the financial support of TOTAL American Services, Inc. and the Natural Sciences and Engineering Research Council of Canada (NSERC) (Grant no. IRCPJ 412045-10), which made this research work possible.

And last but not least, from the bottom of my heart, I would like to express my endless gratitude to my mother, father, lovely sister, and brother-in-law for the absolute support they have provided me throughout my entire life, and without whose love, spiritual encouragement and altruism I would not have finished this thesis. Words are powerless to express what I feel in my heart for them.

RÉSUMÉ

Dans l'industrie, de nombreux procédés nécessitent le contact entre une phase gazeuse et une phase liquide, avec ou sans solide en suspension, et ce afin de donner lieu à une grande variété de réactions chimiques. Bien que de nombreux types de réacteurs peuvent être utilisés à cet effet, au cours de la dernière décennie les réacteurs à colonne à bulles ont reçu une attention particulière car ils offrent certains avantages uniques tels que la facilité d'utilisation, des taux élevés de transfert de masse et de chaleur, et des frais d'entretien réduits en raison de l'absence de pièces mécaniques en mouvement. La conception et la mise à l'échelle d'une colonne à bulles nécessitent une compréhension complète de son hydrodynamique complexe. Ce dernier dépend des propriétés physiques des phases liquides et gazeuses, des conditions d'opération, et des paramètres de conception. A l'heure actuelle, du au manque de connaissance de ces systèmes, la conception des colonnes à bulles nécessite généralement des études expérimentales à différentes échelles (laboratoire, pilote, etc.), ce qui est coûteux en capital et en temps.

Au cours des dernières années, les liquides et les solutions aqueuses en suspension utilisées dans les colonnes à bulles sont visqueuses et présentent habituellement, aux conditions opératoires utilisées, des comportements non newtoniens complexes. De plus, dans les colonnes à bulles utilisant des liquides non-newtoniens, non seulement la viscosité du liquide est habituellement variable selon les conditions d'écoulement, mais également leurs éventuelles propriétés élastiques. Pour cette variété de liquides non-newtoniens possédant des propriétés élastiques, ces dernières sont susceptibles d’affecter et de modifier fortement les comportements des bulles. En dépit de la demande croissante d'utilisation de fluides non newtoniens dans les réacteurs à colonnes à bulles, notre compréhension actuelle des effets des propriétés non-newtoniennes sur différents aspects hydrodynamiques des colonnes à bulles est loin d'être complète. Parmi les quelques études réalisées sur l'effet des propriétés rhéologiques de la phase liquide dans les colonnes de bulles, l'influence de l'élasticité du liquide sur les paramètres hydrodynamiques n'a jamais été étudiée distinctement et les modèles et concepts disponibles à l'heure actuelle sur ce sujet sont insuffisants pour une application industrielle. Afin d'obtenir un aperçu global de la performance des colonnes à bulles utilisant des liquides non-newtoniens, les effets de toutes les propriétés rhéologiques de la phase liquide, et non pas l'effet d'un seul paramètre qu'est la viscosité, doivent être étudiés. Cette thèse

est donc dédiée à l'étude de l'hydrodynamique des colonnes à bulles fonctionnant avec des liquides non-newtoniens possédant des propriétés rhéologiques variées.

Le principe de fonctionnement, les aspects hydrodynamiques de base du réacteur à colonne à bulles, ainsi que les liquides non-newtoniens et leurs propriétés rhéologiques sont brièvement discutés dans les deux premiers chapitres de cette thèse. Le premier objectif de ce travail est de comprendre l'effet des propriétés rhéologiques du liquide sur les différents paramètres hydrodynamiques d'une colonne à bulles. À cet égard, l'effet de la rhéologie de la phase liquide sur l'hydrodynamique d'un réacteur à colonne à bulles à l'échelle pilote est largement étudiée en sélectionnant stratégiquement divers types de liquides. La rétention de gaz et ses variations radiales et axiales, le point de transition du régime opératoire et la taille des bulles sont évalués au moyen de deux sondes à fibre optiques fabriquées dans nos laboratoires, ainsi que plusieurs capteurs de pression. Afin de mieux comprendre l'effet de la rhéologie sur les paramètres hydrodynamiques de la phase gazeuse, plusieurs analyses en fonction du temps et des fréquences sont réalisées sur les signaux de fluctuations de pression. Les effets visqueux et élastiques simultanés des liquides non-newtoniens sont étudiés à l'aide d'une nouvelle approche basée sur les modules dynamiques des solutions viscoélastiques. Il a été trouvé que la viscosité du liquide favorise la coalescence des bulles, alors que son élasticité l'entrave, se comportant comme un solide à l'interface de deux bulles. La présence d'élasticité dans le liquide mène à la réduction de la longueur de corde moyenne des bulles et à l'augmentation de la rétention globale de gaz. Les résultats obtenus dans cette partie du travail sont primordiaux afin d'atteindre le second objectif, qui vise principalement à étudier localement les paramètres hydrodynamiques et à développer de nouvelles corrélations pour estimer la taille des bulles et la rétention de gaz dans les réacteurs à colonne à bulles utilisant des liquides non-newtoniens. Par conséquent, dans la deuxième partie de ce travail, les propriétés locales des bulles telles que leur fréquence, leur longueur de corde et leur vitesse d'ascension ainsi que leurs distributions radiales et axiales, sont évaluées à l'aide de deux sondes à fibres optiques placées à des endroits différents dans le réacteur à colonne à bulles opéré avec différents liquides non-newtoniens. Il a été observé que le profil radial de la fréquence des bulles, de leur longueur de corde et de leur vitesse d'ascension sont relativement plats à basse vitesse superficielle de gaz, mais deviennent paraboliques lorsque la vitesse superficielle du gaz augmente. En outre, à l'aide d'une analyse adimensionnelle, deux corrélations ont été développées afin de prédire la taille des bulles et la rétention de gaz dans les colonnes à bulles opérées avec des liquides non-newtoniens. Ces

deux nouvelles corrélations sont capables de prédire correctement la taille des bulles et la rétention de gaz au sein des colonnes à bulle, à l'aide du rapport entre modules dynamiques des solutions viscoélastiques.

Une variété de procédés industriels tels que la synthèse de Fischer-Tropsch, la synthèse du méthanol, l'oxydation partielle de l'éthylène, l'hydrocraquage des résidus lourds, et l'hydroformylation utilise des colonnes à bulles, mais à haute pression. Par le passé, il a été découvert que la pression d'opération a un effet significatif sur les caractéristiques hydrodynamiques des colonnes à bulles. Par exemple, une augmentation de la pression opératoire conduit normalement à la formation de plus petites bulles au niveau du distributeur de gaz. Bien que l'étude des effets de la pression dans les colonnes à bulles ait fait l'objet de certains travaux de recherche, de nombreuses zones restent à éclairer et il existe encore un grand intérêt des chercheurs et des concepteurs de réacteurs à conduire des études approfondies afin d'élucider l'influence de la pression d'opération sur les différents aspects de l'hydrodynamique et, en conséquence, sur la performance de réacteurs à colonne à bulles.

Afin d'optimiser les procédés industriels cités ci-dessus, il est indispensable d'avoir une compréhension complète de l'effet de la pression d'opération sur la cinétique chimique, les propriétés du liquide (viscosité et tension superficielle), le régime d'écoulement de liquide, la dynamique des bulles (taille des bulles, forme de la bulle, éclatement et taux de coalescence, vitesse d'ascension) et le taux de transfert de chaleur et de masse. Par conséquent, le dernier objectif de ce travail est consacré à étudier l'effet de la pression d'opération sur l'hydrodynamique de la colonne à bulles et en présence de liquides non-newtoniens. A cet effet, un ensemble de réacteurs à haute pression/ haute température, dont une colonne à bulles et un réacteur à lit fluidisé ont été conçus et construits. En plus des réacteurs en tant que tels, cette installation inclus différents équipements tels que des compresseurs, des cylindres de stockage de gaz à haute pression, des éléments chauffants, un réservoir d'alimentation de liquide, une pompe centrifuge pour liquide, des séparateurs gaz-liquide, une unité de contrôle, un système d'acquisition de données, etc. Cette installation expérimentale sera introduite plus en détails au Chapitre 5. Au sein de cette installation et à l'aide de mesures de signaux de pression différentiels et dynamiques, divers caractéristiques hydrodynamiques des colonnes à bulles, comme la rétention totale du gaz et sa distribution axiale, le point de transition de régime d'écoulement, les fluctuations de pression et son écart-type, ont été étudiées. La vitesse superficielle du gaz a été variée de 1 à 35 (cm s^{-1}) couvrant les deux régimes

d'écoulement, homogène et hétérogène. La pression de fonctionnement a également été variée de 0.1 à 1 (MPa) pendant les expériences. Il a été étudié que la rétention totale de gaz augmente à la fois avec la pression opératoire et avec l'élasticité de la phase liquide ; l'impact de la pression est d'autant plus prononcé à de basses pressions d'opération. Il a également été identifié que l'augmentation de la pression d'opération conduit à un décalage du point de transition entre régimes hydrodynamiques à de plus haute vitesses de gaz superficielles. En conclusion, il a été prouvé que non seulement la rhéologie de la phase liquide, mais également la pression d'opération, ont un effet important sur l'hydrodynamique des réacteurs à colonnes à bulles. Les connaissances scientifiques développées dans ce travail peuvent ainsi aider les industriels à mieux décrire les phénomènes présents dans les colonnes bulles utilisant des liquides non-newtoniens très visqueux et des pressions élevées, ce qui leur permettrait une conception, exploitation et mise à l'échelle plus avisée et performante des réacteurs à colonne à bulles commerciaux.

ABSTRACT

Processes based on the contact between gas and liquid/slurry phases are commercially used for performing a variety of chemical reactions. Although different types of reactors are used for this purpose, bubble column reactors have received more attention during the past decade since they offer some unique advantages, such as ease of operation, high rates of heat and mass transfer, and lower maintenance costs due to the absence of moving parts. The design and scale-up of a bubble column reactor require a complete understanding of its complex hydrodynamics, which is influenced by the physical properties of the phases, the operating variables, and the design parameters. Current design procedures for bubble columns involve several steps of pilot-plant experimentation using equipment of different scales, which is expensive and time consuming.

In recent years, the liquid and/or slurry phases which are processed in bubble columns in many applications are viscous and normally demonstrate non-Newtonian behaviors during the process operation. Hydroconversion of heavy oil and petroleum residues, wastewater treatment, processing of fermentation broths, polymer composite processing, and slurry-phase synthesis are some of those processes in which viscous and non-Newtonian liquids are often encountered in bubble column reactors. On the other hand, in bubble columns operating with non-Newtonian liquids, the viscosity changes upon the flow conditions, and also a variety of non-Newtonian liquids possess elastic properties that can affect and alter bubble behavior to a great extent. Although there has been an increasing application of non-Newtonian fluids in bubble column reactors, our present understanding of the effects of non-Newtonian properties on different hydrodynamic aspects of bubble columns is far from complete. Only few studies are reported on the effect of liquid phase rheological properties in bubble columns so that the influence of liquid elasticity on the hydrodynamic parameters such as gas holdup and bubble properties has never been studied distinctly, and the models and concepts currently available on this subject are insufficient for chemical practice. To gain adequate insight into the performance of bubble columns operating with non-Newtonian liquids, the effects of all rheological properties of the liquid phase need to be investigated rather that the effect of a single parameter like viscosity. This thesis is, therefore, dedicated to investigating the hydrodynamics of bubble columns operating with non-Newtonian liquids having different rheological properties.

The operation principle and basic hydrodynamic aspects of the bubble column reactors, as well as non-Newtonian liquids and their rheological properties, are briefly discussed in the first two chapters. The first objective of this work is to understand the effect of the rheological properties of liquid on different hydrodynamic aspects of a bubble column reactor including gas holdup and its radial and axial distributions, bubble size and its axial distribution, standard deviation, power spectral density and average frequency of pressure signals. In this regard, the effect of liquid phase rheology on the hydrodynamics of a pilot-scale bubble column reactor is extensively investigated by strategically selecting various types of liquids. The selected liquids include water as a reference and low-viscosity liquid, an aqueous glucose solution as a highly viscous Newtonian and inelastic liquid, a Boger fluid which has a constant viscosity identical to the glucose solution but it is slightly elastic, and finally two non-Newtonian (shear-thinning) and elastic Carboxymethyl cellulose (CMC) and Xanthan gum solutions. Gas holdup and its radial and axial variations, the operating flow regime transition and bubble size are evaluated by means of two in-house made optical fiber probes and several pressure transducers. Different time-domain and frequency-domain analyses are applied to the pressure fluctuation signals in order to better understand the effect of liquid phase rheology on the gas holdup and bubble size. The simultaneous viscous and elastic effects of non-Newtonian liquids are studied by proposing a new approach based on the dynamic moduli of viscoelastic solutions. It was found that the viscosity of liquid is more favorable for bubble coalescence; however, the elasticity can hinder bubble coalescence as it can demonstrate a solid-like behavior at the interface of two bubbles. The presence of elasticity in the liquid was shown to reduce the average bubble chord length and increase the overall gas holdup. The results obtained in this part of the work are essential for achieving the second objective, which is aimed at studying the local hydrodynamic parameters such as local bubble frequency and bubble rise velocity and developing new correlations to estimate bubble size and gas holdup in bubble column reactors operating with non-Newtonian liquids. Therefore, in the second part of this work, local bubble properties such as bubble frequency, bubble chord length, and bubble rise velocity, as well as their radial and axial distributions, are evaluated by installing two optical fiber probes at various locations within a bubble column reactor operating with different non-Newtonian liquids. It was observed that the radial profiles of bubble frequency, bubble chord length and bubble rise velocity are relatively flat at low superficial gas velocities, while they become parabolic as the superficial gas velocity increases. Moreover, by applying the dimensional analysis, two new correlations are

developed to predict the bubble size and gas holdup in bubble columns operating with non-Newtonian liquids. The two correlations are developed by taking into consideration the ratio between the dynamic moduli of viscoelastic solutions and are capable of accurately predicting both bubble size and gas holdup.

Moreover, a variety of commercial processes such as Fischer-Tropsch synthesis, Methanol synthesis, Partial oxidation of ethylene, Residuum hydrotreating, and Hydroformylation are carried out in bubble columns at elevated pressures. The operating pressure is found to have a significant effect on the hydrodynamic characteristics of bubble columns such as bubble properties and gas holdup. For instance, an increase in the operating pressure normally results in the formation of smaller bubbles at the gas distributor and this is mainly due to the higher gas density at elevated pressure. Although investigating the pressure effects in the bubble columns has been the subject of some research, there is still a strong need toward more studies on the influence of operating pressure on different hydrodynamic aspects, and, accordingly, on the performance of bubble column reactors. Therefore, the last objective of this work is devoted to investigating the effect of operating pressure on the hydrodynamics of bubble column reactors in presence of non-Newtonian liquids. For this purpose, a high-pressure/high-temperature multiphase reactors unit including a bubble column reactor with an inner diameter of 0.152 m and a total height of 4.8 m has been designed and constructed to perform experiments at elevated pressures. The multiphase reactors unit was equipped with different equipment, including air compressors, high-pressure gas storage cylinders, gas heating elements, liquid supply tank, liquid centrifugal pump, gas-liquid separators, PLC control unit, etc. This experimental unit is introduced in more detail in Chapter 5. Various hydrodynamic characteristics of bubble column reactors, such as the total gas holdup and its axial distribution, operating flow regime transition point, pressure fluctuation and its standard deviation have been studied by means of pressure signal measurements with several differential and dynamic pressure traducers. The superficial gas velocity varied from 1 to 35 (cm s^{-1}), covering both homogeneous and heterogeneous flow regimes. Operating pressure also changed from 0.1 to 1 (MPa) during the experiments. The total gas holdup was found to increase with both operating pressure and the elasticity of liquid phase, and the effect of pressure was shown to be more pronounced at lower operating pressures. The operating pressure was shown to shift the flow regime transition point to higher superficial gas velocities. A new correlation was also derived for predicting the gas holdup in bubble column reactors operating at elevated pressure. As a

conclusion, both the rheology of the liquid phase and operating pressure are shown to have important effects on the hydrodynamics of bubble column reactors. Moreover, the scientific findings of the present work may have significant implications for the more accurate design, operation and scale-up of commercial bubble column reactors, where highly viscous and non-Newtonian liquids and high pressures are often applied.

TABLE OF CONTENTS

LIST OF TABLES

LIST OF FIGURES

NOMENCLATURE

Symbols

a	Interfacial surface area (m^{-1})
Bo	Bond number
d_B	Bubble mean diameter (m)
d_O	Diameter of orifice (m)
D_c	Diameter of column (m)
D_p	Diameter of probe (m)
f	Pressure signal frequency (Hz)
f_b	Bubble frequency (Hz)
f_m	Average frequency of the spectrum (Hz)
Fr	Froude number
g	Gravity constant ($m\ s^{-2}$)
Ga	Galilei number
G'	Storage modulus (Pa)
G''	Loss modulus (Pa)
H_C	Column total height (m)
H_0	Unaerated liquid height (m)
j_{gl}	Drift flux ($m\ s^{-1}$)
K	Consistency index ($Pa\ s^n$)
L	Distance from gas distributor (m)
L_b	Bubble chord length (mm)
$L_{b,rms}$	Root mean square of bubble chord length (mm)
M_w	Molecular weight of polymer ($mol\ gr^{-1}$)

n	Flow index (-)
N	Number of bubble/Number of data points (-)
N_o	Number of orifice (-)
N_1	First normal stress difference (Pa)
P	Operating pressure (Pa)
P_n	Pressure time series (Pa)
$\overline{P}$	Mean pressure (Pa)
$P_{xx}^{j}(f)$	Power spectral density of segment *j* (Pa^2 s)
$P_{xx}(f)$	Average power spectral density (Pa^2 s)
Q_g	Gas flow rate (m^3 s^{-1})
r	Radius (m)
R	Column radius (m)
T	Length of time series (s)
t_G	Time that probe spends in the gas phase (s)
t_L	Time that probe spends in the liquid phase (s)
$t_{residence}$	Bubble residence time (s)
t_{rise}	Bubble rise time (s)
$T_{measurement}$	Measurement time (s)
U_g	Superficial gas velocity ($m.s^{-1}$)
$U_{g,transition}$	Superficial gas velocity at transition point (m s^{-1})
U_l	Superficial liquid velocity (m s^{-1})
U_o	Gas velocity at orifice (m s^{-1})
$V_{G,local}$	Local gas volume (m^3)
$V_{L,local}$	Local liquid volume (m^3)
w	Window function

We_o	Orifice weber number (-)
Z	Distance from distributor (m)

Greek letters

$\dot{\gamma}$	Shear rate (s^{-1})
$\mu_{app.}$	Apparent viscosity (Pa s)
μ_g	Gas viscosity (Pa s)
μ_L	Liquid viscosity (Pa s)
ε_g	Gas phase holdup (%)
$\bar{\varepsilon}_g$	Average gas holdup (%)
$\varepsilon_{g,local}$	Local gas phase holdup (%)
$\varepsilon_{g,transition}$	Gas phase holdup at transition point (%)
ε_l	Liquid phase holdup (%)
ρ_g	Gas phase density (kg m^{-3})
ρ_l	Liquid phase density (kg m^{-3})
σ	Surface tension (mN m^{-1})
σ	Standard deviation (Pa)
v_b	Average bubble velocity (m s^{-1})
$v_{b,i}$	Individual bubble velocity (m s^{-1})
ϑ_L	Liquid phase kinematic viscosity (m^2 s^{-1})
ω	Angular frequency (rad s^{-1})

ABBREVIATIONS

CMC:	Carboxymethyl cellulose
DME:	Dimethyl ether
F-T:	Fischer-Tropsch
HP:	High-pressure
HT:	High-temperature
LPMeOH:	Liquid-phase methanol synthesis
MAC:	Maleic acid
MAPE:	Mean absolute percentage error
PAA:	Polyacrylamide
PSD:	Power spectral density

LIST OF APPENDICES

CHAPTER 1 INTRODUCTION

1.1 Motivation

The conservation and management of natural resources are perhaps the most fundamental social, economical, and political challenges for implementing a policy of sustainable development. Economic growth in the twenty-first century will require safe and sustainable resources to support the increasing needs of society. It is therefore vital that we develop and adopt already available technologies for processing more complex raw materials, including non-renewable resources (e.g., heavy petroleum, coal, and minerals), as well as renewable ones. This is a highly strategic issue because these technologies are up-stream from any development. It is also imperative to address the environmental issues that have resulted from the rapid growth of the world population and the corresponding increase in the use of resources, both non-renewable and renewable.

Multiphase flows and processes are used widely in the production of chemical and biotechnological products, fuels and energy, petroleum extraction, and even in environmental engineering. Multiphase reactions and mass transfer operations can be carried out in a variety of contacting devices, such as packed columns, plate and tray columns, bubble column reactors, spray towers, mechanically agitated vessels, etc. (Subrata Kumar Majumder, Kundu, & Mukherjee, 2006). Although multiphase process engineering is an active field of research in academia, general and reliable design criteria for multiphase contactors are still scarce, mainly because of the complexity governing heat, mass transfer and yields in chemical processes. Furthermore, the use of high temperature and/or high pressure during the conversion and the handling of high viscosity materials yields extreme processing conditions for which multiphase process hydrodynamics and related phenomena are not well known, and there are still many issues related to designing processes that operate under such extreme conditions. Although many scientific issues are long-term, the answers to certain pressing issues are of immediate interest to many industries.

In order to provide efficient heat and mass transfer and chemical reactions, the quality of the dispersion of gas bubbles in the liquid or slurry phase is of key importance in many respects, such as polymer devolatilization, boiling, fermentation, cavitation, plastic foam processing, and bubble

absorption, to name a few (H. Z. Li et al., 1998). Although different types of reactors are used as gas–liquid/gas–liquid–solid contactors, bubble column/slurry bubble column reactors are known as one of the most important types of such contactors. In bubble columns, the gas phase is dispersed in a liquid phase in the form of bubbles. They are commercially used in chemical and petrochemical processes, including oxidation, hydrogenation, alkylation, chlorination, polymerization, pharmaceutical, petroleum, biotechnology, and food processing, where a variety of fluids (ranging from low-viscosity and Newtonian to highly viscous and non-Newtonian) are often processed under high-temperature and high-pressure conditions. They are also the central operating unit for the production of primary and secondary metabolites, as well as for several downstream processes such as separation and product recovery by adsorption in bubble flows (Velez-Cordero & Zenit, 2011). Bubble column reactors are very effective for processes where the overall production rate is often controlled by gas-liquid interfacial mass transfer (Koichi Terasaka & Tsuge, 2003). Moreover, one of the most interesting applications of bubble columns is converting natural gas, syngas or coal to liquid fuels and chemicals through a gas-to-liquid processes. Increasing world energy demands, together with the decline of crude oil supplies and the fluctuating fuel markets, mean that gas-to-liquid processes (e.g., the Fischer-Tropsch synthesis, liquid phase methanol synthesis, and dimethyl ether synthesis) should be considered as important energy solutions for the future. Current gas-to-liquid technologies use slurry bubble column reactors with considerably larger column sizes and are now receiving more attention from both the academy and industry.

Although the bubble column reactors are simple from a mechanical point of view, the phenomena that occur in the reactor are quite diverse and complex. Due to the difference between the physical properties of the operating phases (gas, liquid, and solid), the hydrodynamics of bubble columns is complex, which makes their basic engineering design a challenging task. Moreover, most of the processes are carried out under high gas flow rates, pressure, temperature, and solid loading conditions that operation under such extreme conditions can significantly alter the bubble, liquid, and solid flow dynamics and thus their heat and mass transfer characteristics. Therefore, a successful design and scale-up can be achieved only when the influence of different parameters on the performance of bubble columns is completely known. In addition, economic issues related to higher energy costs, the lower quality and intrinsic variability of new feedstock, and the evolution of regulations in terms of health, safety, and the environment, make the design and operation of these reactors much more complex.

The parameters affecting the performance and efficiency of bubble columns can be defined into two classifications: 1) design parameters including reactor size, internals, gas distributor specifications, and catalyst particle size; and 2) operating variables that include gas and liquid flow rates, operating pressure and temperature and catalyst loading (Vinit P Chilekar, van der Schaaf, Kuster, Tinge, & Schouten, 2010; Moustiri, Hebrard, Thakre, & Roustan, 2001; Stoyan Nedeltchev, Jordan, & Schumpe, 2007). For a given chemical process and properties of operating phases, a process design engineer should be able to estimate the optimum column geometry, gas distributor configuration, and superficial gas velocity to achieve optimum mixing, heat, and mass transfer rates between the operating phases, as well as to guarantee the expected product rate (Velez-Cordero & Zenit, 2011). Such estimations need a complete understanding of the functional relations among operating variables and hydrodynamic parameters, such as gas holdup, bubble size and bubble rise velocity, and liquid and solid velocity fields.

Bubble columns have been investigated over the past few decades, and there has been some valuable experimental and theoretical works conducted on this subject. However, most of these studies are limited to studying bubble columns operating with air-water system under ambient conditions. In recent years, viscous liquids and slurries with a variety of rheological properties (including Newtonian, non-Newtonian, and viscoelastic) have been increasingly used for carrying out chemical processes in bubble column reactors. Typical examples include hydroconversion of petroleum residues, wastewater treatment, handling and processing of fermentation broths, polymer devolatilization, composite processing, etc. (Godbole, Schumpe, Shah, & Carr, 1984; Guy, Carreau, & Paris, 1986). For instance, because of the accumulated biomass or the formation of macromolecular products, many microbial culture media behave like highly viscous pseudoplastic liquids. Most of the reaction media in biochemical applications also exhibit a non-Newtonian behaviour (Kawase, Umeno, & Kumagai, 1992; Suh, Schumpe, Deckwer, & Kulicke, 1991) such as processes including Carboxymethyl cellulose (CMC) and Xanthan gum solutions. The bubble-bubble and bubble-liquid interaction phenomena, as well as bubble break-up and coalescence in non-Newtonian fluids, play a key role in such diverse fields. The rheological properties of liquids can dramatically affect the character of the multiphase flows and are shown to have important effects on various hydrodynamic aspects of bubble columns. For example, it has been reported that the elastic characteristics of liquid are responsible for a number of particular phenomena in the bubble columns (Suh et al., 1991).

Although numerous studies are devoted to studying bubble behavior in low-viscous and Newtonian fluids, the understanding of bubble dynamics in viscous and non-Newtonian fluids remains at an elementary stage. Moreover, there is little data and inconsistent information about the effects of liquid rheology on the performance of bubble columns where a swarm of bubbles move through the liquid phase (H. Z. Li et al., 1998). In addition, despite the widespread use of high-pressure bubble columns in a variety of industries (e.g., methanol synthesis at P = 5.5 MPa, resid hydrotreating at P = 5.5–21 MPa, Fischer–Tropsch synthesis at P = 1.5–5.0 MPa, and benzene hydrogenation at P = 5.0 MPa), there are no studies dealing with bubble column reactors operating with viscous and/or non-Newtonian liquids at high pressure conditions, mainly because of the inherently complex nature of bubble phenomena and the difficulties related to the implementation of experimental techniques under such conditions. This significant lack of engineering knowledge and understanding has left many questions to be answered, and many topics are still under discussion in this area (Kemiha, Frank, Poncin, & Li, 2006). Therefore, there is a strong motivation from both theoretical and experimental standpoints to better elucidate the detailed effects of liquid phase properties and operating pressure on bubble dynamics, bubble break-up and coalescence mechanisms, heat and mass transfer and thus the overall performance of bubble columns. Moreover, it is necessary to develop correlations to be able to predict the effect of liquid phase properties and operating pressure on some important hydrodynamic parameters such as gas holdup and bubble size. For example, hydrodynamic studies on the Exxon Donor Solvent coal liquefaction process indicate that many of the correlations available in the literature for evaluating hydrodynamic parameters (e.g., holdup, interfacial area and dispersion coefficients), obtained with cold flow units at ambient conditions and are not applicable for commercial units operating at relatively high pressure (De Lasa, Dogu, Dogŭ, & Ravella, 1992).

1.2 Objectives

As already mentioned, there is a great need to have a complete understanding of the influences of liquid phase properties and operating pressure on different hydrodynamic aspects of bubble column reactors. Thus, the main objective of this research program is *to study the hydrodynamics of bubble column reactors operating with non-Newtonian liquids and at elevated pressures*.

To achieve this, the following specific objectives are defined:

- Understand the effect of non-Newtonian features of liquids on different hydrodynamic aspects of bubble column reactor including the gas holdup and bubble size and their axial and radial distributions by means of several pressure transducers and optical fiber probes.
- Study the local hydrodynamic parameters including the local bubble frequency and bubble rise velocity and develop new correlations to estimate the bubble size and gas holdup in bubble column reactors operating with non-Newtonian liquids, and thus improve the design and scaling-up operations by taking into account the rheological properties of the liquid phase.
- Investigate the effect of operating pressure on the gas holdup, operating flow regime transition and pressure fluctuations in the bubble column reactor operating with non-Newtonian liquids.

Two pilot-scale bubble columns were designed and built to perform the experiments. The first series of experiments were carried out at ambient pressure and in a 0.292-m-diameter bubble column made of Plexiglass with a total height of 2.7 m. The second series of experiments were conducted at elevated pressures in a high-pressure bubble column made of stainless steel with an inner diameter of 0.152 m and a total height of 4.8 m. The effect of liquid phase rheological properties such as shear-thinning, elasticity, and viscoelasticity on the hydrodynamics of bubble column were investigated by strategically choosing several viscous and non-Newtonian liquids. Based on the identified problems and specific objectives, the most important achievement of this study is conducting extensive experiments to investigate the effect of rheological behaviour of different liquids by applying the most reliable, accurate and up-to-date measurement techniques. The feasibility of using different experimental techniques, their accuracy and limitations, and their optimal usage range were examined prior to performing the experiments. Extensive rheological studies were also conducted to characterize the liquids selected in this work. A combination of differential and dynamic pressure transducers and optical fiber probes were applied to scrutinize the global and local behavior of the gas phase and bubbles. Through these techniques, some vital local and global hydrodynamics parameters, such as gas holdup, regime transition point, bubble frequency, bubble size and bubble rise velocity, and their axial and radial distributions, are investigated. Moreover, one part of this work is specifically dedicated to introducing the

rheological properties of the liquid phase into the correlations for predicting bubble size and gas holdup. Knowledge of these parameters is essential for the successful design and operation of bubble columns and slurry bubble column reactors.

1.3 Thesis organization

In the present chapter, the problem under study, research framework, and field of application are introduced, along with the objectives of the study. Chapter 2 presents a critical review of the key relevant literature and recent advances in investigating non-Newtonian liquids and their influence on the hydrodynamic parameters of bubble columns such as gas holdup and bubble properties (i.e., bubble frequency, bubble size, and bubble rising velocity), which helps readers to identify the links between this research and past studies in this area. Chapter 3 provides a detailed rheological study of the liquids applied in this work and the effect of liquid properties on the hydrodynamics of a bubble column operating at ambient conditions. The experimental results reported in Chapter 3 are obtained mainly by performing a variety of analyses on the pressure signals recorded by means of several pressure transducers. Chapter 4 is dedicated to studying the effect of liquid phase rheology on bubble frequency and bubble rise velocity and their axial and radial distribution and developing new correlations for the estimation of gas holdup and bubble size in bubble columns operating with non-Newtonian liquids. Chapter 5 explains the new high-pressure/high-temperature multiphase reactors unit specifically designed and constructed to perform the experiments at elevated pressures. The effect of operating pressure on different hydrodynamic aspects of bubble columns is presented in Chapter 6. Moreover, each individual chapter includes a specific literature review on the relevant subjects. A general discussion on the experimental results obtained in this research is covered in Chapter 7. Finally, a brief conclusion and recommendations for future work in this topic are given in Chapter 8.

CHAPTER 2 LITERATURE REVIEW

2.1 Bubble column reactors

At least at first glance, bubble column reactors are pretty simple. Two or three phases are brought into contact with each other in a cylindrical vessel. One of the contacting phases is gas, which is dispersed into a liquid or slurry phase. The contact between these phases is so intense that they also react together chemically, usually with the aid of a catalyst. Bubble column reactors are designed without any moving mechanical parts and have a simple construction that can safely handle aggressive media, even at high-pressure and high-temperature operating conditions. These unique features make this multiphase reactor one of the most important reactor types in process engineering. Figure 2-1 shows a simple schematic of bubble column reactors used for Fischer-Tropsch (F-T) synthesis. Normally, the length-to-diameter aspect ratio in bubble column reactors is greater than five, and they usually operate with a superficial gas velocity which is an order of magnitude greater that the superficial liquid velocity (De Lasa et al., 1992). The typical range of superficial gas velocity in a bubble column is 1 to 30 cm s^{-1}, and for superficial liquid velocity this range is 0 to 2 cm s^{-1}.

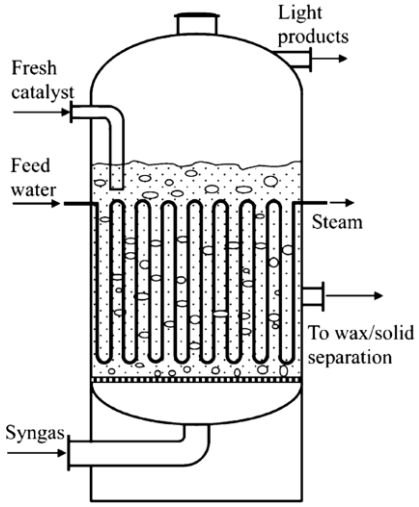

Figure 2-1: Schematic of a bubble column reactor used for F-T synthesis (Wang, Wang, & Jin, 2007).

Bubble columns are widely used in process industries as absorbers, strippers, gas-liquid reactors, etc. Moreover, biotechnology, food processing, and pharmaceutical processes constitute a wide spectrum of chemical industries where highly viscous media are processed in bubble columns (Haque, Nigam, Joshi, & Viswanathan, 1987). A summary of the commercial applications of bubble column reactors is presented in Table 2-1 (Cui, 2005; De Lasa et al., 1992).

Table 2-1: Summary on the commercial applications of bubble column reactors.

Industry	Applications
Chemical	• Hydrogenation of maleic acid (MAC) and saturation of fatty acids • Hydrocracking • Chlorination (production of aliphatic and aromatic chlorinated compounds) • Polymerization (production of polyolefins) • Coal liquefaction • Flue gas desulfurization • Oxidation (adiponitrile synthesis) • Wet-air oxidation
Petrochemical	• Partial oxidation of ethylene to acetaldehyde • Liquid phase methanol (LPMeOH) synthesis • Fischer-Tropsch (F-T) synthesis • Dimethyl ether (DME) synthesis
Biochemical, food, and pharmaceutical	• Fermentation (production of ethanol and mammalian cells) • Cultivation of bacteria • Cultivation of mold fungi • Production of single-cell proteins • Animal cell culture • Treatment of sewage
Metallurgical	• Leaching of ores

Bubble column reactors offer many advantages compared to similar gas-liquid/gas-liquid-solid contactors such as stirred-tank and packed-bed reactors. Some of the most interesting features of bubble column reactors are as follows (Gupta et al., 2009; S. Nedeltchev, Nigam, & Schumpe, 2014):

- Simple to construct and easy to operate.
- Low capital cost due to the small floor space needed.
- Low maintenance and operating costs due to the absence of any moving parts.
- Provide high heat and interphase mass transfer rates at a low energy input.
- Able to operate with very fine catalyst particles (<100 μm), which allows for a large surface area per unit volume and improved liquid-solid mass transfer.
- On-line factors where the catalyst particles can be added and removed continuously, allowing for longer runs without reactor shutdown.
- High selectivity and conversion per pass.
- Able to accommodate large production capacity.
- Uniform temperature distribution and easy temperature control.
- Desirable for processes containing highly exothermic reactions for which efficient interphase contacting is required.

All the above-mentioned advantages have created great interest among chemical and petrochemical industries to replace packed-beds with slurry bubble column reactors. The commercialization of LPMeOH process by Air Products and Chemicals and Eastman Chemicals with funding from the U.S. Department of Energy (Power Generation, 1997) and the commission (in May, 1993) of the Fischer-Tropsch slurry bed process by Sasol (Sasolburg, South Africa) are just two examples of such interest (Inga & Morsi, 1999).

In addition to the numerous advantages of bubble column reactors, they also have some drawbacks that must be taken into consideration for optimum design and operation purposes. Some of these include (Gandhi, Prakash, & Bergougnou, 1999):

- Significant back-mixing in both liquid and gas phases and bubble-bubble interactions at high superficial gas velocities and in the heterogeneous flow regime.
- Substantial side products due to high liquid holdup.
- Catalyst attrition and deactivation as a result of high shear created in the region close to the gas distributor.

- Difficulties related to catalyst separation and recovery, especially in highly viscous slurries containing very fine catalyst particles.
- Difficulties in scaling up.

Because of the extensive applications of bubble columns and the demand of high-production capacity, various constructions and reactor sizes are built in different industries, ranging from a few liters (used, for example, in the growth of plant or animal cells) to thousands of cubic meters (used for wastewater treatment) (Menzel, Weide, Staudacher, Wein, & Onken, 1990). Examples include a single-cell protein unit in Billingham with a total reactor volume of about 2,600 m^3 and a wastewater treatment plant in Leverkusen Bayer operating with a total reactor volume of about 20,000 m^3 (Halard, Kawase, & Moo-Young, 1989). Based on process conditions, heat exchanger coils or other internals may be inserted into the column to increase the heat transfer rate, as can be seen in Figure 2-1. The column may also be sectionalized using a baffle system or perforated plates in order to prevent bubble coalescence and liquid phase back-mixing. In bubble columns, the relevant reactions and transport processes happen on different scales of time and space, ranging from reactions at the molecular level, through turbulence around the gas bubbles and boundary movements, to large-scale flow processes. Moreover, the back-mixing, dilution, dead zones and turbulence also play a large role in selective reactions carried in bubble columns. Depending on the flow of phases, bubble columns can operate as up-flow, down-flow, cocurrent, countercurrent, crosscurrent or semi-batch (batch liquid phase) modes. Among these categories, cocurrent down-flow bubble columns have received more attention since they possess some unique advantages over other types. These include finer and uniform bubble size, negligible bubble coalescence, homogenization of the phases, and longer residence time of the gas phase (Mandal, Kundu, & Mukherjee, 2004).

Depending on the size of catalyst particles, bubble columns can also operate as a slurry reactor or a three-phase fluidized bed reactor in which the catalyst particles are usually suspended in the liquid phase by the action of rising gas bubbles. When the catalyst particles are small (terminal settling velocity of the particle in the liquid less than 7 cm s^{-1}), the bubble column is frequently referred to as a slurry reactor, and is called a three-phase fluidized bed when the particles are relatively large (terminal settling velocity less than 50 cm s^{-1}) (L.-S. Fan, 1989). In addition, the flow of solids may be continuous or in batches.

2.2 Non-Newtonian fluids and rheology

A Newtonian fluid is a fluid whose stress at each point of its flow is linearly proportional to its strain rate at that point. This concept was first introduced by Isaac Newton and is directly analogous to Hook's law for solids. All gases, most common liquids such as water and hydrocarbons, low molecular weight ($M_W < 5000$ or so) liquids and their solutions, molten salts, and liquid metals are all considered Newtonian fluids. On the other hand, over the last few decades, there has been an increasing recognition of the fact that most materials of both practical and industrial interest do not adhere to simple Newtonian fluid behavior, and are accordingly called "rheologically complex" or "non-Newtonian" fluids. The term "rheology" was invented by Professor Eugene Bingham of Lafayette College, Easton, PA, and it means the study of the deformation and flow of matter. The rheology of materials is of great importance in the chemical processing industries (Howard A Barnes, Hutton, & Walters, 1989). There are many examples of materials exhibiting non-Newtonian fluid characteristics: multiphase mixtures such as slurries and emulsions, polymer melts and solutions, soap solutions, personal-care products including cosmetics and toiletries, food products like jams, jellies, cheese, butter, mayonnaise, meat extracts, soups and yoghurt, biological fluids such as blood, synovial fluid, saliva and semen, building materials, natural products including gums, protein solutions and extracts, agricultural and dairy wastes, magmas, and lava, are typical examples of materials exhibiting non-Newtonian fluid characteristics. From these examples, it can be pointed out that non-Newtonian fluid behavior is so widespread that it would not be an exaggeration to say that simple Newtonian fluid behavior is more of an exception than a rule. Moreover, during the last 30 years or so, a new class of synthetic fluids has emerged that display nearly a constant viscosity over a limited range of steady shear and nonequal normal stresses (elastic effects). Materials that exhibit simultaneous characteristics of both an elastic solid and a viscous fluid are called viscoelastic fluids. Furthermore, depending on the time scale of the deformation process, a given material can behave like a solid or a liquid. Polymer melts and solutions, synovial fluid, soap solutions, and many other materials of practical interest exhibit viscoelastic behavior. These materials have some ability to store energy and partially release it upon the removal of stress. As well, viscosity is a property of stress as a result of an instantaneous shear rate, while elasticity is a property of stress due to a stored strain. In fact, the strain first accumulates in the fluid under the shear and then it gradually relaxes (Imaizumi, Kunugi, Yokomine, & Kawara, 2014). Therefore, the stress of an inelastic viscous liquid is related only to

the instantaneous shear rate, while the stress of an elastic body is a function of stored strain from the initial state. There is also another category of materials called "viscoplastic," which describes a material that behaves as a solid below a critical value of stress, but flows like a viscous liquid at greater stress values. In fact, viscoplasticity is characterized by a yield stress, below which the materials will not deform, and above which they will start to flow. Greases, foams, drilling muds, paints, concentrated slurries, blood, foodstuffs, diamond mine tailings, mucus, molten lava, and filled polymers are some common examples of materials showing viscoplastic behavior (Raj P Chhabra & Richardson, 2011; Pal, 2010).

Returning to the historical perspective, it can be remarked that in the early decades of the twentieth century, only the occasional rheological study was undertaken. However, during and after the Second World War, rheology emerged to become very vital from a practical standpoint. It was discovered that when high molecular weight polymers like natural rubber are dissolved in gasoline (to make flamethrower liquids), they exhibit very unusual behavior. It was also observed that when these types of solutions are mixed in an agitated vessel, they climb up the agitating shaft and even out of the vessel. It was then found that the materials used in the flamethrowers are viscoelastic and rod climbing is caused by normal stresses generated by the shearing. This fact was the starting point for original research on material rheology during the War. For rheological measurements, materials are usually investigated under standard flows such as simple steady shear flow, small-amplitude oscillatory-shear flow, and extensional flow (Howard A. Barnes & Hutton, 1993).

When viscosity decreases with increasing shear rate, we call this fluid shear-thinning. It should be mentioned that the shear-thinning type of fluid is the most commonly encountered time-independent fluid behavior. Almost all non-Newtonian fluids display shear-thinning behavior under appropriate conditions (Howard A. Barnes & Hutton, 1993; R. P. Chhabra, 2006; Velez-Cordero & Zenit, 2011). In the case of shear-thinning fluids, the power-law model has been widely used to predict the apparent viscosity and describe their rheological behaviour as follows:

$$\eta = K\dot{\gamma}^{n-1} \tag{2.1}$$

On the other hand, the power-law model cannot be applied in a wide range of shear rate, and its parameters usually show different values in different ranges of shear rate (Kawase & Kumagai,

1991). There are various proposed models in the literature for predicting the apparent viscosity of non-Newtonian fluids whose behaviour does not obey the power-law model. Also, some of these models are based on theoretical fundamentals and are not flexible enough to fit the viscosity data for various types of non-Newtonian fluids (Carreau, Kee, & Daroux, 1979). Some of most important proposed models for predicting the apparent viscosity of non-Newtonian fluids are given in Table 2-2 below.

Table 2-2: Summary of proposed models for predicting apparent viscosity (Carreau et al., 1979; De Kee & Carreau, 1993; Huang & Feng, 1995).

Investigators	**Correlation**
Cross, 1965 (Cross-Williamson model)	$\eta = \eta_0/[1 + \lvert\lambda_1\dot{\gamma}\rvert^{(1-n)}]$
Carreau, 1972	$\eta = \eta_0/[1 + (\lambda_1\dot{\gamma})^2]^{(1-n)/2}$
Carreau-Bird viscosity law	$\frac{\eta - \eta_\infty}{\eta_0 - \eta_\infty} = [1 + (\lambda_3\dot{\gamma})^2]^{(1-n)/2}$
Ellis model	$\frac{\eta}{\eta_0} = 1/\left[1 + \lvert\tau_{12}/\tau_{1/2}\rvert^{(\alpha-1)}\right]$
Yasuda, 1979 (Carreau-Yasuda Model)	$\frac{\eta - \eta_\infty}{\eta_0 - \eta_\infty} = 1/[1 + \lvert t_1\dot{\gamma}\rvert^a]^{(1-n)/a}$

It is worth mentioning that the magnitude of some key rheological parameters such as flow index (n) and zero-shear viscosity (η_0) strongly depends on the choice of rheological model (De Kee & Carreau, 1993).

As the viscosity of non-Newtonian liquids changes with the shear rate, it is therefore very essential to be able to estimate the shear rate in the process flow. The shear rate encountered in any operation can be estimated by dividing the average velocity of the flowing fluid by a characteristic dimension

of the geometry in which the fluid is moving. The approximate magnitude of the shear rate in a number of important industrial and everyday applications is summarized in Table 2-3.

Table 2-3: Typical range of shear rate in some familiar materials and processes (Howard A Barnes et al., 1989).

Situation	Typical range of shear rates (s^{-1})	Application
Sedimentation of fine powders in a suspending liquid	10^{-6}–10^{-4}	Medicines, paints
Levelling due to surface tension	10^{-2}–10^{-1}	Paints, printing inks
Draining under gravity	10^{-1}–10^{1}	Painting and coating. Toilet bleaches
Extruders	10^{0}–10^{2}	Polymers
Chewing and swallowing	10^{1}–10^{2}	Foods
Dip coating	10^{1}–10^{2}	Paints, confectionary
Mixing and stirring	10^{1}–10^{3}	Manufacturing liquids
Pipe flow	10^{0}–10^{3}	Pumping. Blood flow
Spraying and brushing	10^{3}–10^{4}	Spray-drying, painting, fuel atomization
Rubbing	10^{4}–10^{5}	Application of creams and lotions to the skin
Milling pigments in fluid bases	10^{3}–10^{5}	Paints, printing inks
High speed coating	10^{5}–10^{6}	Paper
Lubrication	10^{3}–10^{7}	Gasoline engines

Nishikawa et al. (Lakota, 2007; Nishikawa, Kato, & Hashimoto, 1977) proposed that the existing effective shear rate in a bubble column can be simply estimated by a correlation based on the superficial gas velocity, as follows:

$$\dot{\gamma} = 5000\, U_g \tag{2.2}$$

It is also reported by Nakanoh et al. (Nakanoh & Yoshida, 1980) that at superficial gas velocities (U_g) lower than 4 cm s^{-1}, Eq. (2.2) holds for shear rates in the core section as well as near the wall of the column. On the other hand, at higher U_g, the local average shear rates in the core section of the column are higher than those predicted by Eq. (2.2), while the shear rate values near the column wall are lower than those given by this equation. Henzler proposed that the shear rate is proportional

to the superficial gas velocity by a constant factor of 1500 instead of 5000 (W. D. Deckwer, Nguyen-Tien, Schumpe, & Serpemen, 1982). Furthermore, Pérez et al. (Perez, Porcel, Lopez, Sevilla, & Chisti, 2006) applied a rigorous theoretical analysis to derive some correlations for predicting the shear rate inside the bubble column and stirred tank reactors. They state that the dependency of the shear rate on the superficial gas velocity can be explained using the following equation:

$$\dot{\gamma} = constant\ {U_G}^{1/(n+1)} \tag{2.3}$$

where *n* is the flow index of the power law model. Kawase et al. (Kawase & Kumagai, 1991) also applied the concept of energy dissipation rate to evaluate the apparent viscosity of liquid in the bubble column bioreactors. They reported that their proposed correlation is more accurate for estimating the average shear rate inside the column compared to those available in the literature. It is worth mentioning that the shear rate inside the bubble column in most experimental studies lies in the range of 10-1200 s^{-1}.

As previously mentioned, in many biochemical processes carried out in bubble column reactors, highly viscous and non-Newtonian liquids are involved which normally exhibit a far more complex rheological structure and change the hydrodynamic conditions drastically. For instance, fermentation broths as well as polymer solutions usually display not only viscous and shear-thinning behavior but also elastic properties. Both viscosity and elasticity can dramatically change and control the overall gas and liquid flow pattern, as well as the hydrodynamics in general (Acharya & Ulbrecht, 1978). These effects are in direct relation to the inherently complex rheological properties of these types of liquids (S. B. Li, Ma, Zhu, Fu, & Li, 2012). Unfortunately, there is little consistent information available in the literature concerning the effect of elastic properties on the hydrodynamics of bubble columns (J. R. Liu, Zhu, Fu, Ma, & Li, 2013). One example is the effect of elasticity on the mass transfer coefficient. Hecht et al. (Hecht, Voigt, & Schügerl, 1980) and Schumpe and Dechwer (Schumpe & Deckwer, 1987) reported that the volumetric mass transfer coefficient increases with higher liquid elasticity, whereas Nakanoh and Yoshida (Nakanoh & Yoshida, 1980) and Moo-Young and Kawase (Moo-Young & Kawase, 1987) saw an adverse influence of elasticity. Therefore, with all these gaps in the literature, it seems necessary to accumulate more knowledge about the effect of non-Newtonian liquids, and, in

particular, the effect of elasticity on the hydrodynamics and, hence, on the design, operation and performance of bubble column reactors.

To experimentally investigate the effect of rheological properties in this work, choosing the right liquids is very crucial. The operating liquids should be selected in a way to simulate as closely as possible the rheological behavior of the media that are being processed for example in fermentation, biological, and other processes. As previously mentioned, shear-thinning non-Newtonian liquids are the most common type of non-Newtonian fluids, characterized by a decreasing apparent viscosity with an increasing shear rate. This category of non-Newtonian fluids is also widely used in industry. As some typical non-Newtonian fluids, shear-thinning Carboxy Methyl Cellulose (CMC) and Xanthan gum solutions can model various types of non-Newtonian liquids applied in many industries (S. B. Li, Ma, Fu, Zhu, & Li, 2012). It was reported by Vatai and Tekić (Vatai & Tekić, 1989) that the rheological behaviour of many fermentation and microbiological media can be satisfactorily simulated by the aqueous solutions of CMC. Xanthan gum solution is also used as the model fluid in many experimental studies and has a wide application as a thickener in the food industry. Although both CMC and Xanthan gum solutions are viscoelastic in nature, Xanthan gum solutions behave quite differently by showing a weak gel behaviour (Lakota, 2007). Moreover, Newtonian Glucose solutions are widely used by researchers as viscosity-providing agents. The advantage of Glucose is that it shows a simple Newtonian behavior and, since it is a non-polar solute, it shows a negligible surface activity (Ruzicka, Drahos, Mena, & Teixeira, 2003). Taking this into consideration, the solutions employed in this study were selected in a way to satisfy all the above-mentioned requirements.

2.3 Hydrodynamic aspects of bubble columns

The performance of bubble column reactors is a complicated function of many variables and phenomena. Figure 2-2 illustrates some of the important parameters and phenomena affecting the performance and efficiency of bubble columns.

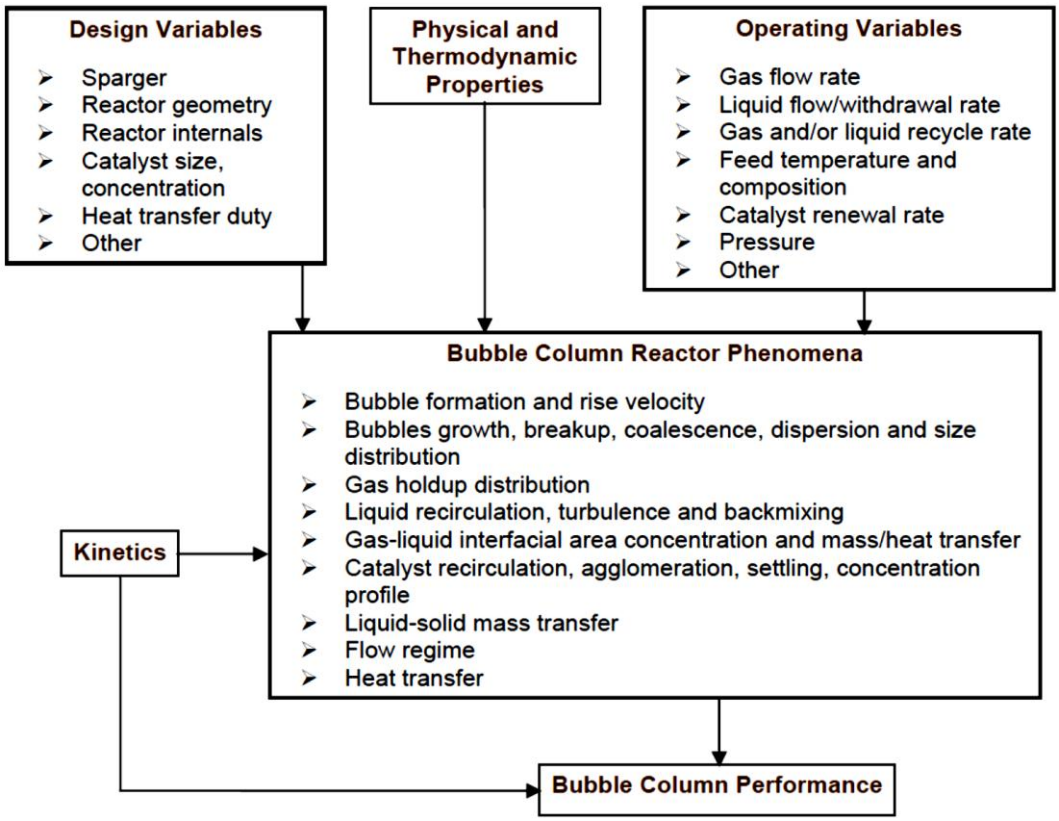

Figure 2-2: Variables and phenomena affecting the performance of bubble columns (P. Chen, 2004).

In bubble columns, the gas phase in the form of bubbles moves in the continuous liquid phase and, accordingly, a satisfactory understanding of the hydrodynamics of gas phase is essential. These are some of the main hydrodynamic parameters and phenomena that play important roles in the accurate design, scale-up, and optimum operation of bubble columns: gas holdup, operating regimes and their transition points, bubble shape and size, bubble rise velocity, bubble-related phenomena such as coalescence and breakage, liquid phase recirculation and mixing, axial dispersion, and volumetric mass transfer coefficient. Moreover, these parameters and phenomena are significantly affected by operating variables such as gas and liquid flow rates, operating pressure and temperature, and liquid and solid physical properties, to name a few.

The hydrodynamic parameters of bubble columns are inherently dependant on each other. Gas holdup, defined as the volume fraction of gas in a given volume of gas-liquid/gas-liquid-solid dispersion, significantly affects the design of bubble columns, since the total volume of the reactor

depends on the maximum gas holdup that must be accommodated. Gas holdup, along with bubble size, defines the interfacial surface area available for mass transfer and reaction. Therefore, it is obvious that the characteristics of a single bubble as well as those of the bubble swarm directly influence the performance and size of the bubble column, which is going to be used for carrying out a diverse range of industrially important processes (Y. T. Shah, Kelkar, Godbole, & Deckwer, 1982). Bubble size and rise velocity is mainly controlled by coalescence and breakup mechanisms. Bubble coalescence and breakup rate is also fundamentally related to the bubbles' geometrical characteristics, how they approach, contact, and interact with each other, and the physical properties of liquid phase. If a bubble enters in the wake of another one under the right conditions, the two bubbles may make contact and coalesce (R. P. Chhabra). In fact, a wake-induced collision can result in coalescence when a pair of large cap bubbles are moving in a liquid that is enough viscous to keep their wakes laminar. However, coalescence may not happen in low-viscosity media. The turbulent wake behind bubbles in low-viscosity liquids is relatively chaotic and intermittent, which imposes a stronger influence than the laminar one in viscous liquids that can diminish the bubble coalescence. Moreover, it is reported that small spherical or ellipsoidal bubbles have a tendency to repel each other unless under very specific conditions (Stewart, 1995). Although many studies have been dedicated to exploring the role of liquid phase rheology on bubble coalescence and breakup, the actual mechanism by which the rheology of the liquid phase influences bubble coalescence and/or breakup remains relatively unknown, as the models that describe bubble interactions are not based on real physical phenomena.

The gas-liquid mass transfer behavior in bubble columns is closely related to the gas holdup through various distinguished flow regimes, as shown in Figure 2-3, among which the homogeneous and heterogeneous flow regimes are the two that are the most industrially useful (Mena, Ruzicka, Rocha, Teixeira, & Drahoš, 2005). Homogeneous bubble flow is normally developed at low superficial gas velocities (U_g < 5 cm s^{-1}), characterized by minor bubble interactions, small bubbles, narrow bubble size distribution, uniform bubble size radial profile, and negligible bubble coalescence and breakup. The small bubbles in homogeneous flow are a few millimeters in diameter and are controlled mainly by the gas sparger and liquid properties. As the superficial gas velocity is increased, the flow becomes unstable, and is referred to as the transition regime, distinguished by the formation of bubble collides and distinct bubble classes. The transition regime may be observed only under certain column geometry and operating conditions. At higher

superficial gas velocities (U_g > 5 cm s^{-1}), small bubbles combine and form larger bubbles of a few centimeters in diameter, which leads to the heterogeneous (churn-turbulent) flow regime, characterized by bimodal bubble size distribution, non-uniform gas holdup radial profile, and liquid circulation. Moreover, the slug flow regime, characterized by bullet-shaped bubbles (extended over the whole column diameter), can be found only in small-diameter columns (D_C < 10 cm) and relatively high superficial gas velocities (Shaikh & Al-Dahhan, 2007).

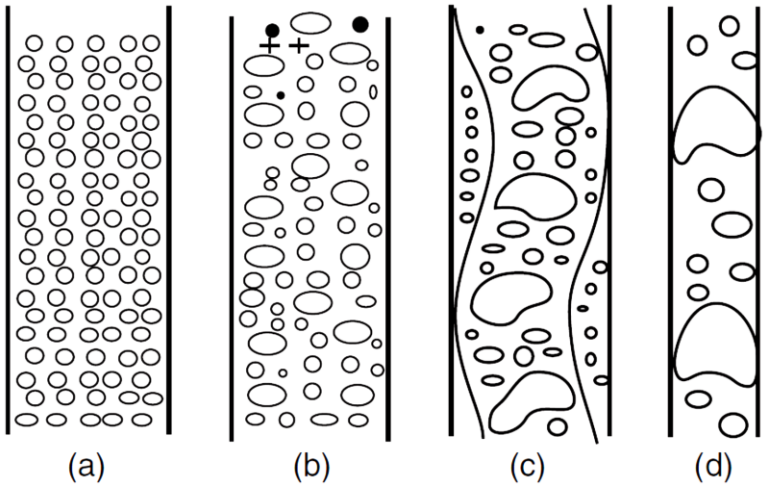

Figure 2-3: Various operating flow regimes in the bubble column reactors: (a) homogeneous; (b) transition; (c) heterogeneous; and (d) slug flow regime (Kantarci, Borak, & Ulgen, 2005).

A significant amount of research has been dedicated to studying the stability of the homogeneous flow regime, since certain biochemical processes require the calm environment and high mass transfer rate resulting from the small bubbles existing in this flow regime. However, the amount of gas throughput and mixing is inadequate in the homogeneous flow regime, which makes it non-applicable for most industrial applications that deal with large operating units and production rates. One of the conventional and accurate methods for characterizing the flow regime in bubble columns is through monitoring the change in the gas holdup with superficial gas velocity. A typical flow regime transition in terms of gas holdup as a function of superficial gas velocity is shown in Figure 2-4. At low gas flow rates, as the superficial gas velocity increases, more bubbles are formed at the gas distributor without significantly influencing bubble size or bubble size distribution. Accordingly, the gas holdup increases almost linearly in this condition. On the other hand, due to

the intense non-linear bubble interactions at higher superficial gas velocities, the increase in the gas holdup with superficial gas velocity is slower and deviates from linearity (R Krishna, Ellenberger, & Hennephof, 1993; Shaikh & Al-Dahhan, 2007). If the gas is distributed in a very good way, the regime transition point (U_{trans}) can be identified by the change in the slope of the gas holdup curve.

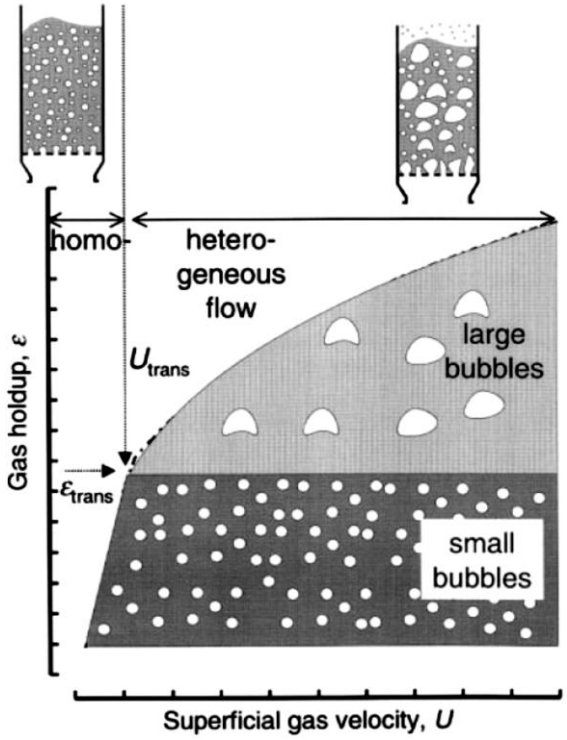

Figure 2-4: Homogeneous and churn-turbulent flow regimes in a gas-liquid bubble column (R. Krishna & Sie, 2000).

The gas holdup and, accordingly, the flow regime transition point are strongly affected by operating conditions and liquid and solid properties. Figure 2-5 schematically exhibits the effect of operating pressure and solid phase properties on the gas holdup and flow regime transition. As can been seen from Figure 2-5, the regime transition point shifts to higher superficial gas velocities at higher pressures. However, although the gas holdup changes according to the catalyst particle wettability, the regime transition seems to be independent of the catalyst's surface properties. It is worth mentioning that an increase in the superficial liquid velocity (in the case of bubble columns

operating with a continuous liquid phase) also shifts the regime transition point to higher gas velocities (De Lasa et al., 1992).

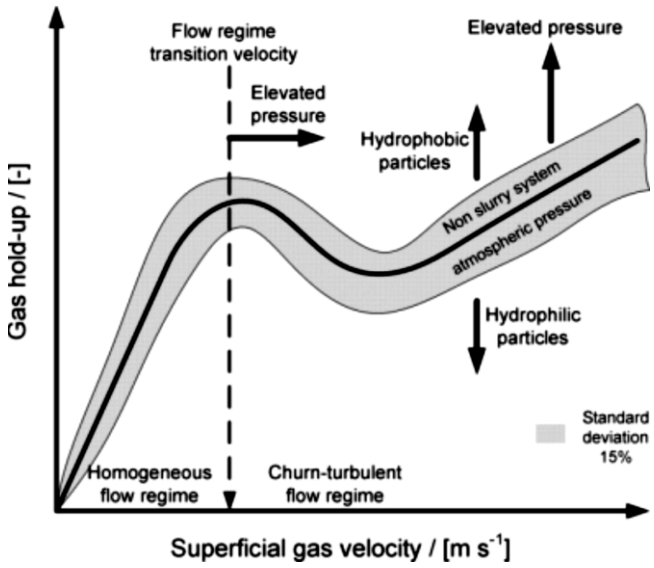

Figure 2-5: Schematic representing the gas holdup as a function of various parameters in slurry bubble column reactors (Vertical arrows: trends in gas hold-up profiles. Horizontal arrow: regime transition velocity trend) (Vinit P Chilekar et al., 2010).

At relatively high gas velocities, the rising bubbles drag liquid upwards in their wake and even between them (in swarms). Due to the difference in the density between the gas and liquid and radially non-uniform gas holdup profile at high gas flow rates, this liquid has to flow down again, which results in developing liquid recirculation patterns in the column. The liquid recirculation strongly affects the mixing in the column and is a function of column geometry, the design of the distributor and internals, and the physical properties of the operating phases. Various liquid recirculation patterns have been proposed by different researchers, as depicted in Figure 2-6. For example, Joshi and Sharma's model describes the flow pattern in a bubble column as a stack of donut-shaped circulation cells (Figure 2-6b), while Zehner's model proposes symmetric circulation cells that span the total column diameter in the bubble columns (Figure 2-6e) (Groen, Oldeman, Mudde, & Van Den Akker, 1996).

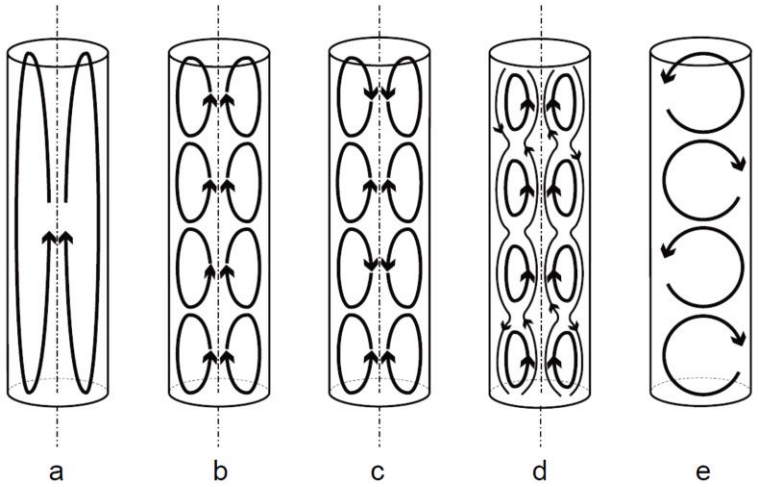

Figure 2-6: Various liquid recirculation patterns in bubble columns reported by researchers: (a) overall liquid circulation pattern; (b) the "donut" model of Joshi and Sharma; (c) counterrotating donuts as proposed by Van Den Akker and Rietema; (d) the interacting donut model from Joshi and Sharma; and (e) the non-symmetric circulation cell model from Zehner (Groen, 2004).

The design of bubble column reactors is a challenging task due to the fact that some important hydrodynamic parameters change with the reactor diameter, and, to a smaller extent, with the column height. Akita and Yoshida (Akita & Yoshida, 1974) pointed out that at a given superficial gas velocity, the average bubble size decreases as the diameter of column increases. It was also reported that with an increasing column diameter, the wall effects on the bubble rise velocity is obvious only in bubble columns operating with viscous liquids. The effect of column diameter on the gas holdup is small except for small-diameter columns. The volumetric mass transfer coefficient also does not change significantly with the column diameter (Eickenbusch, Brunn, & Schumpe, 1995). The choice of gas distributor, and its design, is also critical for mass transfer and, accordingly, the performance of bubble columns. The simplest possibility for sparging the gas is using static spargers such as perforated plates or sintered plates. Both perforated and sintered distributors are commonly used for many kinds of gas-liquid and gas-solid contactors. Sintered plates are suitable for producing small gas bubbles and homogeneous bubble distributions across the entire column cross-section.

Since the current work is aimed mainly at investigating the effects of liquid phase properties and operating pressure on the hydrodynamics of the bubble column, these two subjects are discussed in detail in the following subsections.

2.3.1 Effect of liquid phase properties on hydrodynamics

In a gas-liquid two-phase bubble column, physical properties of the two phases exert varying levels of influence on the hydrodynamic parameters of bubble column reactors, such as gas holdup, bubble size, bubble rise velocity, etc. Among the various physical properties of the liquid phase, liquid viscosity has received more attention in hydrodynamic studies of bubble columns. However, a large amount of work reported previously is based on air-water systems since they are non-toxic and easy to handle, whereas for the chemical industry, this system is only of limited use. Commercial chemistry uses organic solvents more than any other, and most of the reactions are performed under pressure and/or at high temperatures, conditions in which the viscosity of the liquid changes.

Over the last few years, several studies have been dedicated to investigating the effect of liquid viscosity on bubble behavior and the performance of bubble columns. The behaviour of moving bubbles in bubble columns inevitably becomes restricted with increasing liquid viscosity. Viscosity is thus proposed to alter the hydrodynamics according to several mechanisms that influence the formation, coalescence and/or breakup of the bubbles. Bubble coalescence is promoted and, consequently, larger bubbles are formed at higher liquid viscosities (Bukur & Patel, 1989; Godbole, Honath, & Shah, 1982; Gupta et al., 2009). Based on the envisaged application, bubble coalescence may be desirable (to promote separation, for example) or unfavourable (as in chemical reactors where it is desirable to have high interfacial surface area) in the process.

Larger bubbles in viscous liquids rise more quickly and have shorter residence time, resulting in a decrease in the gas holdup (L. S. Fan, Yang, Lee, Tsuchiya, & Luo, 1999). Due to the formation of larger bubbles and decreased gas holdup in viscous liquids, the interfacial surface area also decreases. Moreover, since the larger bubbles have a shorter residence time compared to smaller ones, the portion of smaller bubbles in the population may increase at higher liquid viscosities and thus the small bubble holdup increases with viscosity (Clarke & Correia, 2008). It is also reported

that the temporal increase in the holdup due to the accumulation of small bubbles obeys a first-order kinetics (Sheikhi, Sotudeh-Gharebagh, Zarghami, Mostoufi, & Alfi, 2013). In fact, in highly viscous liquids, the bubble polydispersity turns into a virtual bidispersity, and the bubble population dynamics becomes important. Roughly, a bimodal population includes small (less than 1 mm) and large (above 20 mm) bubbles. The bed establishment time in low-viscosity liquids is virtually zero, while it can take even more than an hour in high-viscosity liquids, where bubble population dynamics is more important (Y. T. Shah et al., 1982).

The effect of viscosity of aqueous Saccharose solutions on gas holdup and flow regime transition was investigated by Zahradnik et al. (Zahradnik et al., 1997) in a bubble column equipped with a perforated plate gas sparger. They found that by increasing the liquid viscosity, the gas holdup decreases remarkably. Moreover, with low-viscosity liquids, they observed a maximum in the gas holdup appearing at relatively low gas velocities, while it disappears at high-viscosity liquids. They attributed this phenomenon to the existence of a homogeneous flow regime at low superficial gas velocities, and the maximum point is considered the point at which the transition to the heterogeneous flow regime occurs. It is worth mentioning that the effect of viscosity on gas holdup may be compensated by adding surfactants or coalescence hindering liquids (e.g., alcohols, electrolytes, and inorganic salts) that tend to increase the gas holdup (Ruzicka et al., 2003).

Yifeng et al. (Yifeng et al., 2008) pointed out that the influence of liquid properties on gas holdup is small in the homogeneous flow regime. According to Godbole et al. (Godbole et al., 1982) and Shaikh and Al-Dahhan (Shaikh & Al-Dahhan, 2007), the formation of large bubbles in a highly viscous medium causes heterogeneous flow to occur at smaller superficial gas velocities. Fan et al. (L. S. Fan et al., 1999) showed that the bubbles rise with higher velocity in liquids with higher viscosity while Yifeng et al. (Yifeng et al., 2008) stated that the bubble rise velocity decreases as the viscosity of liquid increases. It has also been reported by Eickenbush et al. (Eickenbusch et al., 1995) that in bubble columns operating with highly viscous media, the formation of large slug-like bubbles intensifies liquid mixing, however, Yifeng et al. (Yifeng et al., 2008) reported that the liquid axial backmixing is suppressed at higher liquid viscosity. Schäfer et al. (Schafer, Merten, & Eigenberger, 2002) also found that by increasing viscosity, liquid turbulence reduces and, consequently, liquid eddies obtain less energy.

Alvarez et al. (Alvarez, Correa, Navaza, & Riverol, 2001) studied the volumetric mass transfer coefficient in carbon dioxide absorption for several Newtonian sucrose and non-Newtonian CMC solutions in a bubble column reactor. They observed that the mass transfer coefficient decreases by increasing the concentration of sucrose, which is attributed to an increasing viscosity of solution at higher sucrose concentrations. They also showed that at high gas flow rates, the mass transfer coefficient of non-Newtonian CMC solutions increases. They reported that high gas flow rates can create a higher average shear rate inside the column, so the apparent viscosity of shear-thinning CMC solutions decreases in such conditions. This decrease in viscosity leads to a higher diffusivity of carbon dioxide and, accordingly, a higher mass transfer coefficient. Similar results were also reported by Li et al. (S. B. Li, Zhu, Fu, & Ma, 2012). Oxygen transfer in viscous media with yield stress was investigated by Terasaka and Shibata (K. Terasaka & Shibata, 2003) in a bubble column reactor. They indicated that as a consequence of yield stress, the small bubbles do not completely disengage from the system and remain stagnant in the liquid. However, they showed that the yield stress does not have a significant influence on the escapable gas holdup in the slug flow regime. Guy et al. (Guy et al., 1986) studied power consumption, mixing time, liquid circulation time, and gas holdup in a bubble column operating with different Newtonian (water and glycerol) and non-Newtonian (CMC and Polyacrylamide) solutions. They pointed out that in similar conditions, an increase in the viscosity, elasticity, and shear-thinning properties of the liquid decreases mixing efficiency. Also, they have shown that the gas holdup increases as the elasticity of the liquid increases, while it is slightly influenced by the viscosity of liquid. It is reasonable to expect that some phenomena such as bubble coalescence and breakup would be significantly affected by the rheological complexities of the liquid phase (H. Z. Li, Mouline, & Midoux, 2002). However, only a few investigations into the coalescence and breakup of bubbles in non-Newtonian liquids have so far been reported in the literature (R. P. Chhabra, 2006). A summary of the effects of liquid phase properties on different hydrodynamic aspects of bubble columns is given in Table 2-4 (Vinit P Chilekar et al., 2010; L. S. Fan et al., 1999; Gomez-Diaz, Navaza, Quintans-Riveiro, & Sanjurjo, 2009; Hashemi, Macchi, & Servio, 2009; Lakota, 2007; Lau, Peng, Velazquez-Vargas, Yang, & Fan, 2004; Sulaymon & Mohammed, 2010; Urseanu, Guit, Stankiewicz, van Kranenburg, & Lommen, 2003; Waghmare, Rice, & Knopf, 2008; Yang & Fan, 2003; Yifeng et al., 2008).

Table 2-4: Summarized results of liquid properties effects.

Authors	System	Operating Conditions	Observed effects
Fan et al. (1999)	Paratherm NF heat-transfer fluids/ Nitrogen/ Glass beads	P = 0.1 – 19.4 MPa T = 27 – 78 °C U_g = 0 - 36 cm s^{-1}	• Bubble rise velocity increases with viscosity.
Urseanu et al. (2003)	Glucose solutions/ Tellus oil/ Nitrogen	P = 5.6 MPa T = 28 – 78 °C U_g = 0 – 30 cm s^{-1}	• The gas holdup decreases with the liquid viscosity.
Yang et al. (2003)	Paratherm NF heat-transfer fluids/ water/ Air	P = 0.1 – 10.3 MPa T = 27 °C U_g = 0 - 40 cm s^{-1} U_l = 0 - 1 cm s^{-1}	• Liquid axial dispersion coefficient is higher in water system than in the Paratherm system.
Lau et al. (2004)	Paratherm NF heat-transfer fluids/ Nitrogen/ air	P = 0.1 – 4.24 MPa T = 25 – 92 °C U_g = 0 - 40 cm s^{-1}	• k_La is higher in water system than in the Paratherm system (Bubble size).
Lakota (2007)	Water / CMC & Xanthan solutions Air	P= Ambient T= Ambient U_g = 1.8 – 25.2 cm s^{-1} U_l = 0 – 24.8 cm s^{-1}	• The measured gas holdup decreases with increasing effective liquid viscosity.
Yifeng et al. (2008)	Paraffins / Water / K_2CO_3 solutions Air	P= Ambient T= Ambient U_g= 0 - 20 cm s^{-1}	• Increase of liquid viscosity will weaken gas axial backmixing. • With increasing liquid viscosity, bubble rise velocity decreases. • Increase of surface tension leads to lower flow regime transition point and higher overall gas holdup.
Waghmare et al. (2008)	CMC solutions Air	P=Ambient T=25 °C U_g = 0.5 – 1.5 cm s^{-1}	• k_la decreases with the liquid phase viscosity.
Hashemi et al. (2009)	Water Air Resin particles	P= 0.1-4 MPa T= 2-22 °C U_l = 2.5 –20 cm s^{-1}	• The effect of solid concentration was not noticeable in the experimental range investigated.
Gomez-Diaz et al. (2009)	Aqueous solutions of k-carrageenan/ Carbon dioxide	P= 0.1 MPa T=25 °C U_g = 0.13 – 0.21 cm s^{-1}	• k_la decreases with liquid phase viscosity (Polymer concentration). • Gas–liquid specific interfacial area (*a*) decreases with liquid phase viscosity.
Chilekar et al. (2010)	Demineralized water/ Isopar-M oil/ Nitrogen/Air Carbon /Silica particles	P= 0.1-1.3 MPa T = 19 – 23 °C U_g = 0 - 40 cm s^{-1}	• Gas holdup and the flow regime transition point are not influenced by the presence of lyophilic particles at low slurry concentrations up to 3 vol. %. • Interstitial liquid velocity increases by increasing slurry concentration (viscosity).
Sulaymon et al. (2010)	Kerosene solutions/ Air	P= Ambient T= Ambient U_g= 1.09-2.6 cm s^{-1}	• The removal rate of emulsified kerosene decreases with increasing liquid phase viscosity. • The bubble diameter increases by increasing viscosity of liquid phase. • Air holdup decreases by increasing the viscosity of liquid phase.

As already mentioned, a variety of non-Newtonian liquids show elastic properties, but the actual effect of elasticity on bubble coalescence or breakup is not well recognized. In general, elasticity reduces the overall coalescence rate, but its effect becomes more complex when it acts together with viscosity in viscoelastic and shear-thinning solutions (Moo-Young & Kawase, 1987). Although there is some experimental research dedicated to studying the elastic effects on bubble dynamics, their focus is mainly on the behavior of a single bubble moving in a stagnant liquid. However, studies about elastic effects in systems like bubble columns (where a swarm of bubbles are present instead of a single bubble) are still very scarce. The influence of liquid phase rheology on the hydrodynamics of bubble columns will be discussed in more detail in Chapters 3 and 4.

2.3.2 Effect of operating pressure on hydrodynamics

As already explained, many processes in bubble columns are conducted at high pressure and temperature, which conditions can have significant and complex influences on bubble dynamics, multiphase flow, and mass and heat transfer behaviors. Table 2-5 summarizes some industrial applications of bubble columns at high pressures and high temperatures, as well as their typical operating conditions. To succeed in optimizing these processes, the effects of every parameter influencing selectivity and yield have to be accurately studied. A survey of the literature shows that the effect of operating pressure on many parameters has not been investigated thoroughly. There are only a few studies at high pressure (and much fewer at high temperature and high pressure), and, on the other hand, the hydrodynamic models and correlations developed under ambient conditions are not adequate for high-pressure bubble columns. In particular, in a bubble column, gas density is considerably affected by column pressure. Visual observation of the column reveals the formation of smaller bubbles when the pressure is increased, which is attributed to the increase in gas density at elevated pressures (Kemoun, Cheng Ong, Gupta, Al-Dahhan, & Dudukovic, 2001; Rados, Shaikh, & Al-Dahhan, 2005).

Table 2-5: Industrial applications of bubble columns.

Process	Temperature (℃)	Pressure (MPa)	Corresponding reference
Partial oxidation of ethylene to acetaldehyde	**130**	**0.3**	(W.-D. Deckwer, 1992)
Wet-air oxidation of sewage sludge	**200-300**	**4.0-12.0**	(W.-D. Deckwer, 1992)
Oxidation of cumene to phenol	**80-125**	**0.5-0.8**	(W.-D. Deckwer, 1992)
Hydrocilamine formation by hydrogenation	**50-60**	**2.5-3.0**	(W.-D. Deckwer, 1992)
Methanol synthesis:			
(1) BASF	**350-400**	**25.0-35.0**	(Wender, 1996)
(2) Eastman Chemicals, Air-Product, DOE	**220-250**	**5.0-10.0**	(Peng, Toseland, & Tijm, 1999)
Fischer-Tropsch synthesis	**220-270**	**0.1-4.0**	(Fox, 1990) (Jager & Espinoza, 1995)
Hydroformylation processes	**160-200**	**5.0-10.0**	(Wender, 1996)
Residuum hydrotreating	**300-425**	**5.5-21.0**	(Dautzenberg & De Deken, 1984)
Benzene hydrogenation	**180**	**5.0**	(W.-D. Deckwer, 1992)
Methanation	**350**	**6.8**	(Blum & Toman, 1977)
Coal gasification	**980**	**3.0**	(Yosim & Barclay, 1981)

Deckwer et al. (Wolf-Dieter Deckwer, Louisi, Zaidi, & Ralek, 1980) and Kölbel et al. (Kölbel, Borchers, & Langemann, 1961) found that the gas holdup in the bubble column is not affected by operating pressure in the range of 0.1-1.1 MPa, and in superficial gas velocities less than 3 cm s^{-1}. Pohorecki et al. (Pohorecki, Moniuk, Zdrójkowski, & Bielski, 2001) reported that operating pressure has no effect on gas holdup and mean bubble diameter in a bubble column at low superficial gas velocities. Luo et al. (Luo, Lee, Lau, Yang, & Fan, 1999) studied the pressure effects on the gas holdup and bubble size in slurry bubble columns operating with Paratherm NF heat transfer fluid as the liquid phase. Their results show that at relatively high superficial gas velocities

($U_g \geq 6$ cm s^{-1}), the gas holdup increases with pressure, and the pressure effect is more pronounced in slurries with a higher solid concentration. On the other hand, the measurement of bubble size distribution shows that the maximum stable bubble size was significantly smaller at elevated pressures in comparison with that at ambient pressure. They attributed this phenomenon to an increase in the gas inertia and a decrease in the gas-liquid surface tension at elevated pressures. The same effect of pressure on gas holdup at high superficial gas velocities was observed by Kemoun et al. (Kemoun et al., 2001) and Fan et al. (L. S. Fan et al., 1999).

Yang et al. (Yang, Luo, Lau, & Fan, 2000) experimentally and analytically investigated heat transfer phenomena in a high-pressure slurry bubble column operating with Paratherm NF heat transfer fluid. They pointed out that the time-averaged heat transfer coefficient decreases with increasing pressure, which is attributed to variations in the physical properties of the liquid phase, bubble size, and gas holdup at elevated pressures. Behkish et al. (Arsam Behkish, Men, Inga, & Morsi, 2002) studied the volumetric liquid-phase mass transfer coefficient (k_La) and bubble size distribution in a slurry bubble column reactor. They reported that k_La increases with pressure, which is attributed to a decrease in bubble size, and, consequently, an increase in the interfacial area at higher pressures. Similar results on the effect of operating pressure on k_La were obtained by Lau et al. (Lau et al., 2004), who reported that the effect of pressure on k_La is more pronounced in the churn-turbulent flow regime than the bubbling flow regime. The liquid phase axial dispersion coefficient was also measured by Yang and Fan (Yang & Fan, 2003) in bubble columns at high pressures. They found that the axial dispersion coefficient decreases as system pressure increases, which is attributed to the smaller bubble size and lower bubble rise velocity at elevated pressures.

Rados et al. (Rados et al., 2005) studied the effect of operating pressure on gas and solid phase holdup in a slurry bubble column and found that although gas holdup is significantly affected by system pressure, the solid phase holdup slightly increases as pressure is increased. They also investigated the influence of pressure on solid phase velocity and shear stress by means of the Computer Automated Radio Particle Tracking (CARPT) technique, reporting that the average solid axial velocity and shear stress increases with an increase in the pressure. Moreover, Fan et al. (L. S. Fan et al., 1999) investigated the combined effect of pressure and viscosity on the hydrodynamics of bubble columns. They found that the effect of pressure is reduced as the liquid viscosity increases.

The influence of operating pressure on the different hydrodynamic aspects of bubble columns will be reviewed in detail in Chapter 6. Furthermore, the effect of pressure on the hydrodynamics and performance of bubble columns operating with non-Newtonian liquids have not yet been investigated and, thus, performing an accurate and complete research at these conditions will provide invaluable insight into how pressure affects the reactor performance in the presence of non-Newtonian liquids. In this regard, the final objective of the present study is dedicated to studying the effect of pressure on the global hydrodynamics of a bubble column operating with non-Newtonian liquids. For this purpose, a high pressure-high temperature (HP-HT) multiphase reactors unit (including a HP-HT bubble column reactor and a HP-HT fluidized bed reactor) has been designed and constructed at École Polytechnique de Montréal; a description of the unit is given in Chapter 5.

2.3.3 Measurement techniques

A complete understanding of the hydrodynamics and multiphase flow structure in bubble column reactors seeks to apply various highly resolved measurement techniques which are capable of non-destructively probing the properties of all operating phases inside the column. Over the past few decades, a variety of experimental techniques have been developed to characterize multiphase contactors and, in particular, bubble column reactors. The available techniques can be classified into intrusive and non-intrusive ones. Intrusive techniques include impedance (conductivity or resistivity) probes, optical fiber probes, ultrasound probes, endoscopic probes, hot film anemometry, etc. Invasive probes are quite effective if the flow in an opaque vessel needs to be described. They can easily capture local hydrodynamics across a wide range of operating conditions. Beside the difficulties related to the use of every method, the major disadvantage of intrusive techniques is that they must be inserted into the reactor and, thus, interact with the flow field and disturb the dynamics of the operating phases. Therefore, to overcome the drawbacks of intrusive methods, developing reliable non-intrusive techniques is essential. The main advantage of non-intrusive techniques is that there is no measurement interference with the flow field. However, in comparison with intrusive techniques, non-intrusive techniques are relatively expensive (Mueller, 2009).

Non-intrusive techniques used to characterize multiphase flow properties include pressure transducers (differential and dynamic), visualization techniques, particle image velocimetry (PIV), X-ray tomography, γ-ray densitometry, positron emission tomography (PET), radioactive particle tracking (RPT), electrical impedance tomography (EIT), electrical capacitance tomography (ECT), ultrasonic tomography, nuclear magnetic resonance imaging (NMR), laser techniques, etc. Direct visualization is a useful method, but it is limited by the opacity of the system. Another weakness of the visualization techniques is that three-dimensional systems are treated as two-dimensional ones by this method. Hence, the direct visualization method provides only limited information regarding phenomena occurring in multiphase systems.

X-ray computer assisted tomography (CAT) and X-ray-based particle tracking velocimetry (XPTV) can also provide valuable information about local solids velocity, bubble shape, bubble size, bubble rise velocity, bubble growth and bubble breakage in gas-solid or gas-liquid-solid contactors. Non-intrusive laser techniques are also widely used to study bubble behavior. Laser techniques include laser Doppler anemometry (LDA), phase Doppler anemometry (PDA), and laser Doppler velocimetry (LDV). Several phase characteristics can be deduced from laser techniques such as bubble size distribution, liquid velocity and turbulence, velocity and holdup of gas and solid phases. However, laser techniques are limited only to low gas holdup conditions since the laser beam needs to penetrate inside the system.

In addition, positron emission tomography (PET), radioactive particle tracking (RPT), ultrasonic tomography, nuclear magnetic resonance imaging (NMR/MRI), electrical impedance tomography (EIT), and electrical capacitance tomography (ECT) are widely used for tracking particle movement and mapping instantaneous or time-averaged local and/or cross-sectional averaged phase holdups and velocities. The MRI technique has also been applied to the characterization of multiphase flow systems. Although it can provide higher spatial resolution with a relatively fast acquisition time, its relatively high cost and certain fluid property requirements limit its use as a process tomography technique. A summary of the measurement techniques used for characterizing different hydrodynamic aspects of bubble columns is given in Table 2-6. More information on this subject can be found elsewhere (Arsam Behkish, Lemoine, Sehabiague, Oukaci, & Morsi, 2007; H. Jin, Wang, & Williams, 2007; Jordan & Schumpe, 2001; Kemoun et al., 2001; Lau et al., 2004; Luo et al., 1999; Pohorecki, Moniuk, & Zdrójkowski, 1999; Rados et al., 2005; Y Soong, Gamwo,

Romanov, Dilmore, & Hedges, 2006; Vijayan, Schlaberg, & Wang, 2007; Yang & Fan, 2003; Yang et al., 2000).

Table 2-6: Summary of some measurement techniques for characterizing bubble column reactors.

Authors	Experimental technique	Operating Conditions	Measured parameters
Luo et al. (1999)	• Dynamic gas disengagement • PIV • Fiber-optic probe	P = 5.6 MPa T = 28 – 78 °C U_g = 0 – 45 cm s^{-1}	• Gas holdup and bubble size distribution • Flow characteristics • Average bubble size
Yang et al. (2000)	• Heat-transfer probe	P = 0.1 – 4.2 MPa T = 35 – 81 °C U_g = 0 – 20 cm s^{-1}	• Heat transfer coefficient
Kemoun et al. (2001)	• γ-ray based Computed Tomography	P = 0.1 – 0.7 MPa T = 20°C U_g = 2 – 18 cm s^{-1}	• Gas holdup
Pohorecki et al. (2001)	• Photographic technique	P = 0.2 – 1.1 MPa T = 30 – 160 °C U_g = 0.2 – 5.5 cm s^{-1} U_l = 0 – 1 cm s^{-1}	• Bubble size
Yang et al. (2003)	• Differential pressure transducer	P = 0.1 – 10.3 MPa T = 27 °C U_g = 0 – 40 cm s^{-1} U_l = 0 – 1 cm s^{-1}	• Gas holdup and axial liquid dispersion coefficient
Jordan et al. (2003)	• Dynamic gas disengagement	P = 0.1 – 4 MPa T = 20°C U_g = 1 – 20 cm s^{-1}	• Gas holdup
Lau et al. (2004)	• Oxygen desorption method	P = 0.1 – 4.24 MPa T = 25 – 92 °C U_g = 8 – 89 cm s^{-1}	• Volumetric mass-transfer coefficients
Rados et al. (2005)	• γ-radiation source CT • Froth height measurements • Computer Automated Radio Particle Tracking technique (CARPT)	P = 0.1 – 1 MPa T = 20°C U_g = 8 – 45 cm s^{-1}	• Gas holdup • Solids phase velocity and shear stress
Soong et al. (2006)	• Ultrasonic technique	P = 0.1 – 1.36 MPa T = 20 – 200 °C U_g = 0 – 11 cm s^{-1}	• Operating flow regime
Behkish et al. (2007)	• Dynamic gas disengagement • Photographic technique	P = 0.67 - 3 MPa T = 27 – 200 °C U_g = 7 – 39 cm s^{-1}	• Gas holdup, bubble size distribution, and bubble Sauter-mean diameter
Jin et al. (2007)	• Electrical resistance tomography • Dynamic gas disengagement	Ambient P & T U_g = 2 – 13 cm s^{-1}	• Bubble rise velocity and bubble size
Vijayan et al. (2007)	• Electrical resistance tomography	Ambient P & T U_g = 1 – 15 cm s^{-1}	• Void fraction wave to identify flow pattern

Before selecting a measurement technique to study a particular multiphase reactor, it is very important to have at least a qualitative image of the flow inside the vessel. Based on this, the best measurement technique can be chosen and implemented to gain an adequate quantitative flow description (Mueller, 2009). To evaluate hydrodynamic parameters and adequately understand the effect of non-Newtonian liquids in this study, it is essential to choose accurate experimental techniques. To meet these objectives, first, extensive rheological measurements are conducted to characterize the liquids which are going to be used in this work. Also, in order to investigate different hydrodynamic aspects of bubble column locally and globally, a series of pressure transducers and optical fiber probes are applied. A brief description of the measurement techniques used in this work is given below.

2.3.3.1 Rheological properties measurements

Newtonian liquids can be defined only by a single value of viscosity, while non-Newtonian liquids require more rheological parameters (material functions) to be set and measured. In the science of rheology, material functions are evaluated by means of a rheometer. In fact, a rheometer is a piece of laboratory equipment used to study the way in which a liquid, suspension or slurry flow responds to applied standard forces or deformations. In this work, all the rheological measurements are carried out using a modular rheometer (Physica MCR 501, Anton Paar Co.) with different types of geometry, including the cone and plate, concentric cylinder, and double gap setups. A schematic of different geometries used in this work is given Figure 2-7.

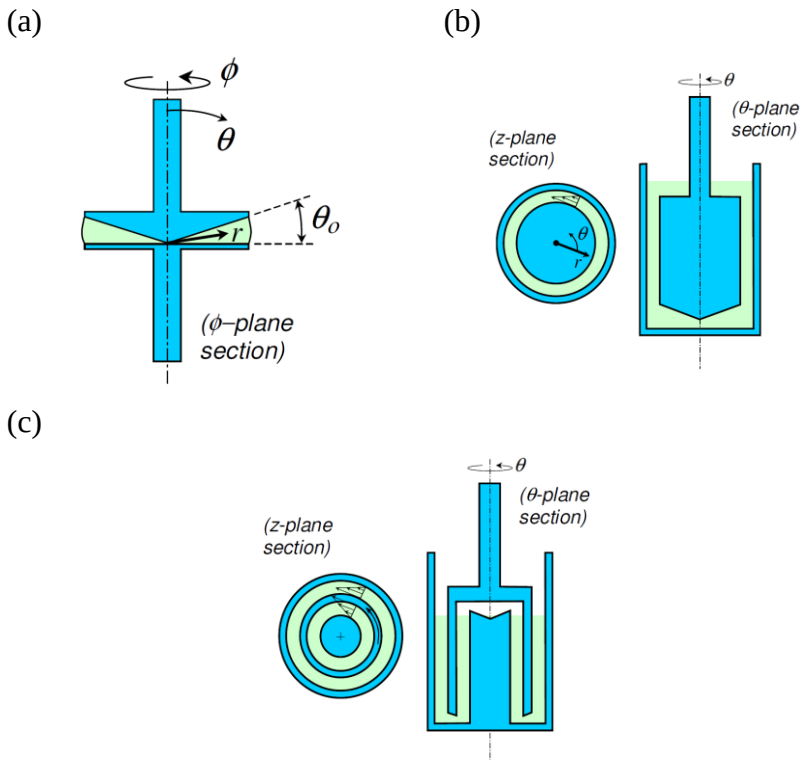

Figure 2-7: Schematic of different geometries used for rheolocial measurments: (a) cone and plate; (b) concentric cylinder; (c) double gap.

Among different standard flows, the simple steady-state and small-amplitude oscillatory shear flow are the most commonly used standard flows in rheological investigations of non-Newtonian fluids. A simple schematic of the aforementioned standard flows is shown in Figure 2-8. In the case of steady-state flow, the stress tensor is constant in time, and the viscosity and first normal stress difference are measured as follows (Morrison, 2001):

$$\mu(\dot{\gamma}) = \frac{-\tau_{21}}{\dot{\gamma}} \tag{2.4}$$

And:

$$N_1 = -(\tau_{11} - \tau_{22}) \tag{2.5}$$

As can be seen, the viscosity for any fluid subjected to steady-state shear flow can be defined as the ratio of the steady-state shear stress to the shear rate. The first normal stress difference is representative of the elastic nature of the fluids and is a function of existing normal stresses in the flow.

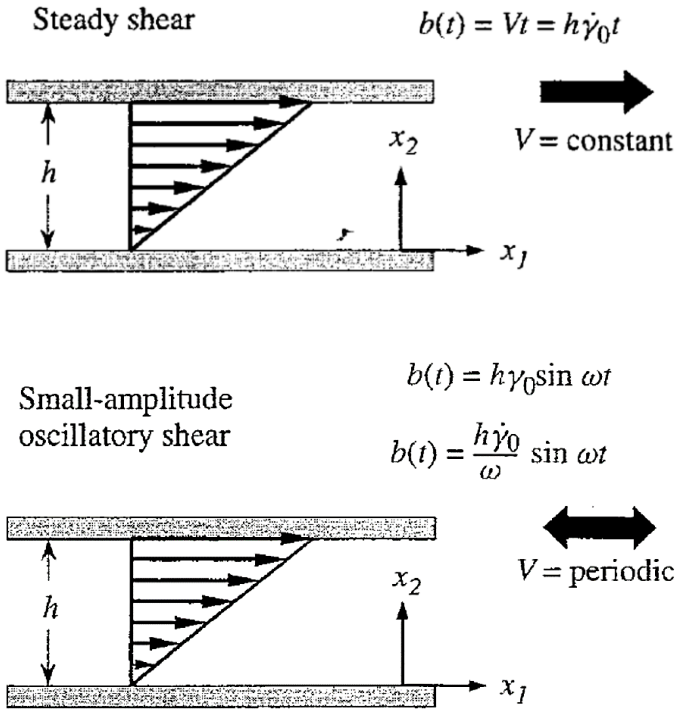

Figure 2-8: Schematic showing how steady-state and small-amplitude oscillatory shear flow are produced.

With the development of commercial rheogoniometers, the use of oscillatory methods in rheological characterization of materials has considerably increased. A general advantage of oscillatory tests is that a single instrument can cover a very wide range of frequency and this is essential when the material has a broad spectrum of relaxation times. The small-amplitude oscillatory shear (SAOS) measurement is widely used to characterize complex fluids by chemists, chemical engineers, and materials scientists. This type of flow can be obtained, for example, when a sample is strained in a periodic manner at low strain amplitude (see Figure 2-8). Accordingly, shear stress produced in this way will be a sine wave with the same frequency as the input strain wave; however, it will usually not be in phase with the input strain and can be written as follows:

$$-\tau_{21}(\omega) = \tau_0 \sin(\omega t + \delta) \tag{2.6}$$

Where δ is the phase difference between the strain wave and stress response, and ω is the frequency of oscillation. Although there are several material functions that can be obtained through the small-amplitude oscillatory shear measurement, the dynamic moduli are the most important ones. The storage and loss moduli can be defined as follows:

$$\frac{-\tau_{21}(\omega)}{\gamma_0} = G' \sin \omega t + G'' \cos \omega t \tag{2.7}$$

Storage modulus: $$G'(\omega) = \frac{\tau_0}{\gamma_0} \cos \delta \tag{2.8}$$

Loss modulus: $$G''(\omega) = \frac{\tau_0}{\gamma_0} \sin \delta \tag{2.9}$$

Where γ_0 is the strain amplitude. The storage modulus, G', is defined as the stress in phase with the strain in a sinusoidal shear deformation divided by strain. It is a measure of the energy stored and recovered per cycle and represents the elastic properties of fluid. The loss modulus, G'', is defined as the stress 90° out of phase with the strain divided by the strain. It is a measure of the energy dissipated or lost as heat per cycle of sinusoidal deformation and represents the viscous properties of fluid. For a Newtonian fluid in SAOS, the response is completely in phase with the strain (G'=0). For an elastic solid that follows Hooke's law (a Hookean solid), the shear-stress response in SAOS is completely in phase with the strain (G''=0). For viscoelastic fluids both G' and G'' are nonzero. More information on the rheological measurements of non-Newtonian liquids can be found elsewhere (Raj P Chhabra & Richardson, 2011; Ferry, 1980; Morrison, 2001).

2.3.3.2 Pressure Transducers

In bubble column reactors, the gas bubbles are first formed at the gas distributor. The bubbles then start to rise along the column height, coalescing and growing in size. The bubbles also drag the liquid, resulting in a global liquid recirculation inside the column. The bubbles eventually rupture

at the liquid surface. All the above-mentioned phenomena can generate either local or global pressure fluctuations in the column. The liquid velocity fluctuations caused by rising gas bubbles, large liquid eddies, and liquid turbulence and gas holdup fluctuations ceased by the passage of large bubbles can be considered the source of local pressure fluctuations. Bubble formation, coalescence, breakup, and eruption, oscillations of the gas-liquid suspension, and mechanical vibrations of the column are some of the sources of global pressure fluctuations. The measurement of pressure fluctuations inside the column is a relatively simple, inexpensive and non-intrusive measurement technique that has already been applied in most multiphase flow studies. In addition, the hydrodynamics of bubble columns has been investigated by analyzing wall pressure fluctuations by many researchers (Gourich et al., 2006; Kumar, Srinivasulu, Munshi, & Khanna, 2013; Lacroix, Aressy, & Carreau, 1997; T. J. Lin, Juang, & Chen, 2001; Park & Kim, 2001). However, one of the drawbacks of pressure fluctuation measurements is the complex output fluctuation signal generated by different pressure sources (V. P. Chilekar et al., 2005).

In order to measure pressure fluctuations, different types of pressure transducers (differential, absolute, and dynamic) are typically installed on the wall of the column along the axial direction. One of the most important hydrodynamic parameters of bubble columns that can be easily measured by differential pressure transducers is gas holdup. The local pressure fluctuations can be simply related to fluctuations of the gas holdup in a gas-liquid two-phase flow, according to the following equation:

$$\frac{dP}{dz} = \rho_G \varepsilon_g g + \rho_L \varepsilon_L g \tag{2.10}$$

Moreover, a variety of pressure signal processing methods and analyses can also be applied to characterize the hydrodynamic aspects of bubble columns. These analyses include statistical, spectral, chaos, Hurst, wavelet transform analysis, etc. Gourich et al. (Gourich et al., 2006), Kumar et al. (Kumar et al., 2013), Letzel et al. (Letzel, Schouten, Krishna, & van den Bleek, 1997) have performed statistical, spectral, and fractal analyses on the pressure fluctuation signals in order to identify flow regimes and their transition points in bubble columns reactors. Chilekar et al. (V. P. Chilekar et al., 2005) have also applied the spectral analysis of pressure fluctuations to estimate bubble size in slurry bubble columns. A summary of various measurements and analyses applied

to pressure signals is given in Figure 2-9. In this work, a series of differential and dynamic pressure transducers are applied to study the effects of liquid phase properties and operating pressure on the gas holdup, operating flow regimes, etc. The analyses and methods used to interpret the pressure signals are explained in detail in Chapter 3.

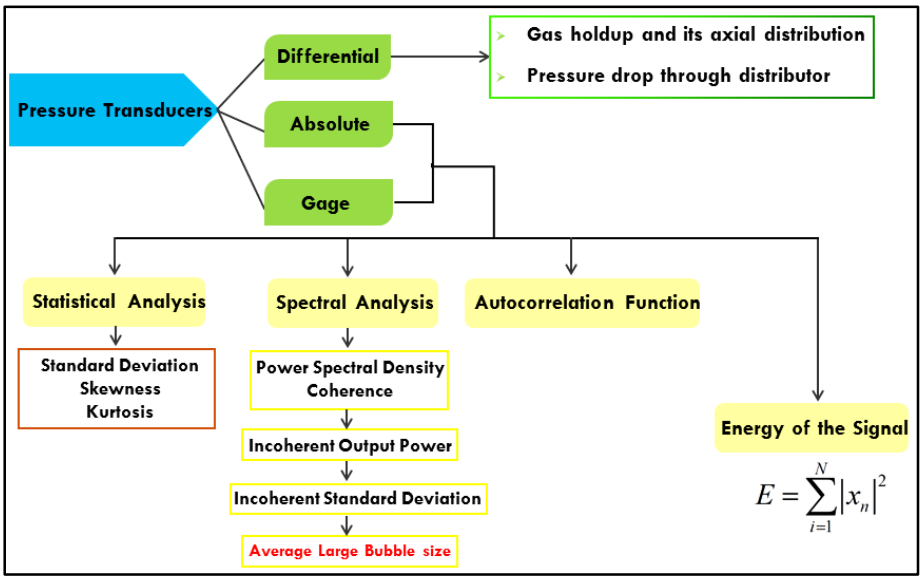

Figure 2-9: Various measurements and analyses caried out on the pressure signals.

2.3.3.3 Optical Fiber Probes

In order to investigate bubble dynamics in bubble column reactors, it is of great importance to use an inexpensive and reliable tool that can capture bubble size, bubble rise velocity, and interfacial area for bubbles from the micron scale of spherical shapes to the millimeter scale of ellipsoidal ones. Optical probes have been widely used for many purposes since the price of fiber optic cable dropped in the 1980s. Optical probes rely on the difference between the refractive indices of two fluids. A light is generated and sent to the system by means of emitting fibers and according to the refractive indices of the operating phases, a part of the light is reflected back and sent to an analyzer device. In a gas-liquid two-phase flow in bubble columns, due to the difference in the refractive indices of the gas and liquid phases, the projected light refracts when the probe tip is inside the bulk of liquid while it reflects back in the presence of gas bubble. The reflected light is then converted to voltage, and after amplification it is recorded in the form of crenel-type voltage

outputs as a function of time. Figure 2-10 displays the working principle of an optical fiber probe.

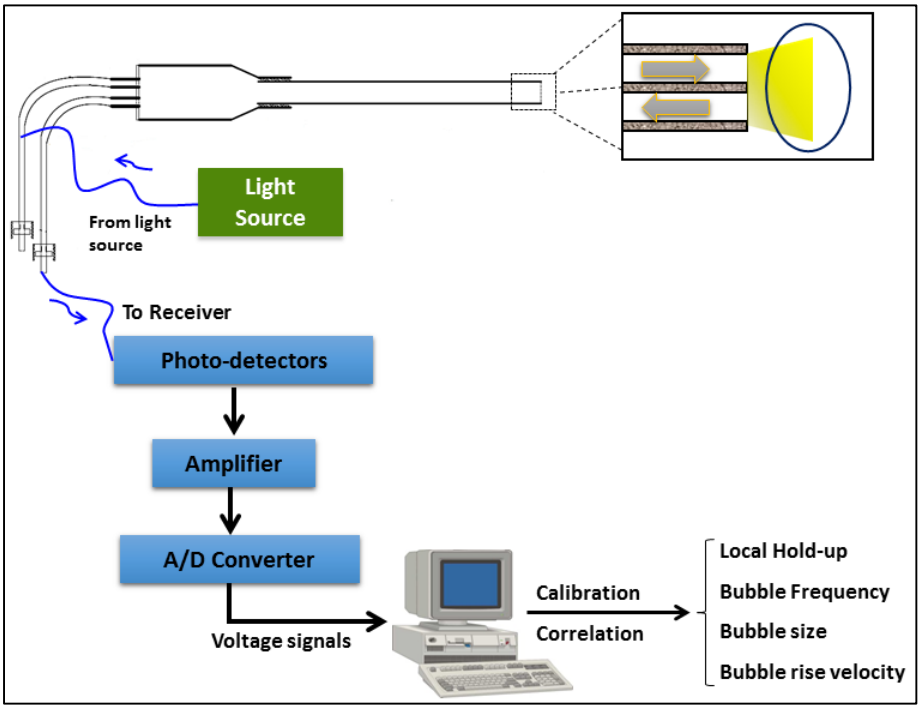

Figure 2-10: Working principle of optical fiber probes.

Optical fiber probes have some unique advantages over other types of probes (e.g., impedance probes). They are simple to use and can be used for opaque media enclosed by a non-transparent vessel, and in non-conductive liquids. Therefore, they can handle a wider range of liquids. The probe size can be as small as 50 μm, and it can also provide high sampling rates. They also do not require routine calibrations, have a better signal-to-noise ratio, and can be used at high-pressure and high-temperature conditions (for example, aluminum-jacketed fibers can operate at temperatures up to 400ºC). However, the main drawback of optical fiber probes is that the bare probe tip must be fully exposed to the flow and can thus disturb the flow and alter the hydrodynamics. The tip of an optical fiber probe is also very fragile and needs to be handled with care (Mueller, 2009). Optical fiber probes are used extensively to measure the local hydrodynamic parameters of bubble columns such as local gas holdup, bubble frequency, bubble size, and bubble rise velocity. The probe can be placed almost anywhere in the bed, thus allowing for the measurement of radial and axial distribution of the above-mentioned hydrodynamic parameters

(Chaumat, Billet-Duquenne, Augier, Mathieu, & Delmas, 2007). However, one of the disadvantages of optical probes in bubble columns is that once it contacts the bubbles, it can modify their shape or velocity; this should be taken into consideration during the interpretation of the results. It is also worth mentioning that optical probes give no information concerning the characteristics of the liquid phase (Magaud, Souhar, Wild, & Boisson, 2001).

In this work, two optical fiber probes are specially designed and fabricated to measure the local gas holdup, bubble frequency, bubble size, and bubble rise velocity and their radial and axial distributions in the bubble column operating with different Newtonian and non-Newtonian liquids. A picture of our in-house-made optical fiber probe is shown in Figure 2-11. It should be mentioned that measuring bubble dynamics in bubble columns has always been a challenging issue, particularly when the column is operating in chaotic heterogeneous regime, which is of industrial interest (Xue, 2004). It is essential to understand how the probe interacts with its environment at the scales of interest and to minimize any disturbing effect of the probe on the flow. The probe may pierce the bubble at different positions, and also bubbles are not always in an ideal spherical shape and these issues need to be taken into consideration when measuring bubble size using optical probes (Chabot, Lee, Soria, & de Lasa, 1992; Mueller, 2009; Saberi, Shakourzadeh, Bastoul, & Militzer, 1995). In measurements with optical fiber probes, several parameters can be adjusted in data acquisition and treatment steps, such as data acquisition frequency, the number of samples per sampling burst, and the number of series of measurements. Adjusting these parameters in their optimal values can lead to measuring a statistically meaningful average at each measurement location. The configuration of optical fiber probes and data treatment methods applied in this work are discussed in greater detail in Chapter 4.

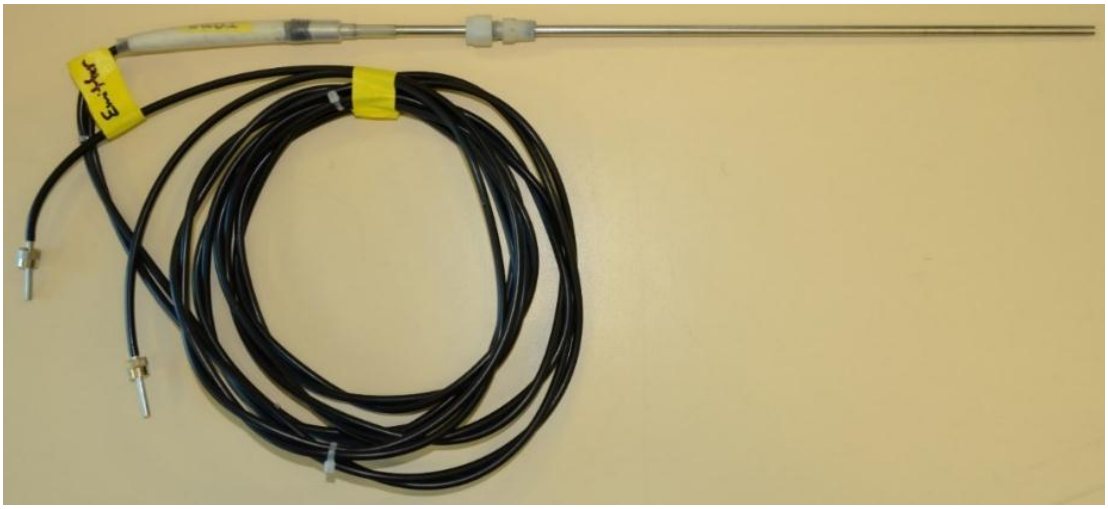

Figure 2-11: The in-house fabricated optical fiber probe used in this study.

CHAPTER 3

ARTICLE 1: THE EFFECTS OF LIQUID PHASE RHEOLOGY ON THE HYDRODYNAMICS OF A GAS-LIQUID BUBBLE COLUMN REACTOR

Amin Esmaeili, Christophe Guy, Jamal Chaouki

Department of Chemical Engineering, École Polytechnique de Montréal, P.O. Box 6079, St. C.V., Montreal, Qc, Canada H3C 3A7

Published in *Chemical Engineering Science* (Volume 129 (2015), Pages 193-207).

Abstract

In this study, the effects of liquid phase rheology on the hydrodynamics of a pilot scale bubble column reactor is extensively investigated by applying various types of test liquids with different rheological characteristics as the operating fluids. Two fiber optic probes and several pressure transducers are used and different time-domain and frequency-domain analyses are applied to perform a comprehensive interpretation of the pressure signals and measure the hydrodynamic parameters of the gas phase such as gas holdup and bubble size. A new approach is proposed based on the dynamic moduli of viscoelastic solutions to better understand the simultaneous viscous and elastic effects. It was observed that the elasticity of the operating liquid reduced the average bubble chord length and increased the total gas holdup. The obtained results reveal that although the viscosity is more favorable for coalescence, the elasticity of the operating liquid can prevent bubble coalescence by showing a solid-like behavior at the interface of two bubbles.

Keywords: Bubble column; Rheology; Hydrodynamics; Pressure fluctuations; Gas holdup; Viscoelastic fluids

3.1 Introduction

Bubble column reactors have a wide range of applications in processes based on the contact between gas and liquid phases, such as the Fischer-Tropsch (FT) synthesis, the liquid phase methanol synthesis (LPMeOH) and the hydroconversion of heavy oils and petroleum residues (Shaikh & Al-Dahhan, 2007; Sheikhi et al., 2013; Wang et al., 2007). These reactors have received a great deal of attention from both academia and industry over the last few decades since they offer excellent heat and mass transfer performance, low operating and maintenance costs because of the absence of moving parts, and are easy to operate (Gandhi et al., 1999; Kantarci et al., 2005; Y. T. Shah et al., 1982).

With the dramatic increase in the world energy demand and the appearance of a new generation of feedstocks, gas-liquid contactors and in particular bubble column reactors have become increasingly important. Although many liquids in industrial processes are low molecular weight and Newtonian-like fluids, an increasing number of high molecular weight solutions with complex internal structure and non-Newtonian behavior are being used in the fields of enhanced oil recovery, wastewater treatment, polymerization processes, and the production of foods and pharmaceuticals. Bubble behavior as the key hydrodynamic factor in bubble column reactors can drastically change in the presence of non-Newtonian fluids. While research on bubble columns is mainly focused on Newtonian fluids, it is of fundamental importance to understand the non-Newtonian effects on the behavior of bubbles and hydrodynamics.

Generally, increasing the liquid phase viscosity has been shown to decrease the total gas holdup and hinder the formation and stability of a homogeneous bubble bed. This negative effect is mainly ascribed to the existence of drag forces enhancing bubble coalescence in the gas sparger zone (Ruzicka et al., 2003; Urseanu et al., 2003; Zahradnik et al., 1997). Schafer et al. (Schafer et al., 2002) pointed out that the turbulence in the liquid phase diminishes by increasing the viscosity and consequently, the liquid eddies obtain less energy and bubble breakage decreases, which results in an increase in bubble size. Larger bubbles with wider bubble size distribution in a highly viscous medium cause the heterogeneous flow regime to appear at lower superficial gas velocities (Clarke & Correia, 2008; Gupta et al., 2009; Su et al., 2008). The negative effects of viscosity on the interfacial area have also been reported in several studies (Clarke & Correia, 2008).

The hydrodynamics of bubbles in non-Newtonian fluids is quite different from that in Newtonian fluids. Previous studies mostly considered Newtonian and non-Newtonian media with simple internal structure and rheological behavior. However, the non-Newtonian characteristics are responsible for a number of particular phenomena that are not observed in Newtonian fluids (Kawase et al., 1992; Kemiha et al., 2006). Gomez-Diaz et al. (Gomez-Diaz et al., 2009) showed that the gas-liquid interfacial area decreases as the viscosity of pseudoplastic *k*-carrageenan solutions increases. Majumder et al. (S. K. Majumder, Kundu, & Mukherjee, 2007) have reported a significant contribution of viscous forces to the bubble-liquid interfacial shear stress and a higher pressure drop in non-Newtonian solutions. Miura et al. (Miura, Katoh, & Kawase, 2012) have indicated that increasing the non-Newtonian properties of Carboxymethyl Cellulose (CMC) and Xanthan gum solutions reduce the gas holdup. Moo-Young and Kawase (Moo-Young & Kawase, 1987) showed that the bubble coalescence rate is higher in the shear-thinning CMC solutions compared to the viscoelastic Polyacrylamide (PAA) solutions. This has been attributed to the resistance effect of the viscoelastic fluid squeezed out between a pair of bubbles, resulting in a decrease of the coalescence rate and the formation of numerous fine bubbles with a long retention time in the PAA solution. On the other hand, it has also been reported that the solid-like properties of elastic liquids can diminish the bubble breakup rate and increase the average bubble size (Suh et al., 1991). Olivieri et al. (Olivieri, Russo, Simeone, Marzocchella, & Salatino, 2011) have investigated the effects of liquid properties on the hydrodynamics of a lab-scale bubble column reactor. Their results showed that the homogeneous flow regime is stabilized in non-Newtonian liquids having elastic properties and the regime transition velocity increases with liquid elasticity.

Due to the inherently complex nature of elasticity, the literature on the effects of elastic properties on the hydrodynamics of bubble columns is scarce and conflicting results have been reported. Therefore, there is still strong motivation to gain a better understanding of the detailed influence of fluid elasticity on hydrodynamics. The effects of increasing viscosity and elasticity on hydrodynamic parameters have been summarized in Table 3-1.

Table 3-1: Summary of the effects of increasing viscosity and elasticity on different hydrodynamic parameters

Parameter	ε_g	$U_{g,tran.}$	Bubble Coalescence	d_b	a
↑ **Viscosity**	↓	↓	↑	↑	↓
↑ **Elasticity**	?	↑	↓	?	?

↑: Increasing ↓: Decreasing ?: No trend reported

Several processing techniques have been developed and utilized to characterize the hydrodynamics of bubble column reactors, including particle image velocimetry, electrical resistance tomography, laser Doppler anemometry, bed vibration signature, optical fiber signals and pressure fluctuations (Alain Cartellier, 1992; Shaikh & Al-Dahhan, 2007; Sheikhi et al., 2013; Wild, Poncin, Li, & Olmos, 2003). Drahos et al. (Drahoš, Zahradník, Punčochář, Fialová, & Bradka, 1991) characterized three basic flow patterns in the bubble column using statistical analysis of pressure fluctuations in both time and frequency domains. They showed that the power spectrum of pressure fluctuations is a useful tool to identify different sources of the pressure fluctuations in the bubble column reactors. Al-Masry et al. (Al-Masry, Ali, & Al-Kalbani, 2007) and Gourich et al. (Gourich et al., 2006) identified the flow regime transition point by statistical and spectral analysis of the differential pressure signals. Barghi et al. (S. Barghi, A. Prakash, A. Margaritis, & M. Bergougnou, 2004) applied the statistical analysis of pressure fluctuation signals combined with gas holdup analysis to study the flow regime transition in a slurry bubble column. Recently, Sheikhi et al. (Sheikhi et al., 2013) studied the hydrodynamic state of a bubble column by analyzing the pressure fluctuations in both time and frequency domains. Moreover, Chilekar et al. (V. P. Chilekar et al., 2005) estimated the average large bubble size in slurry bubble columns using spectral analysis of pressure fluctuation signals. Xu et al. (Xu, Qu, Chaouki, & Guy, 2005) and Schweitzer et al. (Schweitzer, Bayle, & Gauthier, 2001) applied fiber optic probes to evaluate bubble flow characteristics in a bubble column reactor by performing the measurements at several radial and axial positions. Chaumat et al. (Chaumat et al., 2007) established a new methodology for the double optic fiber probe to derive gas holdup, bubble velocity and the mean Sauter diameter in a pilot-scale bubble column operated under high gas flow rate. Chen et al. (W. Chen, Tsutsumi,

Otawara, & Shigaki, 2003) investigated the effect of column scales on the local gas holdup, bubble frequency, bubble size, bubble velocity and flow structure by means of a single-tip optical fiber probe.

The viscosity and also the elasticity of the liquid phase may have strong effects on the bubble and liquid dynamics in bubble columns operating with non-Newtonian liquids. However, these phenomena are not well understood at this stage. Due to the complex rheology of non-Newtonian liquids, studies on the hydrodynamics of bubble columns operating with these types of liquids are still scarce and experimental work in this area is mainly limited to the study of single bubbles moving in stagnant liquids. On the other hand, it is very difficult to separate the viscosity and elasticity effects if they are studied together. Therefore, the main objective of this work is to conduct an extensive experimental study on the simultaneous effects of viscosity and elasticity of non-Newtonian liquids on the most important hydrodynamic parameters of bubble columns such as gas holdup, bubble size, and bubble related parameters. A complete set of non-Newtonian solutions has been strategically chosen to discriminate between the elastic and viscous effects. In order to gain comprehensive insight into the hydrodynamics and bubble properties, the pressure fluctuations are sampled by a series of pressure transducers along the column height and several data analysis approaches and techniques are applied to measure the hydrodynamic parameters and characterize the flow dynamics inside the column. Furthermore, the local measurements are conducted by using two fiber optic probes to evaluate the gas holdup radial distribution and mean bubble chord length.

3.2 Experimental details

3.2.1 Bubble column setup

The experiments described in this study are carried out in a 2.7 m high Plexiglas column with an inside diameter of 0.292 m. Oil-free compressed air is used as the gas phase and injected into the column through a perforated plate distributor with 94 holes that are 1 mm in diameter providing uniform distribution of the gas phase. The air flow rate is adjusted by two rotameters and the superficial gas velocity varies from very low gas velocities up to 0.22 m s^{-1} covering both homogeneous and heterogeneous flow regimes. The liquid phase is fed into the column through a

conical box located at the bottom of the column. Since the liquid phase is operated in a batch mode, the unaerated liquid height is set to 1.1m (L/D=3.8) at the beginning of all experiments. The bubble column setup is schematically shown in Figure 3-1.

3.2.2 Pressure time series and fiber optic probe measurements

Several fast response pressure transducers (response time ~1 ms) flush-mounted on the column wall are used to record pressure in different locations throughout the column height. Three absolute pressure transducers (APTs, OMEGA PX-429) are used to measure pressure fluctuations in the distributor and the middle and top regions of the column at heights of 3.5, 54 and 95.5 cm above the distributor (L/D=0.1, 1.8 and 3.3), respectively. The total average gas holdup and also the gas holdup axial distribution are evaluated by using three differential pressure transducers (DPTs). Along with pressure transducers, two in-house made fiber optic probes are installed at heights of 45 cm (L/D=1.5) and 91 cm (L/D=3.1) in order to measure the local gas holdup radial distributions and mean bubble chord length, as shown in Figure 3-1.

A fiber optic probe utilizes the difference in the reflective index between gas and liquid to detect bubbles inside a gas-liquid dispersion. A ray of light produced by a light source is sent to the column through emitting fiber strands. The light propagates into the liquid medium if the probe tip is immersed in the liquid phase or reflects back when the tip has penetrated inside the bubble. The reflected light is collected by receiving fiber strands and transmitted to an Electrobox Analyzer (PV-4A, Chinese Academy of Science) to treat the output signals. More information on the configuration of our in-house fabricated fiber optic probes can be found in detail elsewhere (Shabanian & Chaouki, 2014).

A data acquisition card (National Instrument, PCI6023E) and LabVIEW software are used to collect and sort the data. The pressure time series are recorded with a frequency of 512 Hz for 180s, which allows a spectrum resolution of up to 256 Hz according to the Shannon-Nyquist sampling criterion (Abbasi, Mostoufi, Sotudeh-Gharebagh, & Zarghami, 2013). Since the bubbles generate pressure fluctuations only up to 50 Hz (V. P. Chilekar et al., 2005), the signals are therefore low-pass filtered at 70 Hz. In order to minimize measurement errors, both pressure and fiber optic data are recorded three times and the average of these three readings is used to calculate

the final values of the gas holdup, bubble chord length, standard deviation and average spectral frequency of pressure signals.

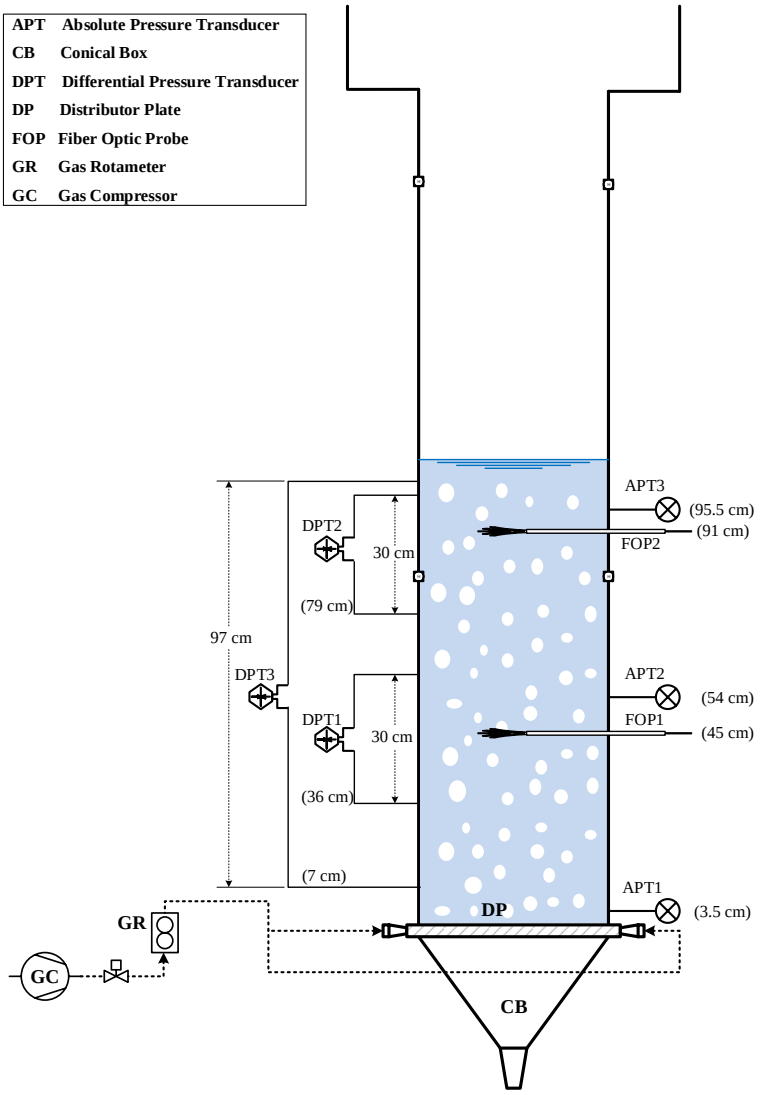

Figure 3-1: Schematic of the bubble column setup.

3.2.3 Materials and rheological characterization

Five types of fluids with different rheological characteristics are strategically chosen in order to discriminate between Newtonian, shear-thinning and elastic behaviors. The test fluids include an aqueous solution of Newtonian glucose syrup (70 vol.% of Glucose Enzose 62DE, Univar,

Canada), an elastic constant-viscosity Boger fluid prepared by dissolving 0.04 wt.% of PAA (Sigma-Aldrich, Canada, M_w~5,000,000-6,000,000) in 60 vol.% of aqueous glucose solution and two viscoelastic and shear-thinning fluids consisting of 0.5 wt.% aqueous solutions of high molecular weight CMC (Grade 7HF, CPKelco, USA) and Xanthan gum (200 mesh, Cambrian, Canada) polymers. All of the solutions are prepared by gently adding the polymers to tap water in a stirred tank of 200 liters at 22 °C. The solutions are left in repose for 24 hours prior to starting experiments. These fluids are specifically chosen for their similar rheological properties to actual industrial media. In fact, shear-thinning non-Newtonian fluids are the most common type of non-Newtonian fluids and are characterized by a decreasing apparent viscosity with increasing shear rate. Is it shown that the rheological behaviour of many fermentation and microbiological media can be satisfactorily simulated by the aqueous solutions of Carboxymethyl Cellulose (CMC). Xanthan gum which is used as the model fluid in many experimental studies is also widely applied as thickener in food and many other industries. Moreover, the Newtonian Glucose and Boger solutions used in this work have a viscosity of about 180 (mPa.s). A survey of the literature shows that the Newtonian viscous liquids applied in bubble columns in many applications have a viscosity very close to that of the Glucose and Boger solutions applied in this work. Regarding all these contexts, the solutions applied in this study, are selected in a way to simulate as closely as possible the rheological behavior of the media which are being used in the food, petrochemical and many other industries. All experiments are also repeated with tap water as the reference fluid. The surface tension of the test liquids is measured using a Dynamic Interfacial Tensiometer equipped with a Wilhelmy plate (DCAT21, Dataphysics, Germany). The test liquids and their physical properties are summarized in Table 3-2. It should be mentioned that all the solutions applied in this study are neither toxic nor flammable and are safe to handle.

Table 3-2: Physical properties of the test liquids at 22 °C.

Test liquid	Composition	Density (kg m^{-3})	Surface tension (mN m^{-1})
Water	-	997.04	71.97
Glucose	70 vol% in water	1293.5	74.33
Boger	60 vol% Glucose +0.04 wt% PAA in water	1251.1	75.28
CMC	0.5 wt% in water	995.65	73.92
Xanthan gum	0.5 wt% in water	995.31	76.07

The rheological studies of the solutions are carried out by a modular compact rheometer (MCR-501, Anton Paar) with a double-gap couette geometry. A simple shear study with a shear rate ranging from 0.1 to 1500 s^{-1} is performed to determine the apparent viscosity, μ_{app} and first normal stress difference, N_1. An oscillatory shear study is performed in the linear viscoelastic regime (at a strain amplitude of 10%) to measure viscous and elastic moduli, G″ and G′, respectively. The apparent viscosity of the solutions is represented in Figure 3-2. The Power-law model can describe the variation of apparent viscosity with the shear rate for the test solutions used in this study (Schowalter, 1960):

$$\mu_{app.} = K\dot{\gamma}^{n-1} \tag{3.1}$$

Where K is the consistency index and n is the flow index of the fluid. As can be seen in Figure 3-2, the rheological behavior of both the Glucose and Boger solutions is Newtonian since their viscosity is constant in all the applied shear rate values while the viscosity of both CMC and Xanthan gum decreases as the shear rate increases, which means they are shear-thinning solutions.

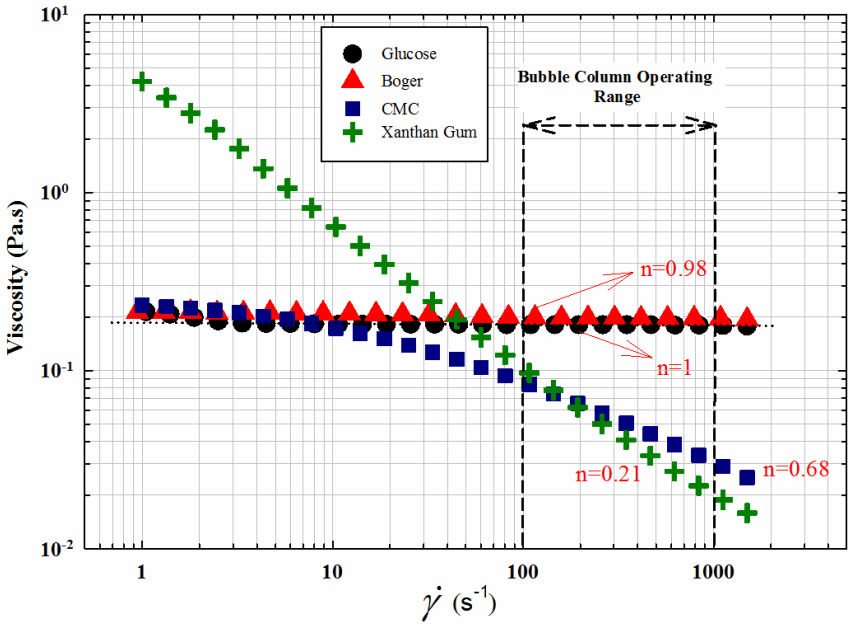

Figure 3-2: Variation of apparent viscosity of the aqueous solutions with shear rate.

Table 3-3 summarizes the fitted parameters of the Power-law model. The higher K means a higher apparent viscosity of the solution and the smaller flow index specifies the more shear-thinning behavior of the solution. The first normal stress difference, N_1, which indicates the presence of elasticity in a fluid, is also measured using a cone-plate geometry under simple shear study and presented in Figure 3-3. Since the glucose solution is a Newtonian fluid without any elasticity, the N_1 for glucose solution is too small to be detected by the rheometer while the three other solutions show a significant N_1 indicating the high elastic characteristic of these solutions. Moreover, the Boger solution shows higher elasticity at high shear rates in comparison with CMC and Xanthan gum solutions. From the simple shear study results, it can be concluded that both CMC and Xanthan gum solutions possess a moderate viscoelastic nature.

Table 3-3: Power law parameters of the test liquids.

Test liquid	K (Pa s^n)	n	Correlation ratio (R^2)
Glucose	0.185	1	0.99
Boger	0.135	0.98	0.98
CMC	0.32	0.68	0.89
Xanthan gum	3.29	0.21	0.92

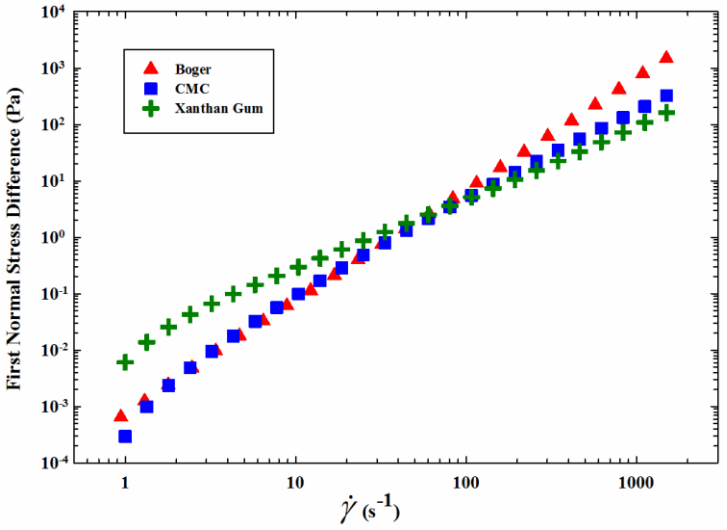

Figure 3-3: First normal stress difference versus shear rate for the test solutions.

In order to gain better insight into the viscoelastic behavior of the solutions, viscous and elastic moduli are measured under small amplitude oscillatory shear and plotted in Figure 3-4 as a function of angular frequency.

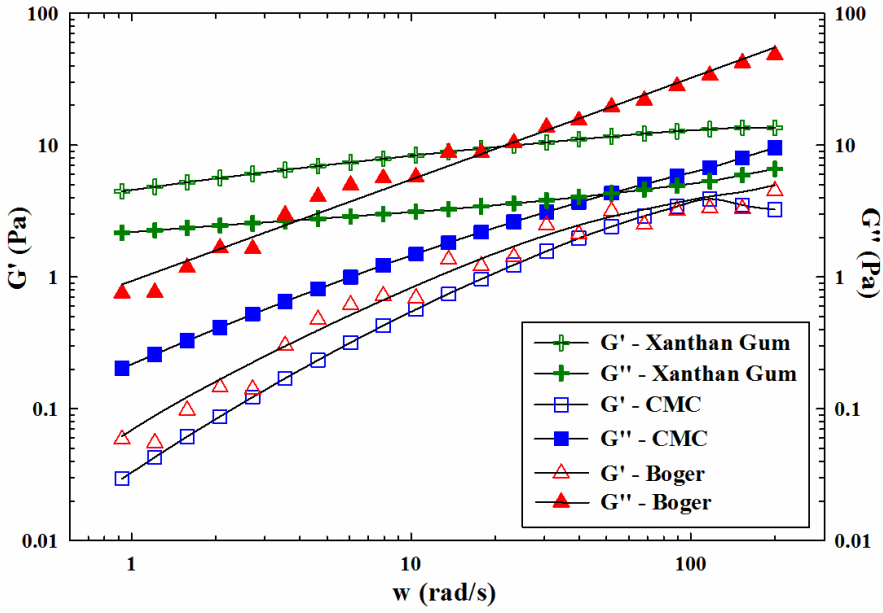

Figure 3-4: Dynamic moduli against the angular frequency for the test solutions.

Figure 3-4 demonstrates that the elastic modulus in the Xanthan gum solution is bigger than the viscous modulus at all applied angular frequencies while the CMC and Boger solutions exhibit a clearly visible dominance of the viscous modulus. In addition, the elasticity plays a more important role in the Boger solution at frequencies less than 70 (rad s^{-1}) and it becomes comparable with those for the CMC solution at higher frequencies. Except for the glucose solution, all three other solutions are viscoelastic, though the Xanthan gum solution behaves in a different way as the ratio $\frac{G'}{G''}$ is over 1. Note that this ratio is almost constant for all liquids over the experimental frequency range. The rheological properties of the test liquids are summarized in Table 3-4.

It is worth mentioning that in bubble column reactors, bubbles rise with a specific bubbling frequency through the column height exerting a specific shear to each element of liquid in their vicinity, which is similar to what the liquid experiences in the small amplitude oscillatory shear experiment. The frequency of this shear applied by the rising bubbles can be considered to be equal to the bubbling frequency, which is experimentally observed as between 5 Hz and 50 Hz. Therefore, the range of angular frequency in the small amplitude oscillatory shear experiments is specifically chosen to cover all the frequencies that the liquid undergoes in the bubble column reactor.

Table 3-4: Rheological properties of the test liquids at 22 °C.

Test liquid	Properties	$\frac{G'}{G''} \approx$	Effects
Glucose	Newtonian and Highly viscous	0	Strong viscosity effects
Boger	Viscoelastic	0.11	Elasticity effects << viscosity effects
CMC	Viscoelastic	0.36	Elasticity effects < viscosity effects
Xanthan gum	Viscoelastic	2.68	Elasticity effects > viscosity effects

3.3 Results and discussion

Several measurements and analyses, including statistical and spectral analyses, are done on the time series pressure fluctuations to put in evidence different phenomena happening in the bubble column in the presence of non-Newtonian fluids. In order to estimate the effective apparent viscosity of a non-Newtonian fluid in the bubble column, the effective average shear rate should be known. Thomasi et al. (Thomasi, Cerri, & Badino, 2010) proposed a correlation, including the power-law model parameters, to estimate the shear rate in a bubble column operating with different Newtonian and non-Newtonian solutions. Furthermore, several researchers have applied the relation developed by Nishikawa (Chisti & Mooyoung, 1989; W. D. Deckwer et al., 1982; Ghosh & Upadhyay, 2007; Nishikawa et al., 1977) for bubble column reactors. According to Nishikawa's model, the average shear rate can be related to the superficial gas velocity by means of a linear function as follows:

$$\dot{\gamma}_{av} = 5000\, U_g \tag{3.2}$$

Where $\dot{\gamma}_{av}$ and U_g are the average shear rate and superficial gas velocity, respectively. By considering the range of superficial gas velocity applied in this study (i.e., 0.02-0.22 m s^{-1}) and using equation 2, the effective shear rate inside the bubble column lies in the range of 100 to 1000 s^{-1}.

3.3.1 The effect of liquid properties on the gas holdup

The average gas holdup, one of the most important hydrodynamic and design parameters of bubble column reactors, is evaluated by measuring the pressure gradients along the column height. The gas holdup can be related to the pressure gradient using the following equation:

$$\epsilon_g = 1 - \frac{1}{\rho_l g}\left(\frac{\Delta P}{\Delta Z}\right) \tag{3.3}$$

Figure 3-5 shows the influence of the rheology of operating solutions upon the overall gas holdup in the column (measured by DPT3 as shown in Figure 3-1).

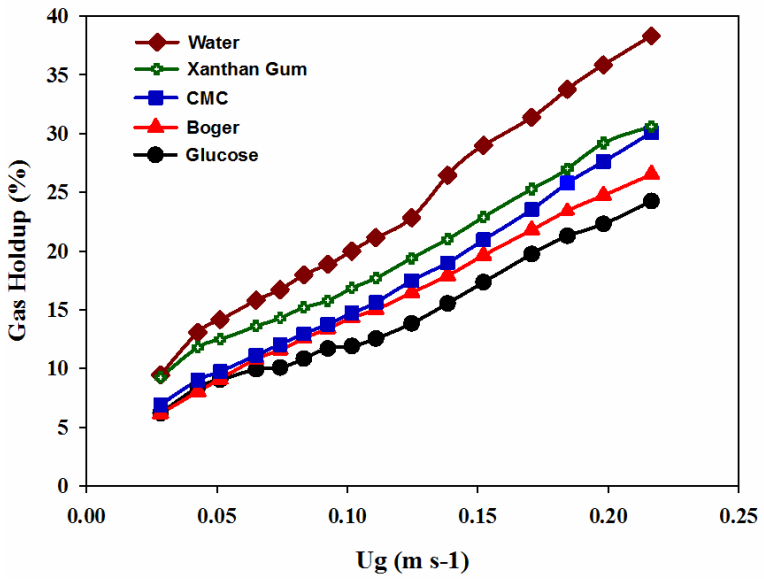

Figure 3-5: Variation of gas holdup with superficial gas velocity for different solutions.

In general, increasing the liquid viscosity reduces the gas holdup, the effect of which can be clearly observed in Figure 3-5 by comparing the gas holdup values of the glucose solution with those of water. The role of bubble coalescence and breakup in determining bubble size distribution, bubble rise velocity distribution, gas holdup and interfacial area is inevitable. The drag forces in low viscosity liquids (e.g., water in this study) are not strong enough to increase the coalescence and, accordingly, the bubble coalescence rate is remarkably low in low viscosity liquids. Hence,

bubbles are normally small with low rise velocity (see section 4.3.2) causing the gas holdup to become higher in the bubble columns operating with such liquids. On the other hand, in viscous liquids, the turbulence and energy of eddies to break the bubbles is reduced and bubble coalescence is promoted, leading to larger and faster bubbles and smaller gas holdup (Ruzicka et al., 2003; Schafer et al., 2002).

In addition, comparing the gas holdup of different operating fluids plotted in Figure 3-5 reveals some important results. The gas holdup for the Boger solution is higher than that for the glucose solution at all superficial gas velocities higher than 0.05 m s^{-1}. Both Boger and glucose solutions have a relatively high and constant viscosity in the entire operating (effective shear rate) range of the column. On the other hand, as previously explained, the Boger fluid shows a remarkable normal force and elastic properties ($\frac{G'}{G''} \ll 1$), especially at higher shear rates (Figure 3-3). Therefore, in comparison with the glucose solution ($\frac{G'}{G''} \approx 0$), the elasticity effects of the Boger solution prevent bubble coalescence. A lower coalescence rate leads to smaller bubbles with low rise velocities and, consequently, results in higher gas holdup in the column.

The behavior of the Xanthan gum solution is more complex. The Xanthan gum solution shows higher gas holdup in comparison with the CMC solution at almost all superficial gas velocities while both solutions show a comparable viscosity and normal force in low effective shear rates inside the column (i.e., 100 to 450 s^{-1} corresponding to U_g= 0.02 to 0.09 m s^{-1}) as shown in Figure 3-2 and Figure 3-3. On the other hand, according to the response of these solutions to small amplitude oscillatory shear depicted in Figure 3-4, it is observed that the Xanthan gum solution has a dominating elastic modulus ($\frac{G'}{G''} > 1$) compared to the CMC solution ($\frac{G'}{G''} < 1$). It seems that the higher gas holdup of the Xanthan gum solution at lower gas velocities is a result of the elastic effects of this solution that prevent bubble coalescence and form smaller bubbles. As seen in Figure 3-2, at higher effective shear rates inside the column (i.e., 450 to 1000 s^{-1} corresponding to U_g= 0.09 to 0.22 m s^{-1}), the viscosity of the Xanthan gum solution drops and is much lower that the viscosity of the CMC solution. Accordingly the higher gas holdup of the Xanthan gum solution at the upper values of the gas velocity can be related more to the decrease in the viscosity of this solution rather than the elasticity effects.

In conclusion, the glucose solution as the highly viscous Newtonian and inelastic fluid shows the lowest gas holdup and water as the low-viscosity Newtonian fluid, has the highest gas holdup inside the column. In fact, the absence of any elastic effect in glucose solution can facilitate the bubble coalescence and thus, leads to presence of larger bubbles and less gas holdup in this system. The three other solutions fall between these two limits and are arranged according to their rheological properties. The elastic properties of the Xanthan gum and Boger solutions that are evident from the values of normal force and storage modulus prevent bubble coalescence and, consequently, increase the gas holdup inside the column. More interestingly, it is obvious that for solutions with similar viscosity, the gas holdup is directly related to the ratio between loss and storage modulus (i.e. $\frac{G'}{G''}$). In other words, for solutions with a similar viscosity, higher values of $\frac{G'}{G''}$ will result in higher gas holdup as observed by comparing the gas holdup of glucose with the Boger solution and that of CMC with the Xanthan gum solution.

The operation and performance of bubble column reactors are strictly governed by the flow regime prevailing in the column. Basically, two flow regimes are observed in bubble column reactors: homogeneous (bubbly) and heterogeneous (churn-turbulent) regimes. A homogeneous flow regime is generally encountered at low superficial gas velocities in which the bubbles are small and there is a narrow bubble size distribution. A heterogeneous flow regime is commonly observed at relatively high superficial gas velocities and characterized by a wide bubble size distribution, the turbulent motion of gas bubbles and liquid circulation. The occurrence of the aforementioned flow regimes strongly depends on the column diameter, gas and liquid phase properties and distributor plate design. In many studies, the change in slope of the gas holdup curve versus the superficial gas velocity is considered as the regime transition point (Gourich et al., 2006; Shaikh & Al-Dahhan, 2013; Shaikh & Al-Dahhan, 2007). However, when the gas holdup curve does not show a rapid change in slope, identification of the transition point will be difficult. In such cases, literature studies have extensively used the drift flux approach proposed by Wallis (Ruzicka et al., 2003; Sheikhi et al., 2013; Vial et al., 2000; Wallis, 1969). The drift flux is the volumetric flux of gas phase relative to a surface moving at the volumetric average velocity of gas-liquid flow systems and in a bubble column with batch operation for the liquid phase is defined as:

$$j_{gl} = U_g(1 - \varepsilon_g) \tag{3.4}$$

The plot of j_{gl} versus ε_g can reveal immediately which regime prevails in the bubble column. A slope change in the plot of the drift flux versus gas holdup corresponds to the passage from homogeneous to heterogeneous regime. The change in slope of the drift flux plot is generally sharper than the change in slope of gas holdup curve. More information on the drift flux model can be found elsewhere (N. Clark & Flemmer, 1985; Shaikh & Al-Dahhan, 2007). The drift flux is plotted versus gas holdup for all the solutions in Figure 3-6.

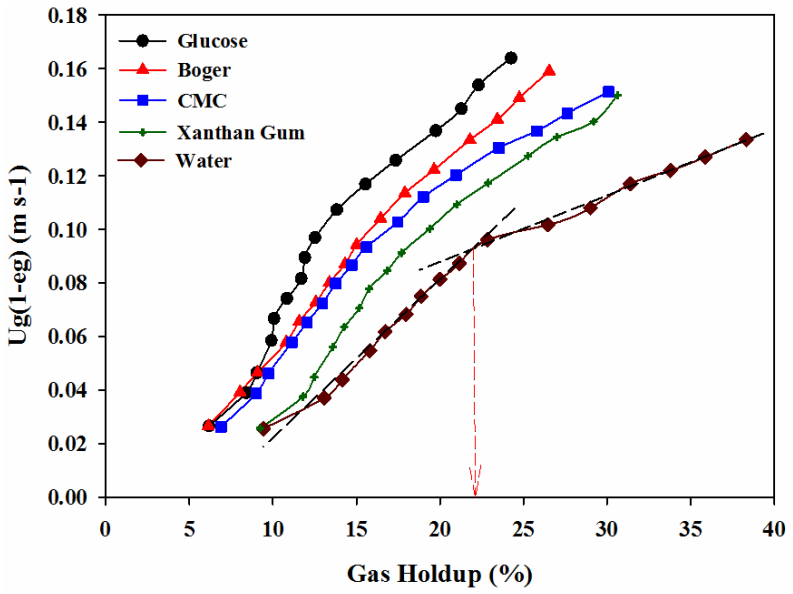

Figure 3-6: Identification of regime transition by Wallis' drift flux approach.

As can be seen from Figure 3-6, the drift flux curve for the water system shows a remarkable change at the gas holdup around 22% (corresponding to U_g= 0.12 m s^{-1}), which represents a change in the flow regime for this system. In contrast, no clear change in slope was observed in the drift flux curve for the other operating viscous solutions. In fact, the primary bubble size in viscous liquids is relatively large, suppressing the stability of the homogeneous flow regime (characterized by small bubbles with narrow bubble size distribution). The flow regime transition therefore appears earlier and the heterogeneous flow regime is developed faster. Even slug flow can already be formed at very low gas velocity in highly viscous liquids (Joshi, 1998; Ruzicka et al., 2003; Y.

T. Shah, Kelkar, B. G., Godbole, S. P. and Deckwer, W.-D., 1982). It has also been reported that in bubble columns with a perforated plate gas distributor with orifice diameters of $d_o > 1$ mm, the homogeneous flow regime is not observed in many cases (Zahradnik et al., 1997).

Generally, the axial distribution of gas holdup in a bubble column consists of three main zones: distributor plate zone, bulk (middle) zone and foam (top) zone (Gandhi et al., 1999). In the present work, the gas holdup values for the middle and top zones of the column are measured using DPT1 and DPT2 (as shown in Figure 3-1), respectively. Figure 3-7 illustrates the axial distribution of the gas holdup for different operating systems. As pointed out in Figure 3-7, for the water, glucose and Boger solutions that have a constant viscosity at all superficial gas velocities applied in this work the gas holdup in the middle and top zones of the column does not differ significantly and has a uniform axial distribution. As already mentioned, the gas holdup in bubble column is depended to the bubble size and liquid circulation. In fact, once the bubbles are formed and detached from the distributor, they undergo interactions and the average bubble size is determined mainly by the balance between coalescence and breakage phenomena inside the column. Moreover, the bubble coalescence becomes more dominant as the distance from the gas distributor increases. According to the results reported in Figure 3-7 for the water, glucose, and Boger, although the higher bubble coalescence at the top zone of the column can lead to larger bubbles and less holdup in this zone, the liquid circulation can increase the bubble residence time and the gas holdup, leading to a uniform gas holdup axial distribution in these solutions. On the other hand, for the CMC and Xanthan gum solutions, which are highly shear-thinning (Figure 3-2), the values of gas holdup in the middle zone are higher than those in the top zone of the column. In bubble columns, a swarm of bubbles rise through the column height and these moving bubbles can exert a specific shear stress to each element of liquid in their vicinity and accordingly deform it. Moreover, in the region closer to the gas distributor, the flow pattern is more stirred, the bubble-bubble and bubble-liquid interactions are developed, the inertia force that the bubbles experience is higher, and consequently the shear rate is higher than in the regions far from the gas distributor. All these effects may cause a higher shear stress to be exerted on the liquid phase in the middle zone of the column (which is close to the gas distributor in this work). In addition, the axial change in gas holdup is observed only for CMC and Xanthan gum solutions that are shear-thinning. Increasing shear stress on the shear-thinning liquids leads to a decrease in their viscosity. Therefore, it can be concluded that since the shear stress exerted on CMC and Xanthan solutions

is higher in the middle zone, the local viscosity of these solutions in the middle zone is less than that in the regions far from the gas distributor. Lower viscosity in the middle zone results in the formation of smaller bubbles and consequently higher gas holdup. Moreover, it seems that the axial distribution of gas holdup is not affected by the elasticity of the solutions nor by the values of $\frac{G'}{G''}$ and it depends more on the shear-thinning properties of the solutions.

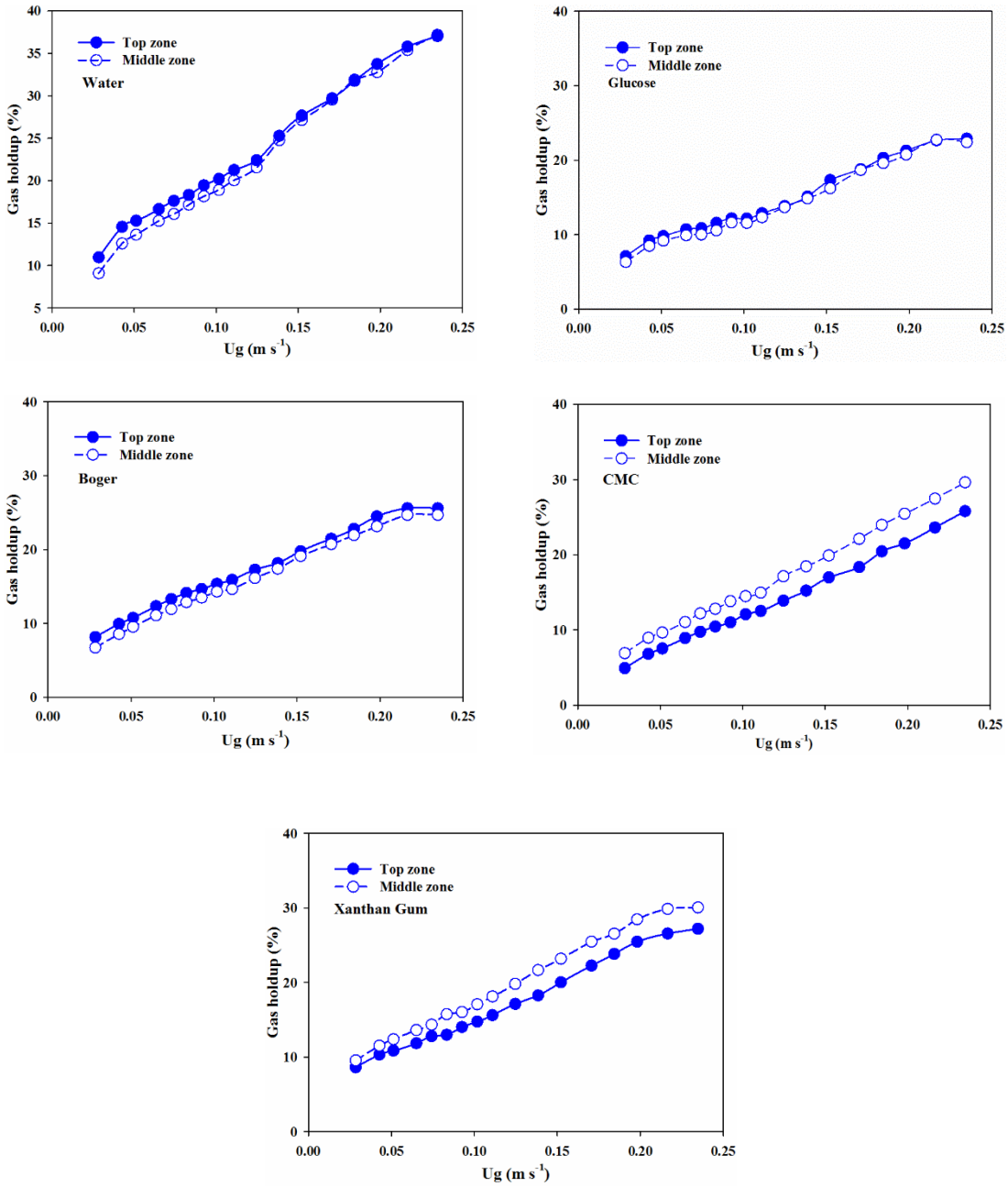

Figure 3-7: Gas holdup axial distribution for different operating solutions.

The radial dependence of gas holdup values measured by fiber optic probes in the middle and top zones of the column for all operating systems are presented in Figure 3-8.

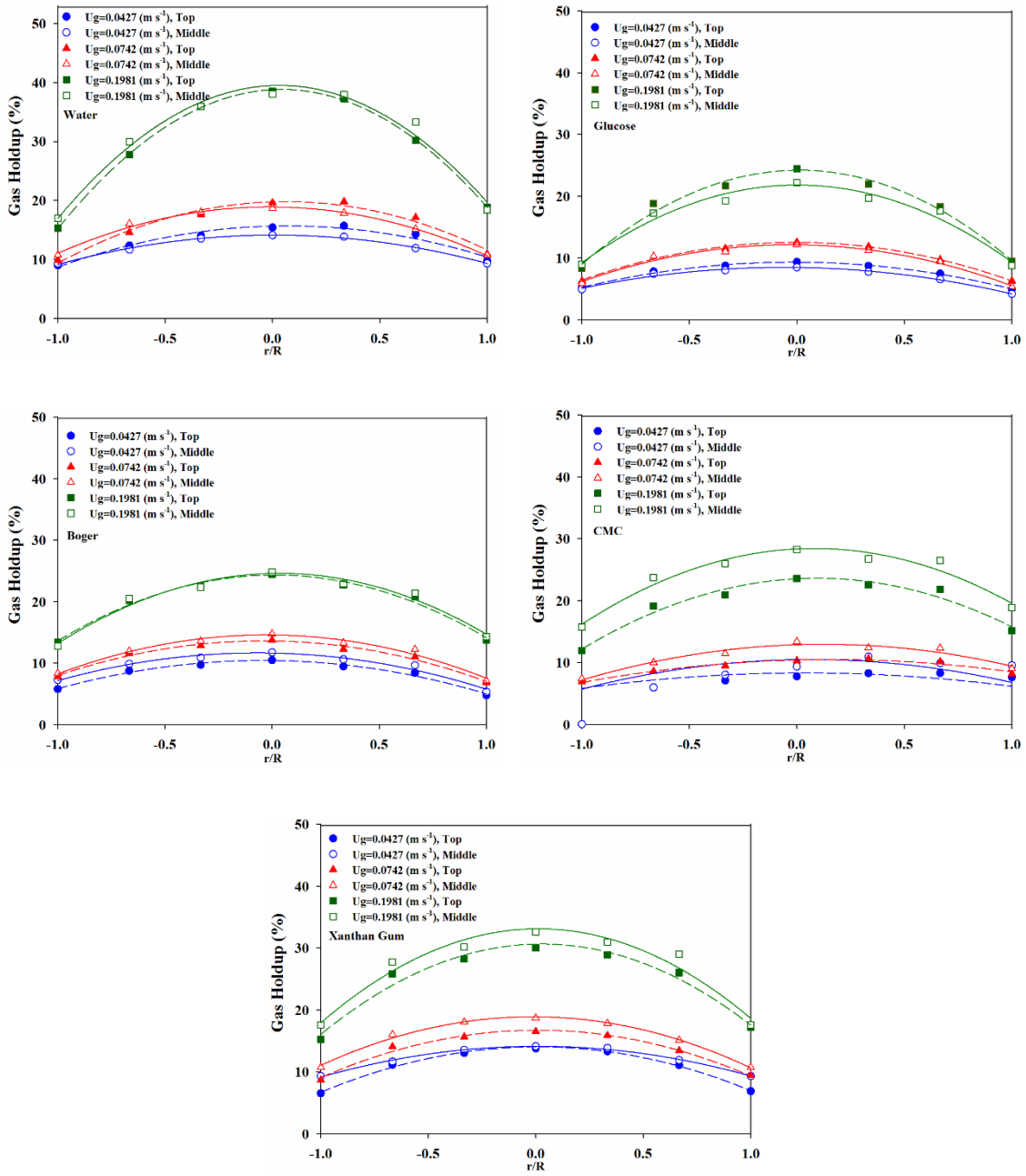

Figure 3-8: Radial dependence of gas holdup for different operating systems and superficial gas velocities in the middle and top zones of the column (at L/D=1.5 and 3.1, respectively).

The shape of the gas holdup profile depends strongly on the superficial gas velocity. As seen in Figure 3-8, in both the middle and top zones of the column, the gas holdup is flatter at low gas velocities while it becomes more parabolic at higher gas velocities for all operating solutions. At low superficial gas velocities, there is a uniform bubble distribution along the column cross section, which results in a uniform gas holdup radial distribution in the column. On the other hand, at high superficial gas velocity, the bubble coalescence is promoted, larger bubbles are formed and a heterogeneous flow regime and liquid circulation is developed. The parabolic gas holdup radial distribution at higher superficial gas velocity is mainly due to the radial variation of liquid velocity and the presence of more bubbles in the center of column in this operating condition. Due to the elastic properties of the Boger solution, the local gas holdup in this solution is slightly higher than those in the glucose solution. Moreover, as seen from the global gas holdup measurements (Figure 3-5), since the Xanthan gum solution shows higher elastic effects ($\frac{G'}{G''} > 1$) and shear-thinning behaviour than the CMC solution does ($\frac{G'}{G''} < 1$), the local gas holdup in the Xanthan gum solution is also higher compared with those in the CMC solution. The observed effects of liquid rheology on the gas holdup evaluated by fiber optic probes are in good accordance with those obtained by differential pressure transducers. It is also worth mentioning that although the average values of gas holdup are directly related to the $\frac{G'}{G''}$, the shape of the radial distribution of gas holdup is independent of $\frac{G'}{G''}$ values.

Comparing the shape of the gas holdup profile in the middle zone with those in the top zone of the column for each operating system reveals that there is not an appreciable change in the shape of gas holdup along the column height for all operating solutions. In both middle and top zones of the column, the gas holdup radial profiles for water and Xanthan gum solutions are steeper compared with those for other operating solutions. Among the solutions applied in this work, water and Xanthan gum have the lowest viscosity in the operating range of the column, therefore the liquid phase circulates more freely with higher velocity and, as a result, the gas holdup radial profile tends to be steeper in these two systems. Moreover, the gas holdup at each radial point and superficial gas velocity for the water, glucose, and Boger systems is almost the same in the middle and top zone of the column. However, in the CMC and Xanthan gum solutions, the gas holdup at the middle zone of the column is higher than that in the top zone of column and this can be observed

almost at each radial point and superficial gas velocity. This is mainly because of the shear-thinning properties of CMC and Xanthan gum solutions and is in a good accordance with the results obtained by differential pressure transducers in Figure 3-7.

3.3.2 Bubble size measurements

In order to study in greater depth and more accurately the effects of the rheological properties of the liquid phase on the local hydrodynamics, the mean bubble size is measured by two fiber optic probes in both middle and top zones of the column. One of the issues with using fiber optic probes is that the bubble diameter cannot be measured by the probe directly since the probe does not always intersect the bubble at its center and also bubbles are not spherical in many processes. Therefore, what is measured by the probe is the bubble chord length. The chord length also is strongly affected by the pierced conditions, such as the pierced position and the angle between the probe and the bubble velocity vector. In literature, there are some studies carried out to evaluate the equivalent bubble diameter from the chord length distribution. With the aid of geometrical probability analysis, it has been shown that the equivalent bubble diameter can be determined by the average measured cord length multiplied by a correction factor of 1.5 (Bai, 2010; Mizushima, Sakamoto, & Saito, 2013; Rojas & Loewen, 2007).

Before measuring the bubble size in this study, a series of single bubble experiments are conducted in a specially designed vessel in order to know where and how the optical fiber probe touches the bubbles. Visual inspection shows that the majority of the bubbles have ellipsoidal and spherical cap shapes rather than having the ideal spherical shape. It is also observed that the output signal from the fiber optic probe shows a clear pick when the probe pierces the bubble in its center and therefore only those picks are considered in calculating the bubble chord length in the signal post-processing step. It should be mentioned that since the bubbles are mainly ellipsoidal, only the average bubble chord length is reported in this study without considering any correction factor. The average bubble chord lengths measured by the fiber optic probes in the middle and top zones of the column are presented in Figure 3-9 for all operating solutions.

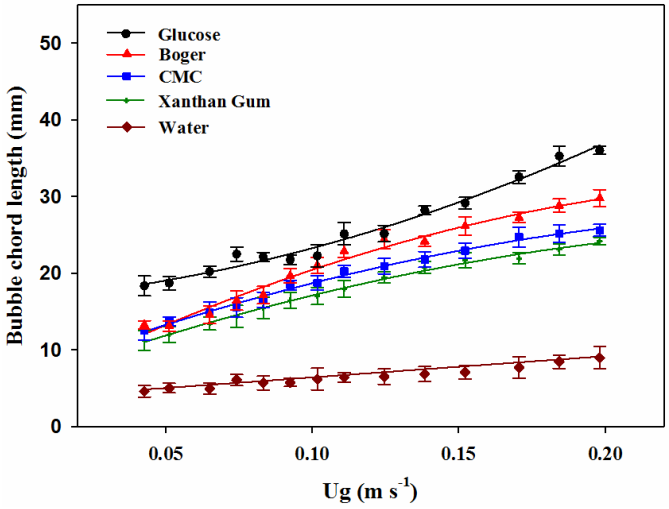

(a)

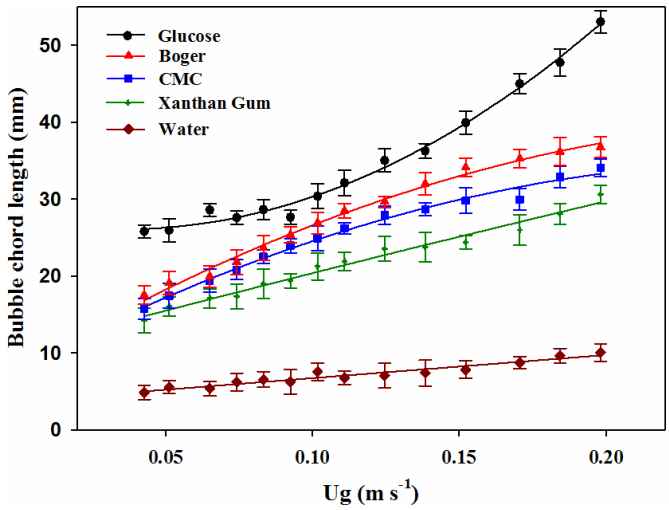

(b)

Figure 3-9: Variation of average bubble chord length with superficial gas velocity for different operating systems: (a) in the middle zone of the column; and (b) in the top zone of the column.

As pointed out from Figure 3-9, in water, the bubble chord length increases slightly with the superficial gas velocity whereas there is a significant change in the bubble chord length with the superficial gas velocity for other operating solutions. At low gas velocities, uniform bubbles are generated at the distributor plate that rise without any significant coalescence while at high gas velocities, the bubble coalescence is more significant which results in existence of larger bubbles in the column. By comparing the bubble chord length in the middle zone (Figure 3-9a) with those

in the top zone (Figure 3-9b) of the column, it can be observed that for all operating solutions, the bubble chord length is larger in the top zone of the column. In fact, the bubble coalescence in more dominant at higher level of the column where the effect of distributor plate is less which leads to a larger average bubble size in the top zone of the column. The glucose and Boger solutions are highly viscous and even at a low superficial gas velocity larger bubbles are produced at the gas distributor in these solutions. On the other hand, the bubble chord length in the Boger solution is smaller than those in the glucose solution in both middle and top zones of the column, as is obvious in Figure 3-9a and Figure 3-9b. Since the Boger solution has a moderate storage modulus and elastic properties ($\frac{G'}{G''} \ll 1$), it seems that bubble coalescence is prevented in the presence of the elastic effects in this solution and, consequently, smaller bubbles are formed compared with the bubble chord length in the Glucose solution, which is not elastic ($\frac{G'}{G''} \approx 0$).

Comparing the bubble chord length of CMC with that of the Xanthan gum solution reveals some important features of non-Newtonian fluids in bubble column reactors. In the middle zone of the column, the bubble chord length in the Xanthan gum solution is slightly smaller than those in the CMC solution. Both CMC and Xanthan gum solutions are shear-thinning with viscosities lower than the glucose solution in the operating range of the column while the Xanthan gum solution has higher storage modulus ($\frac{G'}{G''} > 1$) that diminishes bubble coalescence and keeps bubble chord length smaller in the middle zone, as presented in Figure 3-9a. In the top zone of the column (Figure 3-9b) where the gas distributor effects are less and coalescence phenomena dominate, the difference between bubble chord length in the Xanthan gum and CMC solution is more significant. In the top zone of the column, there is less shear inserted on the liquid phase and as a result the viscosity of CMC and Xanthan gum solutions are probably identical while the effects of the higher storage modulus (elasticity) of the Xanthan gum solution prevent bubble coalescence more and lead to presence of smaller bubbles in this system. The results obtained by the measurement of bubble chord length are consistent with those observed by measuring the gas holdup in previous sections confirming that the higher elastic effect of liquid leads to presence of smaller bubbles and higher gas holdup in the column. Similar to the results obtained by the gas holdup measurements, it is also clear that the bubble chord length in non-Newtonian liquids is strongly dependent on the

value of $\frac{G'}{G''}$. Therefore, it can be concluded that bubble chord length in solutions with high values of $\frac{G'}{G''}$ is smaller than those with low values of $\frac{G'}{G''}$.

Certainly, the most remarkable feature of viscoelastic materials is that they show simultaneous fluid-like and solid-like behaviors under deformation. Several models have been developed to quantitatively describe the behavior of viscoelastic fluids in linear deformation. All these models are constructed mainly by a combination of series of viscous (presented by a damper) and elastic (presented by a spring) components of fluids, such as the Kelvin-Voigt model, Maxwell model, and Burgers model (R. P. Chhabra, 2006). The Kelvin-Voigt model, as depicted in Figure 3-10, consists of a damper and Hookean elastic spring connected in parallel. According to the effects of non-Newtonian behavior on the bubble chord length observed in this study, it seems that the Kelvin-Voigt model can describe well the effects of viscoelastic liquids on bubble size. According to this model, when a thin layer of viscoelastic liquid is compressed between two approaching bubbles, the elastic element of the liquid acts similar to a compressed Hookean elastic spring that can repel two bubbles, prevent bubble coalescence and keep the average bubble size smaller. However, the viscous element of the liquid can display a damper-like behavior that promotes bubble coalescence and, consequently, leads to an increase in the average bubble size.

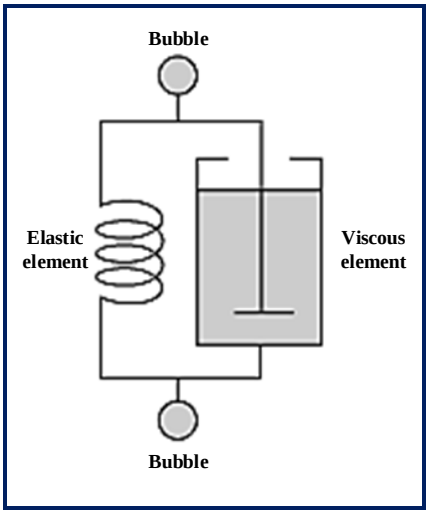

Figure 3-10: A schematic of the viscoelastic model describing the effects of viscous and elastic properties of liquid on the bubbles.

On the other hand, according to the results obtained so far in this study, these two competitive elastic and viscous elements can be replaced by the storage (G') and loss (G'') moduli of the solutions, respectively. It can be concluded that the higher elastic effect of liquid ($\frac{G'}{G''} > 1$) supresses the bubble coalescence and leads to presence of smaller bubbles in the system while the higher viscous effect of liquid ($\frac{G'}{G''} < 1$) is more favorable for bubble coalescence which results in presence of larger bubbles in the system. The advantage of using G' and G'' to interpret the observations is that both of them have the same unit and are measured under the same standard flow conditions in the rheological studies. As already observed from the results of gas holdup and bubble chord length measurements, both gas holdup and bubble chord length are directly dependant on the value of $\frac{G'}{G''}$. This dimensionless ratio can be used as a new approach to discriminate between the elastic and viscous effects of complex liquids and further interpret the effects of non-Newtonian liquids on the hydrodynamic parameters of bubble column reactors. This has not yet been applied by other researchers.

3.3.3 Statistical analysis of the pressure time series

Until now, different analyses have been performed on the pressure and optical fiber signals in order to evaluate the gas holdup and bubble size and their radial and axial distributions. The measurement of pressure fluctuation in the bubble columns is a very simple, non-expensive and effective method in characterizing the hydrodynamics of these type of reactors. Although the pressure fluctuation signals in the bubble column reactors are complex, they include some useful information about the hydrodynamic characteristics of the column that can help to confirm and validate the results obtained by other techniques. In order to extract this information, several analyses should be performed on the pressure fluctuation signals. Among several pressure signal analyses applied by researchers, the statistical analysis has been widely used in many studies. Statistical analysis is based on the estimation of moments of the probability density function (PDF) of a pressure signal. Usually, only standard deviation (square root of the second-order statistical moment) is estimated and higher moments require a large amount of accurate data to be calculated. The standard deviation of pressure fluctuation signal is shown to be a good representative of the average bubble size in the system, in which the larger rising bubbles create pressure fluctuations

with higher amplitude and, consequently, higher standard deviation (S. Barghi, A. Prakash, A. Margaritis, & M. A. Bergougnou, 2004; Johnsson, Zijerveld, Schouten, van den Bleek, & Leckner, 2000; Kumar et al., 2013; Sheikhi et al., 2013). The standard deviation as a measure of data set dispersion from its mean is given by

$$\sigma = \sqrt{\frac{1}{N-1}\sum_{n=1}^{N}(P_n - \bar{P})^2} \tag{3.5}$$

With the mean,

$$\bar{P} = \frac{1}{N}\sum_{n=1}^{N} P_n \tag{3.6}$$

Figure 3-11 exhibits the standard deviation of pressure fluctuations measured in the middle zone of the column (via APT2 as shown in Figure 3-1). From Figure 3-11, it is obvious that the standard deviation increases not only with superficial gas velocity but also with liquid viscosity. This is related to the presence of larger bubbles at higher gas velocities and higher viscosity. In fact, as already explained in the previous sections, the bubble size increases with both superficial gas velocity and liquid viscosity. The larger rising bubbles in viscous solutions and at higher superficial gas velocity create pressure fluctuations with higher magnitude that leads to higher standard deviation of pressure fluctuation signals. The standard deviation in glucose solution is highest while it is lowest in water system and this is in consistent with the results reported in previous section that show the bubble size is smallest and largest in the water and glucose systems, respectively. The elasticity and shear-thinning behavior of the Boger, CMC and Xanthan gum solutions results in smaller bubbles and, consequently, lower standard deviations in the aforementioned solutions compared to the glucose solution. Moreover, as expected, in solutions with identical viscosities, the standard deviation is also a function of $\frac{G'}{G''}$ which is in good agreement with the results of gas holdup and bubble size measurements.

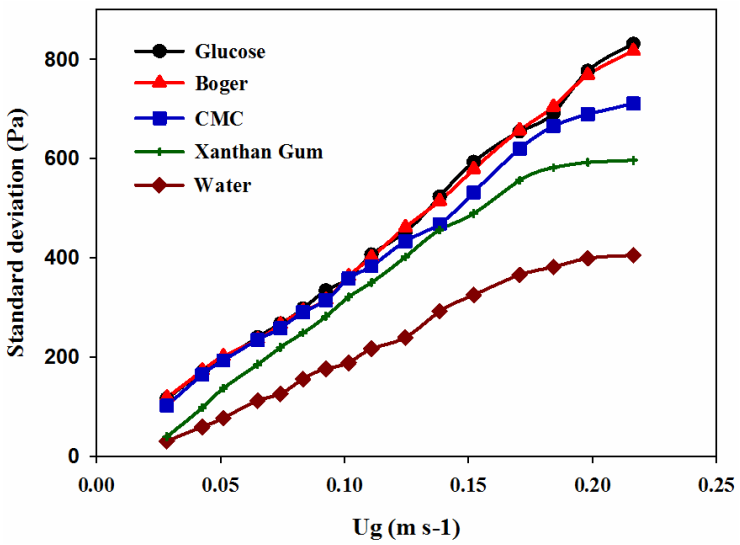

Figure 3-11: Comparison of the standard deviations of pressure fluctuations for different operating solutions in the middle zone of the column.

Similar to the study of gas holdup axial distribution (Figure 3-7), it is worth studying the axial variation of the standard deviation as well. Figure 3-12 compares the standard deviation of pressure fluctuations in the middle and top zones of the column (measured by APT2 and APT3 as shown in Figure 3-1) for different operating solutions. In contrast to the gas holdup axial distribution, the standard deviation of pressure fluctuations is higher in the top zone of the column in comparison with that in the middle zone for almost all operating solutions. This may be due to the high bed level oscillations as a result of bubble rupture, which creates more pressure fluctuations in the top zone of the column. In addition, no definite conclusion can be made on the dependency of axial distribution of standard deviation on $\frac{G'}{G''}$.

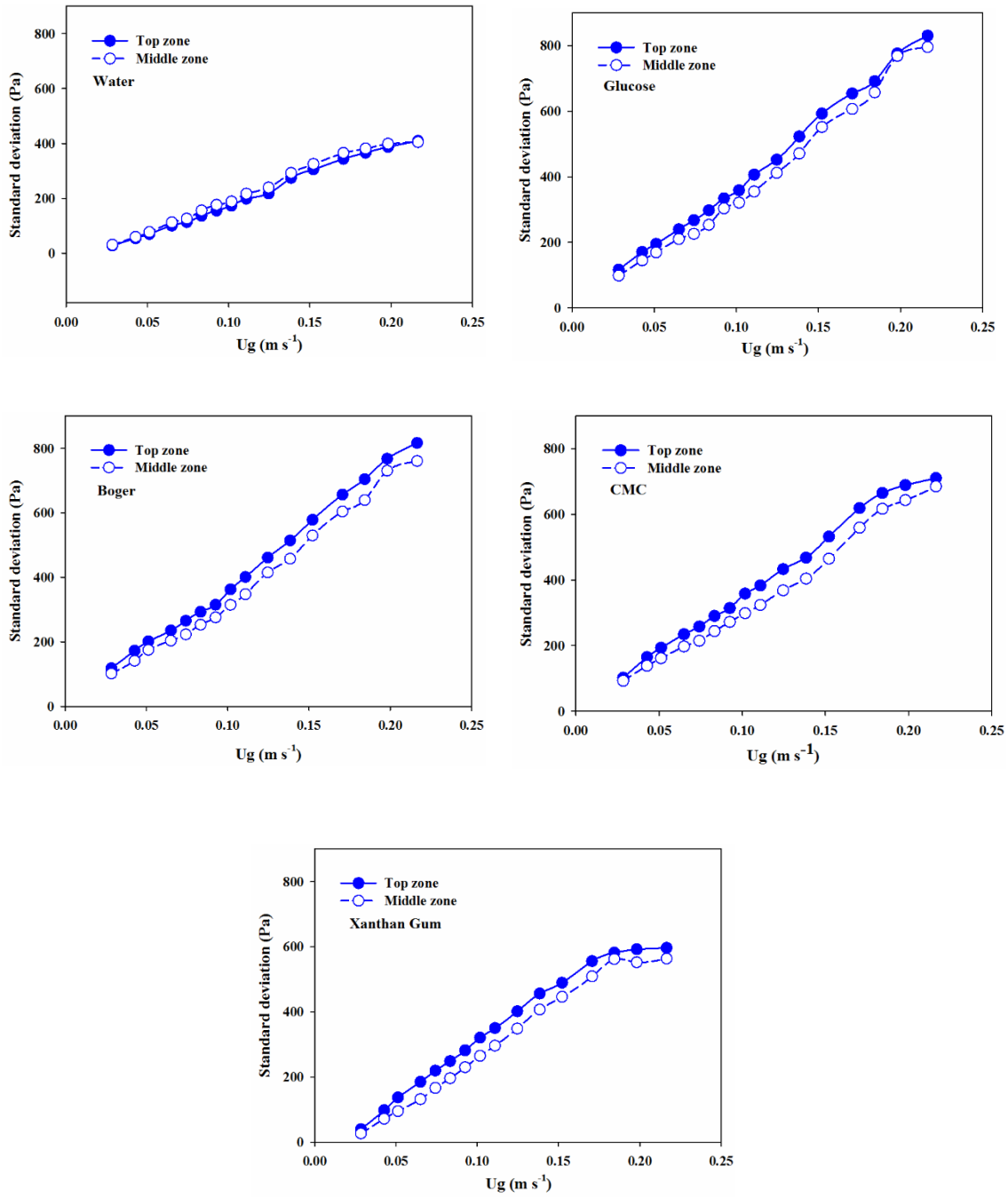

Figure 3-12: Comparison of the standard deviation of the pressure fluctuations in the middle and top zones of the column.

3.3.4 Spectral analysis of the pressure time series

Since the formation, coalescence and breakage of bubbles in non-Newtonian liquids are a complex function of several factors including viscosity, the degree of shear-thinning, and elasticity, further analyses on the time series pressure data are still needed to gain better insight into the complex effects of different rheological properties. Spectral analysis of pressure signals based on the Fourier transform, which is a frequency-domain analysis, has been demonstrated as a valuable tool for this goal, which has not yet been applied for the pressure signals obtained in non-Newtonian liquids (V. P. Chilekar et al., 2005; Vial et al., 2000). In this study, a discrete Fourier transform (Fast Fourier Transform) algorithm is used to convert the measured pressure signals from the time-domain into the frequency-domain. The power spectral density (PSD) can be estimated by the square of the magnitude of the Fourier transform. On the other hand, the variance of such an estimation of PSD is large to some extent. In order to overcome this drawback, the signal is divided into sub-spectra (Welch method) and the PSD is estimated as an average of a number of sub-spectra (Johnsson et al., 2000; Oppenheim & Schafer, 1975; Shabanian & Chaouki, 2014; Welch, 1967). Therefore, if the pressure time series is divided into K segments of distinct lengths of N_s, the PSD of each sub-spectra is given as follows:

$$P_{xx}^{j}(f) = \frac{1}{\sum_{n=1}^{N_s} w^2(n)} \left[\sum_{n=1}^{N_s} P_j(n) w(n) e^{-2i\pi nf} \right]^2 \tag{3.7}$$

Where $P_j(n)$ and $w(n)$ are the pressure time series and window function, respectively. The averaged PSD can then be estimated as follows:

$$P_{xx}(f) = \frac{1}{K} \sum_{j=1}^{K} P_{xx}^{j}(f) \tag{3.8}$$

To evaluate the PSD of the pressure signal in the present study, the pressure time series of APT2 (Figure 1) recorded in different solutions and superficial gas velocities is processed. The time series is divided into segments of 1024 points with an overlap of 50% and a Hamming window as the window function (Oppenheim & Schafer, 1989; Press, Teukolsky, Vetterling, & Flannery,

1992). The pressure signal in the bubble column is affected by several fluctuation sources with specific characteristic frequencies, including the bubble formation, rise, coalescence and breakage and bubble-liquid interactions. For example, small rising bubbles with a diameter of 4 mm can generate pressure fluctuations up to 50 Hz while larger bubbles 4 to 5 cm in diameter generate pressure fluctuations only in the range of 2 to 5Hz. The power spectrum of a signal describes the contribution of each of these fluctuation sources in the spectrum to the overall power of the signal (V. P. Chilekar et al., 2005). Thus, the amplitude, dominant frequency, and frequency distribution of a PSD curve can be used as a characteristic of the bubble properties and behavior inside the column. The PSD curves for different operating solutions at three superficial gas velocities are shown in Figure 3-13. Since in bubble columns only phenomena with a frequency range between 0 to 20 Hz occur (Drahos, Zahradnik, Puncochar, Fialova, & Bradka, 1991), the PSD curves are plotted only in this range. At low superficial gas velocity (Figure 3-13a) all operating solutions show dominant peaks at relatively high frequencies. The glucose solution has a dominant peak at a frequency lower than 5 Hz showing the formation of large bubbles directly at the distributor plate even at low gas velocity and as explained earlier in this study, the high viscosity of the glucose solution reduces the liquid turbulence and increases bubble coalescence and size, respectively. In comparison with the glucose solution, the Boger solution shows a dominant peak at a higher frequency of about 7.5 Hz, which is attributed to the formation of smaller bubbles as the result of elasticity effects. The CMC and Xanthan gum solutions exhibit dominant frequencies of about 8 and 9.8 Hz, respectively. Since both CMC and Xanthan gum solutions are less viscous than the Boger solution, smaller bubbles are therefore formed, leading to dominant peaks at higher frequencies. Moreover, because of the higher elastic effects, the bubble size in the Xanthan gum solution is even smaller than that in the CMC solution, which leads to a higher dominant frequency in this solution. On the other hand, it can also be pointed out that the dominant peak in the spectrum will appear at a higher frequency in the solution with a higher value of $\frac{G'}{G''}$.

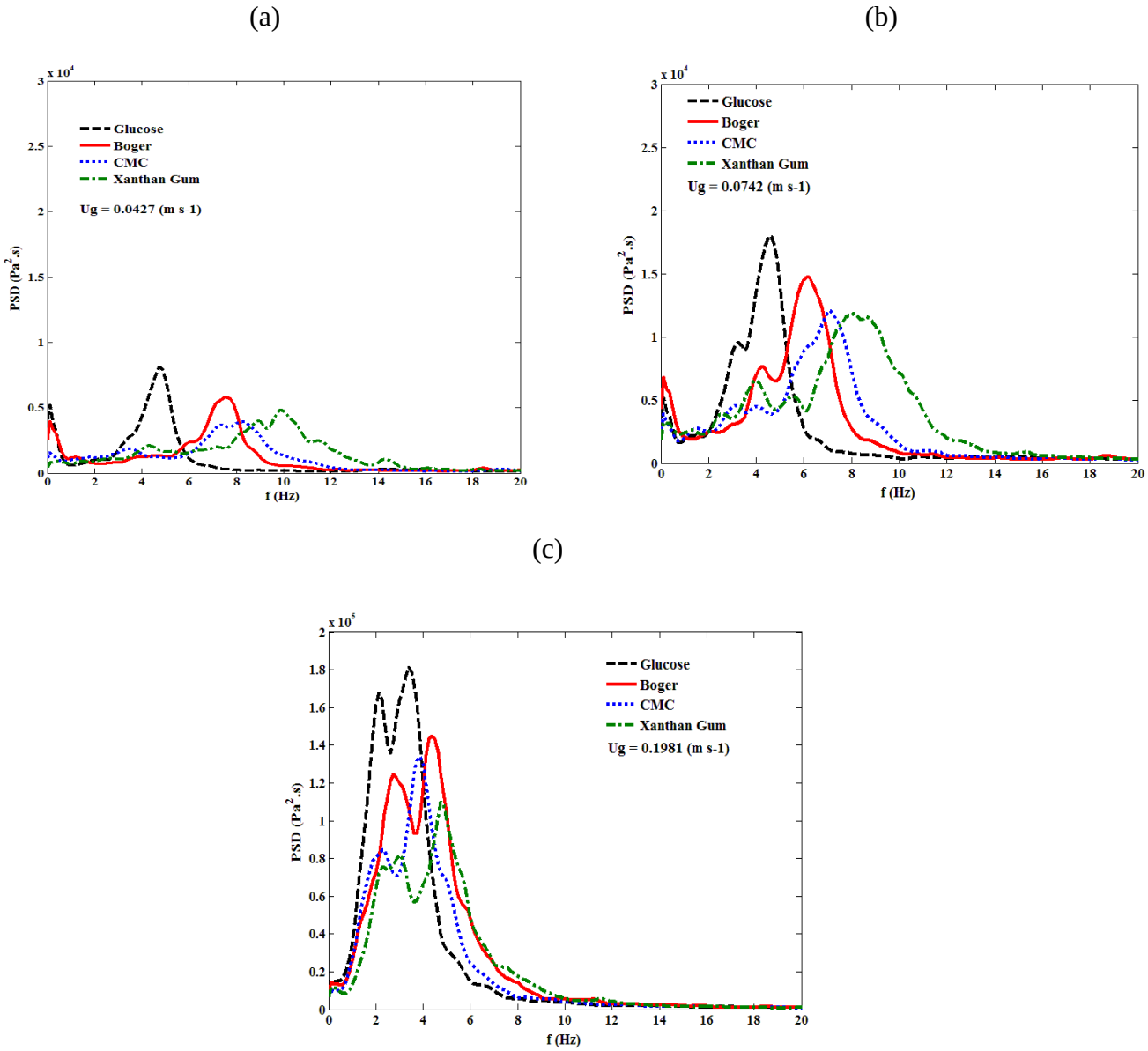

Figure 3-13: Power spectral density of the pressure time series recorded by APT2 for different operating solutions at superficial gas velocities of (a) 0.0427 m s^{-1}, (b) 0.0742 m s^{-1}, and (c) 0.1981 m s^{-1}.

By increasing the superficial gas velocity up to 0.0742 m s^{-1}, as seen in Figure 3-13b, the dominant peaks for all solutions shift to the left side of the spectrum toward lower frequencies with higher amplitudes. It should be pointed out that by increasing the gas velocity, the gas throughputs are

higher and as a result the overall coalescence rate and bubble size increase in all operating systems. The formation of larger bubbles at higher gas velocity causes the dominant peaks to appear at lower frequencies for all operating systems. However, the rheological effects of the solutions still act in the same way as before and there is still a considerable difference between the frequencies of each of the two neighboring peaks representing a remarkable difference in the bubble size in each of the two neighboring solutions. Furthermore, an evolution of secondary dominant peaks at a lower frequency can be observed for all operating systems. At the very high superficial gas velocity of 0.1981 (m s^{-1}), the dominant peaks and overall spectrum shift further toward lower frequencies with a significant increase in the amplitudes. Moreover, the above mentioned secondary peaks are completely developed in almost all operating systems. The appearance of these secondary dominant peaks can be referred to as the existence of two different bubble populations at this high gas velocity. The high rate of bubble coalescence and breakage at a high gas velocity leads to a wide bubble size distribution to be attained. The average frequency of the spectrum, f_m, is another useful measure that provides us with valuable information about the phenomena happening inside the bubble column. The average frequency of a spectrum is given as:

$$f_m = \frac{\int [P_{xx}(f)] f df}{\int [P_{xx}(f)] df} \tag{3.9}$$

The average frequency of the spectrum for different operating solutions is calculated and plotted in Figure 3-14 (the average was taken in the 0-20 frequency band).

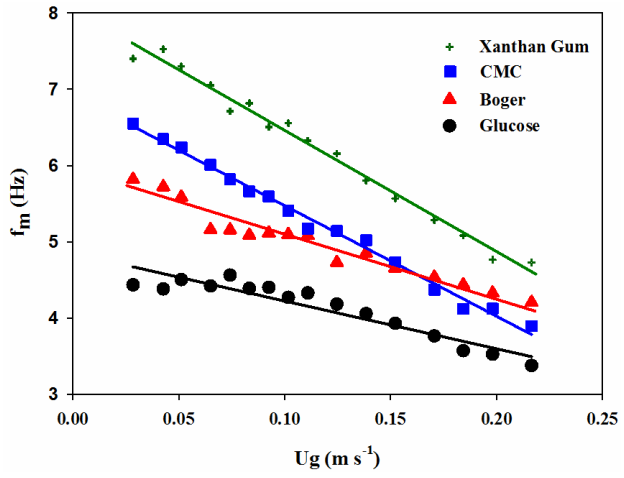

Figure 3-14: Average frequency of the spectrum versus superficial gas velocity for different operating solutions.

Figure 3-14 shows that by increasing the superficial gas velocity the average frequency of the spectrum decreases gradually. As mentioned earlier in this work, coalescence and breakage related mechanisms are known to be the two most influential phenomena on the development of bubble size distribution. In general, by increasing the superficial gas velocity and particularly in the turbulent flow, bubble coalescence becomes dominant leading to the formation of larger bubbles with lower frequencies in the spectrum (Shaikh & Al-Dahhan, 2007). Furthermore, by comparing the average frequency of the solutions with dissimilar rheological behaviors used in this study, the same results obtained by other analytical methods can be achieved. As expected, the lowest values of average frequency belong to the highly viscous glucose solution, which can be attributed to the formation of larger bubbles in this solution. The average frequency of the spectrum in the Boger solution is higher in comparison with the glucose solution. As explained before, the elastic effects of the Boger solution suppress bubble coalescence and result in smaller bubbles. The bubbles in the Xanthan gum solution are smaller due to the higher elasticity and relatively smaller viscosity of this solution in comparison with those of the CMC solution. Therefore, the average frequency of the spectrum for the Xanthan gum solution becomes higher than that for CMC solution.

It is worth mentioning that the average frequency of the spectrum is strongly proportional to the $\frac{G'}{G''}$ ratio in which solutions with a higher $\frac{G'}{G''}$ ratio show a higher average frequency of the spectrum and vice versa. In conclusion, the results of the spectral analysis of the pressure time series are in complete agreement with those obtained by other measurements and analyses in this study. The effects of the rheological behavior of the non-Newtonian solutions used in this study in the form of an increased $\frac{G'}{G''}$ ratio on the hydrodynamic characteristics of the bubble column are summarized in Table 3-5.

Table 3-5: Summary of the effects of increasing the G′/G″ratio on the hydrodynamic characteristics of the bubble column.

Characterictic	ε_g	$U_{g,tran.}$	Bubble Coalescence	Axial and radial distribution of ε_g	L_b	a	Magnitude of Pressure fluctuation	σ	f_m
$\uparrow \frac{G'}{G''}$	↑	↔	↓	↔	↓	↑	↓	↓	↑

↑: Increasing ↓: Decreasing ↔: No effect observed

3.4 Conclusion

The distinct effects of elastic and viscous aspects of several non-Newtonian fluids on the hydrodynamics and bubble related phenomena are experimentally studied in a pilot scale bubble column reactor. Pressure time-series and fiber optic probe signals are recorded along the column height. A comprehensive set of analyses is conducted to post-process the pressure and fiber optic probe signals by taking advantage of both time and frequency domain analyses. A new approach based on the $\frac{G'}{G''}$ ratio has been applied to interpret the simultaneous effects of the elasticity and viscosity of non-Newtonian solutions on the hydrodynamic characteristics of bubble column reactor. It was observed that the negative and coalescing effects of highly viscous liquids on the gas holdup and bubble chord length can be suppressed in the presence of the elastic effects and these effects can be directly explained by comparing the values of $\frac{G'}{G''}$ for different solutions. The axial distribution of gas holdup and bubble chord length is shown to be different in viscoelastic liquids in comparison with those in Newtonian liquids. The statistical and spectral analyses on the pressure time-series also confirm that the elastic aspects of non-Newtonian fluids, which is normally neglected, plays an important role on bubble related phenomena and thus on the hydrodynamics of bubble column reactors. On the other hand, the $\frac{G'}{G''}$ ratio is a dimensionless parameter, including both elastic and viscous effects of non-Newtonian liquids, and the new approach based on using this ratio can provide researchers with a new path to interpret further the effects of non-Newtonian liquids in gas-liquid contactors, which have not yet been considered elsewhere. The rheology of the operating liquid in the bubble column reactors has been

demonstrated to be of great importance and should be considered in detail for a more accurate design, operation and scale-up of multiphase contactors.

CHAPTER 4

ARTICLE 2: LOCAL HYDRODYNAMICS OF BUBBLE COLUMN REACTORS OPERATING WITH NON-NEWTONIAN LIQUIDS: EXPERIMENTS AND MODELS DEVELOPMENT

Amin Esmaeili, Christophe Guy, Jamal Chaouki

Department of Chemical Engineering, École Polytechnique de Montréal, P.O. Box 6079, St. C.V., Montreal, Qc, Canada H3C 3A7

Submitted to the *AICHE Journal*

Abstract

This work is aimed at investigating the effects of liquid phase rheology on the local hydrodynamics of bubble column reactors operating with non-Newtonian liquids. Local bubble properties, including bubble frequency, bubble chord length, and bubble rise velocity, are measured by placing two in-house made optical fiber probes at various locations within a bubble column reactor operating with different non-Newtonian liquids. It was found that the presence of elasticity can noticeably increase the bubble frequency but decreases the bubble chord length and its rise velocity. The radial profiles of bubble frequency, bubble chord length and bubble rise velocity are shown to be relatively flat at low superficial gas velocity while they become parabolic at high superficial gas velocity. Moreover, the bubble size and gas holdup are correlated with respect to dimensionless groups by considering the ratio between dynamic moduli of viscoelastic liquids. The proposed correlations are capable of predicting the experimental data of bubble size and gas holdup within a mean absolute percentage error of 9.3% and 10%, respectively.

Keywords: Bubble column; non-Newtonian liquids; Hydrodynamics; Local measurements; Optical fiber probe; Modeling; Gas Holdup; Bubble size

4.1 Introduction

Escalating global demands for energy and chemicals and environmental considerations are motivating great interest in the design, operation, and optimization of chemical processes toward more efficiency, reduced energy consumption and increased environmental protection. Bubble column reactors are considered as one of the most important types of reactors in petroleum processing, biotechnology, food processing and pharmaceutical processes where highly viscous and non-Newtonian media are often processed. The chemical industries produce about 50 million metric tons of chemicals in bubble columns all over the world.(Bai, 2010; Kantarci et al., 2005; Wang et al., 2007) The rheological behavior of non-Newtonian liquids in many chemical industries can sometimes be very complex. In some cultivation processes, the culture media show a high viscosity and yield stress. Viscous pseudoplastic flow behavior is also found in many concentrated suspensions, slurries, emulsions, and aqueous polymer solutions. In addition, in many industrial processes, the rheological properties of the liquid phase can change within the process (Raj P Chhabra & Richardson, 2011; S. B. Li, Zhu, et al., 2012; Koichi Terasaka & Tsuge, 2003; Velez-Cordero & Zenit, 2011). Several differences are observed between the behavior of Newtonian and non-Newtonian liquids. The non-Newtonian features of fluids are shown to be responsible for some strange phenomena in the processes. Phenomena, such as rod-climbing in agitated vessels, hole-pressure error, die swell, and tubeless siphon, present some of these differences that are of both laboratory interest and industrial and commercial importance (Howard A Barnes et al., 1989; Rodrigue, De Kee, & Fong, 1998).

On the other hand, the motion of bubbles rising in shear-thinning and viscoelastic liquids is one of the research problems in the field of non-Newtonian fluid mechanics. There are a number of interesting phenomena for the case of bubble motion in non-Newtonian liquids. The Uebler effect, the apparent discontinuity in the bubble terminal velocity–volume curve in viscoelastic liquids, and the formation of a negative wake of liquid velocity behind bubbles rising in non-Newtonian liquids are some of the phenomena observed by researchers. For example, the Uebler effect (Metzner, Uebler, & Fong, 1969) denotes a moving bubble that may come to a sudden stop in contraction flows of viscoelastic fluids. It has been shown that as the volume of a rising bubble in viscoelastic liquid increases, a sudden jump in the bubble terminal velocity is observed. This discontinuity in the bubble terminal velocity is attributed to the elastic effects of the fluid. It must

be mentioned that a complete understanding of many of these peculiar phenomena is still limited (De Kee, Chhabra, & Dajan, 1990; Herrera-Velarde, Zenit, Chehata, & Mena, 2003; Imaizumi et al., 2014; Pillapakkam, Singh, Blackmore, & Aubry, 2007; Pilz & Brenn, 2007). The behavior of individual bubbles in non-Newtonian liquids has been investigated by many researchers. Most of these investigations have shown that the flow field around a bubble rising in viscoelastic liquids contains three distinct zones: (1) an upward flow in front of the bubble, which is similar to that in the Newtonian case and (2) a central downward negative wake behind the bubble, and a hollow cone upward flow surrounding the negative wake zone that begins on the sides of the bubble and is largely extended backward (Kemiha et al., 2006).

Otake et al. (Otake, Tone, Nakao, & Mitsuhashi, 1977) studied the coalescence and breakup phenomena taking place in a swarm of bubbles. They observed when the trailing bubble reaches close enough to the leading bubble, it is accelerated and gathered into the back of the leading bubble. They reported a critical distance at which the leading bubble begins to exert a remarkable influence on the one following and this distance is about 3 to 4 times the diameter of the leading bubble. It was found that coalescence occurs at the critical distance where more than half of the projected area of the trailing bubble is overlapped with that of the leading bubble. On the other hand, it has been realized that breakup takes place in the case of overlapping less than about half of the projected area of the trailing bubble. They also observed that the extent of bubble coalescence is largely determined by the liquid viscosity as a higher viscosity is more favorable for coalescence than for breakup. Indeed, bubble coalescence is a complex process and entails three steps: (1) In the first step, the following bubble enters the wake behind the leading bubble;. (2) Depending upon the size and velocity of the following bubble, it experiences much less drag in the wake and as a result it approaches the leading bubble quickly until they collide and are then separated by a thin film of liquid. This step is controlled essentially by the hydrodynamics of the bulk liquid; and (3) The outer forces press the two bubbles together for a sufficiently long time, and the liquid is gradually drained from the film until it ruptures and coalescence occurs. This step is controlled more by the hydrodynamics of the thin film. The rate of film thinning in this step determines whether coalescence will happen or not. If the film drainage time is longer than the period of collision and contact, the two bubbles may separate rather than coalesce. It can be expected that the rheological complexities of the liquid phase significantly influence the coalescence process. The elasticity of liquids is shown to have a tendency to decrease the

coalescence rate. Thus, liquids with strong elasticity may reduce the overall coalescence rate considerably (Acharya & Ulbrecht, 1978; R. P. Chhabra, 2006; T.-J. Lin & Lin, 2009).

In processes involving gas-liquid dispersions, bubbles are frequently colliding and thus may separate from each other or coalesce. The overall coalescence and breakup processes are governed by a balance between inertia force, surface tension force, viscous drag force, elastic force and buoyancy (W. Fan, Jiang, Zhu, Ma, & Li, 2008). The bubble coalescence and breakup processes in bubble columns operating with non-Newtonian liquids exert remarkable influences on the local bubble properties, such as bubble frequency, bubble size, and bubble rise velocity than can directly affect the mass transfer and chemical reactions rate (Acharya & Ulbrecht, 1978; J. Liu, Zhu, Fu, & Ma, 2014). For example, the variation in the liquid-side volumetric mass transfer coefficient ($k_L a$) is primarily due to the variations in the specific interfacial area (a). The specific interfacial area is a function of gas holdup and bubble size. The gas holdup is also related to bubble frequency, bubble size, and its rise velocity.

Therefore, to properly design and efficiently operate a bubble column reactor operating with non-Newtonian liquids, understanding and accumulating enough knowledge about the effects of such media on the local hydrodynamics of bubble columns is of considerable importance. Previous experimental efforts on bubble columns operating with rheologically complex liquids were mostly made on global investigations while local measurements of bubble properties are very scarce. Furthermore, experimental data on the local bubble properties make it possible to gain detailed insight on the performance of bubble columns in such media. In the bubble columns, one encounters groups of bubbles that move in the form of a swarm and it is basically impossible to observe the individual coalescence and breakup events in such an environment. In contrast to the extensive studies on the single bubble moving in non-Newtonian liquids, the systems involving a swarm of bubbles, such as the bubble columns, have received only scant attention.(R. P. Chhabra, 2006) Indirect and non-visual measurements of bubble size and chemical concentration can be applied as an alternative to study bubble coalescence and breakup but these techniques are still very difficult to use and interpreting their results in terms of actual bubble behavior is complicated. Measurement methods have not yet been able to resolve the details of the coalescence event. Moreover, although bubble columns have been the topic of much research in the last decade, no reliable general model has been developed to consider the rheological properties of the liquid phase in predicting the hydrodynamic parameters such as gas holdup and bubble size.

In a previous work of the authors (Amin Esmaeili, Guy, & Chaouki, 2015), the influence of the liquid phase rheology on the global hydrodynamics of a bubble column reactor was extensively investigated and a new approach was proposed based on the dynamic moduli of viscoelastic solutions to better understand the simultaneous viscous and elastic effects of liquid phase. The main goal of the present work is to discover what actually happens to the local bubble properties in the presence of non-Newtonian liquids. As the starting point of this work, the effects of liquid phase rheology on bubble frequency, bubble size, bubble rise velocity, and their radial distributions in a bubble column have been evaluated by applying two in-house made fiber optic probes. In order to discriminate between Newtonian, shear-thinning and elastic behaviors, several types of fluids with different rheological characteristics were strategically chosen.

Previous models available in literature were generally developed to predict the bubble size and gas holdup in bubble column reactors operated with Newtonian liquids. There was no universal correlation to predict the aforementioned hydrodynamic parameters when the non-Newtonian liquids were used and considerable discrepancies were frequently observed among the predictions of different models. Additionally, the correlations were normally given in dimensional forms and were in reasonable agreement with only the data, which were used to obtain them. To overcome these drawbacks, in the last part of this work, two correlations have been developed based on dimensionless numbers by introducing the dynamic moduli of the liquid phase into the correlations to predict the bubble size and gas holdup in bubble columns operating with non-Newtonian liquids.

4.2 Experimental procedure

4.2.1 Apparatus

The heart of the experimental setup in this study is a 2.7 m high Plexiglas column with an inside diameter of 0.292 m. Oil-free compressed air is used as the gas phase, fed from the bottom of the column through a perforated plate (94×1 mm diameter holes with a density of 1400 holes m^{-2} arranged in a 27 mm square pitch). The column is equipped with two precise rotameters to measure and control the gas flow rate. The superficial gas velocity varies from 0.03 m s^{-1} up to 0.22 m s^{-1} covering both the homogeneous and heterogeneous flow regimes. The liquid phase is fed into the column through a conical box located at the bottom of the column. Since the liquid phase is

operating in batch mode, the unaerated liquid height is set to 1.1 m (*L/D=3.8*) at the beginning of all experiments. In order to check the reproducibility of data and minimize the measurement errors, the experiments at each superficial gas velocity are repeated three times and the average of these three measurements is used to calculate the hydrodynamic parameters. More details on the bubble column setup and data acquisition method can be found in the earlier work of the present authors (Amin Esmaeili et al., 2015).

4.2.2 Non-Newtonian solutions, preparation and rheological characterization

In order to find the proper non-Newtonian liquids to fulfill the objectives of this study, several polymer solutions with different rheological characteristics were pre-tested and finally three Carboxymethyl Cellulose (CMC, Grade 7HF, CPKelco, USA) and three Xanthan gum (200 mesh, Cambrian, Canada) aqueous polymer solutions at concentrations ranging from 0.3 to 0.7 wt.% were found to be appropriate candidates for this work. The selected polymer powders have the tendency to form lumps when dispersed into water. Due to their rapid swelling in water, an appropriate mixing method must be chosen to overcome this problem. One of the most popular methods for preparing a homogenous aqueous solution of these polymers is to add them directly into the vortex of a vigorously stirred body of water (Chambers, 1978). Furthermore, the rate of adding the polymers should be slow enough to prevent particle agglomeration, but fast enough to add all of the powders before the vortex disappears. Therefore, in the present study, all of the solutions were prepared by gently adding a known weight of polymers into a known weight of tap water in a continuously stirred tank of 200 liters at 22 °C. The agitation was maintained until a homogenous and clear solution was produced (after 6-10 hours depending on the concentration of polymer).

To compare the viscosity, shear-thinning and elasticity effects of the fluids, a 70 vol.% aqueous solution of Newtonian glucose syrup (Enzose 62DE, Univar, Canada) and an elastic constant-viscosity Boger fluid were also prepared. The Boger fluid was prepared by dissolving 0.04 wt.% of Polyacrylamide (PAA, Sigma-Aldrich, Canada, M_w~5,000,000-6,000,000) powder in 60 vol.% of aqueous glucose solution. It is worth mentioning that the PAA powder cannot be dissolved in a glucose solution at ambient temperature. Therefore, a separate agitation vessel equipped with a heating element was used to prepare the Boger fluid at 60 °C. The solutions were left to rest for

24 hours prior to starting the experiments. The non-Newtonian liquids used in this study fulfill three conditions: (1) they are all viscoelastic; (2) show a shear-thinning behavior; and (3) cover a wide range of viscosity and elasticity. All experiments were also repeated with tap water as the low viscosity, inelastic and Newtonian reference liquid. The surface tension of the test liquids were measured with use of a dynamic interfacial tensiometer (DCAT21, Dataphysics, Germany). The physical properties of the test liquids are given in Table 4-1.

Table 4-1: Physical properties of the test liquids at 22 °C.

Test liquid		**Density ($kg\ m^{-3}$)**	**Surface Tension ($mN\ m^{-1}$)**
Water		997.04	71.97
Glucose		1293.50	74.33
Boger		1251.10	75.28
	Concentration (wt.%)		
CMC	**0.3**	996.21	73.70
	0.5	995.65	73.92
	0.7	995.10	74.28
Xanthan gum	**0.3**	995.98	75.83
	0.5	995.31	76.07
	0.7	994.61	77.02

The rheological characterization of the test liquids was carried out by a modular compact rheometer (MCR-501, Anton Paar) with a double-gap couette geometry. In order to measure the apparent viscosity (μ_{app}), steady-shear experiments were conducted in a shear rate range of 1 to 1500 s^{-1} (which corresponds to the range of shear rates in the column). The apparent viscosity of the solutions as a function of shear rate is represented in Figure 4-1. As expected and it is obvious from Figure 4-1, both the Glucose and Boger solutions show constant viscosity over the range of shear rates applied in the rheometer and, thus, are Newtonian. On the other hand, the CMC and Xanthan gum solutions exhibit a strong deviation from Newtonian type of fluids by showing shear-thinning behaviors. In addition, increasing the concentration of CMC and Xanthan gum polymers in these solutions leads to higher viscosity and stronger shear-thinning behavior.

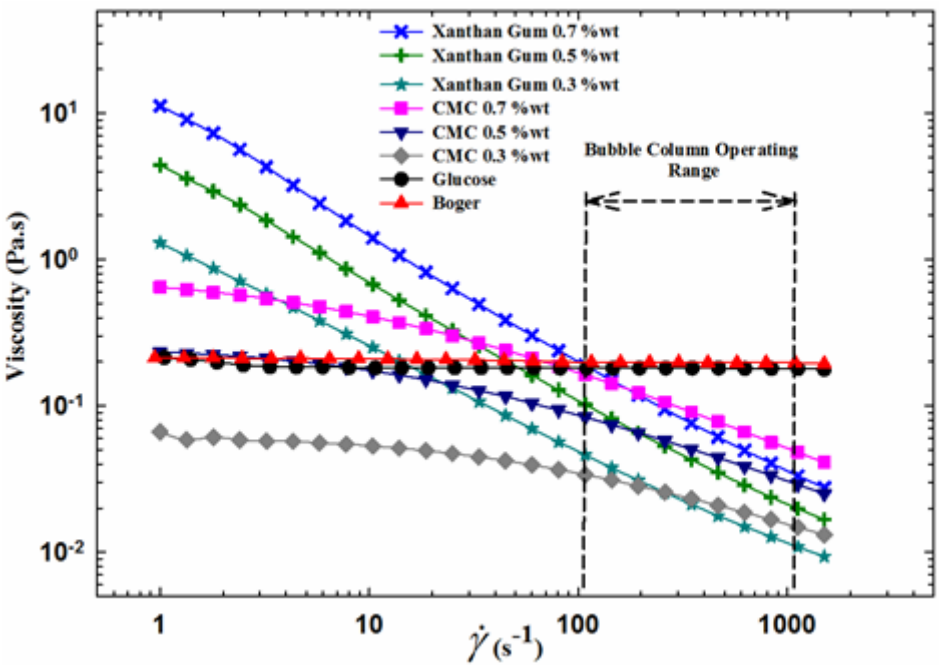

Figure 4-1: Variation of the apparent viscosity of the solutions with shear rate.

Various models are proposed in the literature to predict the apparent viscosity of shear-thinning liquids (Carreau et al., 1979; De Kee & Carreau, 1993). In the present study, we have examined different models and eventually it was found that the power law model can perfectly characterize the behavior of the test solutions. The power law model can predict the apparent viscosity as a function of shear rate as follows (Schowalter, 1960):

$$\mu_{app.} = K\dot{\gamma}^{n-1} \tag{4.1}$$

Where *K* is the consistency index and is directly related to the viscosity of the solution. *n* is the flow index of the fluid and indicates the degree of shear-thinning. The power law parameters for the solutions applied in this study are summarized in Table 4-2. The higher *K* means higher apparent viscosity of the solution and the smaller flow index specifies the more shear-thinning behavior of the solution. As it is obvious from the values of parameters *K* and *n* in Table 4-2, increasing the concentration of polymer in both CMC and Xanthan gum solutions results in a higher apparent viscosity and stronger shear-thinning behavior.

Table 4-2: Power law parameters for the liquids used in this study.

Test liquid		K (Pa s^n)	n	Correlation ratio (R^2)
Glucose		0.185	1	0.99
Boger		0.135	0.98	0.98
	Concentration (wt.%)			
CMC	**0.3**	0.08	0.79	0.93
	0.5	0.32	0.68	0.89
	0.7	0.88	0.61	0.93
Xanthan gum	**0.3**	1.01	0.31	0.97
	0.5	3.29	0.21	0.92
	0.7	7.06	0.16	0.92

Another parameter that can be measured through the steady-shear experiments is the first normal stress difference, which is a measure of the elasticity of the solution. Historically, the first normal stress difference in steady-shear flow is the first evidence of the presence of elasticity in the solution. Although the first normal stress difference is useful in the solution characterization, it is not suitable for interpreting the rheological effects of solutions for the goal of this study. Therefore, using other parameters that can describe the simultaneous effects of elasticity and viscosity is more desirable. However, today, thanks to the widespread availability of convenient and accurate measurements, such as the dynamic moduli via oscillatory frequency sweep tests, less normal stress measurements are made. In an oscillatory frequency sweep test, the speed of sample deformation is changed in its linear viscoelastic range and this can be done when the frequency of oscillation is ramped while the amplitude is held constant (Bui et al., 2012; Morrison, 2001).

According to our previous work (Amin Esmaeili et al., 2015), it was found that along with the apparent viscosity, storage modulus (G') and loss modulus (G'') of viscoelastic solutions can be considered as appropriate candidates for a complete description of the rheological effects of viscoelastic solutions in bubble column reactors. In the present study, an oscillatory amplitude sweep test is performed first to define the linear viscoelastic range at a constant frequency of 10 rad s^{-1} and a strain amplitude ramp from 1 to 300%. It is observed that the linear viscoelastic response lies in strains of less than 15%. Once the range of linear viscoelasticity is defined, the

oscillatory frequency sweep tests are conducted at a constant strain of 10% and a frequency ramp from 1 to 200 rad s^{-1} in order to measure G' and G'' of the solutions. The results of the oscillatory frequency sweep test for the solutions used in this work are illustrated in Figure 4-2. Since the glucose solution is not elastic, it does not show any measurable G' during the tests. Therefore, only the dynamic moduli of viscoelastic solutions are reported in Figure 4-2.

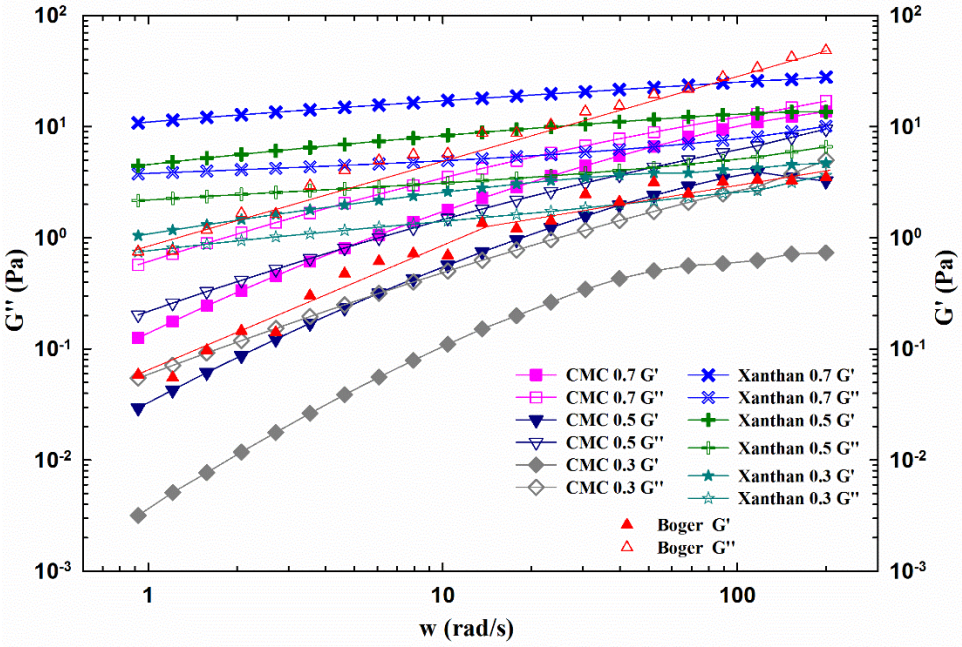

Figure 4-2: The variation of dynamic moduli of the test solutions with angular frequency.

The low and high frequencies correspond to slow and fast deformations of fluid, respectively. However, the G' and G'' data can be used to evaluate if the response of the fluid to deformation at a specific frequency is a viscous response or an elastic one. At a given frequency, if G' is smaller than G'' ($\frac{G'}{G''} < 1$), the response of the fluid to deformation is dominated by viscosity and the fluid behaves more viscously while when G' is higher than G'' ($\frac{G'}{G''} > 1$), the fluid acts more elastically. Experimental results (Figure 4-2) show that increasing the concentration of polymers increases G' and G'' in both CMC and Xanthan gum solutions. Another important observation in Figure 4-2 is that for all CMC solutions, the $\frac{G'}{G''}$ ratio is less than unity corresponding to a dominating viscous

response in the CMC solutions at any given frequency. In contrast, the $\frac{G'}{G''}$ ratio is more than unity for all Xanthan gum solutions signifying the stronger elastic behavior and the dominance of the elastic property of the Xanthan gum solutions in the investigated range of frequency. Moreover, for the Boger solution, the G' values are very small compared with the G'' values, which means the Boger solution is elastic but with a strong viscous property. The rheological properties of the test solutions are summarized in Table 4-3.

Table 4-3: Rheological properties of the test liquids at 22 °C.

Test liquid		**Properties**	$\frac{G'}{G''} \approx$	**Effects**
Glucose		Newtonian and Highly viscous	**0**	Strong viscosity effects
Boger		Viscoelastic	**0.11**	Elasticity << viscosity
	Concentration (wt.%)			
CMC	**0.3**	Viscoelastic	**0.20**	Elasticity < viscosity
	0.5	Viscoelastic	**0.36**	Elasticity < viscosity
	0.7	Viscoelastic	**0.54**	Elasticity < viscosity
Xanthan gum	**0.3**	Viscoelastic	**1.60**	Elasticity > viscosity
	0.5	Viscoelastic	**2.68**	Elasticity < viscosity
	0.7	Viscoelastic	**3.26**	Elasticity < viscosity

Since the range of the deformation frequency that the liquid phase experiences in a bubble column is very narrow (from 5 Hz to 50 Hz particularly in the bubble column used in this study), the $\frac{G'}{G''}$ ratio is almost constant in this range and thus only the average values of $\frac{G'}{G''}$ ratio are reported in Table 4-3. More details about this subject can be find elsewhere (Amin Esmaeili et al., 2015). It should be noted that the rheological properties of the solutions cannot be exactly reproduced since they are affected by degradation and the mixing technique. Therefore, to avoid any uncertainty associated with the change in the rheological properties, the solutions were sampled and

characterized several times during preparation and the experiments to ensure stable and constant values of rheological parameters.

4.2.3 Fiber Optic Probes Measurements

A fiber optic probe is sensitive to the change in the refractive index of the phase in contact with the probe tip. An opto-electronic box generates a light beam and sends it to the optical fibers of the probe. The light is refracted when the probe tip lies in liquid while it is reflected back when the probe tip penetrates the bubbles. The reflected light signals are received and transformed into voltage by photoelectric multipliers and sent to the data acquisition board to be saved. The miniaturization of fiber optic probes permits an accurate measurement of local hydrodynamics even at high gas velocity or in opaque systems. In this study, two single-tip optical fiber probes were fabricated with the aim of investigating the local bubble properties (including bubble frequency, bubble size and its rise velocity). The main part of the probes contains 72 emitting and receiving plastic fiber strands each having a diameter of 250 μm with the core refractive index and numerical aperture of 1.49 and 0.5, respectively. These fiber strands are uniformly mixed together and are arranged in an alternative array at the center of probe tip that make them to function in a similar manner to a single-tip probe. The fiber strands are protected by a stainless tube with a tip and body diameter of 3 and 4.7 mm, respectively. This configuration makes it possible to detect the information of a wide range of bubble sizes and to avoid the disturbance of the flow. More details about our in-house made optical fiber probes can be found elsewhere (Shabanian & Chaouki, 2014). The output from the fiber optic probe is a series of crenel-like pulses. Figure 4-3 schematically shows a typical signal of the fiber optic probe created when a single bubble passes the probe. As shown in Figure 4-3, when a gas bubble penetrates the probe and starts moving upward, the intensity of the reflected light changes from point A to point B. It is obvious that the detection of the gas-liquid interface does not result in an instantaneous change of the output voltage, but a transient exists between the air and liquid voltage levels. The bubble rise time, t_{rise}, is defined as the time taken for the voltage level to rise from level A to level B. As long as the bubble covers the entire cross area of the probe tip, the voltage level remains constant (from point B to point C). Once the bubble starts leaving the probe tip, the voltage level decreases until the complete departure of bubbles (from point C to point D). The bubble residence time, $t_{residence}$, can

be defined as the time interval from the start of the ascending slope to the start of the descending slope (i.e., from point A to point C).

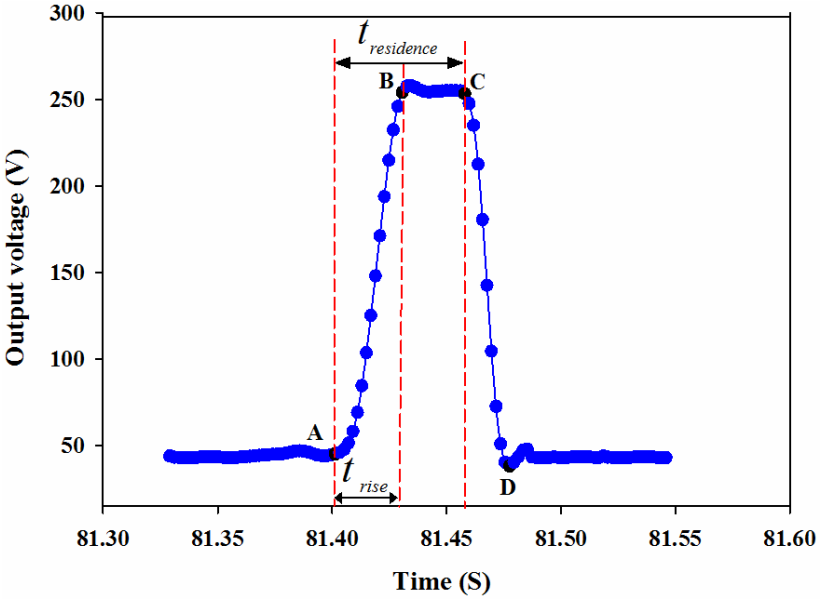

Figure 4-3: Typical voltage signal caused by the passage of a single bubble across the probe tip.

The local gas holdup is defined as the fraction of volume occupied by the dispersed gas phase within a known volume of fluid mixture (Mueller, 2009):

$$\varepsilon_{G,local} = \frac{V_{G,local}}{V_{G,local} + V_{L,local}} \tag{4.2}$$

The Ergodic theory declares that the ensemble average is equivalent to the time average. By considering the Ergodic hypothesis, the spatially (volume) averaged local gas holdup (Eq.(4.2)) can be replaced by its equivalent time-averaged local gas holdup (Mueller, 2009):

$$\varepsilon_{G,local} = \frac{t_G}{t_G + t_L} \tag{4.3}$$

In the present work, the time-averaged gas holdup was defined as the ratio of time that the probe spends in the gas phase divided by the total measurement time at each point of space within the

column, as follows:

$$\varepsilon_{G,local} = \frac{\sum_{i=1}^{n} t_{residence,i}}{T_{measurement}} \tag{4.4}$$

To study the effects of liquid phase rheology on the radial distribution of bubble properties, the probes were placed in seven different radial positions across the column diameter (i.e., r= -0.148, -0.1, -0.05, 0, 0.05, 0.1 and 0.148 m). The average gas holdup can then be deduced by using the radial local gas holdup profile as follows:

$$\bar{\varepsilon_G} = \frac{1}{\pi R^2} \int_0^R \varepsilon(r)(2\pi r \mathrm{d}r) \tag{4.5}$$

The bubble frequency at any radial position is measured by:

$$f_b = \frac{N}{T_{measurement}} \tag{4.6}$$

Where N is the number of bubbles recorded in time $T_{measurement}$. Cartellier et al. (Alain Cartellier, 1990, 1992; A. Cartellier & Barrau, 1998) developed an alternative method to measure bubble velocity by doing a detailed analysis on the output voltage of a single fiber optic probe. Serdula and Loewen (Serdula & Loewen, 1998) and Rojas and Loewen (Rojas & Loewen, 2007) applied this method to measure bubble size and they proposed that this method represents a promising technique for bubble size measurements. Based on this method, the bubble velocity can be calculated by measuring the time taken by the head of bubble to move from the bottom to the top of the probe tip (i.e., t_{rise}) from:

$$v_{b,i} = \frac{D_{probe}}{t_{rise}} \tag{4.7}$$

The mean bubble velocity is then calculated by taking the arithmetic mean of individual bubbles velocities as follows:

$$v_b = \frac{1}{N}\sum_{n=1}^{N} v_{b,i} \tag{4.8}$$

The bubble residence time, $t_{residence}$, is the time period that the probe tip is present in the bubble that is proportional to the bubble chord length. Once the bubble velocity is known, the bubble chord length can be calculated by multiplying the bubble velocity with the bubble residence time as follows:

$$L_{b,i} = v_{b,i} \times t_{residence} \tag{4.9}$$

Before measuring the bubble properties in this study, a series of single bubble experiments were conducted in a specially designed vessel in order to know where and how the optical fiber probes touch the bubbles. It is worth mentioning that at each space point within the column and for any given superficial gas velocity, measurements were usually taken for three minutes to insure a sufficiently long measurement time providing a good statistical representation for the sampled point. Moreover, to facilitate the comparison between different effects of liquid phase rheology on the bubble frequency and bubble rise velocity, only the results for CMC and Xanthan gum solutions in a concentration of 0.5 wt.% are displayed and the data for other concentrations are mainly used in developing the correlations for bubble size and gas holdup prediction.

4.3 Results and Discussion

4.3.1 The effect of liquid phase rheology on bubble frequency

Bubble frequency as a function of superficial gas velocity in the middle (L/D =0.41) and top (L/D=0.95) zone of the column is shown in Figure 4-4.

(a) (b)

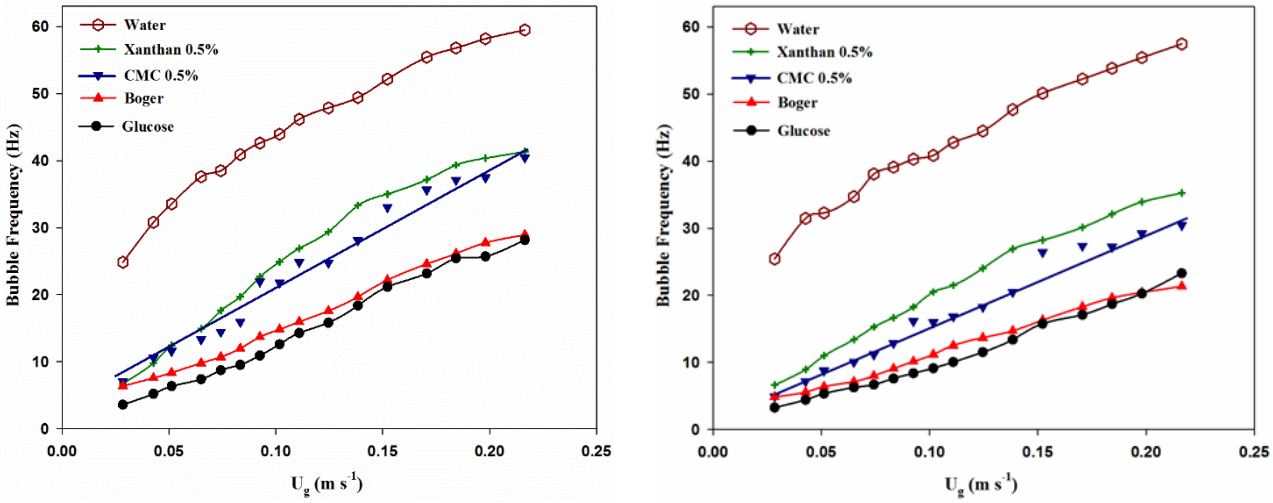

Figure 4-4: Variation of bubble frequency with superficial gas velocity for different solutions: (a) in the middle zone of the column and (b) in the top zone of the column.

Kuncová and Zahradnik (Kuncová & Zahradník, 1995) investigated the effects of liquid viscosity on the gas holdup and bubble frequency in a bubble column containing Newtonian Saccharose solution. They have shown that increasing the liquid viscosity decreases the bubbling frequency, which has a negative effect on the stability of the homogeneous bubbling regime. As is obvious from Figure 4-4, the bubble frequency increases with superficial gas velocity in both the middle and top zones of the column. As the superficial gas velocity increases, the gas throughputs increase and, consequently, the number of bubbles formed in the gas distributor is higher. Comparing the bubble frequency of different solutions reveals that water, which has the lowest viscosity, shows the highest bubble frequency, while the Glucose solution, as the most viscous solution, has the lowest bubble frequency, which is in good agreement with the results reported by Kuncová and Zahradnik (Kuncová & Zahradník, 1995). In fact, increasing the viscosity results in the existence of large drag forces promoting the formation of larger bubbles and bubble coalescence in the distributor zone and, therefore, lower bubble frequency. Bubble frequency in the Boger solution, which has a viscosity identical to the Glucose solution but is slightly elastic ($\frac{G'}{G''} \ll 1$), is slightly higher than that in the Glucose solution ($\frac{G'}{G''} \approx 0$). Since CMC and Xanthan gum solutions are

shear-thinning and less viscous in the column operating range (see Figure 4-1), the bubble frequency in these solutions is considerably higher than that in the Glucose and Boger solutions. On the other hand, the bubble frequency in the Xanthan gum solution is higher than that in CMC solution in both the middle and top zones of the column. According to the results of the oscillatory frequency sweep tests depicted in Figure 4-2, it can be observed that the Xanthan gum solution has a dominating elastic modulus ($\frac{G'}{G''} > 1$) compared to the CMC solution ($\frac{G'}{G''} < 1$). It seems that the higher elasticity effects in the Xanthan gum solution prevent bubble coalescence and, consequently, lead to presence of more bubbles and higher bubble frequency in this system. Moreover, except for water, the bubble frequency in the middle zone of the column is higher than that in the top zone of the column indicating the dominating coalescence effects along the column height that lead to formation of larger bubble and a decrease in the number of bubbles in viscous solutions. These results are in good agreement with the results reported in Chapter 3 on the effect of rheological properties of liquids on the gas holdup and bubble size. It is worth mentioning that the effects of superficial gas velocity on bubble frequency diminish with increasing viscosity.

The radial profile of bubble frequency in the middle and top zones of the column at three selected superficial gas velocities is presented in Figure 4-5 for all operating solutions. As can be seen from Figure 4-5, the bubble frequency radial profiles change from flat at low superficial gas velocity to parabolic at high superficial gas velocity. This evolution in the shape of the bubble frequency radial profile is obvious for almost all operating liquids, which is consistent with the radial profile of bubble frequency reported by Xue et al. (Xue, 2004; Xue, Al-Dahhan, Dudukovic, & Mudde, 2008)

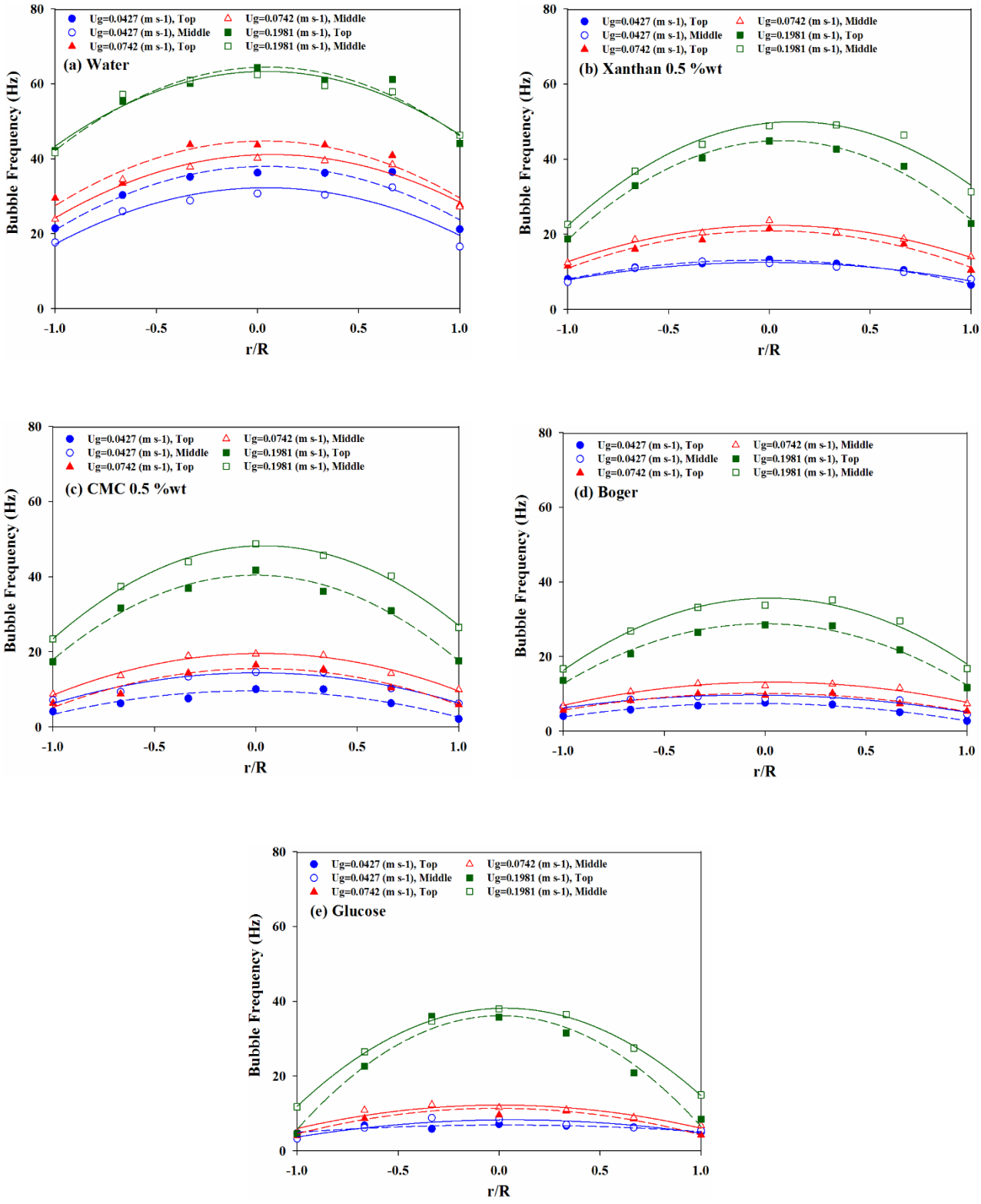

Figure 4-5: Radial dependence of bubble frequency for different operating systems and superficial gas velocities in the middle and top zones of the column.

4.3.2 The effect of liquid phase rheology on bubble rise velocity

Bubble rise velocity is one of the key hydrodynamic parameters in bubble column reactors that is used in evaluating the drag forces and in computational fluid dynamics. However, the information available in the literature provides essentially the experimental results on the single bubble rise velocity and not a swarm of bubbles in viscous and non-Newtonian liquids. In this study, the mean bubble rise velocity for different operating solutions in the middle and top zone of the column is obtained experimentally and plotted in Figure 4-6.

(a) (b)

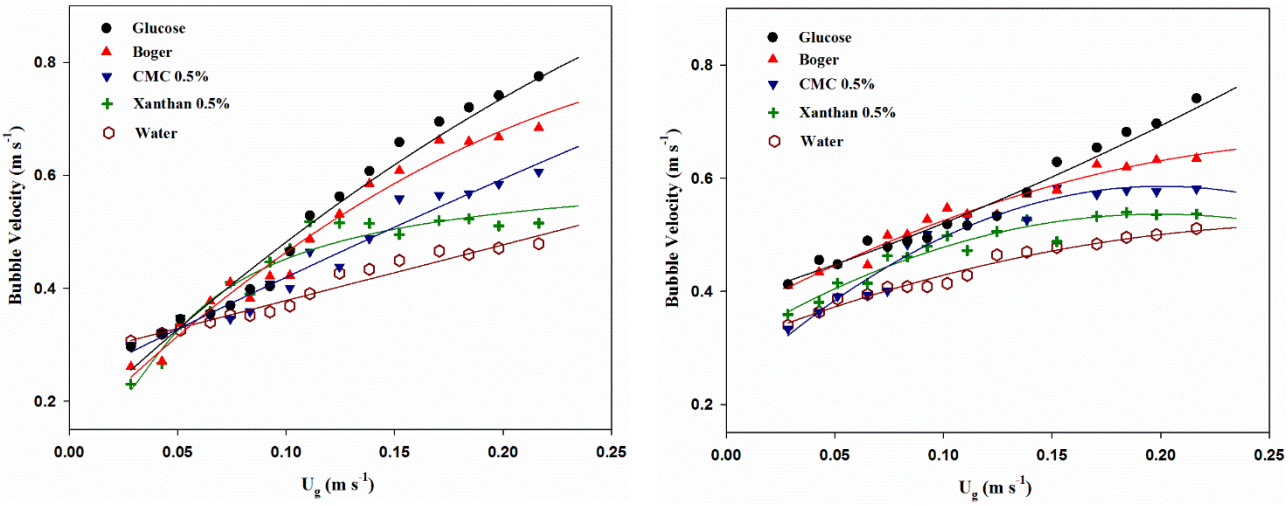

Figure 4-6: Mean bubble rise velocity versus superficial gas velocity for different operating solutions: (a) in the middle zone of the column and (b) in the top zone of the column.

Figure 4-6 demonstrates that the mean bubble rise velocity increases by increasing the superficial gas velocity for all operating liquids in both the middle and top zones of the column. This can be related to the higher inertia forces exerted on the bubbles in the gas distributor at higher superficial gas velocities. Moreover, the change in the bubble rise velocity with superficial gas velocity is more significant in the middle zone of the column rather than in the top zone of the column, which is far from the gas distributor.

The bubble rise velocity is directly related to the bubble size. Due to the buoyancy force effects, bigger bubbles rise faster. The effects of liquid phase rheology on bubble size have been studied in the previous work of the authors (Amin Esmaeili et al., 2015). Although there is no clear effect of the liquid phase rheology on the bubble rise velocity at low superficial gas velocities (i.e., $U_g \leq$ 0.14 m s^{-1}), there is a noticeable difference in the bubble rise velocity for different solutions at higher superficial gas velocities. As it can be observed in Figure 4-6, bubbles rise with the lowest velocity in water while they move faster in viscous solutions.

The bubble rise velocity is highest in the Glucose solution since the bubble size in this liquid is bigger than in the other liquids (Amin Esmaeili et al., 2015). The elastic effects in the Boger fluid ($\frac{G'}{G''} \ll 1$) lead to smaller bubble sizes and, thus, slower moving bubbles in comparison with the Glucose. It is also reported by Soto et al. (Soto, Goujon, Zenit, & Manero, 2006) that the presence of normal stresses (elasticity) in liquid can change the bubble shape, which evidently causes a drag reduction and, consequently, an increase in the bubble velocity. The bubble size in the Xanthan gum solution with dominating elastic effects ($\frac{G'}{G''} > 1$) is smaller than that in the CMC solution ($\frac{G'}{G''} < 1$) (Amin Esmaeili et al., 2015). In addition, due to the shear-thinning characteristics and elastic effects of CMC and Xanthan gum solutions, the passage of bubbles in these liquids can lead to a local decrease in the viscosity. A combination of all these effects may cause bubbles to rise slower in Xanthan gum solutions as is obvious in Figure 4-6.

Figure 4-7 shows the bubble rise velocity radial profile obtained under different superficial gas velocities in the middle and top zones of the column for all operating liquids.

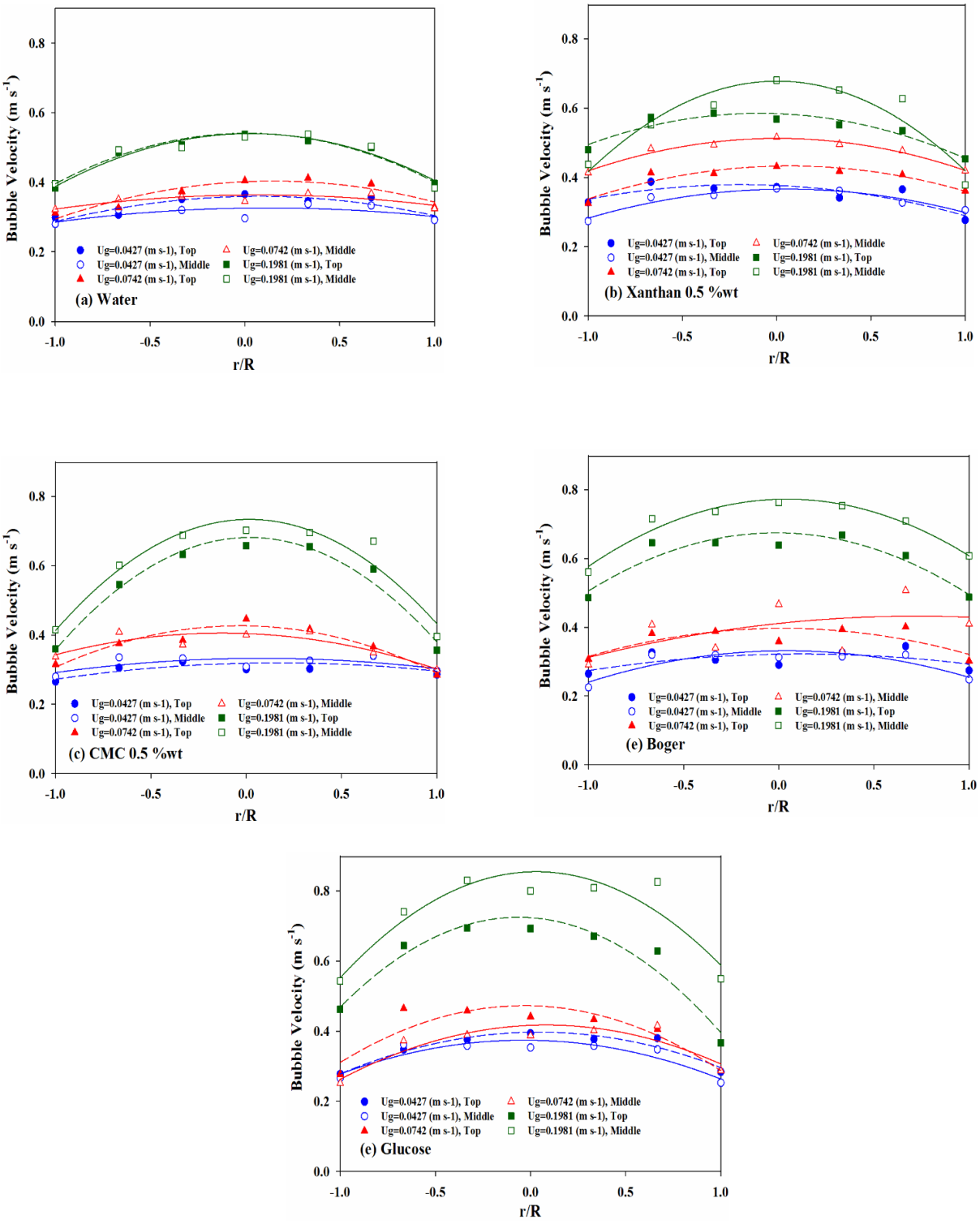

Figure 4-7: Bubble rise velocity profile evolution for different operating systems and superficial gas velocities in the middle and top zones of the column.

As it is evident in Figure 4-7, the superficial gas velocity has a significant effect on the shape of the bubble rise velocity profile. At low superficial gas velocities, the bubbles move upward with a relatively uniform radial velocity while at high superficial gas velocities, the radial profile of the bubble rise velocity is pronounced due to the existence of a strong internal liquid circulation enhancing bubble rise speed in the central core of the column. Therefore, as it is obvious from

Figure 4-7, at low superficial gas velocities the bubble rise velocity profile is relatively flat while it becomes more parabolic at a high superficial gas velocity with a clear maximum at the center of the column and a minimum near the wall. This trend can be observed for almost all fluids applied in this study.

4.3.3 The effect of operating conditions on the bubble chord length radial profile

The effects of liquid phase rheology on the bubble chord length have been completely explained elsewhere (Amin Esmaeili et al., 2015). In this work, only the bubble chord length radial distributions, which are measured under different superficial gas velocities in the middle and top zones of the column, are presented in Figure 4-8.

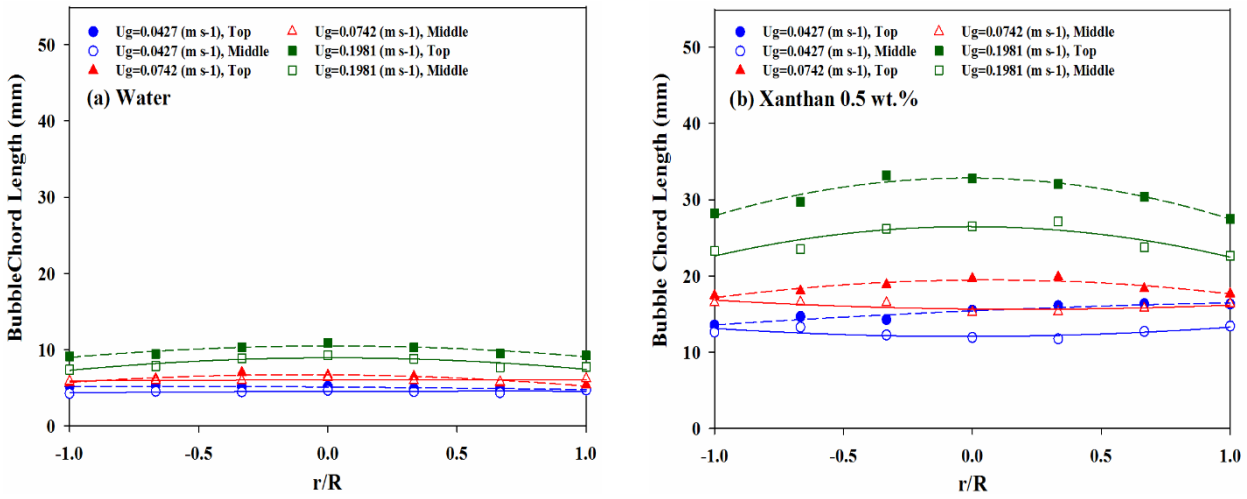

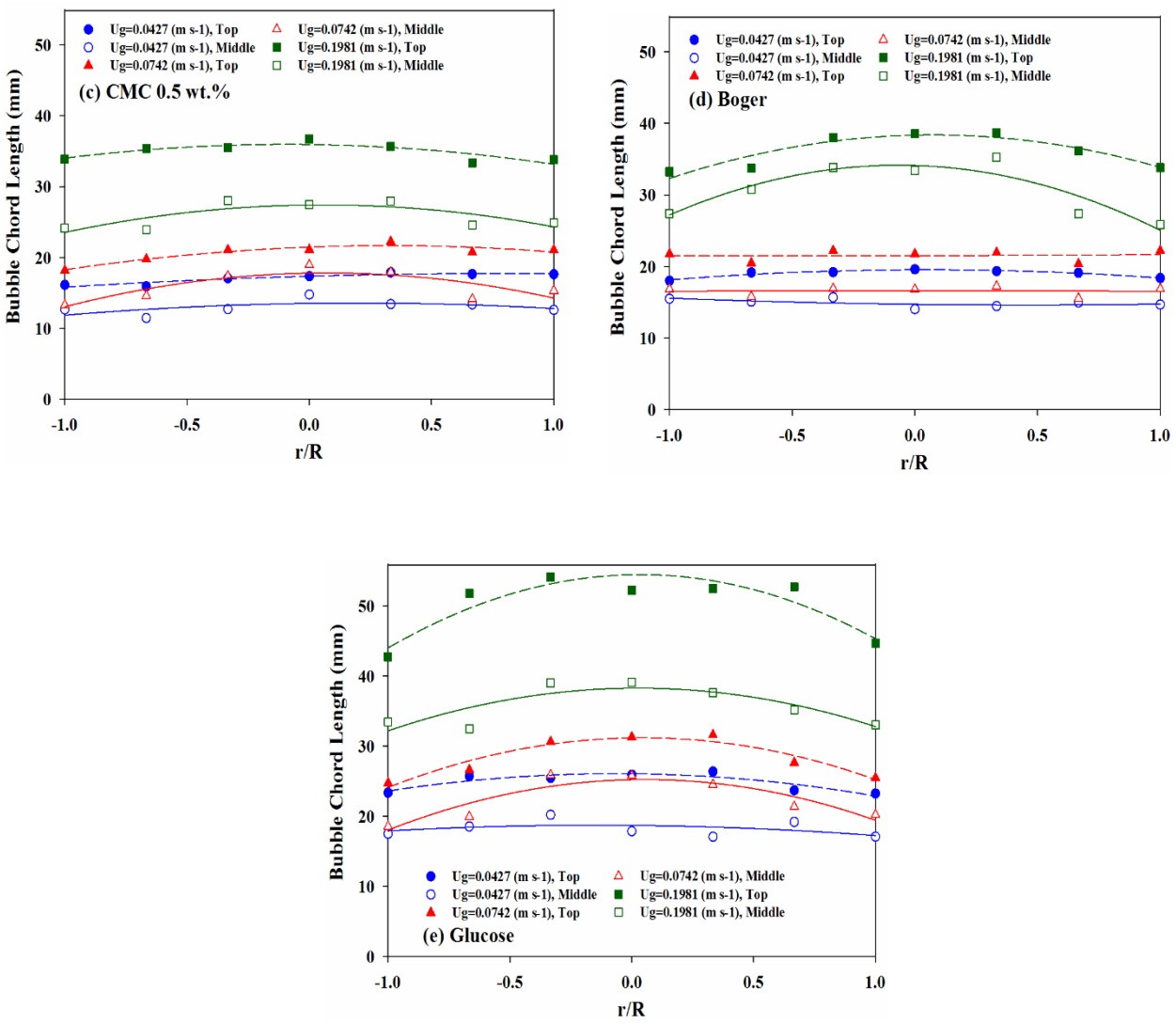

Figure 4-8: Radial profiles of bubble chord length at different superficial gas velocities determined in the middle and top zones of the column.

The superficial gas velocity does not alter the bubble chord length profile to any significant extent in water. On the other hand, the bubble chord length radial profiles in other operating liquids are fairly uniform at low superficial gas velocities in both the middle and top zones of the column. However, at higher superficial gas velocities the bubble chord length changes significantly along the radial direction. To better understand the axial variation in the bubble chord length, the values of this parameter in the middle and top zones of the column are compared by calculating the root mean square defined as follows:

$$L_{b,rms} = \sqrt{\frac{1}{N}\sum_{i=1}^{N}\left[L_{\mathrm{b},i}(Top\ zone) - L_{\mathrm{b},i}(Middle\ zone)\right]^2} \tag{4.10}$$

The root mean square of the bubble chord length is calculated for different solutions and is presented in Table 4-4.

Table 4-4: Root mean square of the bubble chord length.

Test liquid		$L_{b,rms}$ (mm)	**Change Trend**
Water		0.8035	↑
Glucose		10.4802	↑
Boger		6.6854	↑
	Concentration (wt.%)		
CMC	**0.3**	4.4948	↑
	0.5	6.4967	↑
	0.7	6.5000	↑
Xanthan gum	**0.3**	2.8352	↑
	0.5	4.3931	↑
	0.7	6.1921	↑

↑: Increasing

According to the values of the root mean square of the bubble chord length reported in Table 4-4, it is obvious that the bubble chord length in water does not differ significantly along the column height, while in Glucose and Boger solutions, the bubble chord length increases remarkably as they rise toward the column surface. As explained earlier in this work, the highly viscous Glucose solution promotes bubble coalescence and, consequently, the bubbles become bigger as they rise upward in the column. The root mean square of the bubble chord length in the Boger solution is smaller than that in the Glucose solution. In comparison with Glucose, the Boger solution is slightly elastic ($\frac{G'}{G''} \ll 1$) and the elasticity effects of the Boger solution can hinder bubble coalescence and, therefore, the bubble chord length changes less axially compared to the Glucose solution. In both CMC and Xanthan gum solutions, the root mean square increases with increasing polymer concentration. Moreover, since the elastic effects are dominant in Xanthan gum solutions

($\frac{G'}{G''} > 1$) in comparison with those in CMC solutions ($\frac{G'}{G''} < 1$), as a result, the root mean square at each identical concentration (viscosity) in Xanthan gum solution is less than that in CMC solutions.

4.3.4 Developing models for predicting bubble size and gas holdup

The gas holdup and bubble size are the two main hydrodynamic parameters of bubble columns. The gas holdup has a great impact upon the design of bubble column reactors. The total volume of the reactor for any operating conditions is determined by the maximum gas holdup that must be accommodated. The gas holdup in combination with the bubble size influences the specific interfacial area available for mass transfer and the reaction rate. As it has already been mentioned, viscous Newtonian and non-Newtonian media are frequently processed in bubble columns in many industries. The design of the bubble column reactors is primarily conducted by the use of empirical or semi-empirical correlations based mainly on the experimental data. Therefore, for a proper design, optimization, and scale-up of bubble columns, it is extremely important to use correct correlations to estimate the gas holdup and bubble size in such media. To date, the correlations available in literature are applicable mostly in Newtonian media and deviate significantly from experimental data when used in non-Newtonian and viscoelastic liquids. To overcome this problem, two correlations are proposed with the aid of our experimental data to better predict the bubble size and gas holdup in bubble columns operating with a wide range of non-Newtonian and viscoelastic liquids. The gas holdup and bubble chord length measured in the experimental fluids are fully reported in our previous work (Amin Esmaeili et al., 2015) and are used in this study to develop the correlations for predicting bubble size and gas holdup.

One of the issues in using fiber optic probes is that the bubble diameter cannot be measured by the probe directly since the probe does not always intersect the bubble at its center and also because bubbles are not spherical in many processes. Therefore, only the bubble chord length can be measured by means of optical fiber probes rather than bubble diameter. The chord length is also strongly affected by the pierced conditions, such as the pierced position and the angle between the probe and the bubble velocity vector. In literature, there have been several studies carried out to evaluate the equivalent bubble diameter from the chord length distribution. With the aid of

geometrical probability analysis for nearly spherical bubbles, it was shown that the equivalent mean bubble diameter can be determined by the average measured cord length multiplied by a correction factor of 1.5 (Boyer, Duquenne, & Wild, 2002; Rojas & Loewen, 2007; Saberi et al., 1995; Takeo, 1971; Thang & Davis, 1979; Ueyama, Morooka, Koide, Kaji, & Miyauchi, 1980) and this correction factor was used in the present study to convert the mean bubble chord length to the equivalent mean bubble diameter.

Dimensionless analysis is applied in order to derive a generalized correlation for bubble size that would include the relative effects of the physical and rheological properties of the liquid phase and operation conditions. According to the observations made during the experiments, bubble size was conceivably affected by the following factors involving three dimensions (mass, time and length):

$$d_B = f(D_c, \sigma, \rho_L, \mu_L, U_g, g, G', G'') \tag{4.11}$$

Applying Buckingham's π theorem specifies that four independent dimensionless groups can be formed as follows:

$$\pi_1 = \frac{gD_c^2\rho_L}{\sigma} \qquad \pi_2 = \frac{gD_c^3}{\vartheta_L^2} \qquad \pi_3 = \frac{U_g}{\sqrt{gD_c}} \qquad \pi_4 = \frac{G'}{G''}$$

Rearranging Eq. (4.11) by considering the dimensionless groups leads to:

$$\frac{d_B}{D_c} = f\left(\frac{gD_c^2\rho_L}{\sigma}, \frac{gD_c^3}{\vartheta_L^2}, \frac{U_g}{\sqrt{gD_c}}, \frac{G'}{G''}\right) \tag{4.12}$$

The first dimensionless group on the right side of Eq. (4.12) that includes the effect of surface tension is the Bond number (*Bo*), which is a measure of the importance of the surface tension forces compared to the body forces. The second group is the Galilei number (*Ga*), which is the gravity forces divided by the viscous forces and mainly represents the influence of liquid viscosity. The effect of superficial gas velocity is taken into account in the third group that is the Froude number (*Fr*), which is the ratio of the body inertia to the gravitational forces and, finally, the last

dimensionless group introduces the effects of the rheological properties of the liquid phase in the model.

Our experimental results show that the bubble size and gas holdup change with the rheological effects of the liquid phase depending on the ratio of $\frac{G'}{G''}$ being more or less than unity. In order to develop a correlation that can be applicable in both Newtonian ($\frac{G'}{G''} = 0$) and viscoelastic ($\frac{G'}{G''} \neq 0$) solutions and to emphasise the effect of $\frac{G'}{G''}$ ratio, the best form for the effect of rheological properties is found to be exponential. By considering the exponential form for the rheological effects and rearranging Eq. (4.12) according to the dimensionless numbers defined, the following correlation is proposed:

$$\frac{d_B}{D_c} = \alpha_1 \, Bo^{\alpha_2} \, Ga^{\alpha_3} \, Fr^{\alpha_4} \, e^{\alpha_5\left(1-\frac{G'}{G''}\right)} \tag{4.13}$$

Similar analysis has been done by Akita and Yoshida (Akita & Yoshida, 1974). However, by considering the rheological effects of the liquid phase in the correlation, we subsequently employed a modification on the original correlation proposed by Akita and Yoshida (Akita & Yoshida, 1974).

In order to estimate the effective apparent viscosity of a non-Newtonian fluid in the bubble column, the effective average shear rate should be known. Unknown shear rates and apparent viscosities can lead to the incorrect design and poor performance of bubble columns operating with non-Newtonian liquids. Several researchers have applied the relation proposed by Nishikawa et al. (Nishikawa et al., 1977) for bubble column reactors. According to Nishikawa et al. (Nishikawa et al., 1977), the average shear rate can be related to the superficial gas velocity by means of a linear function as follows (Chisti & Mooyoung, 1989; W. D. Deckwer et al., 1982; Ghosh & Upadhyay, 2007):

$$\dot{\gamma}_{av} = 5000 \, U_g \tag{4.14}$$

Where $\dot{\gamma}_{av}$ and U_g are the average shear rate and superficial gas velocity, respectively. By considering the range of superficial gas velocity applied in this study and using Eq. (4.14), the effective shear rate inside the bubble column lies in the range of 100 to 1000 s^{-1}.

The constants of Eq. (4.13) are then evaluated using the Genetic Algorithm method (*ga function*) in MATLAB by fitting the data of a viscous Newtonian solution (i.e., Glucose) and non-Newtonian viscoelastic solutions (i.e., CMC, Xanthan, and Boger); that means a total of 136 data points. By replacing the evaluated constants in Eq. (4.13), the final form of correlation for the prediction of bubble size will be as follows:

$$\frac{d_B}{D_c} = 18.7\, Ga^{-0.15}\, Fr^{0.53}\, e^{0.1\left(1-\frac{G'}{G''}\right)} \tag{4.15}$$

$$1.4 \times 10^7 < Ga < 2.4 \times 10^{11}$$

$$0.06 < Fr < 0.138$$

$$0 < \frac{G'}{G''} < 3.26$$

The agreement between the experimental and predicted bubble size is within the mean absolute percentage error (MAPE), standard error, and 95% prediction interval of 9.3%, ±2.8 mm, and ±6 mm, respectively. In order to have a better view of the validity of the derived correlation, the bubble sizes measured experimentally are compared with those predicted by Eq. (4.15) for different solutions and are displayed in Figure 4-9.

From Figure 4-9, it can be seen that the proposed correlation can predict the experimental data with fairly good accuracy. The present correlation predicts an increase in the bubble size with increasing liquid viscosity, superficial gas velocity and decreasing $\frac{G'}{G''}$. This latter trend is consistent with the results obtained experimentally and can satisfactorily describe the influence of the fluid rheology on bubble size. Moreover, as seen in Table 4-1, surface tension does not differ significantly among the fluids used in this work and, consequently, the Bond number that includes the surface tension term does not change remarkably in the operating range of the column. Therefore, the model cannot be correlated with this group and as a result it does not appear in the final form of the proposed correlation.

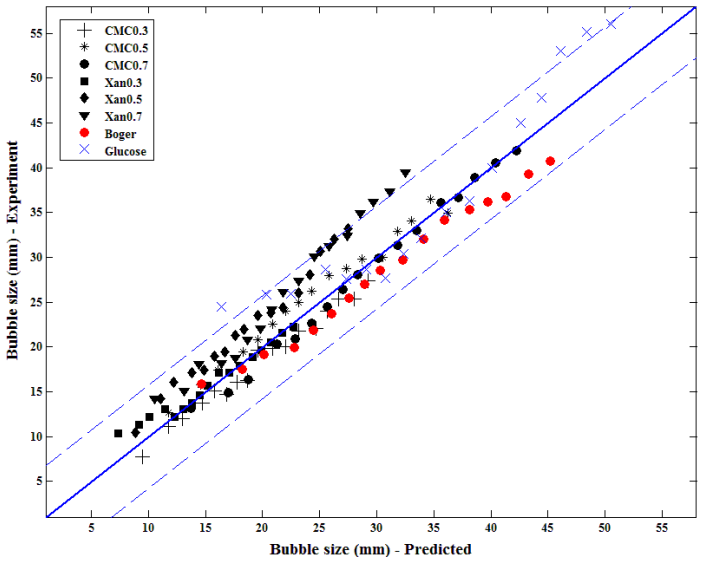

Figure 4-9: Comparison between the experimental and predicted value of bubble size.

A comprehensive literature survey was conducted to find the most reliable models available to predict the bubble size and gas holdup in bubble column reactors. Akita and Yoshida (Akita & Yoshida, 1974) have developed a model based on dimensionless numbers that can predict the bubble size in bubble columns operating in the presence of liquids with different viscosities. They have shown that there is good accordance between the bubble size measured experimentally with those predicted by their correlation. Wilkinson et al. (Wilkinson, Haringa, & Van Dierendonck, 1994) have proposed an empirical equation to estimate the bubble size in bubble columns operating with several types of liquid and gas phases. Gaddis and Vogelpohl (Gaddis & Vogelpohl, 1986) also theoretically developed an equation to predict the bubble diameter in quiescent liquids under constant gas flow conditions. Their equation has been shown to be valid for predicting the bubble diameter in a wide range of operating regimes and in liquids with viscosities from very low up to very high values. Table 4-5 summarizes the aforementioned models.

Table 4-5: Summary of the bubble size models proposed by different researchers.

Research group	Correlation proposed	Range of parameters
Akita and Yoshida (Akita & Yoshida, 1974)	$\frac{d_B}{D_c} = 26(Bo)^{-0.50}(Ga)^{-0.12}(Fr)^{-0.12}$	$0.009 \leq u_g \leq 0.07\ m\ s^{-1}$ $0.077 \leq D_c \leq 0.30\ m$ $0.001 \leq \mu_L \leq 0.021\ Pa.s$
Wilkinson et al. (Wilkinson et al., 1994)	$d_B = \left(\frac{8.8\sigma}{g\rho_L}\right)^{0.5}\left(\frac{u_g\mu_L}{\sigma}\right)^{-0.02}\left(\frac{\sigma^3\rho_L}{g\mu_L^4}\right)^{-0.06}\left(\frac{\rho_L}{\rho_g}\right)^{0.11}$	$0 \leq u_g \leq 0.2\ m\ s^{-1}$ $D_c = 0.158\ m$ $0.001 \leq \mu_L \leq 0.021\ Pa.s$
Gaddis and Vogelpohl (Gaddis & Vogelpohl, 1986)	$d_B = \left[\left(\frac{6d_0\sigma}{\rho_L g}\right)^{4/3} + \left(\frac{81v_L Q_g}{\pi g}\right) + \left(\frac{135Q_g^2}{4\pi^2 g}\right)^{4/5}\right]^{1/4}$	$10 \leq Q_g \leq 84\ (\times 10^{-6}\ m^3\ s^{-1})$ $0.0002 \leq d_o \leq 0.006\ m$ $0.001 \leq \mu_L \leq 1\ Pa.s$

The models summarized in Table 4-5 are compared with the proposed correlation in this work in Figure 4-10. The prediction parameters for different models are also reported in Table 4-6.

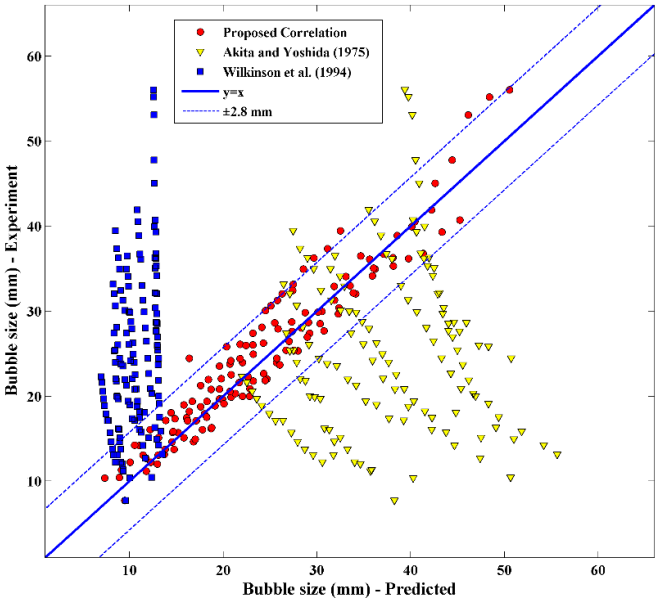

Figure 4-10: Comparison between the different models proposed for bubble size prediction.

Table 4-6: Prediction parameters for different bubble size models.

Research group	MAPE	Standard Error (mm)	95% prediction error (mm)
Akita and Yoshida (Akita & Yoshida, 1974)	76.5%	±17.2	±34.2
Wilkinson et al. (Wilkinson et al., 1994)	52.7%	±17.4	±34.4
Gaddis and Vogelpohl (Gaddis & Vogelpohl, 1986)	392%	±92	±182
Proposed model in this study	9.3%	±2.8	±6

Figure 4-10 shows that the proposed correlation in this study can predict the experimental data much better than the models reported in the literature. The applicability of Eq. (4.15) in predicting the bubble size measured in viscous and Newtonian fluids by other researchers is also examined using the bubble size data reported by Soong et al. (Y. Soong, Harke, Gamwo, Schehl, & Zarochak, 1997), Kuncová and Zahradnik (Kuncová & Zahradník, 1995), and Akita and Yoshida (Akita & Yoshida, 1974) and the obtained results are reported in Table 4-7. It is observed that Eq. (4.15) can predict the bubble size data measured by Soong et al. (Y. Soong et al., 1997), Kuncová and Zahradnik (Kuncová & Zahradník, 1995), and Akita and Yoshida (Akita & Yoshida, 1974) with a total MAPE and standard error of 28% and ±3.4 mm, respectively. Moreover, no experimental data of bubble size measured in non-Newtonian fluids was found to survey the accuracy of Eq. (4.15) in predicting bubble size in non-Newtonian fluids.

Table 4-7: Prediction parameters for different data series of bubble size.

Data series	System	Number of points	MAPE	Standard Error (mm)
Soong et al. (Y. Soong et al., 1997)	Drakeol-10 oil	8	22%	±4.2
Kuncová and Zahradnik (Kuncová & Zahradník, 1995)	Saccharose solutions	32	25%	±1.9
Akita and Yoshida (Akita & Yoshida, 1974)	Glycol solutions	16	38%	±4.1
	Total	56	28%	±3.4

The same procedure that was carried out to develop the bubble size model was repeated to develop a correlation for predicting the gas holdup. The constants of the derived correlation were determined by fitting the gas holdup data obtained in our previous work (Amin Esmaeili et al., 2015) and the final form of the developed correlation is as follows:

$$\varepsilon_g = 0.13\, Ga^{0.14}\, Fr^{0.73}\, e^{-0.1\left(1-\frac{G'}{G''}\right)} \tag{4.16}$$

$$1.4 \times 10^7 < Ga < 2.4 \times 10^{11}$$

$$0.06 < Fr < 0.138$$

$$0 < \frac{G'}{G''} < 3.26$$

Figure 4-11 displays a comparison between the gas holdup values measured experimentally with those predicted by Eq. (4.16) for different solutions. The MAPE, standard error, and 95% prediction interval of the fitting are 10%, ±2.3%, and ±4.7%, respectively. The comparison indicates very good agreement between the experimental and predicted values.

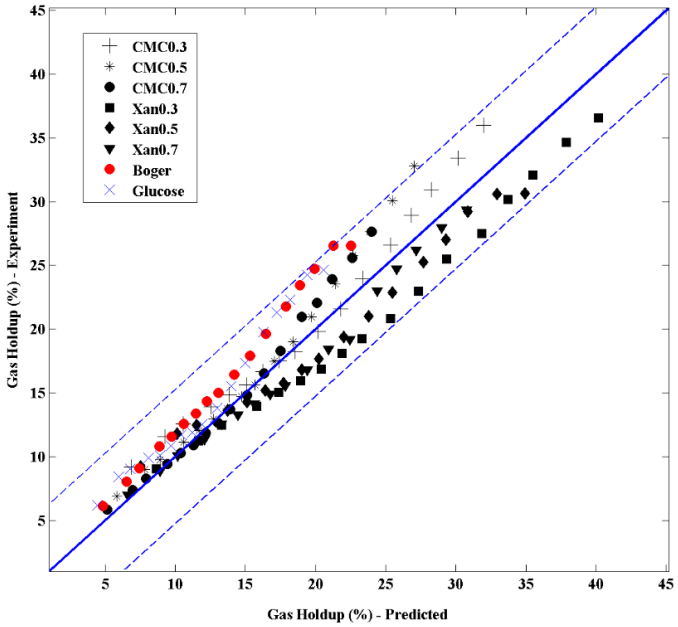

Figure 4-11: Comparison between the experimental values of gas holdup with those predicted by the proposed correlation.

Various correlations are available in the literature to predict the gas holdup in the bubble column reactors. Kawase and Moo-Young (Kawase & Moo-Young, 1986) have developed a correlation to predict the gas holdup in both Newtonian and non-Newtonian liquids. They reported fairly good agreement between the gas holdup predicted by their correlation with that measured experimentally in water, CMC, and Corn Syrup solutions in bubble columns equipped with both perforated and porous plate spargers. Schumpe and Deckwer (Schumpe & Deckwer, 1987) have proposed a correlation, which has the same dimensionless groups as the correlation developed by Akita and Yoshid (Akita & Yoshida, 1973). Their model is useful to predict the gas holdup in a wide range of viscous and non-Newtonian liquids with an average error of 8.1%. Hikita et al. (Hikita, Asai, Tanigawa, Segawa, & Kitao, 1980) have presented a dimensionless correlation for the gas holdup by considering the effects of physical properties of liquid and gas phases. They have shown that their correlation is able to predict the experimental data with an average deviation of 4.2%.

Table 4-8 summarizes the correlations that have been widely used to predict the gas holdup for different Newtonian and non-Newtonian solutions in bubble columns. Comprehensive sets of models for predicting hydrodynamic parameters of bubble columns have been reported elsewhere.(Arsam Behkish, 2004; A. Behkish, Lemoine, Oukaci, & Morsi, 2006; Gupta et al., 2009; Kantarci et al., 2005; Y. T. Shah et al., 1982). The accuracy of the models presented in Table 4-8 in predicting the gas holdup is compared with that of the model developed in this work and illustrated in Figure 4-12.

Table 4-8: Summary of the gas holdup models proposed by different researchers.

Research group	Correlation proposed	Range of parameters
Kawase and Moo-Young (Kawase & Moo-Young, 1986)	$\varepsilon_g = 0.24n^{-0.6}\left(\frac{u_g}{\sqrt{gD_c}}\right)^{0.84-0.14n}\left(\frac{gD_c^3}{v_L^2}\right)^{0.07}$	$0.008 \leq u_g \leq 0.285\ m\,s^{-1}$ $0.14 \leq D_c \leq 0.35\ m$ $0.28 \leq n \leq 1$ $0.001 \leq K \leq 1.22\ Pa.s^n$
Schumpe and Deckwer (Schumpe & Deckwer, 1987)	$\varepsilon_g = 0.20\left(\frac{gD_c^2\rho_L}{\sigma}\right)^{-0.13}\left(\frac{gD_c^3}{v_L^2}\right)^{0.11}\left(\frac{u_g}{\sqrt{gD_c}}\right)^{0.54}$	$0.14 \leq D_c \leq 0.35\ m$ $1.2 \times 10^7 \leq Ga \leq 6.5 \times 10^{10}$ $3.0 \times 10^{-3} \leq Fr \leq 2.2 \times 10^{-1}$ $0.0011 \leq (u_g\mu_L/\sigma) \leq 0.089$ $2.5 \times 10^{-11} \leq (g\mu_L^4/\rho_L\sigma^3) \leq 1.9 \times 10^{-6}$
Hikita et al. (Hikita et al., 1980)	$\varepsilon_g = 0.672\left(\frac{u_g\mu_L}{\sigma}\right)^{0.578}\left(\frac{g\mu_L^4}{\rho_L\sigma^3}\right)^{-0.131}\left(\frac{\rho_g}{\rho_L}\right)^{0.062}\left(\frac{\mu_g}{\mu_L}\right)^{0.107}$	$8.4 \times 10^{-5} \leq (\rho_g/\rho_L) \leq 1.9 \times 10^{-3}$ $1.0 \times 10^{-3} \leq (\mu_g/\mu_L) \leq 1.8 \times 10^{-2}$

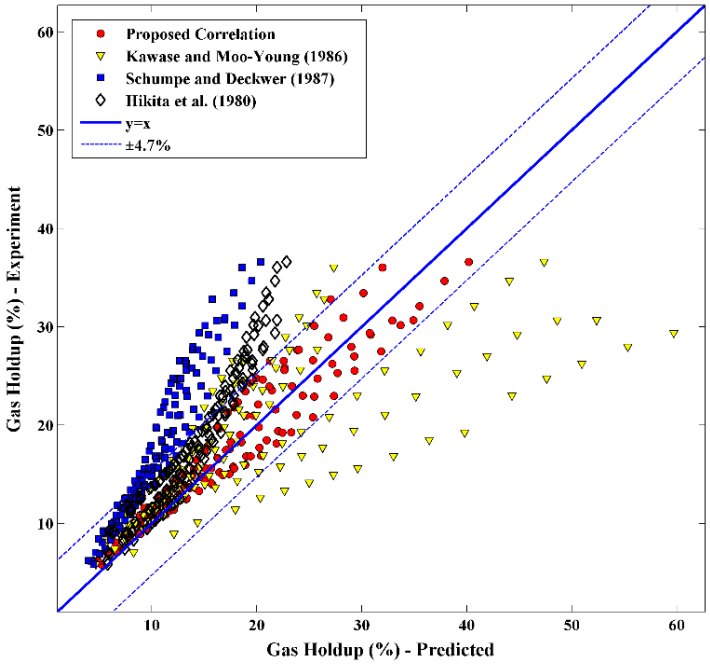

Figure 4-12: Comparison between the different models proposed for the gas holdup prediction.

The prediction parameters are calculated for different gas holdup models and compared with those of the proposed correlation in Table 4-9.

Table 4-9: Prediction parameters for different gas holdup models.

Research group	MAPE	Standard Error (%)	95% prediction error (%)
Kawase and Moo-Young (Kawase & Moo-Young, 1986)	29%	±8.1	±17.9
Schumpe and Deckwer (Schumpe & Deckwer, 1987)	38%	±8.3	±18.3
Hikita et al. (Hikita et al., 1980)	20%	±5.2	±11.6
Proposed model in this study	10%	±2.3	±4.7

Similar to the work that has been done for the bubble size correlation, the proposed correlation for the gas holdup is also examined to have a better understanding of the accuracy of Eq. (4.16) in predicting the gas holdup data reported in the literature. The results show that Eq. (4.16) can predict the gas holdup in viscous Newtonian Glycerol solutions reported by Li et al. (S. B. Li, Zhu, et al., 2012) and the gas holdup data measured by Kuncová and Zahrabnik (Kuncová & Zahradník, 1995) in viscous Newtonian Saccharose solutions with a total MAPE and standard error of 20% and ±1%, respectively. The detailed prediction parameters are reported in Table 4-10.

Table 4-10: Prediction parameters for different data series of gas holdup.

Data series	System	Number of points	MAPE	Standard Error (%)
Li et al. (S. B. Li, Zhu, et al., 2012)	Glycerol solutions	15	31%	±0.5%
Kuncova and Zahradnik (Kuncová & Zahradník, 1995)	Saccharose solutions	23	10%	±1.5%
	Total	38	20.5%	±1%

In addition, it is essential to know the accuracy of Eq. (4.16) in predicting the gas holdup data measured in non-Newtonian liquids. A survey of the literature shows that although there is a variety of experimental data of gas holdup measured in non-Newtonian liquids, no $\frac{G'}{G''}$ value is reported by the corresponding researchers for the non-Newtonian liquid used during their experiments. To overcome this drawback, the gas holdup experimental data reported by several researchers (Fransolet, Crine, Marchot, & Toye, 2005; Haque, Nigam, & Joshi, 1986; Kawase, Halard, & Moo-Young, 1987; Kawase & Moo-Young, 1986; Lakota, 2007; S. B. Li, Zhu, et al., 2012) are fitted by Eq. (4.16) and the values of the $\frac{G'}{G''}$ ratio are calculated as the fitting parameter. The $\frac{G'}{G''}$ values calculated by this method are summarized in Table 4-11.

Table 4-11: The range of G′/G″ ratio calculated using different gas holdup experimental data.

Data series	**System (solution)**	**Number of points**	$\frac{G'}{G''}$ **range**
Li et al. (S. B. Li, Zhu, et al., 2012)	CMC	25	0.79-1.04
	PAA	20	0.94-1.73
Kawase and Moo-Young (Kawase & Moo-Young, 1986)	CMC	27	0.11-0.93
Lakota (Lakota, 2007)	CMC	19	0.11-1.05
	Xanthan gum	24	0.91-1.18
Fransolet et al. (Fransolet et al., 2005)	Xanthan gum	40	0.01-0.63
Kawase et al. (Kawase et al., 1987)	Carbopol	11	0.23-0.49
	CMC	11	0.25-0.6
Haque et al. (Znad, Báleš, Markoš, & Kawase, 2004)	CMC	46	0.12-0.54
	Total	**223**	**0.01-1.73**

As evident in Table 4-11, almost all the values of the $\frac{G'}{G''}$ ratio predicted by Eq. (4.16) for the CMC solutions used by different researchers are less than unity. Moreover, except for the experimental data of Fransolet et al. (Fransolet et al., 2005), the values of the $\frac{G'}{G''}$ ratio predicted for the Xanthan

gum solutions are mainly more than unity and are in good agreement with the $\frac{G'}{G''}$ ratio measured experimentally for CMC and Xanthan gum solutions in this work (see Table 4-3). PAA solutions are also highly elastic and the values of the $\frac{G'}{G''}$ ratio as predicted by Eq. (4.16) for the PAA solution are mostly more than unity. These high values of the $\frac{G'}{G''}$ ratio can be attributed to the stronger elastic effects in PAA solutions. Similar to the CMC solutions, the $\frac{G'}{G''}$ ratio predicted for the Carbopol solution is less than unity. However, there is not enough information on the rheological properties of Carbopol solutions reported in the literature to justify the values of the $\frac{G'}{G''}$ ratio predicted for Carbopol solution in this study and it needs to be investigated in future studies. The overall range of the $\frac{G'}{G''}$ ratio reported in Table 4-11 (i.e., 0.01-1.73) is within the range of applicability of Eq. (4.16) (i.e., 0-3.26), which confirms the accuracy of Eq. (4.16) in predicting the gas holdup data measured experimentally by other researchers. It may be concluded that the correlations developed in this work can provide a reasonable estimation of the bubble size and gas holdup in bubble columns operating with viscous Newtonian and non-Newtonian viscoelastic solutions.

4.4 Conclusion

The distinct effects of the elasticity and viscosity of several non-Newtonian liquids on the local hydrodynamic parameters of a bubble column reactor are experimentally studied by means of two in-house made optical fiber probes. It was observed that the elasticity of the liquid increases the bubble frequency while it can diminish the bubble rise velocity. The bubble frequency in viscoelastic liquids with comparable apparent viscosity is markedly higher in solutions with dominating elastic effects. The shape of the radial profiles of bubble chord length, bubble frequency, and bubble rise velocity are shown to be relatively independent of the type of operating liquids. The axial distribution of the bubble chord length in different solutions is compared by calculating the root mean square of the bubble chord length and it was observed that the axial distribution of the bubble chord length is smaller in solutions with dominating elastic effects. The experimental results confirm that the elastic aspects of non-Newtonian liquids, which are normally neglected, have a significant effect on the local hydrodynamic parameters of the bubble columns. The new approach using the $\frac{G'}{G''}$ ratio, which is a dimensionless parameter including both elastic and viscous effects, was found to be an appropriate method to interpret further the effects of non-Newtonian liquids on the local hydrodynamics of gas-liquid contactors. Two dimensionless correlations were also developed by introducing the simultaneous effects of the viscosity and elasticity of liquids in the form of the $\frac{G'}{G''}$ ratio to predict the bubble size and gas holdup that has not yet been considered elsewhere. The proposed correlations are recommended for predicting bubble size and gas holdup in bubble column reactors operating with non-Newtonian liquids with a wide range of viscosity and elasticity and will distinguish this work from a number of conventional research works in this field.

CHAPTER 5

HP-HT BUBBLE COLUMN REACTOR: DESIGN, CONSTRUCTION, AND OPERATION

5.1 Introduction

As previously mentioned, although relatively simple in construction, slurry bubble reactors are still difficult to design and scale-up, primarily due to the lack of detailed information on hydrodynamics and mass transfer over a wide range of industrial operating conditions; there is thus a strong need for more research and experimental investigation in this area. In this regard, the final part of the present work is aimed at investigating the effect of elevated pressure on different hydrodynamic aspects of bubble column reactors. Thus, in order to perform the experiments at high pressure, a new HP-HT multiphase reactor unit including a bubble column and fluidized bed reactor has been designed and constructed at the Chemical Engineering Department of École Polytechnique de Montréal, in collaboration with the Natural Sciences and Engineering Research Council of Canada (NSERC) and TOTAL American Service Inc. The objective of this proposed research program is to investigate the hydrodynamics of multiphase processes under extreme conditions that are applicable to a broad range of technologies and processes, and more specifically to develop phenomenological hydrodynamic models for multiphase processes involved in petrochemical and energy production. The specific objectives are to contribute to the fundamental understanding of multiphase reactors, and also to develop new and improved processes in association with TOTAL. Another objective is to train highly qualified specialists in the development and implementation of these new technologies. Moreover, various original measurement techniques that have already been developed or are under development will be employed. These techniques have been used in many projects so far and will continue to be used in this research program. It is also worth mentioning that this project is considered one of the major contributions within the framework agreement in place between École Polytechnique de Montréal and TOTAL.

In many processes, slurry bubble column reactors operate under high temperature (up to 400 ℃) and high pressure (up to 3 MPa). The maximum superficial gas velocity is also around 0.35 m s^{-1} in many applications. Therefore, to best achieve our research objectives, it is important to correctly take into account the following points:

- Design and build a pilot-scale experimental setup to be used under extreme conditions and be equipped with different internal configurations (internals and gas distributor design).
- The slurry bubble column reactor should operate at a high superficial gas velocity and a high solid concentration to improve conversion rate and volumetric productivity.
- An appropriate reactor diameter needs to be chosen. The choice of diameter and the operating conditions is a compromise between the quality of the experimental data obtained for an adequate extrapolation and some constraints related to the compressor and the inherent university limitations.
- The reactor, gas distributor design and presence of internals affect the hydrodynamics of bubble columns.

To start with, an appropriate location must be chosen and prepared for installing the reactor and other necessary equipment. The selected location has to pass several safety measures as defined by the school. In the following sections, the design and construction of HP-HT bubble column reactor and equipment used in the HP-HT multiphase reactor unit will be discussed.

5.2 HP-HT bubble column reactor

The HP-HT bubble column reactor is made of stainless steel (SS316) and includes five pieces connected with four INOX 316L flanges. The column's active section is 5 m high and 0.15 m in diameter. The reactor is equipped with two different types of heating elements (a flanged heating element and a series of wall heating elements). These heating elements are covered with heavy-duty insulation jackets, allowing for less energy loss and a more efficient operation of the column. The schematic of the HP-HT bubble column reactor is shown in Figure 5-1. Figure 5-2 and Figure 5-3 also show different views and pictures of the HP-HT bubble column reactor, including the reactor and its structure. The operating conditions achievable in the reactor are given in Table 5-1.

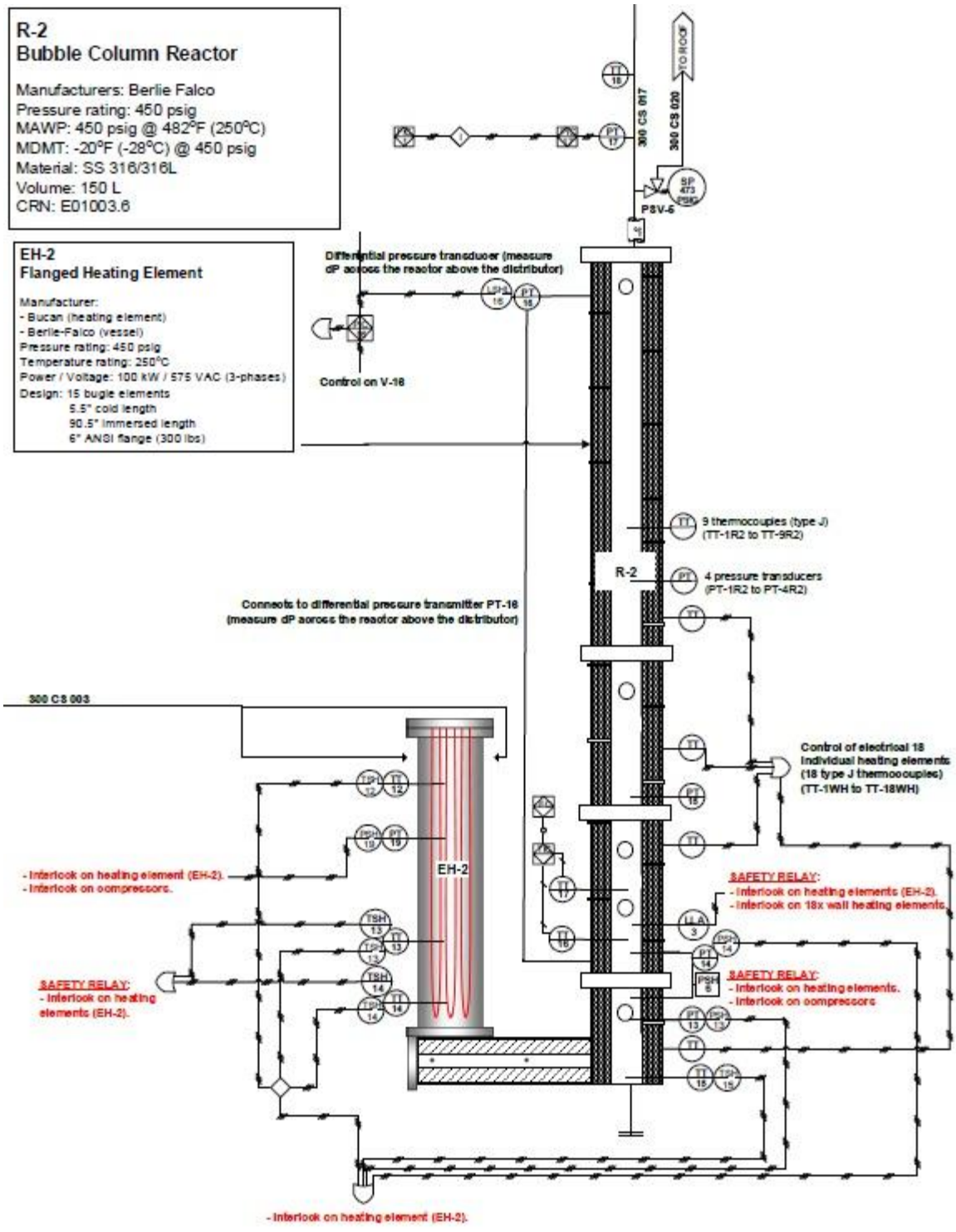

Figure 5-1: Schematic of the HP-HT bubble column reactor.

(a) (b)

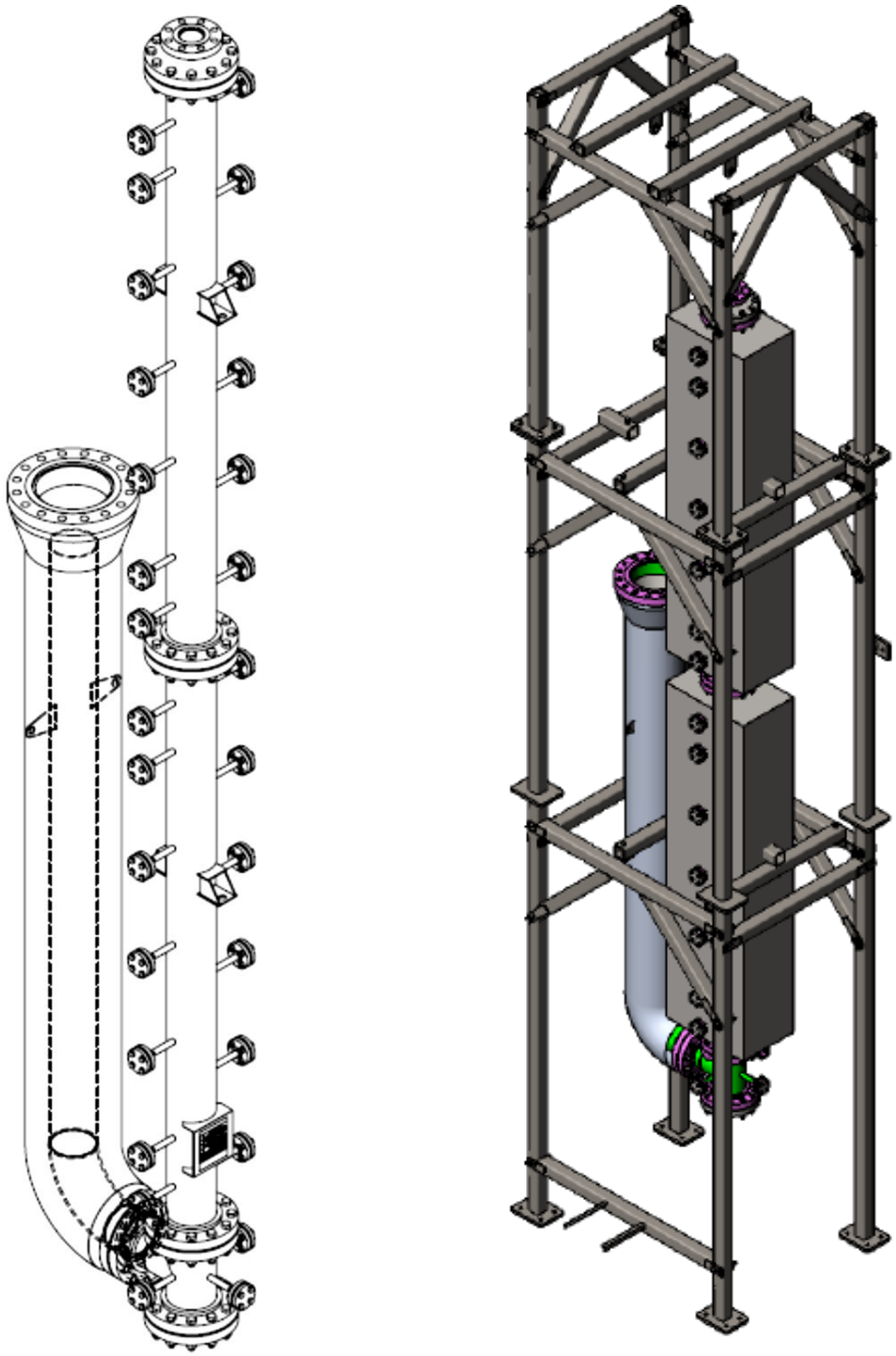

Figure 5-2: Different views of the HP-HT bubble column reactor: (a) side view; and (b) structural view.

(a) (b)

Figure 5-3: Photographs of the HP-HT bubble column reactor.

Table 5-1: Operating conditions of the HP-HT bubble column reactor.

Parameter	**Range**
Pressure (P)	
Capability	0.1 – 3 MPa
Design	0 – 3.1 MPa
Temperature (T)	
Capability	Ambient – 200 ^{o}C
Design	Ambient – 250 ^{o}C
Superficial gas velocity (U_g)	0.1 – 0.5 m s^{-1}
Solid particle size range (d_p)	60 – 500 µm
Solid particle density range (ρ_p)	1000 – 2500 kg m^{-3}

The high-pressure air provided by the compressors is first injected into the flanged heating element (EH-2 in Figure 5-1) through the gas stream 300 C8 003 (Figure 5-1) and then introduced to the column by a gas sparger. Although different types of spargers are used to distribute the gas in bubble column reactors, the perforated plate distributor is the most common. In this research program, the HP-HT bubble column reactor is equipped with a perforated plate distributor made of a stainless steel plate, which is 6 mm in thickness. The distributor includes 24 holes that are 1 mm in diameter, spaced in a square pitch (with a total orifice density of 1316 orifices per m^2) to provide a uniform distribution of the gas phase. A schematic of the distributor plate designed and fabricated for the HP-HT bubble column in this project is shown in Figure 5-4.

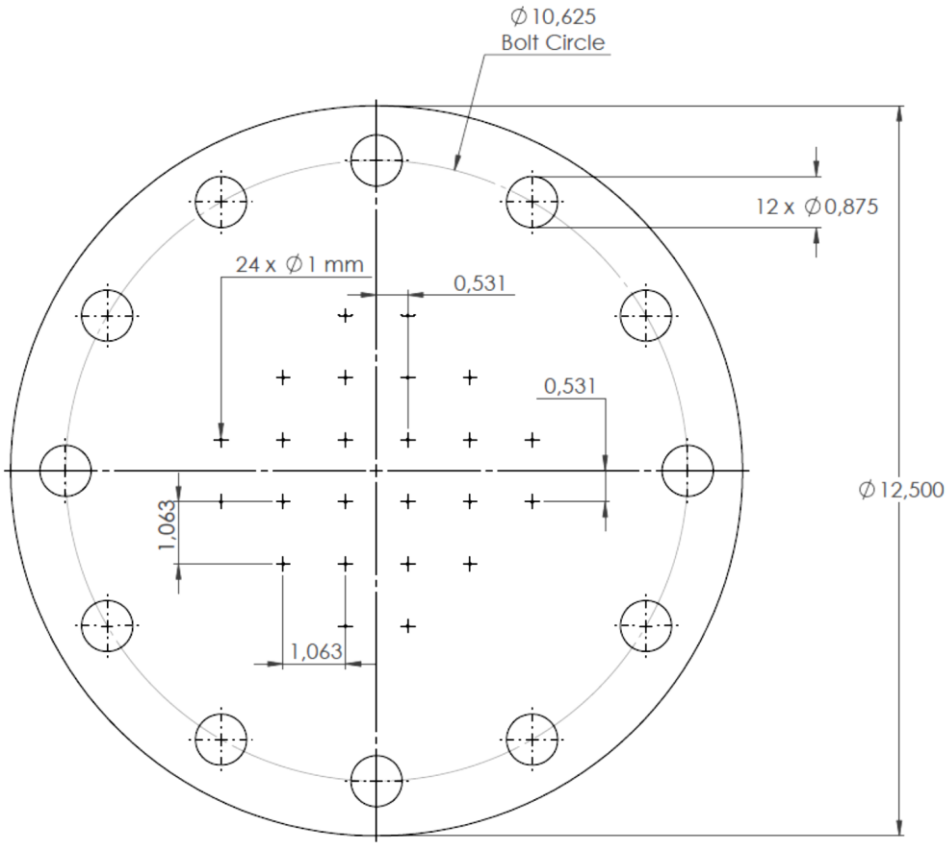

Figure 5-4: Schematic of the perforated plate distributor.

5.3 Air compressors and high pressure air tank

Compressed air is provided by a system of two redundant compressors capable of pressurizing the reactor and compensate for the pressure drop across the distributor plate. During normal operation, each one of the two compressors can deliver a maximum flow rate of 70.8 m^3 h^{-1} (at 25 ℃ and 473 psi). The compressors feed a tank (400 gallons rated at 450 psi) that will be used, via a pressure regulator, to control the total pressure of the gas fed to the reactor. A schematic of the compressors system is presented in

Figure 5-5, and a photograph of the compressor system is shown in Figure 5-6. Air flows out of the compressors (C-1/A and C-1/B) through a high-pressure filter F-1 to ensure that gas is lube- and oil-free before being fed to the tank T-1.

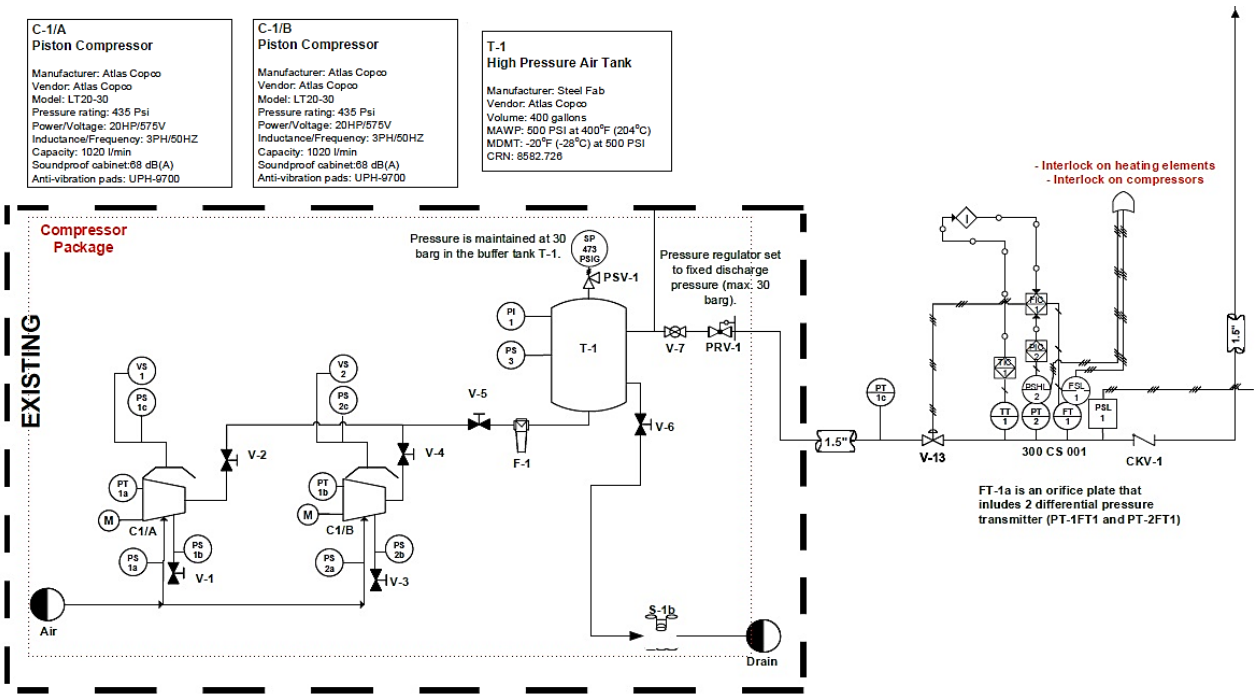

Figure 5-5: A schematic of the air compressor system.

Figure 5-6: A photograph of the air compressor system.

The tank T-1 is equipped with a pressure relief valve (PSV-1) to ensure that the maximum pressure limit of the system is respected inside the tank. The pressure limit is set at the max design pressure, plus a 5% margin (450 psig + 5% = 473 psig). PSV-1 is designed to handle a flow of two compressors, delivering a total of 141.6 $m^3 h^{-1}$ at 20℃ and 435 psia (maximum flow rate from two compressors - Atlas Copco LT20-30). An oil-water separator S-1b is located on the drain stream downstream of the compressors and the tank T-1 in order to ensure that water can be safely disposed of. The pressure downstream of tank T-1 is adjusted with the pressure regulator PRV-1 on stream 300 CS 001, which is controlled manually by the operator. A modulating valve (V-13 in

Figure 5-5) is used to control the pressurization rate of the reactor. Valve V-13 is slowly opened by the PLC unit to pressurize the reactor with a maximum rate of 10 psi per minute. Moreover, another modulating valve has been installed downstream of the reactor to adjust the gas mass flow

rate (superficial gas velocity). A pressure safety valve (PSV-5 in Figure 5-1) is also installed on the bubble column outlet stream (300 CS 017).

5.4 Heating systems

To heat up the bubble column reactor, two different heating systems will be used, as described below.

5.4.1 Flanged electrical heating element

In order to preheat the entering compressed air, a flanged electrical heating element (EH-2 in Figure 5-1) is used upstream of the distributor. The power of the flanged electrical heating element was selected in order to heat an air flow of 730 scfm at 20 bara to a temperature of 200℃. In this regard, a 100 kW flanged heater was selected. This is, to achieve the maximum power that could be fitted in a 0.152-m flange. The U-shape of the electrical heater EH-2 and bubble column ensures that water backflow into the stream 300 CS 003 is impossible.

5.4.2 Wall electrical heating elements

A series of external electrical heating elements (18×) are also located around the reactor wall to increase the bed temperature up to 200℃. The heating elements are controlled using 18 temperature transmitters located along the reactor. The power of the wall heating elements was selected in order to heat the bed of liquid water ($c_{p,w}$ = 4.3 and ρ_w = 996 kg m^{-3}) and silica sand particles (c_{ps} = 0.9 kJ kg^{-1} K^{-1}) to 200℃ in one hour. Moreover, the bubble column is equipped with a low level alarm (LLA-3), which will turn off all heating elements (EH-2 and the 18 wall heating elements) in case there is not enough liquid inside the column.

5.5 Liquid storage and feeding system

The schematic of liquid storage and the feeding system is displayed in Figure 5-7. A pressurized Tank (T-2 in Figure 5-7) will be manually filled with distilled water prior to operation. The water tank T-2 is equipped with a high level switch, which will provide a visual alarm to the operator once the tank is full. The water tank T-2 is also equipped with a low level alarm, which will turn off all heating elements on the bubble column. A pump (P-1 in Figure 5-7) will be used to inject

water inside the bubble column, and a level transmitter will control the liquid level in the column. The water flow into the bubble column will be controlled by two automated modulating valves: V-31 and V-16. These two valves follow each other and function as ON/OFF valves. However, their opening can be adjusted via the PLC unit. To prevent pressurized hot gas from flowing towards the pump P-1 in case of a malfunction, a check valve (CKV-2) is located on stream 300 CS 013 downstream of the pump. The water pump maximum capacity is selected in a way to be higher than the maximum evaporation rate from the bubble column, which corresponds to 22 lpm (Ug = 2 m s^{-1} at 15 bara and 200℃).

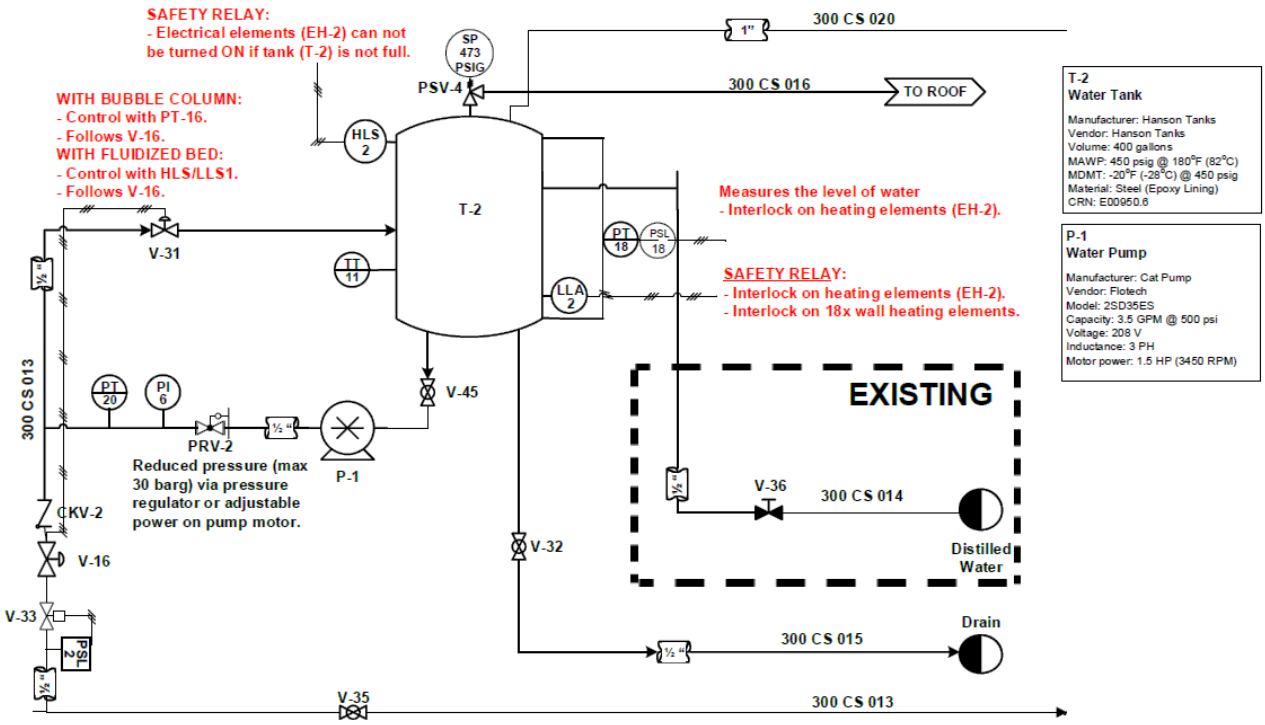

Figure 5-7: Schematic of the liquid storage tank and liquid pump.

5.6 Heat exchanger and gas-liquid separators

Due to the high exhaust gas temperatures, evaporation will occur and steam will be present in the bubble column reactor exhaust gas. Therefore, the outlet stream of the bubble column is connected to a heat exchanger to condense the steam and return it to the bubble column. A schematic of the heat exchanger system is shown in Figure 5-8. The sizing of this heat exchanger (HE-1) is

performed such that it must be able to remove the power inputted by the flanged electoral element EH-2 (100 kW) and the wall heating elements (18 kW); it has been built as per the ASME code for 250℃ and 450 psig.

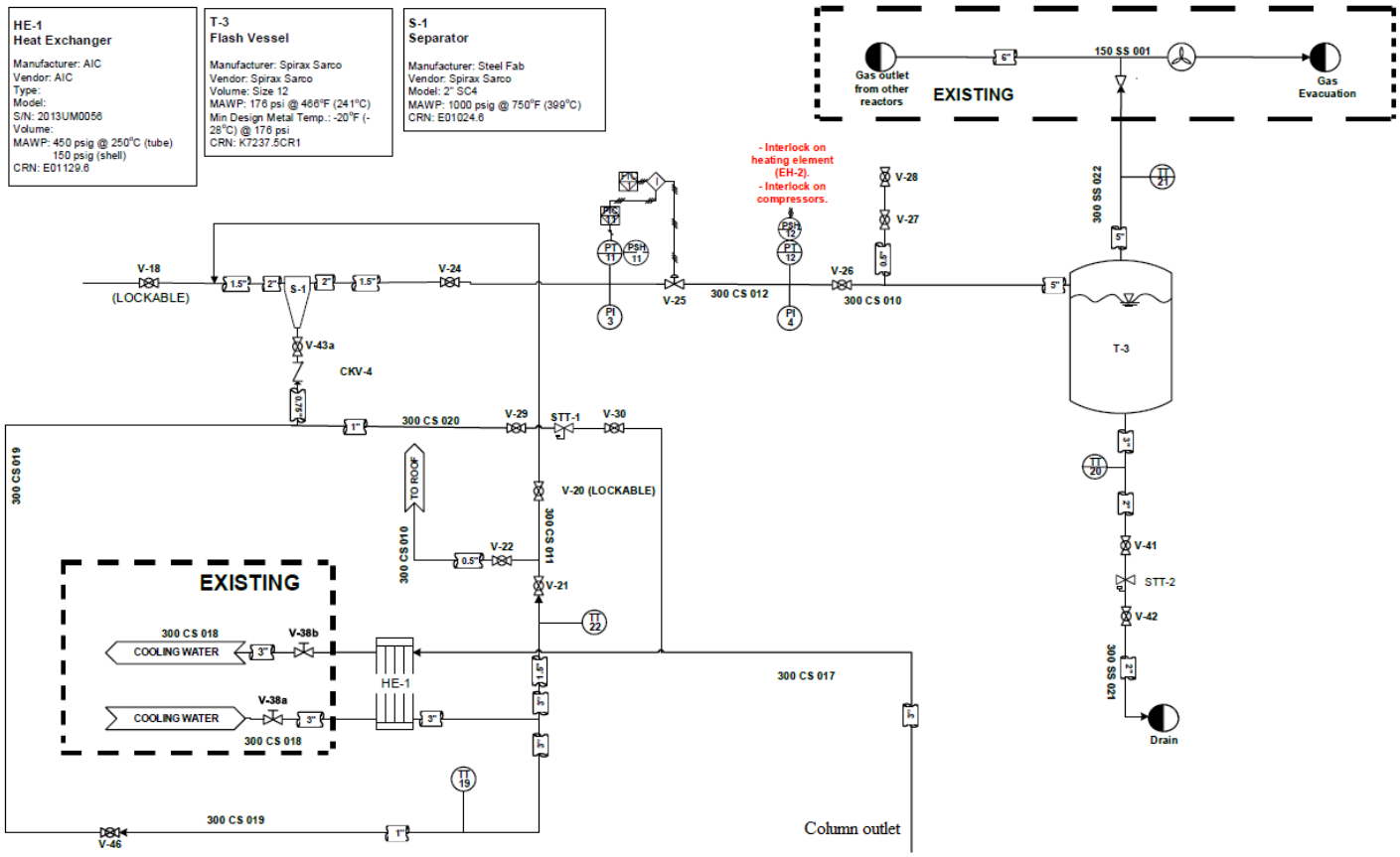

Figure 5-8: A Schematic of the heat exchanger and gas-liquid separators.

The remaining water vapour in the exhaust air is recovered in the separator (S-1) and flash tank (T-3). To separate the steam and water droplets from the air prior to disposal in the gas manifold, stream 300 CS 010 is connected to a detention tank (flash tank) T-3. At the flach tank, the gas pressure is lowered to atmospheric and water condenses. The tank T-3 has a drain with manual valves V-41 and V-42. The gas outflow of the tank 300 CS 022 is connected to the existing manifold 150 SS 001, which discharges to the atmosphere via a fan. This manifold operates at slightly sub-atmospheric pressure with a fan and discharges onto the roof of the building. A photograph of the separator and flash tank is provided in Figure 5-9.

It is worth mentioning that prior to running the experiments, several troubleshooting steps were undertaken to assure the stable operation of the bubble column. Moreover, a series of safety inspections and hydrostatic tests were conducted to verify that the unit can operate in a very safe mode.

Figure 5-9: Photograph of the separator and the flash tank.

CHAPTER 6

ARTICLE 3: EFFECT OF ELEVATED PRESSURE ON THE HYDRODYNAMIC ASPECTS OF A PILOT-SCALE BUBBLE COLUMN REACTOR OPERATING WITH NON-NEWTONIAN LIQUIDS

Amin Esmaeili, Sherif Farag, Christophe Guy, Jamal Chaouki

Department of Chemical Engineering, École Polytechnique de Montréal, P.O. Box 6079, St. C.V., Montreal, Qc, Canada H3C 3A7

Submitted to Chemical Engineering Journal

Abstract

The effect of elevated pressure on the hydrodynamics of a pilot-scale bubble column reactor has been studied in presence of non-Newtonian liquid phase. Various hydrodynamic characteristics of the bubble column reactor, including the total gas holdup and its axial distribution, operating flow regime transition point, pressure fluctuation and its standard deviation have been evaluated by means of several pressure traducers along the column height. The superficial gas velocity and operating pressure varied from 1 to 35 (cm s^{-1}) and 0.1 to 1.0 (MPa), respectively. It was found that the total gas holdup increases with both operating pressure and the elasticity of the liquid phase. The operating flow regime transition point was shifted to higher superficial gas velocities at elevated pressures. The standard deviation of pressure fluctuations was also found to increase with operating pressure but to decrease with the elasticity of the liquid phase. A new correlation has also been developed to predict the gas holdup in bubble columns operating at elevated pressures. The new correlation was shown to be able to predict the experimental data of gas holdup within a mean absolute percentage error of 20%.

Keywords: Bubble column reactor; Viscoelastic liquids; High pressure; Hydrodynamics; Gas holdup; Regime transition; Pressure fluctuations

6.1 Introduction

Bubble columns are known as one of the most applicable pieces of production equipment in the chemical industry. The simple design, construction, and absence of any mechanically moving part are some of the advantages of bubble columns that make them very suitable for high pressure operations. The obvious advantage of operation at high pressure is that the solubility of the gas phase reactants increases with pressure. Fischer-Tropsch synthesis, methanol synthesis, partial oxidation of ethylene, residuum hydrotreating, and hydroformylation processes are some of the commercial applications of bubble column reactors in processing chemicals at high pressure (Dautzenberg & De Deken, 1984; L.-S. Fan, 1989; Haque et al., 1987; T. J. Lin & Fan, 1999). Several works have been dedicated to study the bubble column reactors operating at high pressure over the past few years. It has been pointed out by Rollbusch et al. (P. Rollbusch et al., 2013) that at elevated pressures, smaller bubbles are formed at the gas distributor and bubble coalescence is inhibited due to the higher gas density and momentum. Sagert and Quinn (Norman H. Sagert & Quinn, 1976; Norman H Sagert & Quinn, 1977) also observed that bubble coalescence decreases at a higher system pressure. Lin et al. (T. J. Lin, Tsuchiya, & Fan, 1999) investigated the effects of pressure on the gas holdup through in-situ measurements of the physical properties of fluids, such as the density and viscosity of the liquid phase and the interfacial tension in a bubble column reactor. Their results showed an increase in the gas holdup with increasing pressure. They also reported that the bubble formation, coalescence and breakup rates are strongly influenced by the system pressure. Oyevaar et al. (Oyevaar, Bos, & Westerterp, 1991) reported that the influence of pressure on the gas holdup originates from the formation of smaller bubbles at the gas distributor. Schafer et al. (Schafer et al., 2002) determined the bubble size distribution in a lab-scale bubble column operated with different liquids at pressures up to 50 bars. They found that the bubble size significantly changed by pressure and the initial and stable bubble sizes were smaller at elevated pressures. It has been stated by Jiang et al. (Jiang, Lin, Luo, & Fan, 1995) that the bubble size distribution becomes narrower and thus, the average bubble size decreases at higher system pressure. Behkish et al. (Arsam Behkish, 2004) have also shown that the gas holdup and mass transfer coefficient increase with pressure and that is attributed to the increase in the holdup of small bubbles. Jin et al. (H. B. Jin, Qin, Yang, He, & Guo, 2013) investigated the radial variation of bubble properties in a bubble column under high pressure. They noted that the bubble swarm rises with a lower velocity at a higher system pressure. They also indicated that the higher gas

density at elevated pressures causes a lower bubble stability, an increased bubble breakup probability and, as a result, a reduced bubble size. In fact, the gravity of bubbles is higher at a higher gas density while the buoyancy of bubbles does not change. Therefore, the overall force balance of bubbles changes and, accordingly, the bubble rise velocity decreases. Jin et al. (H. Jin, Yang, Zhang, & Tong, 2004) studied the hydrodynamics of a large-scale bubble column using the dynamic gas disengagement method. They showed that the rising velocity of the swarm of small bubbles and the holdup of large bubbles decrease, whereas the holdup of small bubbles increases with an increase in operating pressure. Kemoun et al. (Kemoun et al., 2001) reported that the gas holdup radial profile tends to become relatively flatter at a higher operating pressure compared to that at ambient pressure. Shaikh and Al-Dahhan (Shaikh & Al-Dahhan, 2005) also noted that the flatter gas holdup radial distribution at higher pressure is due to the decrease in the bubble coalesscense rate. It is worth mentioning that the mechanism of bubble formation can be explained by a general force balance considering the contributions of the pressure difference between the inside and outside of the bubble, inertial forces, interfacial tension force at gas sparger, viscous resistance, and gas momentum. The smaller bubble size at pressurized conditions can be attributed to the stronger gas momentum contribution as a result of increased gas density and not to the smaller interfacial surface tension at higher pressure. Therefore, bubble detachment can occur earlier under such conditions resulting in smaller initial bubble size.

Ong (B. Ong, 2003) also evaluated the gas holdup, the time-averaged liquid velocity and the turbulence by means of Computed Tomography and Computer Automated Radioactive Particle Tracking in a bubble column at elevated pressures and high superficial gas velocities. They have shown that the gas holdup and liquid recirculation increase with pressure. Moreover, the turbulent normal stresses and eddy diffusivities decrease at elevated pressures as a result of a reduction in bubble size. The reported experimental results by Oyevaar et al. (Oyevaar & Westerterp, 1989), Letzel et al. (Letzel et al., 1997), Lin et al. (T. J. Lin et al., 1999), and Urseanu et al. (Urseanu et al., 2003) suggest that the transition from uniform bubbling regime toward the heterogeneous regime is delayed at higher pressures. Therefore, the regime transition occurs at higher superficial gas velocities and gas holdups under such conditions. However, it is not yet well understood why the regime transition shifts to higher superficial gas velocities at higher pressures and there is also a discrepancy between the positions of the transition point reported by different researchers. Therefore, there is still a need for much research in the mechanistic understanding of this flow

regime transition. A literature review on the most recent works investigating the effects of pressure on the different hydrodynamic aspects of bubble column reactors is summarized in Table 6-1.

Table 6-1: Overview of the most recent literature studies on bubble columns at elevated pressure.

Reference	System	Apparatus and Conditions	Methodology	Key Findings
Jin et al. (H. B. Jin et al., 2013)	Air/Water	P= 0.5 – 2.0 MPa U_g= 11 – 32 cm s^{-1} D= 0.3 m H= 6.6 m	Conductivity probe	- The bubble swarm rising velocity and Sauter mean diameter decreased with higher system pressure.
Ong et al. (B. C. Ong, Gupta, Youssef, Al-Dahhan, & Dudukovic, 2009)	Air/Water	P= 0.1 and 0.4 MPa U_g= 2 – 30 cm s^{-1} D= 0.162 m H= 2.5 m	γ-Ray Computed Tomography	- At 0.4 MPa, the sparger design did not have a significant effect on the gas holdup profiles compared to atmospheric pressure conditions.
Shaikh and Al-Dahhan (Shaikh & Al-Dahhan, 2005)	Air/Therminol LT	P= 0.4 and 1.0 MPa U_g=1 - 20 and 100 cm s^{-1} D= 0.162 m H= 2.5 m	Computed Tomography	- The regime transition was found to be delayed to higher superficial gas velocities with an increase in the operating pressure. - At higher pressures, a transition occurred over a range of superficial gas velocities rather than at a single point.
Rados et al. (Rados et al., 2005)	Air/Water/ Glass beads	P = 0.1 – 1.0 MPa T = 20°C U_g = 8 – 45 cm s^{-1} D= 0.162 m H= 2.5 m	Computer Automated Radioactive Particle Tracking	- Bubble breakup and gas holdup increased with pressure while the bubble coalescence rate decreased at elevated pressures. - Bubble size was smaller at elevated pressures. - Solids holdup profile decreased with pressure.
G. Q. Yang et al. (Yang & Fan, 2003)	Air/Water/ Paratherm NF heat-transfer fluid	P = 0.1 – 10.3 MPa T = 27 °C U_g = 0 – 40 cm s^{-1} U_l = 0 – 1 cm s^{-1} D= 0.05 and 0.10 m H= 0.55 and 0.9 m	Steady-state thermal dispersion technique	- Axial liquid dispersion coefficient decreased with pressure.

Table 6-1. Continued.

Reference	System	Apparatus and Conditions	Methodology	Key Findings
Maalej et al. (Maalej, Benadda, & Otterbein, 2003)	$N_2/CO_2/Na_2CO_3$-$NaHCO_3$/NaOH	P= 1 – 10 MPa U_g= 0.025 – 3 cm s^{-1} D= 0.046 m H= 0.25 m	Gas–liquid absorption with chemical reaction	- The mass transfer coefficient, k_L, was shown to be independent of pressure. Furthermore, increasing the pressure resulted in a decrease of k_G and k_Ga for a given gas flow rate.
Urseanu et al. (Urseanu et al., 2003)	N_2/Tellus oil/ Glucose solutions	P= 0.1 – 5.6 MPa U_g= 1 – 15 cm s^{-1} μ_L = up to 0.55 Pa s D= 0.15 and 0.23 m H= 1.22 m	Differential pressure transducers	- Increasing the operation pressure led to a considerable increase in the total gas holdup. - The effect of the pressure on gas holdup gradually disappeared as the liquid viscosity increased.
Jordan et al. (Jordan, Terasaka, Kundu, & Schumpe, 2002)	N_2/O_2/Ethanol/ 1-Butanol/Toluene/ Water	P= 0.1 – 1.0 MPa U_g= 1 – 15 cm s^{-1} D= 0.115 m H= 1.37 m	Optical sensor	- Gas holdup and volumetric mass transfer coefficients increased with the gas density to the power of 0.24. - The effect of pressure was negligible at gas velocities below 1 cm s^{-1} and gas densities below 0.1 kg m^{-3}.
Schafer et al. (Schafer et al., 2002)	N_2/Water/ Cyclohexane and Na_2SO_4 solutions	P= up to 5 MPa T= up to 175 °C D= 0.054 m	Photography	- Increasing the operating pressure reduced surface tension slightly and increased gas density significantly. Both effects reduced the stable bubble size.
Behkish et al. (Arsam Behkish et al., 2002)	$H_2/CO/N_2/CH_4$/ Isopar-M and Hexane mixture/Iron oxides catalyst and glass beads	P= 0.17 – 0.8 MPa U_g= 8 – 20 cm s^{-1} D= 0.316 m H= 2.8 m	- Transient physical gas absorption technique - Dynamic gas disengagement	- The coalescence tendency of gas bubbles due to the presence of high solid concentration appeared to prevail over the effect of pressure.

As already mentioned, in most applications, bubble column reactors are typically operated at high superficial gas velocities and elevated pressures. However, the majority of previous studies reported in the literature are restricted to characterizing bubble columns operating at ambient and low operating pressures and superficial gas velocities. In spite of the wealth of knowledge provided by these previous studies, the information required for the design, scale-up and optimum operation of such reactors at high pressure is still incomplete.

Other applications of bubble column reactors also include operating with viscous and non-Newtonian liquids at high pressure (e.g., hydrotreating petroleum residuum and heavy oil). However, the available studies dealing with bubble column reactors operating with viscous and non-Newtonian liquids at high-pressure condition is limited compared with the extensive amount of published data on the characteristics of bubble columns operating with air-water system under ambient conditions (Philipp Rollbusch et al., 2015). Urseanu et al. (Urseanu et al., 2003) conducted a series of experiments in a bubble column with viscous Newtonian liquids at high pressure. They found that the effect of pressure on gas holdup gradually disappears as the liquid viscosity increases. On the other hand, it is reported by Stegeman et al. (Stegeman, Knop, Wijnands, & Westerterp, 1996) that the pressure effect in pure water is small, whereas its effect is more pronounced in viscous liquids. Ishiyama et al. (Ishiyama, Isokawa, Sawai, & Kojima, 2001) also showed that the gas holdup in the nitrogen-water system increases with the system pressure. On the other hand, they found a maximum for the gas holdup in the carbon dioxide-water system at the pressure of 0.6 MPa and then the gas holdup decreased as the pressure was increased up to 1.3 MPa. They attributed this phenomenon to the increased viscosity of water saturated with carbon dioxide at higher pressures.

The bubble properties as well as the hydrodynamics of bubble columns in the presence of non-Newtonian liquids and at high pressure are remarkably different from those operating with low viscosity and Newtonian liquids at atmospheric pressure. However, due to the lack of reliable measurement techniques that can be applied at high pressure and difficulties with conducting experiments under such operating conditions, there is little data and few experimental works on this subject and the knowledge on the mechanism of pressure influence in the presence of non-Newtonian liquids is not sufficient at this stage. Therefore, understanding the simultaneous effects of the non-Newtonian liquid phase properties and elevated pressures is of fundamental importance for better design, optimization, and scale-up purposes of bubble columns operating under such

conditions. In our previous works (Amin Esmaeili et al., 2015; A. Esmaeili, Guy, & Chaouki, 2015, Submitted to AIChE J.), the effect of the rheological properties of liquid phase on the hydrodynamics of a bubble column reactor has been extensively investigated at ambient pressure. In this work, the simultaneous effects of liquid phase rheological properties and operating pressure have been studied in a pilot-scale bubble column reactor by means of analyzing the pressure signals.

6.2 Experimental

6.2.1 Bubble column reactor

The experiments are conducted using a high-pressure/high-temperature multiphase flow unit. The schematic of the multiphase flow unit is shown in Figure 6-1. The unit is comprised of a high-pressure bubble column, two air compressors, two high-pressure gas storage cylinders, gas heating elements, a liquid supply tank, liquid pump, two gas-liquid separators, and the PLC control unit. Since the liquid phase is operated under batch condition, the static liquid height is adjusted to 1.05 m (L/D=6.9) prior to any measurement. The air is first compressed and charged to the two high-pressure gas storage cylinders. The gas cylinders are essentially used to absorb the pressure fluctuations created by the compressors (Model: LT20-30, Atlas Copco, Canada) and provide a stable gas flow rate and operating pressure.

The compressed air is then fed into the bottom of the column via a perforated plate gas distributor and mixed with the liquid phase in the plenum section. The bubble column reactor is made of stainless steel and can be operated at pressures up to 3 MPa and temperatures up to 300 °C. The column has an inner diameter of 0.152 m and a total height of 4.8 m. Several large-diameter ports are drilled in the column wall through the column height at equal distances of 0.2 m for the insertion of probes for various types of measurements. The inlet gas pressure is adjusted using a spring-loaded pressure reducing regulator (Type 630, Big Joe™). The superficial gas velocity and the system pressure are simultaneously regulated and controlled by two pneumatic ball values (Model: 15A-N47P-SW-V60, Habonim) located at the inlet and outlet of the column, respectively. The geometrical specifications of the bubble column system and the selected operating conditions are summarized in Table 6-2.

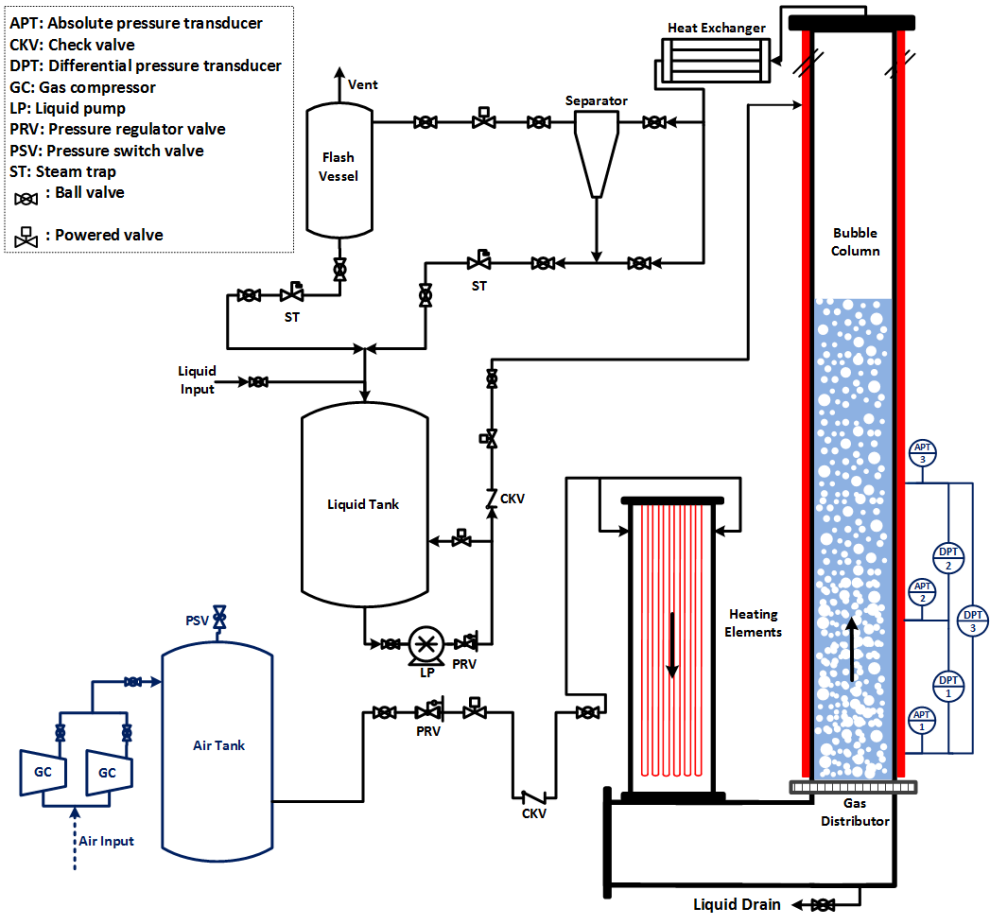

Figure 6-1: A schematic diagram of the experimental unit.

A series of fast response differential and dynamic pressure transducers (response time < 1 ms) flush-mounted on the column wall along the active height of the column measure the gas holdup and pressure fluctuations. Two piezoelectric sensors (Model: 113B26, ICP® sensors, PCB Inc.) are installed at heights of 0.2 m (L/D=1.3) and 0.6 m (L/D=3.9) above the distributor plate to record the dynamic pressure fluctuations in the middle and top zones of the column, respectively. The total average gas holdup and also the gas holdup in different sections of the column are measured by means of three differential pressure transducers (Model: CE5NBA20, Viatran Inc.). A data acquisition card (National Instrument, USB-6211) along with LabVIEW software are used to collect and sort the data. The pressure fluctuations are recorded at a frequency of 512 Hz for 120s. In order to reduce the number of measurement errors, the pressure data are registered three times

and the average of these three readings is used to calculate the final values of the gas holdup and other hydrodynamic parameters.

Table 6-2: Geometrical specifications of the bubble column and distributor plate.

Parameter	**Value**
Column diameter, D_C	0.152 m
Column total height, H_C	4.8 m
Static liquid height, H_0	1.05 m
Operating pressure, P	0.1-1.0 MPa
Superficial gas velocity range, U_g	1-35 (cm s^{-1})
Gas Distributor:	
Distributor type	Perforated plate
Plate thickness	0.006 m
Orifice arrangement	0.027 m spaced square pitch
Orifice diameter, d_o	0.001 m
Number of orifice, N_o	24
Orifice density	1316 (orifices m^{-2})

The pressure influence on the hydrodynamics is strongly affected by the gas distributor design. It is reported by Oyevaar et al. (Oyevaar et al., 1991) that the effect of pressure on the gas holdup in bubble columns equipped with a perforated plate is always found to be stronger compared with those equipped with a porous plate. Stable flow through the distributor plate is obtained when the orifice Weber number (ratio of the gas initial force to the interfacial tension force) is greater than two as follows (Arsam Behkish, 2004):

$$We_o = \frac{\rho_g U_o^2 d_o}{\sigma} = \frac{\rho_g U_g^2 D_c^4}{N_o^2 d_o^3 \sigma} \geq 2 \tag{6.1}$$

Therefore, the operating conditions are chosen in a way to insure a stable bubble flow through the perforated plate used in this study. It is also worth mentioning that there is no incentive to operate the bubble column reactors at very high superficial gas velocities since the high power consumption and short gas residence time are not economical.

6.2.2 Materials and rheological study

In order to discriminate between Newtonian, shear-thinning and elastic behaviors, five types of fluids with different rheological characteristics are objectively chosen. The selected liquids are a 70 vol.% aqueous solution of Newtonian Glucose syrup (Enzose 62DE, Univar, Canada), an elastic constant-viscosity Boger fluid prepared by dissolving 0.04 wt.% of PAA (Sigma-Aldrich, Canada, M_w~5,000,000-6,000,000) in 60 vol.% of aqueous Glucose solution and two viscoelastic fluids consisting of 0.5 wt.% aqueous solutions of high molecular weight CMC (Grade 7HF, CPKelco, USA) and Xanthan gum (200 mesh, Cambrian, Canada) polymers. All of the solutions are prepared by gently adding a known weight of polymers into a known weight of water in a continuously stirred tank of 200 liters at 22 °C. The solutions are left to rest for 24 hours prior to starting the experiments. All experiments are also repeated with water as the reference fluid. The surface tension of the test liquids is measured with a Dynamic Interfacial Tensiometer equipped with a Wilhelmy plate (DCAT21, Dataphysics, Germany).

The rheological characterization of the solutions is carried out in a modular compact rheometer (MCR-501, Anton Paar) with a double-gap Couette geometry. A simple shear study with a shear rate ranging from 0.1 to 1500 s^{-1} is conducted in order to measure the apparent viscosity (μ_{app}). An oscillatory shear study is also performed in the linear viscoelastic regime (at a strain amplitude of 10%) to determine the dynamic moduli of viscoelastic solutions. The apparent viscosity of the solutions is represented in Figure 6-2. The parameter "n" in Figure 6-2 indicates the flow index of the fluid measured by using the Power-law model for shear-thinning liquids as follows (Schowalter, 1960):

$$\mu_{app} = K\dot{\gamma}^{n-1} \tag{6.2}$$

As is obvious from Figure 6-2, the rheological behavior of both Glucose and Boger solutions is Newtonian since their viscosity is constant over the range of shear rates applied in the rheometer while the CMC and Xanthan gum solutions exhibit a strong deviation from Newtonian type of fluids by showing shear-thinning behaviors.

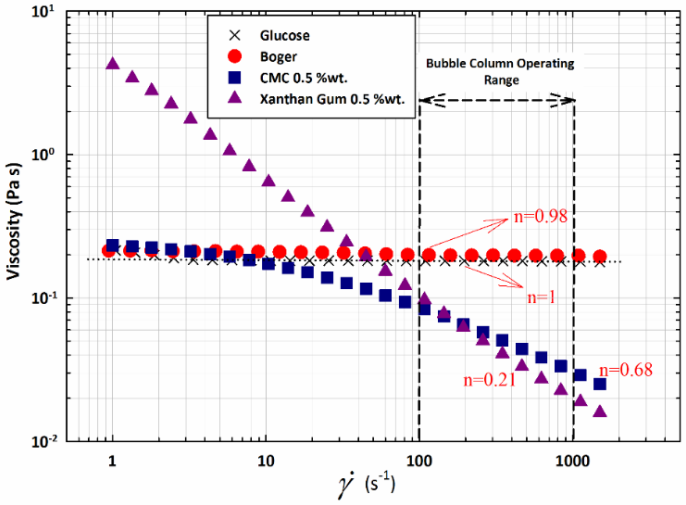

Figure 6-2: Variation of the apparent viscosity of the aqueous solutions with shear rate.

In the previous works of the authors (Amin Esmaeili et al., 2015; A. Esmaeili et al., 2015, Submitted to AIChE J.), it was found that along with the apparent viscosity, the storage modulus (G′) and loss modulus (G″) of viscoelastic solutions can be considered as appropriate factors for a complete description of the rheological effects of viscoelastic solutions in bubble column reactors. Therefore, in order to gain a better understanding of the viscoelastic behavior of the solutions, storage and loss moduli are measured under small amplitude oscillatory shear and reported in Figure 6-3 as a function of angular frequency. More details on the rheological measurements can be found elsewhere (A. Esmaeili et al., 2015, Submitted to AIChE J.).

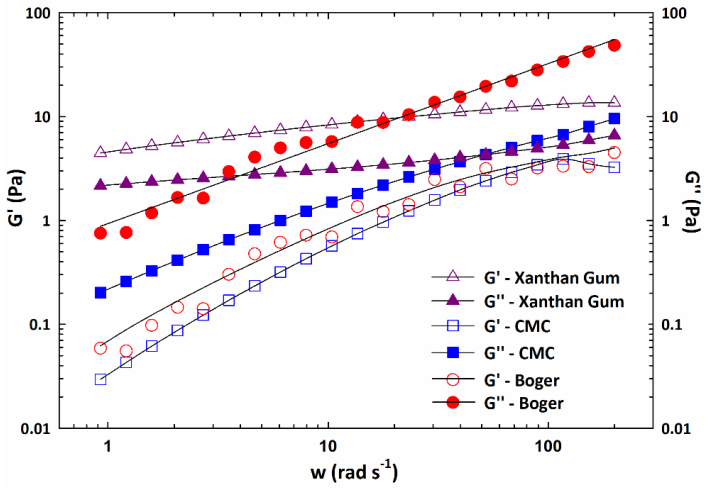

Figure 6-3: Dynamic moduli versus angular frequency for the test solutions.

Figure 6-3 demonstrates that the elastic modulus in the Xanthan gum solution is higher than the viscous modulus ($\frac{G'}{G''} > 1$) signifying the stronger elastic behavior and the dominance of the elastic properties of the Xanthan gum solution at all applied angular frequencies. In contrast, for the CMC and Boger solutions, the $\frac{G'}{G''}$ ratio is less than unity corresponding to a clearly visible dominance of the viscous modulus at any given frequency. In conclusion, except the Glucose solution, all three other solutions are viscoelastic, though the Xanthan gum solution behaves in a different way as the $\frac{G'}{G''}$ ratio is over unity for this solution. It should be noted that this ratio is almost constant for all solutions in the experimental frequency range. The physical and rheological properties of the test liquids are summarized in Table 6-3.

Table 6-3: Rheological and physical properties of the test liquids at 22 °C.

Test liquid	**Composition**	**Density (kg m^{-3})**	**Surface Tension (mN m^{-1})**	**Properties**	$\frac{G'}{G''} \approx$	**Effects**
Water	-	997.04	71.97	-	0	Low-viscous liquid
Glucose	70 vol.% in water	1293.5	74.33	Newtonian and Highly viscous	0	Strong viscosity effects
Boger	60 vol.% Glucose + 0.04 wt.% PAA in water	1251.1	75.28	Viscoelastic	0.11	Elasticity effects << viscosity effects
CMC	0.5 wt.% in water	995.65	73.92	Viscoelastic	0.36	Elasticity effects < viscosity effects
Xanthan gum	0.5 wt.% in water	995.31	76.07	Viscoelastic	2.68	Elasticity effects > viscosity effects

It is worth mentioning that in bubble column reactors and at any given superficial gas velocity, bubbles rise with a specific bubbling frequency through the column height exerting a specific shear to each element of liquid in their vicinity. This shear can be considered to be similar to what the liquid experiences in the small amplitude oscillatory shear experiment. The frequency of this shear applied by the rising bubbles can be identical to the bubbling frequency, which is typically less than 100 Hz for the operating conditions applied in this work (A. Esmaeili et al., 2015, Submitted to AIChE J.). Therefore, the range of angular frequency in the small amplitude oscillatory shear experiments is specifically chosen to cover all the frequencies that the liquid may undergo in the

bubble column reactor used in this study. Moreover, since most of the liquids are almost non-compressible at low or medium pressures, the viscosity of liquids is independent of the applied range of pressure in this work.

6.3 Results and discussion

The superficial gas velocity, the operating pressure as well as the liquid phase properties play an important role in the hydrodynamic aspects of bubble column reactors. In the following sections, the simultaneous effects of the above-mentioned operating conditions on the various hydrodynamic parameters is discussed. Several measurements and analyses are done on the time series pressure signals to investigate the gas holdup, the operating flow regime transition, and different phenomena happening in the bubble column in the presence of non-Newtonian liquids and at elevated pressures.

6.3.1 Effect of pressure on the gas holdup

The gas holdup is one of the most important hydrodynamic and design parameters that has a great impact upon the design of bubble column reactors. The total volume of the reactor for any operating conditions is determined by the maximum gas holdup that must be accommodated. In this study, the total time-averaged gas holdup is evaluated by measuring the pressure gradient between two points located at the distance of 0.2 and 1 m from the distributor plate, respectively (see DPT3 in Figure 6-1). The gas holdup is related to the pressure gradient by:

$$\varepsilon_g = 1 - \frac{1}{\rho_l g}\left(\frac{\Delta P}{\Delta Z}\right) \tag{6.3}$$

The effect of operating pressure on the gas holdup for different solutions used in this study is shown in Figure 6-4. The gas holdup is strongly affected by the superficial gas velocity and operating pressure. Therefore, a dimensionless group of parameters including the superficial gas velocity and the gas density (as a representative parameter for considering the pressure effects) is defined in the form of $\left(\frac{U_g^4 \rho_g}{\sigma g}\right)$ in order to describe the effect of superficial gas velocity and operating pressure simultaneously.

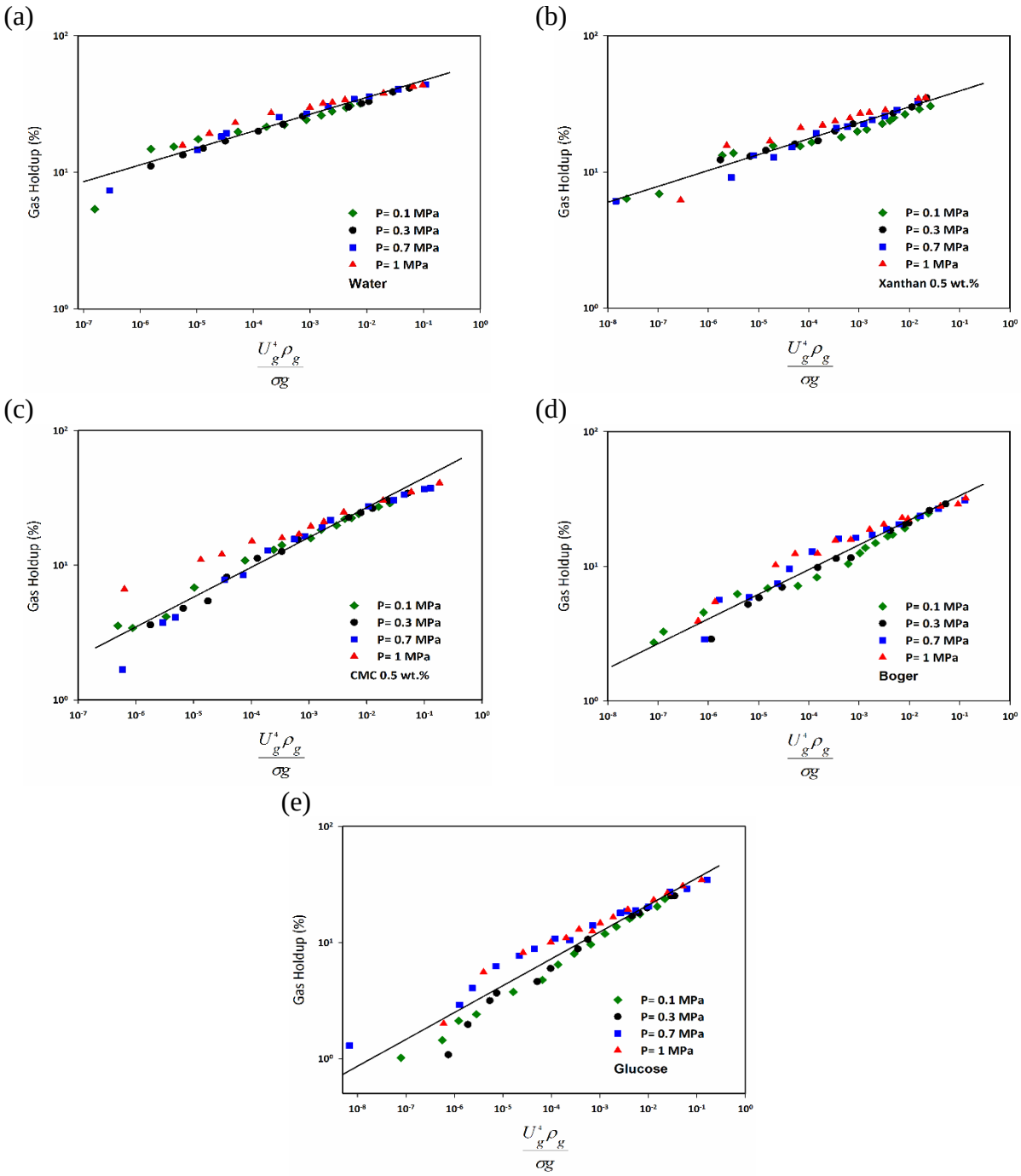

Figure 6-4: Variation of gas holdup with operating pressure for different solutions: (a) Water; (b) Xanthan gum 0.5 wt.%; (c) CMC 0.5 wt.%; (d) Boger; and (e) Glucose.

Figure 6-4 shows that the total gas holdup increases by increasing both the superficial gas velocity and the operating pressure and this trend can be observed for all the solutions applied in this study.

In fact, increasing the operating pressure results in an increase in the gas density, which is responsible for the formation of smaller bubbles at the distributor plate. Smaller bubbles rise with lower velocity along the column height and thus the gas holdup is higher under this condition. It is also widely accepted that the elevated pressure is mainly responsible for reducing the coalescence tendency of the gas bubbles (Arsam Behkish, 2004). The influence of pressure on the gas holdup is not strong at low superficial gas velocities (i.e., $U_g \leq 6\ cm\ s^{-1}$), however, it becomes more significant at higher superficial gas velocities. In order to make these effects more evident, the increase in the gas holdup in two different ranges of superficial gas velocity is given in Table 6-4. As pointed out in this table, the increase in the gas holdup with pressure, is more significant at higher superficial gas velocities ($U_g > 6\ cm\ s^{-1}$) than in lower superficial gas velocities ($U_g \leq 6\ cm\ s^{-1}$) and this can be observed for all liquids applied in this work. This phenomena can be attributed to the unstable bubble flow (low Weber number) at low superficial gas velocities (Arsam Behkish, 2004). It is also reported by Clark (K. N. Clark, 1990) that under low superficial gas velocities, the bubble size and, accordingly, the gas holdup are influenced more by the interfacial tension at the gas distributor than the operating pressure.

Table 6-4: Effect of pressure on the gas holdup in different ranges of superficial gas velocity.

Test liquid	$\Delta\varepsilon_g$ **for** $\Delta P = 1\ MPa$	
	$U_g \leq 6\ cm\ s^{-1}$	$U_g > 6\ cm\ s^{-1}$
Water	8.1%	11.0%
Xanthan 0.5 wt.%	5.2%	12.1%
CMC 0.5 wt.%	6.7%	10.5%
Boger	4.1%	9.7%
Glucose	5.2%	10.8%

To better understand the simultaneous effects of the operating pressure and liquid phase properties on the gas holdup, this parameter for all solutions and at two operating pressures of 0.1 and 1.0 MPa is plotted separately and presented in Figure 6-5.

(a) (b)

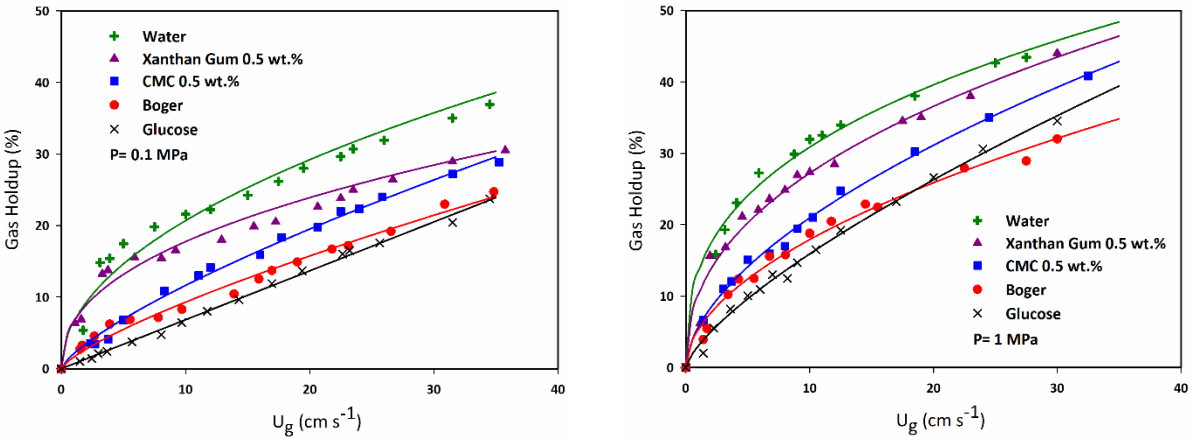

Figure 6-5: Effect of liquid properties on the gas holdup at different operating pressures: (a) P= 0.1 MPa; and (b) P= 1.0 MPa.

In our previous work (Amin Esmaeili et al., 2015; A. Esmaeili et al., 2015, Submitted to AIChE J.), a new approach based on the $\frac{G'}{G''}$ ratio was developed and applied to interpret the simultaneous effects of the elasticity and viscosity of non-Newtonian solutions on the global and local hydrodynamic parameters of bubble column reactors. It was found that the coalescing effects of highly viscous liquids on the gas holdup and bubble size decreased in the presence of elastic effects and these effects can be directly explained by comparing the values of $\frac{G'}{G''}$ for different solutions. As is obvious from Figure 6-5, at any given superficial gas velocity, the gas holdup in water (as the low viscosity liquid) is highest while it has the lowest values in the Glucose solution that has a high viscosity. As already seen in Figure 6-3, the Xanthan gum solution has a dominating elastic modulus ($\frac{G'}{G''} > 1$) compared to the CMC solution ($\frac{G'}{G''} < 1$). Therefore, the higher gas holdup in the Xanthan gum solution is a result of the higher elastic effects that can prevent bubble coalescence and form smaller bubbles in this solution. The effects of the rheological properties of the solutions at elevated pressures are the same as at ambient pressure, which is clear from Figure 6-5. The gas holdups in Boger solutions are slightly higher than those in the Glucose solution at pressure of 0.1 MPa while there is no clear difference between them at higher pressure of 1.0 MPa.

6.3.2 Gas holdup axial distribution at high pressure

Based on the geometry of the bubble column, three different zones with their respective gas holdup can be identified as follows: (1) distributor zone in which gas holdup depends on the distributor design; (2) bulk or middle zone where the gas holdup is controlled more by the liquid circulation; and (3) top zone in which the gas holdup is large due to the formation of a layer of froth above the liquid (Arsam Behkish, 2004). The gas holdup in the middle and top regions of the column is measured by means of DPT1 and DPT2 (as shown in Figure 6-1), respectively. Figure 6-6 demonstrates the axial distribution of the gas holdup for different solutions at P=1.0 MPa.

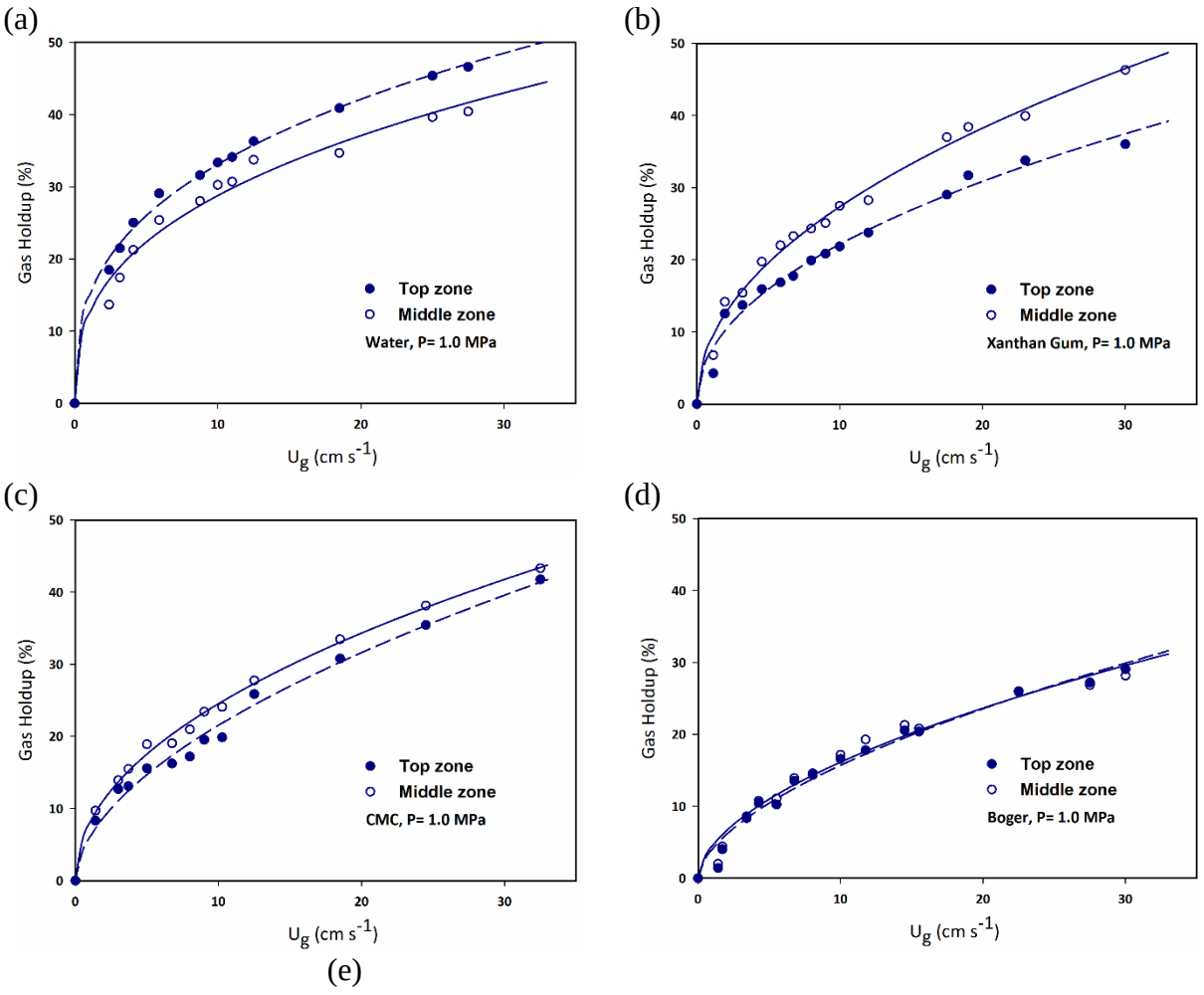

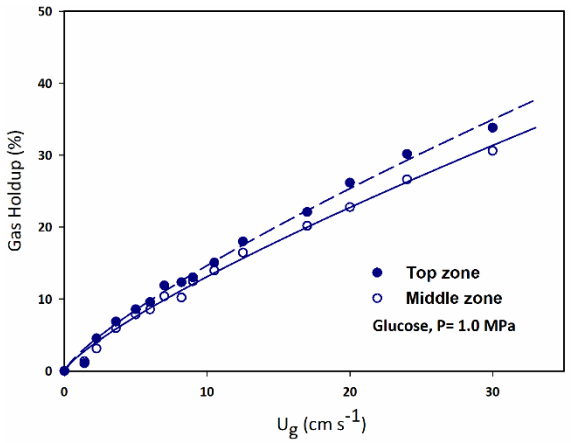

Figure 6-6: Gas holdup axial distribution for different operating solutions at P= 1.0 MPa: (a) Water; (b) Xanthan gum 0.5 wt.%; (c) CMC 0.5 wt.%; (d) Boger; (e) Glucose.

As can be seen in Figure 6-6, the gas holdup in the top zone of the column is higher than that in the middle zone of the column for water while there is no significant difference between the gas holdup measured in the middle and top zones of the column for Boger and Glucose especially at low superficial gas velocities. However, the gas holdup for the Xanthan gum and CMC solutions in the middle zone is higher than that in the top zone of the column. In bubble column reactors, a swarm of bubbles rises through the column height and these moving bubbles can exert a specific shear stress on each element of liquid in their vicinity and accordingly deform it. On the other hand, in the region closer to the gas distributor, the flow pattern is more stirred, the bubble-bubble and bubble-liquid interactions are developed, the inertia force that the bubbles experience is higher, and consequently the shear rate in this region is higher than that in the regions far from the gas distributor. All these effects may cause a higher shear stress to be exerted on the liquid phase in the middle zone of the column. Increasing shear stress on the shear-thinning liquids leads to a decrease in their viscosity and the higher gas holdup in the middle zone of the column for Xanthan gum and CMC solutions can be attributed to their shear-thinning properties. It can be concluded that since the shear stress exerted on Xanthan gum and CMC solutions is higher in the middle zone, the local viscosity of these solutions in the middle zone is less than that in the top zone of the column. Lower viscosity results in the formation of smaller bubbles and consequently higher gas holdup. Moreover, the difference in the gas holdup in middle and top zone of the column is more obvious

for the Xanthan gum solution than for the CMC solution and the reason is the higher shear-thinning behaviour of the Xanthan gum solution used in this work (as previously explained in Figure 6-2).

The higher gas holdup in the top zone of the column for water can be due to the expansion of the gas bubbles rising toward the surface of the liquid and the developed liquid circulation that increases the residence time of small bubbles and thus increases the gas holdup in the top zone of the column. It is worth mentioning that similar results are also found for lower operating pressures applied in this work but only one selected pressure is presented in this section. Furthermore, it seems that the axial distribution of gas holdup is not affected by the elasticity of the solutions and is independent of the values of $\frac{G'}{G''}$ ratio, whereas it is related more to the shear-thinning properties of the solutions.

6.3.3 Effect of pressure on the operating flow regime transition

Basically, two flow regimes are observed in the bubble column reactors: (1) homogeneous or bubbly flow regime; and (2) heterogeneous or churn-turbulent flow regime. The homogeneous flow regime, which contains small and uniform bubbles is generally observed at low superficial gas velocities while the heterogeneous flow regime is commonly encountered at high superficial gas velocities and characterized by a wide bubble size distribution, the turbulent motion of gas bubbles and the presence of the liquid circulation cells.

Normally, the point at which the slope of the ε_g - U_g curve changes, can be considered as the regime transition point (Gourich et al., 2006; Shaikh & Al-Dahhan, 2013; Shaikh & Al-Dahhan, 2007). In addition, literature studies have extensively used the drift flux approach proposed by Wallis (Ruzicka et al., 2003; Sheikhi et al., 2013; Vial et al., 2000; Wallis, 1969). The drift flux in a bubble column is defined as the volumetric flux of gas relative to a surface moving at the average velocity of gas-liquid flow systems and can be expressed using the relative velocity between the gas and liquid phases as follows:

$$j_{gl} = \varepsilon_g(1-\varepsilon_g)\left[\frac{U_g}{\varepsilon_g} - \frac{U_l}{\varepsilon_l}\right] \tag{6.4}$$

That for a bubble column with batch operation for the liquid phase (i.e., $U_l = 0\ cm\ s^{-1}$), it can be simplified to:

$$j_{gl} = U_g(1 - \varepsilon_g) \tag{6.5}$$

A slope change in the plot of the drift flux versus gas holdup can be considered as the transition point. Figure 6-7 shows the drift flux plotted versus gas holdup for water at different operating pressures.

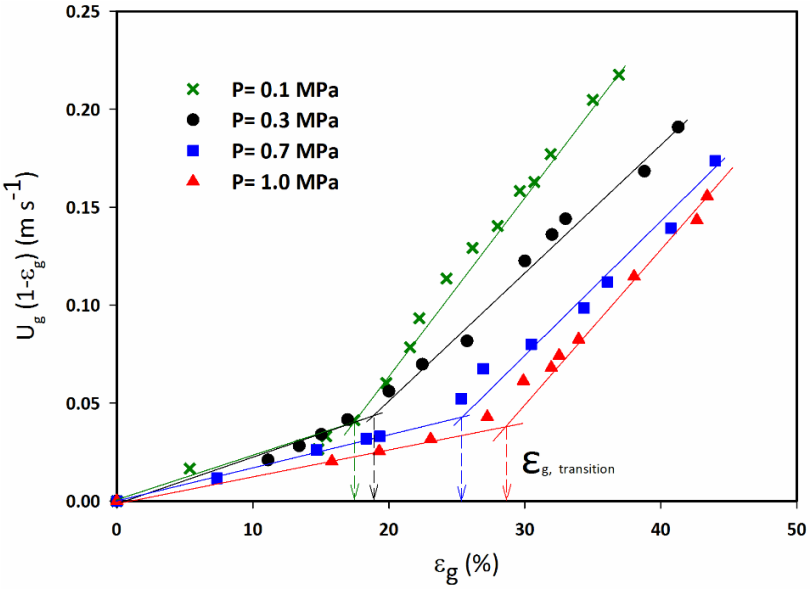

Figure 6-7: Identification of regime transition by Wallis' drift flux approach for water.

As pointed out in Figure 6-7, as the pressure increases, the change in the slope of the drift flux curve versus gas holdup occurs at higher gas holdups (corresponding to higher superficial gas velocities), which means the transition from homogeneous to heterogeneous flow regime is delayed and occurs at higher superficial gas velocities. Maleej et al. (Maalej et al., 2003) showed that an increase in pressure shifts the flow regime transition point to the higher gas holdups and decreases the rise velocity of large bubbles in the heterogeneous flow regime. It has been reported by Cui (Cui, 2005) that the effect of pressure on the flow regime transition is mainly due to the formation of smaller bubbles and narrower bubble size distribution under high pressure that delay the flow regime transition. Similar justifications on the effect of elevated pressures on the flow regime transition have been reported by other researchers (Arsam Behkish, 2004; Y Kang, Cho, Woo, &

Kim, 1999). However, Shaikh and Al-Dahhan (Shaikh & Al-Dahhan, 2005) observed that at ambient conditions, the change in the flow regime is noticeable while the flow regime changes gradually over a region of superficial gas velocities (rather that at a single point) at elevated pressures. The Wallis' drift flux approach is also applied to study the effect of pressure on the flow regime transition in the other solutions used in the present work. Table 6-5 includes the flow regime transition velocities for different solutions and pressures evaluated by Walls' drift flux approach.

Table 6-5: Flow regime transition velocity for different solutions.

Test liquid	$U_{g,transition}$ $(cm\ s^{-1})$			
	P= 0.1 MPa	**P= 0.3 MPa**	**P= 0.7 MPa**	**P= 1.0 MPa**
Water	5.2108	6.3424	6.8438	7.2491
Xanthan gum	3.28	4.0467	4.775	4.614
CMC	-	-	3.3725	3.3294
Boger	2.8486	3.9763	4.718	4.6989
Glucose	-	-	3.9625	4.3694

- : not detected

As seen in Table 6-5, the flow regime transition velocity for water increases with pressure and the same effect is observed for the Xanthan gum and Boger solutions. The homogeneous flow regime can be considered inexistent in many viscous systems (Urseanu et al., 2003). Although, increasing the pressure can allow the bubbling phenomena to be stable and the bubbly flow regime to remain even at relatively high superficial gas velocities, operating at high pressure has a less pronounced effect in viscous liquids than in low-viscous ones. Nevertheless, as is obvious from Table 6-5, for the Xanthan gum solution, the flow regime transition occurs at lower superficial gas velocities compared to those for water. The transition velocity for the CMC solution could be detected only at high pressures of 0.7 and 1.0 MPa, which are also shown to be lower than those for the Xanthan gum solution. It can be concluded that at low pressures, the flow regime is already in the heterogeneous flow for the CMC solution. It is reported that at ambient conditions, the homogeneous bubble flow regime in CMC solutions can be achieved only at gas velocities below a critical one ($\sim$0.5 cm s^{-1}); this critical velocity is a function of the apparent viscosity of the

solution (Velez-Cordero & Zenit, 2011). Kawase and Moo-Young (Kawase & Moo-Young, 1986) also found that for highly viscous non-Newtonian liquids at ambient pressure, the homogeneous flow regime occurs only at very low gas velocities (U_g < 1.3 cm s^{-1}).

Moreover, the dominating elastic modulus ($\frac{G'}{G''} > 1$) in the Xanthan gum solution leads to the existence of smaller bubbles in this solution compared to the CMC solution with the dominance of viscous effects ($\frac{G'}{G''} < 1$) and, therefore, the homogeneous flow regime is more stable and the flow regime transition occurs at higher velocities in the Xanthan gum solution. The flow regime transition in the Boger solution occurs at lower gas velocities compared to Water and the Xanthan gum solution. Similar to the CMC solution, the flow regime transition velocity for the Glucose solution could also not be detected at pressures of 0.1 and 0.3 MPa. Bubble coalescence in the Glucose solution which is highly viscous and inelastic, results in the formation of large bubbles and, hence, the flow regime is already in the heterogeneous flow regime at low pressures while at higher pressures, smaller bubbles are formed that can delay the flow transition and for this reason, a regime transition point can be observed for the Glucose solution at higher pressure. The Boger solution is highly viscous but it is slightly elastic ($\frac{G'}{G''} \ll 1$) and due to the elastic effects, smaller bubbles are formed in this solution compared to that in Glucose solution which is not elastic. Therefore, the formation of smaller bubbles in the Boger solution causes the homogeneous flow regime to appear even at the low pressures of 0.1 and 0.3 MPa and the regime transition point to be detected at these low pressures. Reilly et al. (Reilly, Scott, Debruijn, & MacIntyre, 1994) and Wilkinson et al. (Wilkinson, Spek, & van Dierendonck, 1992) correlated the gas holdup at the regime transition point as a function of physical properties as given in Table 6-6.

Table 6-6: Proposed model for predicting the gas holdup at regime transition point.

Researchers	**Correlation**
Reilly et al. (Reilly et al., 1994)	$\varepsilon_{g,trans} = 0.59B^{1.5}\sqrt{\rho_g^{0.96}\sigma^{0.12}/\rho_l}$, *B=3.85*
Wilkinson et al. (Wilkinson et al., 1992)	$\varepsilon_{g,trans} = 0.5\exp(-193\rho_g^{-0.61}\mu_l^{0.5}\sigma^{0.11})$

The gas holdup at the regime transition point for different solutions and operating pressures is determined from the experimental data and displayed in Figure 6-8 as a function of gas density. Also, the gas holdup at regime transition point predicted by the correlations of Reilly et al. and Wilkinson et al. for water are plotted in Figure 6-8.

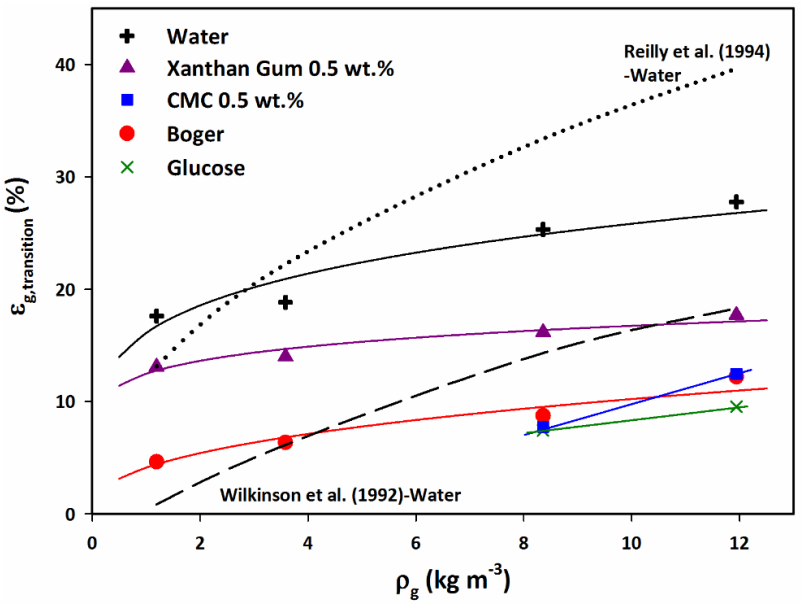

Figure 6-8: The variation of gas holdup at the transition point with pressure for different solutions.

As it can be seen from Figure 6-8, for water system, the gas holdup at regime transition point determined experimentally is lower than that predicted by the correlation of Reilly et al. at elevated pressures. On the other hand, the experimental gas holdups at regime transition point overlap those predicted by the correlation of Wilkinson et al. It is worth mentioning that the predictions of the correlation of Reilly et al. for other solutions is almost identical to those for water system and the reason is that this correlation does not include the effect of liquid viscosity. In addition, although the correlation of Wilkinson et al. includes the effect of liquid viscosity, the gas holdup at regime transition point predicted by this correlation for other solutions is found to be very small (< 3%).

6.3.4 Effect of operating pressure on the pressure fluctuations

The pressure fluctuations signal in the bubble columns is a complex function of fluctuations from several sources, such as the gas input line fluctuations, the bubble formation, rise, coalescence and breakage, bubble-liquid interactions, liquid circulations, and liquid surface fluctuations (Drahoš et al., 1991). The effect of operating pressure on the pressure fluctuations at high superficial gas velocity is shown in Figure 6-9.

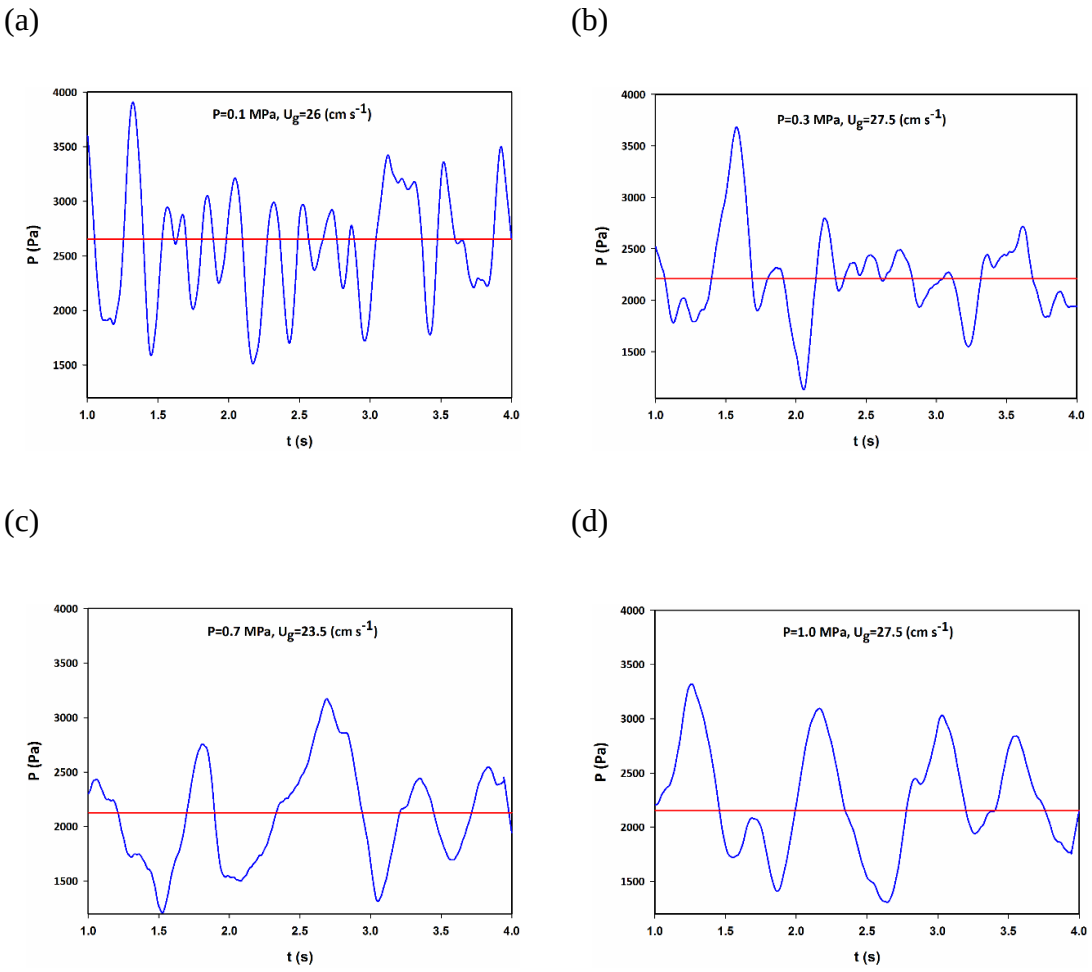

Figure 6-9: Variation of pressure fluctuations with operating pressure for water: (a) P= 0.1 MPa; (b) P= 0.3 MPa; (c) P= 0.7 MPa; and (d) P= 1.0 MPa.

The most important observation in Figure 6-9 is that the pressure fluctuations at P= 1.0 MPa is completely different as compared to that in P= 0.1 MPa indicating an inherent different bed hydrodynamics at elevated pressures. Pressure fluctuation signals in pressurized bubble columns

are complex since the bubbles behave highly irregularly in such conditions (Y. Kang, Cho, Woo, Kim, & Kim, 2000; Park & Kim, 2001). As observed in Figure 6-9, the pressure fluctuation signals at all operating pressures have random appearances and there is no clear periodicity in the fluctuations. However, the amplitude of pressure fluctuations increases relatively with an increase in the operating pressure and this can be attributed to the more complicated bubble-liquid interactions at elevated pressures. Lin et al. (T. J. Lin et al., 2001) also reported similar effects of the increased pressure on the pressure fluctuations in bubble column reactors. As previously explained, at elevated pressures, smaller bubbles are formed at the gas distributor, the bubbling frequency is higher, and due to the higher gas holdup in such conditions the bubble interactions with the liquid phase are promoted. A combination of all these effects results in a higher amplitude in the pressure fluctuations at higher pressures. In addition, the same effects of superficial gas velocity and operating pressure are observed for other solutions used in this study but no definite conclusion can be made on the effects of the rheological properties of solutions on the pressure fluctuations just by visual observation of the fluctuations; and there is a need for more qualitative investigations in this case.

6.3.5 Effect of operating pressure on the standard deviation of pressure fluctuations

Statistical analysis of pressure signals has widely been applied in many studies to characterize the hydrodynamics in bubble column reactors (S. Barghi et al., 2004; Cui, 2005; Johnsson et al., 2000; Kumar et al., 2013; Sheikhi et al., 2013). Statistical analysis is based on the estimation of moments of the probability density function of a pressure signal. Usually, only standard deviation (square root of the second-order statistical moment) is estimated and higher moments require a large amount of accurate experimental data. In order to evaluate the effects of various parameters on the pressure fluctuations and thus the hydrodynamic of the bubble column, the standard deviation of pressure fluctuations is evaluated and studied in this section. The standard deviation as a measure of data set dispersion from its mean is given by

$$\sigma = \sqrt{\frac{1}{N-1}\sum_{n=1}^{N}(P_n - \bar{P})^2} \tag{6.6}$$

Where $\bar{P}$ is the mean pressure and is defined by

$$\bar{P} = \frac{1}{N}\sum_{n=1}^{N} P_n \tag{6.7}$$

The variation of standard deviation with operating pressure for different solutions is presented in Figure 6-10.

(a)

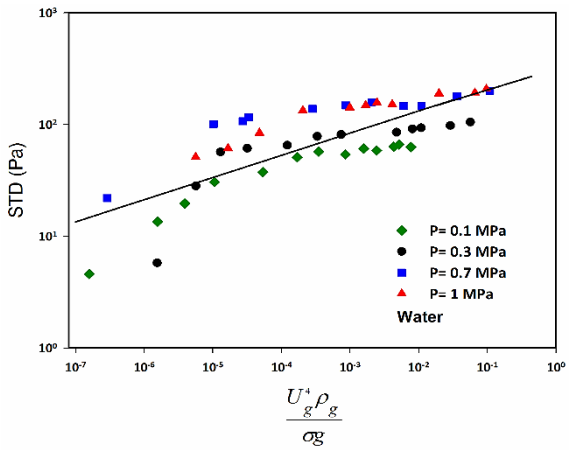

(b)

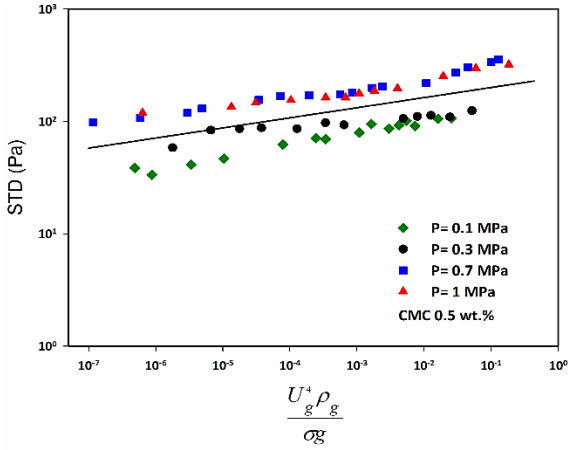

(c)

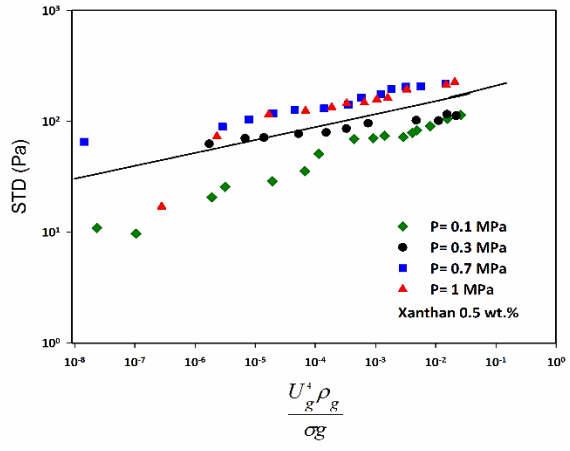

(d)

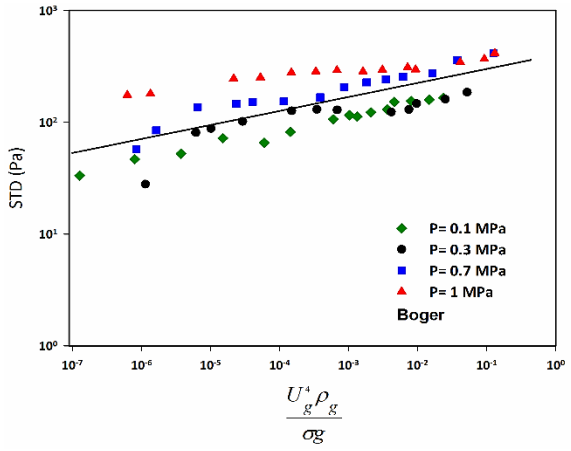

(e)

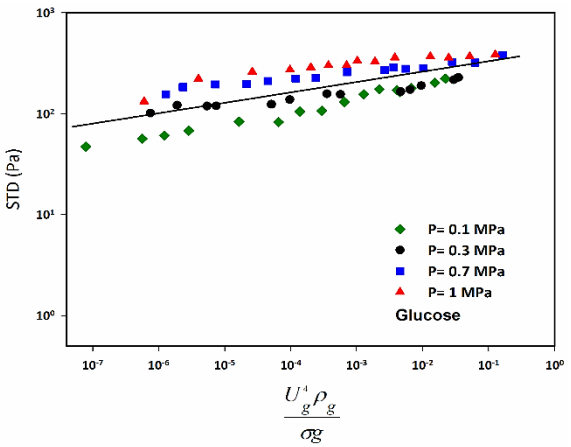

Figure 6-10: Variation of standard deviation with operating pressure for different solutions: (a) Water; (b) Xanthan gum 0.5 wt.%; (c) CMC 0.5 wt.%; (d) Boger; and (e) Glucose.

It can be pointed out from Figure 6-10 that for almost all solutions, the standard deviation increases with both superficial gas velocity and operating pressure. This trend is closely associated with the trend in the gas holdup (see Figure 6-4). As already mentioned in this study, as the superficial gas velocity increases, the heterogeneous flow regime characterized by large rising bubbles with relatively high velocity, the turbulent motion of gas bubbles, and liquid circulation become dominant. The larger bubbles and more turbulence at higher superficial gas velocities create more pressure fluctuations and, accordingly, the standard deviation is higher. Furthermore, the gas density and momentum increases with an increase in the operating pressure. When the gas density increases, the liquid phase disturbances will increase as well. Higher bubbling frequency and bubble-liquid interactions at elevated pressures also introduce higher turbulence intensity into the liquid phase and create more pressure fluctuations. All the above-mentioned phenomena can lead to an increase in the standard deviation at elevated pressures. In order to have better insight into the simultaneous effects of the operating pressure and the liquid phase properties, the standard deviation for all solutions at two pressures of 0.1 MPa and 1.0 MPa is plotted separately and shown in Figure 6-11.

(a) (b)

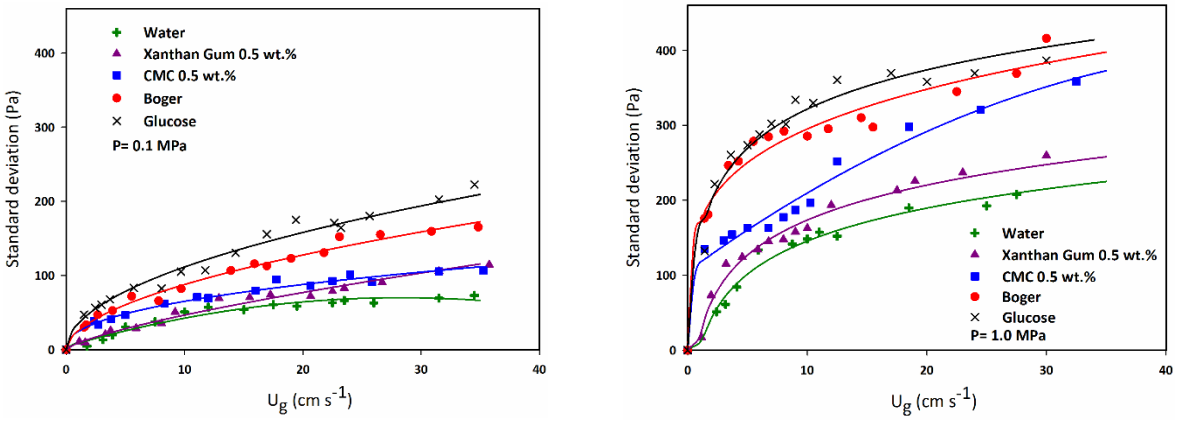

Figure 6-11: Variation of standard deviation with operating pressure for different solutions: (a) P= 0.1 MPa; and (b) P= 1.0 MPa.

In a previous work of the author (Amin Esmaeili et al., 2015), it was found that at ambient pressure, the standard deviation increases with the liquid viscosity, which was attributed to the presence of larger bubbles in the viscous liquids. As seen in Figure 6-11, at any given superficial gas velocity, the standard deviation of the Glucose solution is highest and the one for water is lowest. This is obvious for almost all of the applied operating pressures. The bubble size in Glucose as the highly viscous and inelastic liquid is shown to be larger than that in water (Amin Esmaeili et al., 2015). Therefore, the larger bubbles in the Glucose solution can generate higher pressure fluctuations and thus higher standard deviation, as observed in Figure 6-11. The Boger solution is slightly elastic ($\frac{G'}{G''} \ll 1$) and the bubbles in this solution are smaller compared to those in the Glucose solution (Amin Esmaeili et al., 2015). The lower standard deviation in the Boger solution can be attributed to the elastic effects of this solution that prevent the bubble coalescence and form smaller bubbles. There is no clear difference between the standard deviations for the Xanthan gum and CMC solutions at pressure of 0.1 MPa. However, at higher pressure of 1.0 MPa, the standard deviation in the CMC solution is relatively higher than that in the Xanthan gum solution. The Xanthan gum solution has a dominating elastic modulus ($\frac{G'}{G''} > 1$) compared to the CMC solution ($\frac{G'}{G''} < 1$) and due to the higher elastic effects, the bubble size in the Xanthan gum solution is smaller than that in the CMC solution. Hence, the lower standard deviation in the Xanthan gum solution can be related to

the presence of smaller bubbles in this solution in comparison with that in the CMC solution. The influences of the elevated pressure on the different hydrodynamic aspects of the bubble column are summarized in Table 6-7.

Table 6-7: Summary of the effects of elevated pressure on the hydrodynamic characteristics of bubble column.

Characterictic	ε_g	$U_{g,transition}$	$\varepsilon_{g,transition}$	**Axial distribution of** ε_g	**Amplitude of pressure fluctuations**	σ
$\uparrow \boldsymbol{P}$ **:**	↑	↗	↗	↔	↗	↑

↑: Increasing ↗: Slightly increasing ↔: No clear effect observed

6.3.6 Developing a correlation for predicting gas holdup

Empirical and/or semi-empirical correlations are often used for the design purposes of bubble column reactors. Therefore, in order to conduct a proper design and scale-up of bubble columns, it is of great importance to use correct correlations for predicting different hydrodynamic parameters and, in particular, the gas holdup. On the other hand, most of the correlations available in the literature are developed based on the experimental data obtained at ambient conditions and are not able to be predict the gas holdup at elevated pressures. To overcome this issue, in this study, a new correlation is developed by applying the dimensional analysis in order to accurately predict the gas holdup in bubble columns operating at elevated pressures and with a wide range of non-Newtonian and viscoelastic liquids. Based on the observations made during the experiments, the gas holdup is influenced by the following parameters involving three dimensions (mass, time and length):

$$\varepsilon_g = f(D_c, \sigma, \rho_L, \rho_g, \mu_L, U_g, g, G', G'') \tag{6.8}$$

Where the gas density accounts for the effect of operating pressure. Applying the Buckingham's π theorem specifies that five independent dimensionless groups can be formed as follows:

$$\pi_1 = \frac{gD_c^2\rho_L}{\sigma} \qquad \pi_2 = \frac{gD_c^3}{\vartheta_L^2} \qquad \pi_3 = \frac{U_g}{\sqrt{gD_c}} \qquad \pi_4 = \frac{G'}{G''} \qquad \pi_5 = \frac{\rho_g}{\rho_L}$$

Rearranging Eq. (6.8) by considering the dimensionless groups leads to:

$$\varepsilon_g = f\left(\frac{gD_c^2\rho_L}{\sigma}, \frac{gD_c^3}{\vartheta_L^2}, \frac{U_g}{\sqrt{gD_c}}, \frac{G'}{G''}, \frac{\rho_g}{\rho_L}\right) \tag{6.9}$$

The first dimensionless group on the right side of Eq. (6.9) is the Bond number (Bo) that consider the effect of surface tension. The second group is the Galilei number (Ga), which is the gravity force divided by the viscous force and represents mainly the influence of liquid viscosity. The effect of superficial gas velocity is taken into account in the third dimensionless group, which is the Froude number (Fr). The fourth dimensionless group, which is the ratio between the dynamic moduli of viscoelastic liquids, introduces the effect of the rheological properties of the liquid in the model. The effect of operating pressure is also introduced in the form of the gas density in the last dimensionless group. According to the experimental results, the gas holdup is dependent on the rheological properties of the liquid phase based on the ratio of $\frac{G'}{G''}$ being more or less than unity. Therefore, in order to develop a correlation that is applicable in both Newtonian and viscoelastic solutions, the best form for the effect of rheological properties was found to be exponential. By considering all the above-mentioned points and rearranging Eq. (6.9) according to the defined dimensionless groups, the final form of the correlation for the gas holdup is given by:

$$\varepsilon_g = a\, Bo^b\, Ga^c\, Fr^d\, e^{e\left(1-\frac{G'}{G''}\right)}\left(\frac{\rho_g}{\rho_L}\right)^f \tag{6.10}$$

The coefficients in Eq. (6.10) are evaluated using the Genetic Algorithm method in MATLAB by fitting the experimental data of the gas holdup measured in this work and those measured under ambient pressure in a bubble column with a diameter of 0.29 m in our previous works (Amin Esmaeili et al., 2015; A. Esmaeili et al., 2015, Submitted to AIChE J.); that means a total of 359 data points. Replacing the evaluated coefficients in Eq. (6.10) gives the final form of the correlation as follows:

$$\varepsilon_g = 0.13\, Ga^{0.14}\, Fr^{0.73}\, e^{-0.1\left(1-\frac{G'}{G''}\right)}\left(\frac{\rho_g}{\rho_L}\right)^{0.05} \tag{6.11}$$

The agreement between the gas holdups measured experimentally and that predicted by Eq. (6.11) is within the mean absolute percentage error (MAPE), standard error, and 95% prediction interval of 20%, ±3.3%, and ±9%, respectively. It is worth mentioning that Eq. (6.11) predicts an increase in the gas holdup with an increase in the superficial gas velocity, operating pressure (gas density), and $\frac{G'}{G''}$, but a decrease in the gas holdup with an increase in the liquid viscosity. All these predictions are consistent with the results obtained experimentally in this study. Moreover, the liquids used for performing the experiments have similar surface tension (see Table 6-3) and for this reason the Bond number that displays the effect of liquid surface tension force does not appear in the final form of the correlation. In order to have a better understanding about the validity of the proposed correlation, the experimental values of gas holdup are compared with those predicted by Eq. (6.11) for different solutions and are shown in Figure 6-12. As can be seen in Figure 6-12, the proposed correlation can predict the experimental data of gas holdup with fairly good accuracy.

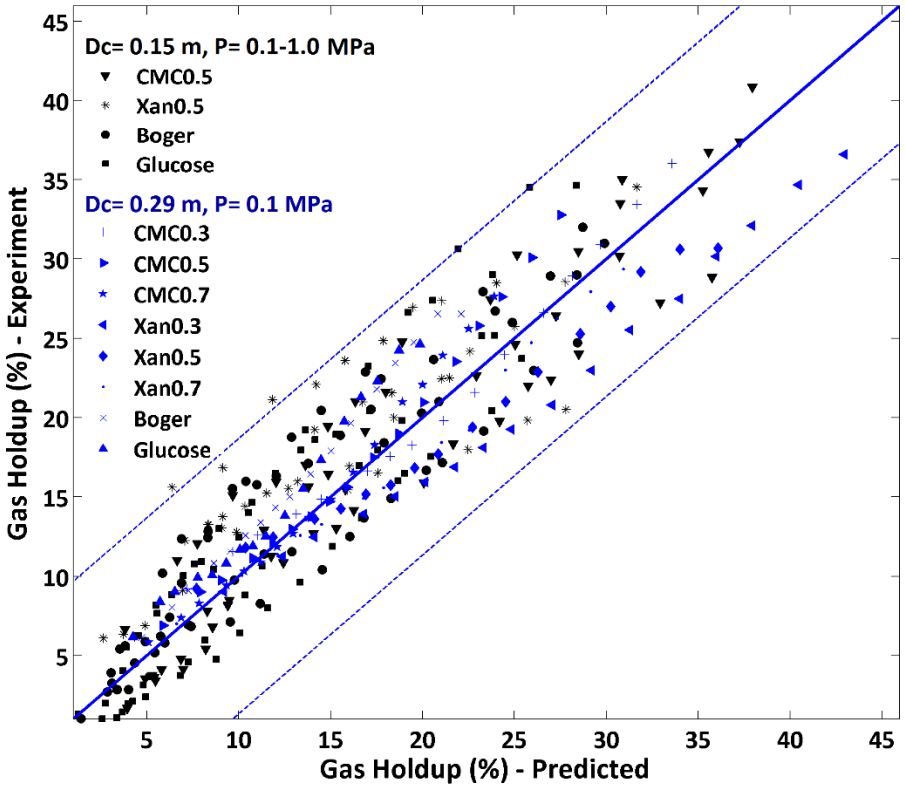

Figure 6-12: Comparison between the experimental and predicted value of gas holdup.

In order to evaluate the accuracy of the correlations proposed for gas holdup by other researchers, a literature survey was conducted to find the most applicable models reported for predicting the gas holdup in bubble column reactors operating at elevated pressures. There are some correlations in the literature that claimed to incorporate the influence of operating pressure (gas density). The correlation of Hammer et al. (Hammer et al., 1984) is shown to be able to predict the gas holdup in various organic liquids in pressures up to 0.7 MPa with good agreement. Idogawa et al. (Idogawa, Ikeda, Fukuda, & Morooka, 1985) developed a correlation to predict the gas holdup in various liquid phases, including methanol, ethanol, acetone, and aqueous alcohol solutions at pressures up to 5 MPa. Hikita et al. (Hikita et al., 1980) also proposed a dimensionless correlation for the gas holdup in pure liquids and aqueous solutions of non-electrolytes. They have shown that their model is able to correlate the experimental data with an average deviation of 4.2%. The above-mentioned correlations are summarized in Table 6-8.

Table 6-8: Summary of the gas holdup models proposed by different researchers.

Researchers	**Correlation proposed**	**Range of applicability**
Hammer et al. (Hammer et al., 1984)	$\frac{\epsilon_g}{1-\epsilon_g} = 0.4\left(\frac{u_g\mu_L}{\sigma}\right)^{0.87}\left(\frac{\mu_L^4 g}{\rho_L\sigma^3}\right)^{-0.27}\left(\frac{\rho_g}{\rho_L}\right)^{0.17}$	$P = 0.1-0.7\ MPa$ $T = 263-293\ K$ $D = 10.6, 20\ cm$ $U_g = 0.5-13\ cm\ s^{-1}$
Idogawa et al. (Idogawa et al., 1985)	$\frac{\epsilon_g}{1-\epsilon_g} = 0.059{u_g}^{0.8}{\rho_g}^{0.17}\left(\frac{\sigma}{72}\right)^{-0.22\exp(-P)}$	$P = 0.1-5\ MPa$ $T = 284-293\ K$ $D = 5\ cm$ $H/D = 16.6$ $U_g = 0.5-5\ cm\ s^{-1}$
Hikita et al. (Hikita et al., 1980)	$\epsilon_g = 0.672\left(\frac{u_g\mu_L}{\sigma}\right)^{0.578}\left(\frac{g\mu_L^4}{\rho_L\sigma^3}\right)^{-0.131}\left(\frac{\rho_g}{\rho_L}\right)^{0.062}\left(\frac{\mu_g}{\mu_L}\right)^{0.107}$	$0.0011 \le (u_g\mu_L/\sigma) \le 0.089$ $2.5\times10^{-11} \le (g\mu_L^4/\rho_L\sigma^3) \le 1.9\times10^{-6}$ $8.4\times10^{-5} \le (\rho_g/\rho_L) \le 1.9\times10^{-3}$ $1.0\times10^{-3} \le (\mu_g/\mu_L) \le 1.8\times10^{-2}$

Figure 6-13 also compares the predictions of the correlations given in Table 6-8 with those of the proposed correlation in this work. The prediction parameters for different correlations are also reported in Table 6-9.

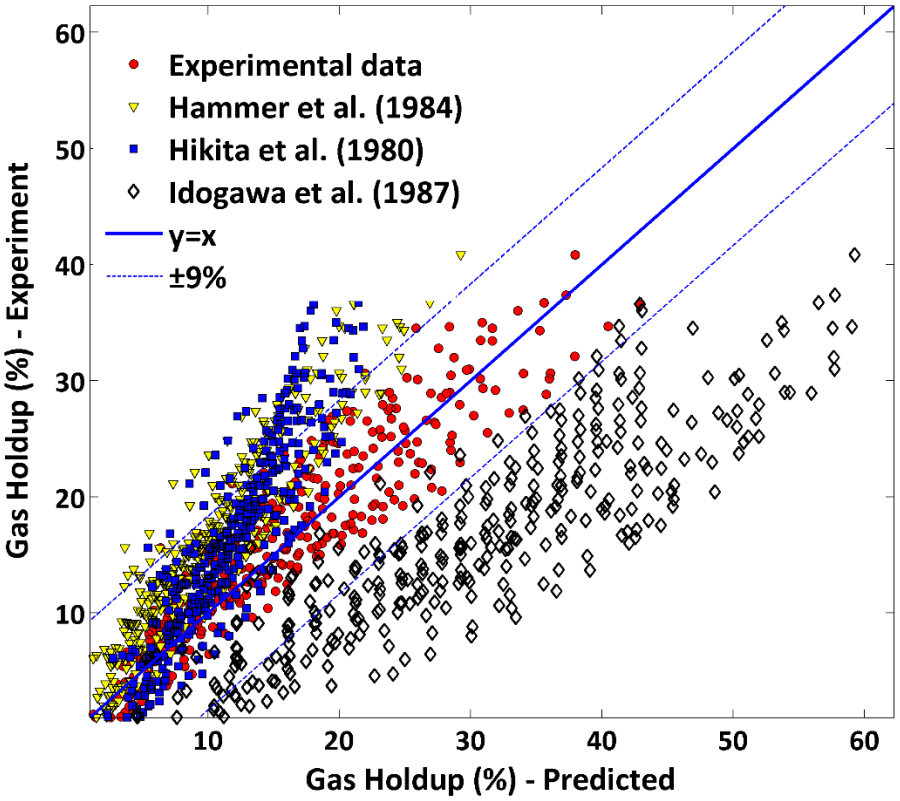

Figure 6-13: Comparison between different correlations proposed for predicting the gas holdup at elevated pressures.

Table 6-9: Prediction parameters for different gas holdup correlations.

Researchers	MAPE	Standard Error (%)	95% prediction error (%)
Hammer et al. (1984)	37%	±7.1	±18
Hikita et al. (1980)	36%	±6.8	±17
Idogawa et al. (1987)	117%	±15.5	±38
Proposed model in this study	20%	±3.3	±9

As is obvious from Figure 6-13, the correlation proposed in this study for gas holdup, can predict the experimental data more accurately than that reported in the literature. In addition, the

correlation proposed by Hammer et al. (Hammer et al., 1984) can also provide a relatively reasonable prediction of the gas holdup measured experimentally.

6.4 Conclusion

The effects of elevated pressure on the various hydrodynamic characteristics have been extensively investigated in a pilot-scale bubble column reactor operating with viscous and non-Newtonian liquids. Pressure signals are recorded using a series of pressure transducers along the column height to evaluate the gas holdup and standard deviation of pressure fluctuation and their axial variations. The obtained results show that the total gas holdup increases by pressure and that effect is more pronounced at lower operating pressures and higher superficial gas velocities. The gas holdup for Newtonian liquids increases axially while it decreases for shear-thinning liquids at high pressures. The transition from homogeneous to heterogeneous flow regime is delayed at higher pressures and it is found that the superficial gas velocity and gas holdup at the transition point also increase with pressure. The pressure fluctuation signals at all operating pressures have random appearances and it was observed that the amplitude of the pressure fluctuations increases relatively with an increase in the operating pressure. The standard deviation is also found to increase with superficial gas velocity and operating pressure. The rheological properties of the liquids at high pressure act almost in the same way as at low and ambient pressures and both elasticity and viscosity have considerable effects on the hydrodynamics parameters of bubble column even at elevated pressures. The $\frac{G'}{G''}$ ratio, which is a dimensionless parameter including both elastic and viscous effects of liquids, was also found to be an appropriate factor to distinguish the simultaneous effects of elastic and viscous responses of liquids at high operating pressures. The effect of pressure on the gas holdup indicates that the studies carried out at atmospheric pressure are not useful under high pressure conditions and will underestimate the bed expansion. In addition, a new correlation has been proposed to predict the gas holdup by considering the simultaneous effects of operating pressure and the rheological properties of the liquid phase. The developed correlation in this work is shown to be capable of predicting the gas holdup in bubble columns operating with viscous and non-Newtonian liquids at elevated pressures appropriately. The findings of the present work can have a significant impact on the design of commercial bubble column reactors, where highly viscous non-Newtonian liquids and high pressures are often applied.

CHAPTER 7 GENERAL DISCUSSION

The hydrodynamics and performance of bubble column reactors are strongly determined by liquid phase properties and operating pressure. The inherently complex nature and rheological behavior of non-Newtonian fluids bring some hydrodynamic complexities to bubble columns that are not observed in those operating with Newtonian fluids. Operating pressure also changes gas density, which is responsible for various phenomena in the bubble column reactors. The optimal design and operation of bubble columns thus require a complete understanding of hydrodynamics in presence of non-Newtonian fluids and elevated pressure, since a variety of industries are increasingly processing viscous and non-Newtonian liquids at elevated pressures. The objective of this work is, therefore, to shed light on the hydrodynamic aspects of bubble columns operating with non-Newtonian liquids and at high pressures.

In the first step of this work, a bubble column reactor with a transparent wall operating at ambient conditions was constructed in order to perform the experimental works and to study the influence of liquid phase properties on the hydrodynamics. Several aqueous liquid solutions were objectively chosen in order to discriminate among Newtonian, shear-thinning and viscoelastic behaviors. Two single-tip optical fiber probes were also designed, fabricated, and tested with the aim of investigating hydrodynamic parameters locally. The effect of rheological behavior of non-Newtonian liquids on the different hydrodynamic aspects of bubble column was first explored in Chapter 3, in which a comprehensive set of time and frequency domain analyses were performed on the pressure signals. It was found that the elastic properties of liquids can suppress bubble coalescence, minimize average bubble size and, therefore, increase the total gas holdup. The axial distribution of gas holdup in Newtonian liquids was shown to be completely different, compared to non-Newtonian and viscoelastic liquids. The gas holdup for CMC and Xanthan gum solutions at the middle zone of the column was found to be higher than in the top zone of the column; this was attributed to shear-thinning properties of these solutions. The regime transition from homogeneous to heterogeneous flow regime was also studied by applying the drift flux approach. A regime transition point was observed for the water system at U_g= 0.12 m s^{-1}, while there was no detectable regime transition point for the viscous and non-Newtonian liquids.

A new approach based on the ratio between the dynamic moduli of viscoelastic liquids, i.e. $\frac{G'}{G''}$, was introduced to recognize the distinct effects of elasticity and viscosity of viscoelastic liquids. The $\frac{G'}{G''}$ ratio is a dimensionless parameter, including both elastic and viscous effects of viscoelastic liquids. Therefore, it is a useful parameter to discriminate between the elastic and viscous effects of non-Newtonian liquids and to further interpret the effects of non-Newtonian liquids on the hydrodynamic parameters of bubble column reactors. It was found that in liquids with higher values of $\frac{G'}{G''}$, the bubble chord length is smaller and the gas holdup is higher. Statistical analysis was also performed to evaluate the standard deviation of the pressure fluctuation signals. It was observed that the elasticity of liquid leads to lower standard deviation, which was attributed to the presence of smaller bubbles in liquids with higher elastic effects. Spectral analysis was also conducted by means of a discrete Fourier transform algorithm in order to evaluate the power spectral density of the pressure signals, as well as the average frequency of the spectrum. The results reveal that the dominant peaks in the power spectral density curve appear at lower frequencies as the superficial gas velocity increases. The average frequency of the spectrum was shown to be lowest in the viscous and inelastic Glucose solution, which was attributed to the formation of larger bubbles in this solution. Moreover, it was pointed out that the average frequency of the spectrum is strongly dependant on the $\frac{G'}{G''}$ ratio in which the solution with a higher $\frac{G'}{G''}$ ratio shows a higher average frequency of the spectrum, and vice versa. The results obtained by statistical and spectral analyses indirectly confirm the impacts of liquid phase rheology on bubble dynamics.

The effects of liquid phase rheology on the local hydrodynamic parameters of bubble columns was primarily investigated in Chapter 4. Bubble frequency, bubble chord length and bubble rise velocity and their axial and radial distributions were evaluated using our two in-house-made optical fiber probes. It was found that bubble frequency decreases with liquid viscosity, while it increases with the elasticity of liquid. On the other hand, the elasticity of liquid was shown to diminish bubble rise velocity mainly because of the formation and presence of smaller bubbles in liquids with dominating elastic effects. Except for the water system, the bubble frequency in the middle zone of the column was observed to be higher than that in the top zone of the column, indicating dominating coalescence phenomena along the column height in viscous solutions, which lead to a decrease in the number of bubbles. The axial distribution of the bubble chord length in different

solutions were also compared by evaluating the root mean square of the bubble chord length, and it was revealed that the axial distribution of the bubble chord length is smaller in solutions with dominating elastic effects. The $\frac{G'}{G''}$ ratio was also found to be an appropriate factor for discriminating between the effects of elasticity and viscosity of non-Newtonian liquids on the local hydrodynamic parameters of bubble columns. In the last part of Chapter 4, two correlations were developed for predicting bubble size and gas holdup by applying dimensional analysis and considering the simultaneous effects of the elasticity and viscosity of liquids in the form of the $\frac{G'}{G''}$ ratio. The proposed correlations were shown to be able to predict both bubble size and gas holdup measured experimentally in this study within a mean absolute percentage error of 9.3% and 10%, respectively. The applicability of the proposed correlations in predicting bubble size and gas holdup measured in viscous and Newtonian liquids by other researchers was also examined using bubble size and gas holdup data reported by various researchers. It was observed that the agreements between the prediction of the proposed correlations in this study and the bubble size and gas holdup data reported by other authors were within a mean absolute percentage error of 28% and 20%, respectively. It was also essential to determine the accuracy of the developed correlations in predicting bubble size and gas holdup measured and reported by other researchers in non-Newtonian liquids. A survey of the relevant literature showed that there is no reliable experimental data for bubble size measurements in non-Newtonian liquids. On the other hand, although there are several series of experimental data of gas holdup measured in non-Newtonian liquids by other authors, no $\frac{G'}{G''}$ values are reported by the corresponding authors for the non-Newtonian liquids used during their experiments. To overcome this issue, the experimental data on gas holdup reported by other researchers (Fransolet et al., 2005; Haque et al., 1986; Kawase et al., 1987; Kawase & Moo-Young, 1986; Lakota, 2007; S. B. Li, Zhu, et al., 2012)are fitted to the developed correlation in this study, and the value of $\frac{G'}{G''}$ ratio is evaluated as the fitting parameter. By doing so, it was found that the overall range of $\frac{G'}{G''}$ ratio evaluated by this method (i.e., 0.01-1.73) was within the range of applicability of the correlation developed in this study for predicting the gas holdup (i.e., 0-3.26). This confirms the accuracy of the new correlation in predicting the gas holdup data measured experimentally by other researchers in bubble columns operating with non-Newtonian liquids.

A variety of industries, process chemicals at high pressure in bubble columns; however, the majority of previous research on bubble column reactors is restricted to characterizing bubble columns operating at ambient pressure. The hydrodynamics of bubble columns operating with non-Newtonian liquids and at high pressure is remarkably different from that of bubble columns operating with low viscosity and Newtonian liquids at ambient pressure. Therefore, the last objective of this work is studying the effects of elevated pressure (up to 1 MPa) on various hydrodynamic characteristics of bubble columns operating with non-Newtonian liquids. In order to carry out the experiments at elevated pressures, a high-pressure bubble column reactor was designed and constructed. The new high-pressure bubble column reactor and related equipment used for operating the reactor were discussed in Chapter 5. Chapter 6 was devoted to evaluating the total gas holdup and its axial distribution, operating flow regime transition point, pressure fluctuation and its standard deviation, by analyzing the pressure signals at elevated pressures and in different viscous and non-Newtonian solutions. For all the solutions applied, it was observed that the total gas holdup increases by increasing operating pressure, and that effect was more pronounced at higher superficial gas velocities. In Newtonian liquids, gas holdup increased axially, while it decreased axially in the shear-thinning liquids. It was found that the transition from the homogeneous to heterogeneous flow regime was shifted to higher superficial gas velocities at elevated pressures. The superficial gas velocity and gas holdup at the regime transition point was also higher at elevated pressures. The pressure signals appeared to fluctuate completely randomly at all operating pressures; however, the amplitude of the pressure fluctuations increased as the operating pressure increased. The standard deviation of pressure fluctuations was also observed to increase with operating pressure, but to decrease with the elasticity of the liquid phase.

In general, the current available phenomenological models and correlations for predicting the gas holdup and bubble size are mainly applicable for bubble column reactors operating with low-viscosity liquids at ambient conditions, and the models that consider non-Newtonian liquids and pressure effects are scarce in the literature. In this regard, a new correlation was developed to predict gas holdup in bubble columns operating at elevated pressure with viscous and non-Newtonian liquids. The new correlation was shown to be able to predict the experimental data of gas holdup within a mean absolute percentage error of 20%.

CHAPTER 8 CONCLUSION AND RECOMMENDATIONS

8.1 Concluding remarks

The effect of rheological behavior of different Newtonian and non-Newtonian liquids and operating pressure on bubble properties and the hydrodynamics of bubble column reactors was extensively investigated. Two pilot-scale bubble column reactors were designed and constructed in order to perform the experiments across a wide range of operating conditions. A detailed study was also conducted on the effects of liquid phase rheology on bubble-related phenomena by performing various analyses on the pressure fluctuation signals. A new approach was proposed based on the dynamic moduli of viscoelastic solutions to better understand the simultaneous effects of the elasticity and viscosity of liquids. To evaluate the local hydrodynamic parameters, two optical fiber probes were also designed and fabricated. In addition, two correlations were derived by considering the rheological parameters of viscoelastic liquids in order to predict bubble size and gas holdup in bubble column reactors operating with viscous and non-Newtonian liquids.

Furthermore, a series of experiments were conducted to study the effects of elevated pressure on the different hydrodynamic aspects of bubble column reactors operating with non-Newtonian liquids at high pressure. By considering the pressure effects, a correlation in the form of dimensionless groups was also developed to predict gas holdup at elevated pressure.

8.2 Original contributions

This study provides a large amount of information about the hydrodynamics of bubble column reactors operating with non-Newtonian liquids and at elevated pressure. The findings of this work are particularly useful for design and scale-up purposes, which, in turn, can lead to a variety of improvements not only in overall economic efficiency but specifically in the energy- and resource-efficiency of chemicals production plants, all of which will make a solid contribution to a sustainable chemistry. The liquids applied in this work are selected in a way to simulate as closely as possible the properties and behavior of typical viscous and non-Newtonian liquids which are being processed in a variety of industries. Therefore, the experimental results obtained in this study

can be considered as a valuable reference to the industrial applications of non-Newtonian liquids in bubble columns in many areas, such as the food, biochemical and petrochemical industries. The most important achievement of this study is the extensive experimental work conducted to investigate the effect of rheological behaviour of different non-Newtonian liquids by applying two reliable and accurate measurement techniques (i.e., pressure transducers and optical fiber probes) and several methods of data analysis. The specific novel aspects of this study are as follows:

1. Detailed investigation on the impact of liquid phase rheological properties on bubble behavior and different hydrodynamic characteristics of bubble column reactors.

2. The proposal of a new approach based on the ratio between dynamic moduli of viscoelastic fluids that can provide researchers with a new way to interpret the effects of non-Newtonian liquids in gas-liquid contactors, which have not yet been considered elsewhere.

3. An extensive study on the local hydrodynamics of bubble column reactors operating with non-Newtonian liquids by means of two in-house-made optical fiber probes.

4. An exploration of the influence of elevated pressure on the global hydrodynamic parameters of bubble column reactors in the presence of non-Newtonian liquids.

5. The development of new correlations for predicting bubble size and gas holdup by considering the rheological properties of liquid phase and operating pressure, and validating them by the experimental data obtained both in this study and in the existing literature.

8.3 Future work and recommendations

The optimal design, scale-up, and operation of bubble column reactors can be achieved by having a complete knowledge about the impact of different design parameters and operating variables on the hydrodynamics of the gas phase as well as the flow dynamics of the liquid/slurry phase. Developing phenomenological models that take into account the influence of all operating variables such as superficial gas velocity, operating pressure and temperature, liquid phase properties, and the properties of solid particles is necessary to achieve this goal. The literature review shows that in the case of bubble columns operating with non-Newtonian liquids, the effects of many factors

such as operating temperature, liquid phase velocity, the properties of solid particles, and the design of the gas distributor and internals have not been well investigated, so there is still a strong motivation for conducting more research to study the impact of all influential parameters in bubble column reactors. Considering the above-mentioned points, some avenues for future research are recommended, as follows:

1) The complex multiphase flow and mixing behaviour in the bubble column reactors can often be described by the flow dynamics of the liquid phase, including liquid velocity and flow pattern, recirculation and axial dispersion. Liquid recirculation can significantly affect the bubble rising path, as well as bubble coalescence and breakage. Therefore, investigating the dynamics of the non-Newtonian liquid phase by means of some reliable and accurate non-intrusive measurement techniques such as radioactive particle tracking (RPT), particle image velocimetry (PIV), X-ray and γ-ray tomography, and laser techniques can provide us with valuable information about the dynamics of the liquid phase in bubble columns operating with non-Newtonian liquids which is useful for design purpose.

2) The operating temperature can significantly change the physical and rheological properties of the liquid phase and, accordingly, the hydrodynamics of bubble columns. In this regard, further studying the impact of operating temperature on the different hydrodynamic aspects of the bubble column operating with non-Newtonian liquids and developing models that consider temperature effects would be of great interest.

3) In this study, the global hydrodynamic parameters of a bubble column reactor were investigated at elevated pressure in presence of non-Newtonian liquids. Developing a new optical fiber probe or any other useful technique for the local characterization of bubble columns operating at such conditions will be essential for further experimentation.

4) Studying the mass transfer and/or reactive behavior of non-Newtonian liquids at elevated pressures and/or temperatures will also be very important for design, scale-up and operation purposes.

5) One of the most important parameters that can considerably affect the hydrodynamics of bubble columns is the presence of solid (catalyst) particles in the dispersion. Although applying high concentrations of catalyst is desirable in many new processes, the basic knowledge about the

apparent viscosity of liquid-solid suspension is still lacking in the literature. The interaction between the solid particles and non-Newtonian fluids, as well as their effects on the overall hydrodynamics and performance of bubble columns, are not well known at this stage. Therefore, investigating the impact of solid particles in the presence of a non-Newtonian liquid phase, especially at elevated pressures and temperatures, would be interesting from both an academic and industrial point of view. This can be performed by applying different measurement techniques, such as densitometry, RPT, etc.

6) Since the gas distributor design influences bubble characteristics, studying the effect of different gas distributor designs on the hydrodynamics of bubble columns operating with non-Newtonian liquids and at elevated pressures and temperatures is necessary for a better design and scale-up of bubble columns operating under such conditions. The presence of internals and their impact would also be interesting to further explore.

BIBLIOGRAPHY

Abbasi, M., Mostoufi, N., Sotudeh-Gharebagh, R., & Zarghami, R. (2013). A novel approach for simultaneous hydrodynamic characterization of gas-liquid and gas-solid systems. *Chemical Engineering Science, 100*, 74-82. doi: DOI 10.1016/j.ces.2012.12.031

Acharya, A., & Ulbrecht, J. J. (1978). Note on the influence of viscoelasticity on the coalescence rate of bubbles and drops. *AIChE J., 24*(2), 348-351. doi: 10.1002/aic.690240227

Akita, K., & Yoshida, F. (1973). Gas Holdup and Volumetric Mass Transfer Coefficient in Bubble Columns. Effects of Liquid Properties. *Industrial & Engineering Chemistry Process Design and Development, 12*(1), 76-80. doi: 10.1021/i260045a015

Akita, K., & Yoshida, F. (1974). Bubble Size, Interfacial Area, and Liquid-Phase Mass Transfer Coefficient in Bubble Columns. *Industrial & Engineering Chemistry Process Design and Development, 13*(1), 84-91. doi: 10.1021/i260049a016

Al-Masry, W. A., Ali, E. M., & Al-Kalbani, M. N. (2007). Prediction of regime transitions in bubble columns using acoustic and differential pressure signals. *Chemical Engineering Journal, 133*(1–3), 139-149. doi: http://dx.doi.org/10.1016/j.cej.2007.02.025

Alvarez, E., Correa, J. M., Navaza, J. M., & Riverol, C. (2001). Theoretical prediction of the mass transfer coefficients in bubble columns operating in churn-turbulent flow regime. Study in Newtonian and non-Newtonian fluids under different operation conditions. *Heat and Mass Transfer, 37*(4-5), 343-350.

Bai, W. (2010). *Experimental and numerical investigation of bubble column reactors.* (Doctoral), Eindhoven University of Technology, Enschede, Netherlands. Retrieved from http://www.tue.nl/en/publication/ep/p/d/ep-uid/244052/

Barghi, S., Prakash, A., Margaritis, A., & Bergougnou, M. (2004). Flow regime identification in a slurry bubble column from gas holdup and pressure fluctuations analysis. *The Canadian Journal of Chemical Engineering, 82*(5), 865-870.

Barghi, S., Prakash, A., Margaritis, A., & Bergougnou, M. A. (2004). Flow regime identification in a slurry bubble column from gas holdup and pressure fluctuations analysis. *Canadian Journal of Chemical Engineering, 82*(5), 865-870.

Barnes, H. A., & Hutton, J. F. (1993). *An Introduction to Rheology* (3rd ed.). Amsterdam, Netherlands: Elsevier Science Publishers.

Barnes, H. A., Hutton, J. F., & Walters, K. (1989). *An introduction to rheology* (Vol. 3): Elsevier.

Behkish, A. (2004). *Hydrodynamic and mass transfer parameters in large-scale slurry bubble column reactors.* (3158739 Doctoral Dissertation), University of Pittsburgh, Ann Arbor. ProQuest Dissertations & Theses Full Text database.

Behkish, A., Lemoine, R., Oukaci, R., & Morsi, B. I. (2006). Novel correlations for gas holdup in large-scale slurry bubble column reactors operating under elevated pressures and temperatures. *Chemical Engineering Journal, 115*(3), 157-171.

Behkish, A., Lemoine, R., Sehabiague, L., Oukaci, R., & Morsi, B. I. (2007). Gas holdup and bubble size behavior in a large-scale slurry bubble column reactor operating with an organic liquid under elevated pressures and temperatures. *Chemical Engineering Journal, 128*(2), 69-84.

Behkish, A., Men, Z., Inga, J. R., & Morsi, B. I. (2002). Mass transfer characteristics in a large-scale slurry bubble column reactor with organic liquid mixtures. *Chemical Engineering Science, 57*(16), 3307-3324.

Blum, D., & Toman, J. (1977). *Three-phase Fluidization in a Liquid-phase Methanator.* Paper presented at the AIChE Symp. Ser.

Boyer, C., Duquenne, A.-M., & Wild, G. (2002). Measuring techniques in gas–liquid and gas–liquid–solid reactors. *Chemical Engineering Science, 57*(16), 3185-3215. doi: http://dx.doi.org/10.1016/S0009-2509(02)00193-8

Bui, B., Saasen, A., Maxey, J., Ozbayoglu, M. E., Miska, S. Z., Yu, M., & Takach, N. E. (2012). Viscoelastic Properties of Oil Based Drilling Fluids. *Annual Transactions of the Nordic Rheology Society, 20*.

Bukur, D. B., & Patel, S. A. (1989). Hydrodynamic studies with foaming and non-newtonian solutions in bubble columns. *The Canadian Journal of Chemical Engineering, 67*(5), 741-751. doi: 10.1002/cjce.5450670505

Carreau, P. J., Kee, D. D., & Daroux, M. (1979). An analysis of the viscous behaviour of polymeric solutions. *The Canadian Journal of Chemical Engineering, 57*(2), 135-140. doi: 10.1002/cjce.5450570202

Cartellier, A. (1990). Optical probes for local void fraction measurements: Characterization of performance. *Review of Scientific Instruments, 61*(2), 874-886. doi: doi:http://dx.doi.org/10.1063/1.1141457

Cartellier, A. (1992). Simultaneous void fraction measurement, bubble velocity, and size estimate using a single optical probe in gas–liquid two-phase flows. *Review of Scientific Instruments, 63*(11), 5442-5453. doi: doi:http://dx.doi.org/10.1063/1.1143416

Cartellier, A., & Barrau, E. (1998). Monofiber optical probes for gas detection and gas velocity measurements: optimised sensing tips. *International Journal of Multiphase Flow, 24*(8), 1295-1315. doi: http://dx.doi.org/10.1016/S0301-9322(98)00033-0

Chabot, J., Lee, S. L. P., Soria, A., & de Lasa, H. I. (1992). Interaction between bubbles and fibre optic probes in a bubble column. *The Canadian Journal of Chemical Engineering, 70*(1), 61-68. doi: 10.1002/cjce.5450700110

Chambers, B. C. (1978).

Chaumat, H., Billet-Duquenne, A. M., Augier, F., Mathieu, C., & Delmas, H. (2007). On the reliability of an optical fibre probe in bubble column under industrial relevant operating conditions. *Experimental Thermal and Fluid Science, 31*(6), 495-504. doi: http://dx.doi.org/10.1016/j.expthermflusci.2006.04.018

Chen, P. (2004). *Modeling the fluid dynamics of bubble column flows.* Washington University, 2004. Department of Chemical Engineering.

Chen, W., Tsutsumi, A., Otawara, K., & Shigaki, Y. (2003). Local Bubble Dynamics and Macroscopic Flow Structure in Bubble Columns with Different Scales. *The Canadian Journal of Chemical Engineering, 81*(6), 1139-1148. doi: 10.1002/cjce.5450810603

Chhabra, R. P. *Bubbles, Drops, and Particles in Non-Newtonian Fluids* (Second ed.). Boca Raton, FL: CRC Press ,Taylor & Francis Group, 2007.

Chhabra, R. P. (2006). *Bubbles, Drops, and Particles in Non-Newtonian Fluids* (Second ed.). Boca Raton, FL: CRC Press ,Taylor & Francis Group.

Chhabra, R. P., & Richardson, J. F. (2011). *Non-Newtonian flow and applied rheology: engineering applications*: Butterworth-Heinemann.

Chilekar, V. P., van der Schaaf, J., Kuster, B. F., Tinge, J. T., & Schouten, J. C. (2010). Influence of elevated pressure and particle lyophobicity on hydrodynamics and gas–liquid mass transfer in slurry bubble columns. *Aiche Journal, 56*(3), 584-596.

Chilekar, V. P., Warnier, M. J. F., van der Schaaf, J., Kuster, B. F. M., Schouten, J. C., & van Ommen, J. R. (2005). Bubble size estimation in slurry bubble columns from pressure fluctuations. *Aiche Journal, 51*(7), 1924-1937. doi: Doi 10.1002/Aic.10427

Chisti, Y., & Mooyoung, M. (1989). On the Calculation of Shear Rate and Apparent Viscosity in Airlift and Bubble Column Bioreactors. *Biotechnology and Bioengineering, 34*(11), 1391-1392. doi: DOI 10.1002/bit.260341107

Clark, K. N. (1990). The effect of high pressure and temperature on phase distributions in a bubble column. *Chemical Engineering Science, 45*(8), 2301-2307. doi: http://dx.doi.org/10.1016/0009-2509(90)80109-R

Clark, N., & Flemmer, R. (1985). Predicting the holdup in two-phase bubble upflow and downflow using the Zuber and Findlay drift-flux model. *Aiche Journal, 31*(3), 500-503.

Clarke, K. G., & Correia, L. D. C. (2008). Oxygen transfer in hydrocarbon-aqueous dispersions and its applicability to alkane bioprocesses: A review. *Biochemical Engineering Journal, 39*(3), 405-429. doi: DOI 10.1016/j.bej.2007.11.020

Cui, Z. (2005). *Hydrodynamics in a bubble column at elevated pressures and turbulence energy distribution in bubbling gas-liquid and gas-liquid-solid flow systems.* (3160828 Ph.D.), The Ohio State University, Ann Arbor. ProQuest Dissertations & Theses Full Text database.

Dautzenberg, F., & De Deken, J. (1984). Reactor developments in hydrotreating and conversion of residues. *Catalysis Reviews Science and Engineering, 26*(3-4), 421-444.

De Kee, D., & Carreau, P. J. (1993). Friction factors and bubble dynamics in polymer solutions. *The Canadian Journal of Chemical Engineering, 71*(2), 183-188. doi: 10.1002/cjce.5450710203

De Kee, D., Chhabra, R. P., & Dajan, A. (1990). Motion and coalescense of gas bubbles in non-Newtonian polymer solutions. *Journal of Non-Newtonian Fluid Mechanics, 37*(1), 1-18. doi: http://dx.doi.org/10.1016/0377-0257(90)80001-G

De Lasa, H., Dogu, G., Dogŭ, G., & Ravella, A. (1992). *Chemical reactor technology for environmentally safe reactors and products* (Vol. 225): Springer Science & Business Media.

Deckwer, W.-D. (1992). *Bubble Column Reactors*. Chichester, England: John Wiley and Sons.

Deckwer, W.-D., Louisi, Y., Zaidi, A., & Ralek, M. (1980). Hydrodynamic properties of the Fischer-Tropsch slurry process. *Industrial & Engineering Chemistry Process Design and Development, 19*(4), 699-708.

Deckwer, W. D., Nguyen-Tien, K., Schumpe, A., & Serpemen, Y. (1982). Oxygen mass transfer into aerated CMC solutions in a bubble column. *Biotechnology and Bioengineering, 24*(2), 461-481. doi: 10.1002/bit.260240215

Drahos, J., Zahradnik, J., Puncochar, M., Fialova, M., & Bradka, F. (1991). Effect of Operating-Conditions on the Characteristics of Pressure-Fluctuations in a Bubble Column. *Chemical Engineering and Processing, 29*(2), 107-115. doi: Doi 10.1016/0255-2701(91)87019-Y

Drahoš, J., Zahradník, J., Punčochář, M., Fialová, M., & Bradka, F. (1991). Effect of operating conditions on the characteristics of pressure fluctuations in a bubble column. *Chemical Engineering and Processing: Process Intensification, 29*(2), 107-115. doi: http://dx.doi.org/10.1016/0255-2701(91)87019-Y

Eickenbusch, H., Brunn, P. O., & Schumpe, A. (1995). Mass transfer into viscous pseudoplastic liquid in large-diameter bubble columns. *Chemical Engineering and Processing: Process Intensification, 34*(5), 479-485. doi: http://dx.doi.org/10.1016/0255-2701(95)00626-5

Esmaeili, A., Guy, C., & Chaouki, J. (2015). The effects of liquid phase rheology on the hydrodynamics of a gas–liquid bubble column reactor. *Chemical Engineering Science, 129*(0), 193-207. doi: http://dx.doi.org/10.1016/j.ces.2015.01.071

Esmaeili, A., Guy, C., & Chaouki, J. (2015, Submitted to AIChE J.). Local Hydrodynamics of Bubble Column Reactors Operating with non-Newtonian Liquids: Experiments and Models Development.

Fan, L.-S. (1989). *Gas-liquid-solid fluidization engineering*. Boston: Butterworth-Heinemann.

Fan, L. S., Yang, G. Q., Lee, D. J., Tsuchiya, K., & Luo, X. (1999). Some aspects of high-pressure phenomena of bubbles in liquids and liquid-solid suspensions. *Chemical Engineering Science, 54*(21), 4681-4709.

Fan, W., Jiang, S., Zhu, C., Ma, Y., & Li, H. (2008). Study on bubble formation in non-Newtonian fluids by laser image technique. *Optics & Laser Technology, 40*(2), 389-393. doi: http://dx.doi.org/10.1016/j.optlastec.2007.07.002

Ferry, J. D. (1980). *Viscoelastic properties of polymers*: John Wiley & Sons.

Fox, J. M. (1990). Fischer-Tropsch reactor selection. *Catalysis Letters, 7*(1), 281-292.

Fransolet, E., Crine, A., Marchot, P., & Toye, D. (2005). Analysis of gas holdup in bubble columns with non-Newtonian fluid using electrical resistance tomography and dynamic gas disengagement technique. *Chemical Engineering Science, 60*(22), 6118-6123. doi: DOI 10.1016/j.ces.2005.03.046

Gaddis, E. S., & Vogelpohl, A. (1986). Bubble formation in quiescent liquids under constant flow conditions. *Chemical Engineering Science, 41*(1), 97-105. doi: http://dx.doi.org/10.1016/0009-2509(86)85202-2

Gandhi, B., Prakash, A., & Bergougnou, M. A. (1999). Hydrodynamic behavior of slurry bubble column at high solids concentrations. *Powder Technology, 103*(2), 80-94. doi: Doi 10.1016/S0032-5910(98)00182-X

Ghosh, U. K., & Upadhyay, S. N. (2007). Gas Holdup and Solid-Liquid Mass Transfer in Newtonian and non-Newtonian Fluids in Bubble Columns. *The Canadian Journal of Chemical Engineering, 85*(6), 825-832. doi: 10.1002/cjce.5450850604

Godbole, S. P., Honath, M. F., & Shah, Y. T. (1982). HOLDUP STRUCTURE IN HIGHLY VISCOUS NEWTONIAN AND NON-NEWTONIAN LIQUIDS IN BUBBLE COLUMNS. *Chemical Engineering Communications, 16*(1-6), 119-134. doi: 10.1080/00986448208911090

Godbole, S. P., Schumpe, A., Shah, Y. T., & Carr, N. L. (1984). Hydrodynamics and mass transfer in non-Newtonian solutions in a bubble column. *Aiche Journal, 30*(2), 213-220. doi: 10.1002/aic.690300207

Gomez-Diaz, D., Navaza, J. M., Quintans-Riveiro, L. C., & Sanjurjo, B. (2009). Gas absorption in bubble column using a non-Newtonian liquid phase. *Chemical Engineering Journal, 146*(1), 16-21. doi: DOI 10.1016/j.cej.2008.05.022

Gourich, B., Vial, C., Essadki, A. H., Allam, F., Soulami, M. B., & Ziyad, M. (2006). Identification of flow regimes and transition points in a bubble column through analysis of differential pressure signal - Influence of the coalescence behavior of the liquid phase. *Chemical Engineering and Processing, 45*(3), 214-223. doi: DOI 10.1016/j.cep.2005.09.002

Groen, J. (2004). *Scales and structures in bubbly flows.* PhD Thesis, Delft University of Technology, The Netherlands.

Groen, J., Oldeman, R., Mudde, R., & Van Den Akker, H. (1996). Coherent structures and axial dispersion in bubble column reactors. *Chemical Engineering Science, 51*(10), 2511-2520.

Gupta, P. P., Merchant, S. S., Bhat, A. U., Gandhi, A. B., Bhagwat, S. S., Joshi, J. B., . . . Kulkarni, B. D. (2009). Development of Correlations for Overall Gas Hold-up, Volumetric Mass Transfer Coefficient, and Effective Interfacial Area in Bubble Column Reactors Using Hybrid Genetic Algorithm-Support Vector Regression Technique: Viscous Newtonian and Non-Newtonian Liquids. *Industrial & Engineering Chemistry Research, 48*(21), 9631-9654. doi: 10.1021/ie801834w

Guy, C., Carreau, P., & Paris, J. (1986). Mixing characteristics and gas hold-up of a bubble column. *The Canadian Journal of Chemical Engineering, 64*(1), 23-35.

Halard, B., Kawase, Y., & Moo-Young, M. (1989). Mass transfer in a pilot plant scale airlift column with non-Newtonian fluids. *Industrial & Engineering Chemistry Research, 28*(2), 243-245. doi: 10.1021/ie00086a019

Hammer, H., Schrag, H., Hektor, K., Schonau, K., Kusters, W., Soemarno, A., . . . Napp, W. (1984). New sub functions on hydrodynamics, heat and mass transfer for gas/liquid and gas/liquid/solid chemical and biochemical reactors. *Front. Chem. Reac. Eng, 464*.

Haque, M. W., Nigam, K. D. P., & Joshi, J. B. (1986). Hydrodynamics and mixing in highly viscous pseudo-plastic non-newtonian solutions in bubble columns. *Chemical Engineering Science, 41*(9), 2321-2331. doi: http://dx.doi.org/10.1016/0009-2509(86)85082-5

Haque, M. W., Nigam, K. D. P., Joshi, J. B., & Viswanathan, K. (1987). Studies on gas holdup and bubble parameters in bubble columns with (carboxymethyl)cellulose solutions. *Industrial & Engineering Chemistry Research, 26*(1), 86-91. doi: 10.1021/ie00061a016

Hashemi, S., Macchi, A., & Servio, P. (2009). Gas–liquid mass transfer in a slurry bubble column operated at gas hydrate forming conditions. *Chemical Engineering Science, 64*(16), 3709-3716.

Hecht, V., Voigt, J., & Schügerl, K. (1980). Absorption of oxygen in countercurrent multistage bubble columns—III Viscoelastic liquids. Comparison of systems with high viscosity. *Chemical Engineering Science, 35*(6), 1325-1330. doi: http://dx.doi.org/10.1016/0009-2509(80)85125-6

Herrera-Velarde, J. R., Zenit, R., Chehata, D., & Mena, B. (2003). The flow of non-Newtonian fluids around bubbles and its connection to the jump discontinuity. *Journal of Non-Newtonian Fluid Mechanics, 111*(2-3), 199-209. doi: Doi 10.1016/S0377-0257(03)00055-7

Hikita, H., Asai, S., Tanigawa, K., Segawa, K., & Kitao, M. (1980). Gas hold-up in bubble columns. *The Chemical Engineering Journal, 20*(1), 59-67. doi: http://dx.doi.org/10.1016/0300-9467(80)85006-4

Huang, P. Y., & Feng, J. (1995). Wall Effects on the Flow of Viscoelastic Fluids around a Circular-Cylinder. *Journal of Non-Newtonian Fluid Mechanics, 60*(2-3), 179-198. doi: Doi 10.1016/0377-0257(95)01394-2

Idogawa, K., Ikeda, K., Fukuda, T., & Morooka, S. (1985). EFFECTS OF GAS AND LIQUID PROPERTIES ON THE BEHAVIOR OF BUBBLES IN A BUBBLE COLUMN UNDER HIGH-PRESSURE. *Kagaku Kogaku Ronbunshu, 11*(4), 432-437.

Imaizumi, Y., Kunugi, T., Yokomine, T., & Kawara, Z. (2014). Viscoelastic fluid behaviors around a rising bubble via a new method of mesh deformation tracking. *Chemical Engineering Science, 120*, 167-173. doi: http://dx.doi.org/10.1016/j.ces.2014.07.036

Inga, J. R., & Morsi, B. I. (1999). Effect of Operating Variables on the Gas Holdup in a Large-Scale Slurry Bubble Column Reactor Operating with an Organic Liquid Mixture. *Industrial & Engineering Chemistry Research, 38*(3), 928-937. doi: 10.1021/ie980384q

Ishiyama, H., Isokawa, Y., Sawai, J., & Kojima, H. (2001). Hydrodynamics in a small size pressurized bubble column. *Chemical Engineering Science, 56*(21), 6273-6278.

Jager, B., & Espinoza, R. (1995). Advances in low temperature Fischer-Tropsch synthesis. *Catalysis Today, 23*(1), 17-28.

Jiang, P., Lin, T.-J., Luo, X., & Fan, L.-S. (1995). Flow visualization of high pressure (21 MPa) bubble column: bubble characteristics. *Chemical Engineering Research & Design, 73*(A3), 269-274.

Jin, H., Wang, M., & Williams, R. (2007). Analysis of bubble behaviors in bubble columns using electrical resistance tomography. *Chemical Engineering Journal, 130*(2), 179-185.

Jin, H., Yang, S., Zhang, T., & Tong, Z. (2004). Bubble Behavior of a Large-Scale Bubble Column with Elevated Pressure. *Chemical Engineering & Technology, 27*(9), 1007-1013.

Jin, H. B., Qin, Y. J., Yang, S. H., He, G. X., & Guo, Z. W. (2013). Radial Profiles of Gas Bubble Behavior in a Gas-Liquid Bubble Column Reactor under Elevated Pressures. *Chemical Engineering & Technology, 36*(10), 1721-1728. doi: DOI 10.1002/ceat.201200551

Johnsson, F., Zijerveld, R. C., Schouten, J. C., van den Bleek, C. M., & Leckner, B. (2000). Characterization of fluidization regimes by time-series analysis of pressure fluctuations. *International Journal of Multiphase Flow, 26*(4), 663-715. doi: http://dx.doi.org/10.1016/S0301-9322(99)00028-2

Jordan, U., & Schumpe, A. (2001). The gas density effect on mass transfer in bubble columns with organic liquids. *Chemical Engineering Science, 56*(21), 6267-6272.

Jordan, U., Terasaka, K., Kundu, G., & Schumpe, A. (2002). Mass Transfer in High-Pressure Bubble Columns with Organic Liquids. *Chemical Engineering & Technology, 25*(3), 262-265.

Joshi, J. B. e. a. (1998). Gas Hold-up Structure in Bubble Column Reactors. *PINSA, 4*(64A), 441-567.

Kang, Y., Cho, Y., Woo, K., & Kim, S. (1999). Diagnosis of bubble distribution and mass transfer in pressurized bubble columns with viscous liquid medium. *Chemical Engineering Science, 54*(21), 4887-4893.

Kang, Y., Cho, Y. J., Woo, K. J., Kim, K. I., & Kim, S. D. (2000). Bubble properties and pressure fluctuations in pressurized bubble columns. *Chemical Engineering Science, 55*(2), 411-419.

Kantarci, N., Borak, F., & Ulgen, K. O. (2005). Bubble column reactors. *Process Biochemistry, 40*(7), 2263-2283. doi: DOI 10.1016/j.procbio.2004.10.004

Kawase, Y., Halard, B., & Moo-Young, M. (1987). Theoretical prediction of volumetric mass transfer coefficients in bubble columns for Newtonian and non-Newtonian fluids. *Chemical Engineering Science, 42*(7), 1609-1617. doi: http://dx.doi.org/10.1016/0009-2509(87)80165-3

Kawase, Y., & Kumagai, T. (1991). Apparent Viscosity for Non-Newtonian Fermentation Media in Bioreactors. *Bioprocess Engineering, 7*(1-2), 25-28.

Kawase, Y., & Moo-Young, M. (1986). Influence of non-Newtonian flow behaviour on mass transfer in bubble columns with and without draft tubes. *Chemical Engineering Communications, 40*(1-6), 67-83. doi: 10.1080/00986448608911691

Kawase, Y., Umeno, S., & Kumagai, T. (1992). The Prediction of Gas Hold-up in Bubble Column Reactors - Newtonian and Non-Newtonian Fluids. *Chemical Engineering Journal and the Biochemical Engineering Journal, 50*(1), 1-7. doi: Doi 10.1016/0300-9467(92)80001-Q

Kemiha, M., Frank, X., Poncin, S., & Li, H. Z. (2006). Origin of the negative wake behind a bubble rising in non-Newtonian fluids. *Chemical Engineering Science, 61*(12), 4041-4047. doi: http://dx.doi.org/10.1016/j.ces.2006.01.051

Kemoun, A., Cheng Ong, B., Gupta, P., Al-Dahhan, M. H., & Dudukovic, M. P. (2001). Gas holdup in bubble columns at elevated pressure via computed tomography. *International Journal of Multiphase Flow, 27*(5), 929-946. doi: http://dx.doi.org/10.1016/S0301-9322(00)00037-9

Kölbel, H., Borchers, E., & Langemann, H. (1961). Größenverteilung der Gasblasen in Blasensäulen. Teil I: Einflüsse von Flüssigkeitsviscosität und Säuleninnendruck. *Chemie Ingenieur Technik, 33*(10), 668-675. doi: 10.1002/cite.330331004

Krishna, R., Ellenberger, J., & Hennephof, D. (1993). Analogous description of the hydrodynamics of gas-solid fluidized beds and bubble columns. *The Chemical Engineering Journal and the Biochemical Engineering Journal, 53*(1), 89-101.

Krishna, R., & Sie, S. T. (2000). Design and scale-up of the Fischer–Tropsch bubble column slurry reactor. *Fuel Processing Technology, 64*(1–3), 73-105. doi: http://dx.doi.org/10.1016/S0378-3820(99)00128-9

Kumar, S., Srinivasulu, N., Munshi, P., & Khanna, A. (2013). Flow regime transition identification in three phase co-current bubble columns. *Canadian Journal of Chemical Engineering, 91*(3), 516-523. doi: Doi 10.1002/Cjce.21688

Kuncová, G., & Zahradník, J. (1995). Gas holdup and bubble frequency in a bubble column reactor containing viscous saccharose solutions. *Chemical Engineering and Processing: Process Intensification, 34*(1), 25-34. doi: http://dx.doi.org/10.1016/0255-2701(94)00563-X

Lacroix, C., Aressy, M., & Carreau, P. J. (1997). Linear viscoelastic behavior of molten polymer blends: A comparative study of the Palierne and Lee and Park models. *Rheologica Acta, 36*(4), 416-428. doi: Doi 10.1007/Bf00396328

Lakota, A. (2007). Effect of Highly Viscous Non-Newtonian Liquids on Gas Holdup in a Concurrent Upflow Bubble Column. *Acta Chim. Slov., 54*, 678–687.

Lau, R., Peng, W., Velazquez-Vargas, L., Yang, G., & Fan, L.-S. (2004). Gas-liquid mass transfer in high-pressure bubble columns. *Industrial & Engineering Chemistry Research, 43*(5), 1302-1311.

Letzel, H. M., Schouten, J. C., Krishna, R., & van den Bleek, C. M. (1997). Characterization of regimes and regime transitions in bubble columns by chaos analysis of pressure signals. *Chemical Engineering Science, 52*(24), 4447-4459. doi: Doi 10.1016/S0009-2509(97)00290-X

Li, H. Z., Mouline, Y., Funfschilling, D., Marchal, P., Choplin, L., & Midoux, N. (1998). Evidence for in-line bubble interactions in non-Newtonian fluids. *Chemical Engineering Science, 53*(12), 2219-+. doi: Doi 10.1016/S0009-2509(98)00048-7

Li, H. Z., Mouline, Y., & Midoux, N. (2002). Modelling the bubble formation dynamics in non-Newtonian fluids. *Chemical Engineering Science, 57*(3), 339-346. doi: Doi 10.1016/S0009-2509(01)00394-3

Li, S. B., Ma, Y. G., Fu, T. T., Zhu, C. Y., & Li, H. Z. (2012). The Viscosity Distribution around a Rising Bubble in Shear-Thinning Non-Newtonian Fluids. *Brazilian Journal of Chemical Engineering, 29*(2), 265-274.

Li, S. B., Ma, Y. G., Zhu, C. Y., Fu, T. T., & Li, H. Z. (2012). Turbulent Characteristic of Liquid Around a Chain of Bubbles in Non-Newtonian Fluid. *Chinese Journal of Chemical Engineering, 20*(5), 883-888.

Li, S. B., Zhu, C. Y., Fu, T. T., & Ma, Y. G. (2012). Study on the mass transfer of bubble swarms in three different rheological fluids. *International Journal of Heat and Mass Transfer, 55*(21-22), 6010-6016. doi: DOI 10.1016/j.ijheatmasstransfer.2012.06.011

Lin, T.-J., & Lin, G.-M. (2009). Mechanisms of in-line coalescence of two-unequal bubbles in a non-Newtonian fluid. *Chemical Engineering Journal, 155*(3), 750-756. doi: http://dx.doi.org/10.1016/j.cej.2009.09.019

Lin, T. J., & Fan, L. S. (1999). Heat transfer and bubble characteristics from a nozzle in high-pressure bubble columns. *Chemical Engineering Science, 54*(21), 4853-4859.

Lin, T. J., Juang, R. C., & Chen, C. C. (2001). Characterizations of flow regime transitions in a high-pressure bubble column by chaotic time series analysis of pressure fluctuation signals. *Chemical Engineering Science, 56*(21–22), 6241-6247. doi: http://dx.doi.org/10.1016/S0009-2509(01)00258-5

Lin, T. J., Tsuchiya, K., & Fan, L.-S. (1999). On the measurements of regime transition in high-pressure bubble columns. *The Canadian Journal of Chemical Engineering, 77*(2), 370-374. doi: 10.1002/cjce.5450770224

Liu, J., Zhu, C., Fu, T., & Ma, Y. (2014). Systematic Study on the Coalescence and Breakup Behaviors of Multiple Parallel Bubbles Rising in Power-law Fluid. *Industrial & Engineering Chemistry Research, 53*(12), 4850-4860. doi: 10.1021/ie4037565

Liu, J. R., Zhu, C. Y., Fu, T. T., Ma, Y. G., & Li, H. Z. (2013). Numerical simulation of the interactions between three equal-interval parallel bubbles rising in non-Newtonian fluids. *Chemical Engineering Science, 93*, 55-66. doi: DOI 10.1016/j.ces.2013.01.060

Luo, X. K., Lee, D. J., Lau, R., Yang, G. Q., & Fan, L. S. (1999). Maximum stable bubble size and gas holdup in high-pressure slurry bubble columns. *Aiche Journal, 45*(4), 665-680.

Maalej, S., Benadda, B., & Otterbein, M. (2003). Interfacial area and volumetric mass transfer coefficient in a bubble reactor at elevated pressures. *Chemical Engineering Science, 58*(11), 2365-2376. doi: http://dx.doi.org/10.1016/S0009-2509(03)00085-X

Magaud, F., Souhar, M., Wild, G., & Boisson, N. (2001). Experimental study of bubble column hydrodynamics. *Chemical Engineering Science, 56*(15), 4597-4607. doi: http://dx.doi.org/10.1016/S0009-2509(01)00110-5

Majumder, S. K., Kundu, G., & Mukherjee, D. (2006). Efficient dispersion in a modified two-phase non-Newtonian downflow bubble column. *Chemical Engineering Science, 61*(20), 6753-6764. doi: http://dx.doi.org/10.1016/j.ces.2006.07.019

Majumder, S. K., Kundu, G., & Mukherjee, D. (2007). Pressure drop and bubble-liquid interfacial shear stress in a modified gas non-Newtonian liquid downflow bubble column. *Chemical Engineering Science, 62*(9), 2482-2490. doi: DOI 10.1016/j.ces.2007.01.074

Mandal, A., Kundu, G., & Mukherjee, D. (2004). Studies on frictional pressure drop of gas-non-Newtonian two-phase flow in a cocurrent downflow bubble column. *Chemical Engineering Science, 59*(18), 3807-3815. doi: http://dx.doi.org/10.1016/j.ces.2004.03.037

Mena, P., Ruzicka, M., Rocha, F., Teixeira, J., & Drahoš, J. (2005). Effect of solids on homogeneous–heterogeneous flow regime transition in bubble columns. *Chemical Engineering Science, 60*(22), 6013-6026.

Menzel, T., Weide, T. I. D., Staudacher, O., Wein, O., & Onken, U. (1990). Reynolds Shear-Stress for Modeling of Bubble Column Reactors. *Industrial & Engineering Chemistry Research, 29*(6), 988-994. doi: Doi 10.1021/Ie00102a007

Metzner, A., Uebler, E., & Fong, C. (1969). Converging flows of viscoelastic materials. *AIChE J., 15*(5), 750-758.

Miura, H., Katoh, T., & Kawase, Y. (2012). Gas-liquid mass transfer in co-current three-phase fluidized beds with non-Newtonian fluids: Theoretical models based on the energy dissipation rate. *Chemical Engineering Journal, 185*, 337-346. doi: DOI 10.1016/j.cej.2012.01.065

Mizushima, Y., Sakamoto, A., & Saito, T. (2013). Measurement technique of bubble velocity and diameter in a bubble column via single-tip optical-fiber probing with judgment of the pierced position and angle. *Chemical Engineering Science, 100*, 98-104. doi: DOI 10.1016/j.ces.2013.01.046

Moo-Young, M., & Kawase, Y. (1987). Gas hold-up and mass transfer in a bubble column with viscoelastic fluids. *The Canadian Journal of Chemical Engineering, 65*(1), 113-118. doi: 10.1002/cjce.5450650118

Morrison, F. A. (2001). Understanding Rheology: Oxford University Press.

Moustiri, S., Hebrard, G., Thakre, S., & Roustan, M. (2001). A unified correlation for predicting liquid axial dispersion coefficient in bubble columns. *Chemical Engineering Science, 56*(3), 1041-1047.

Mueller, S. G. (2009). *Optical measurements in gas-liquid stirred tanks.* (PhD Doctrol Dissertation), Washington University in St. Louis, Ann Arbor. ProQuest Dissertations & Theses Full Text database.

Nakanoh, M., & Yoshida, F. (1980). Gas Absorption by Newtonian and Non-Newtonian Liquids in a Bubble Column. *Industrial & Engineering Chemistry Process Design and Development, 19*(1), 190-195. doi: 10.1021/i260073a033

Nedeltchev, S., Jordan, U., & Schumpe, A. (2007). Correction of the penetration theory based on mass-transfer data from bubble columns operated in the homogeneous regime under high pressure. *Chemical Engineering Science, 62*(22), 6263-6273.

Nedeltchev, S., Nigam, K. D. P., & Schumpe, A. (2014). Prediction of mass transfer coefficients in a slurry bubble column based on the geometrical characteristics of bubbles. *Chemical Engineering Science, 106*, 119-125. doi: DOI 10.1016/j.ces.2013.11.030

Nishikawa, M., Kato, H., & Hashimoto, K. (1977). Heat Transfer in Aerated Tower Filled with Non-Newtonian Liquid. *Industrial & Engineering Chemistry Process Design and Development, 16*(1), 133-137. doi: 10.1021/i260061a607

Olivieri, G., Russo, M. E., Simeone, M., Marzocchella, A., & Salatino, P. (2011). Effects of viscosity and relaxation time on the hydrodynamics of gas-liquid systems. *Chemical Engineering Science, 66*(14), 3392-3399. doi: DOI 10.1016/j.ces.2011.01.027

Ong, B. (2003). *Experimental investigation of bubble column hydrodynamics: effect of elevated pressure and superficial gas velocity.* (Ph.D. Ph.D.), Washington University

Ong, B. C., Gupta, P., Youssef, A., Al-Dahhan, M., & Dudukovic, M. P. (2009). Computed Tomographic Investigation of the Influence of Gas Sparger Design on Gas Holdup Distribution in a Bubble Column. *Industrial & Engineering Chemistry Research, 48*(1), 58-68.

Oppenheim, A. V., & Schafer, R. W. (1975). *Digital signal processing*. Englewood Cliffs, NJ: Prentice-Hall.

Oppenheim, A. V., & Schafer, R. W. (1989). *Discrete-Time Signal Processing.*: Prentice-Hall.

Otake, T., Tone, S., Nakao, K., & Mitsuhashi, Y. (1977). Coalescence and breakup of bubbles in liquids. *Chemical Engineering Science, 32*(4), 377-383. doi: http://dx.doi.org/10.1016/0009-2509(77)85004-5

Oyevaar, M., Bos, R., & Westerterp, K. (1991). Interfacial areas and gas hold-ups in gas—liquid contactors at elevated pressures from 0.1 to 8.0 MPa. *Chemical Engineering Science, 46*(5), 1217-1231.

Oyevaar, M., & Westerterp, K. (1989). Mass transfer phenomena and hydrodynamics in agitated gas—liquid reactors and bubble columns at elevated pressures: State of the art. *Chemical Engineering and Processing: Process Intensification, 25*(2), 85-98.

Pal, R. (2010). *Rheology of particulate dispersions and composites*: CRC Press.

Park, S. H., & Kim, S. D. (2001). Wavelet transform analysis of pressure fluctuation signals in a three-phase fluidized bed. *Korean Journal of Chemical Engineering, 18*(6), 1015-1019. doi: Doi 10.1007/Bf02705635

Peng, X. D., Toseland, B. A., & Tijm, P. J. A. (1999). Kinetic understanding of the chemical synergy under LPDMETM conditions—once-through applications. *Chemical Engineering Science, 54*(13–14), 2787-2792. doi: http://dx.doi.org/10.1016/S0009-2509(98)00343-1

Perez, J. A. S., Porcel, E. M. R., Lopez, J. L. C., Sevilla, J. M. F., & Chisti, Y. (2006). Shear rate in stirred tank and bubble column bioreactors. *Chemical Engineering Journal, 124*(1-3), 1-5. doi: DOI 10.1016/j.cej.2006.07.002

Pillapakkam, S. B., Singh, P., Blackmore, D., & Aubry, N. (2007). Transient and steady state of a rising bubble in a viscoelastic fluid. *Journal of Fluid Mechanics, 589*, 215-252. doi: doi:10.1017/S0022112007007628

Pilz, C., & Brenn, G. (2007). On the critical bubble volume at the rise velocity jump discontinuity in viscoelastic liquids. *Journal of Non-Newtonian Fluid Mechanics, 145*(2-3), 124-138. doi: DOI 10.1016/j.jnnfm.2007.05.015

Pohorecki, R., Moniuk, W., & Zdrójkowski, A. (1999). Hydrodynamics of a bubble column under elevated pressure. *Chemical Engineering Science, 54*(21), 5187-5193. doi: http://dx.doi.org/10.1016/S0009-2509(99)00238-9

Pohorecki, R., Moniuk, W., Zdrójkowski, A., & Bielski, P. (2001). Hydrodynamics of a pilot plant bubble column under elevated temperature and pressure. *Chemical Engineering Science, 56*(3), 1167-1174.

Press, W. H., Teukolsky, S. A., Vetterling, W. T., & Flannery, B. P. (1992). *Numerical Recipes in C: The Art of Scientific Computing*. New York: Cambridge University Press.

Rados, N., Shaikh, A., & Al-Dahhan, M. H. (2005). Solids flow mapping in a high pressure slurry bubble column. *Chemical Engineering Science, 60*(22), 6067-6072. doi: DOI 10.1016/j.ces.2005.04.087

Reilly, I., Scott, D., Debruijn, T., & MacIntyre, D. (1994). The role of gas phase momentum in determining gas holdup and hydrodynamic flow regimes in bubble column operations. *The Canadian Journal of Chemical Engineering, 72*(1), 3-12.

Rodrigue, D., De Kee, D., & Fong, C. F. C. M. (1998). Bubble velocities: further developments on the jump discontinuity. *Journal of Non-Newtonian Fluid Mechanics, 79*(1), 45-55. doi: Doi 10.1016/S0377-0257(98)00072-X

Rojas, G., & Loewen, M. R. (2007). Fiber-optic probe measurements of void fraction and bubble size distributions beneath breaking waves. *Experiments in Fluids, 43*(6), 895-906. doi: 10.1007/s00348-007-0356-5

Rollbusch, P., Bothe, M., Becker, M., Ludwig, M., Grünewald, M., Schlüter, M., & Franke, R. (2015). Bubble columns operated under industrially relevant conditions – Current understanding of design parameters. *Chemical Engineering Science, 126*(0), 660-678. doi: http://dx.doi.org/10.1016/j.ces.2014.11.061

Rollbusch, P., Tuinier, M., Becker, M., Ludwig, M., Grunewald, M., & Franke, R. (2013). Hydrodynamics of High-Pressure Bubble Columns. *Chemical Engineering & Technology, 36*(9), 1603-1607. doi: DOI 10.1002/ceat.201300308

Ruzicka, M. C., Drahos, J., Mena, P. C., & Teixeira, J. A. (2003). Effect of viscosity on homogeneous-heterogeneous flow regime transition in bubble columns. *Chemical Engineering Journal, 96*(1-3), 15-22. doi: DOI 10.1016/j.cej.2003.08.009

Saberi, S., Shakourzadeh, K., Bastoul, D., & Militzer, J. (1995). Bubble size and velocity measurement in gas—liquid systems: Application of fiber optic technique to pilot plant scale. *The Canadian Journal of Chemical Engineering, 73*(2), 253-257. doi: 10.1002/cjce.5450730213

Sagert, N. H., & Quinn, M. J. (1976). The coalescence of H2S and CO2 bubbles in water. *The Canadian Journal of Chemical Engineering, 54*(5), 392-398. doi: 10.1002/cjce.5450540503

Sagert, N. H., & Quinn, M. J. (1977). Influence of high-pressure gases on the stability of thin aqueous films. *Journal of Colloid and Interface Science, 61*(2), 279-286.

Schafer, R., Merten, C., & Eigenberger, G. (2002). Bubble size distributions in a bubble column reactor under industrial conditions. *Experimental Thermal and Fluid Science, 26*(6-7), 595-604. doi: Pii S0894-1777(02)00189-9

Doi 10.1016/S0894-1777(02)00189-9

Schowalter, W. R. (1960). The application of boundary-layer theory to power-law pseudoplastic fluids: Similar solutions. *AIChE J., 6*(1), 24-28. doi: 10.1002/aic.690060105

Schumpe, A., & Deckwer, W. D. (1987). Viscous media in tower bioreactors: Hydrodynamic characteristics and mass transfer properties. *Bioprocess Engineering, 2*(2), 79-94. doi: 10.1007/BF00369528

Schweitzer, J. M., Bayle, J., & Gauthier, T. (2001). Local gas hold-up measurements in fluidized bed and slurry bubble column. *Chemical Engineering Science, 56*(3), 1103-1110. doi: http://dx.doi.org/10.1016/S0009-2509(00)00327-4

Serdula, C. D., & Loewen, M. R. (1998). Experiments investigating the use of fiber-optic probes for measuring bubble-size distributions. *Oceanic Engineering, IEEE Journal of, 23*(4), 385-399. doi: 10.1109/48.725233

Shabanian, J., & Chaouki, J. (2014). Local characterization of a gas–solid fluidized bed in the presence of thermally induced interparticle forces. *Chemical Engineering Science, 119*, 261-273. doi: http://dx.doi.org/10.1016/j.ces.2014.08.037

Shah, Y. T., Kelkar, B. G., Godbole, S. P., & Deckwer, W. D. (1982). Design parameters estimations for bubble column reactors. *AIChE J., 28*(3), 353-379. doi: 10.1002/aic.690280302

Shah, Y. T., Kelkar, B. G., Godbole, S. P. and Deckwer, W.-D. (1982). Design parameters estimations for bubble column reactors. *AIChE J., 28*, 353–379.

Shaikh, A., & Al-Dahhan, M. (2005). Characterization of the hydrodynamic flow regime in bubble columns via computed tomography. *Flow Measurement and Instrumentation, 16*(2-3), 91-98. doi: DOI 10.1016/j.flowmeasinst.2005.02.004

Shaikh, A., & Al-Dahhan, M. (2013). A new method for online flow regime monitoring in bubble column reactors via nuclear gauge densitometry. *Chemical Engineering Science, 89*, 120-132. doi: DOI 10.1016/j.ces.2012.11.023

Shaikh, A., & Al-Dahhan, M. H. (2007). A review on flow regime transition in bubble columns. *International Journal of Chemical Reactor Engineering, 5*.

Sheikhi, A., Sotudeh-Gharebagh, R., Zarghami, R., Mostoufi, N., & Alfi, M. (2013). Understanding bubble hydrodynamics in bubble columns. *Experimental Thermal and Fluid Science, 45*, 63-74. doi: DOI 10.1016/j.expthermflusci.2012.10.008

Soong, Y., Gamwo, I., Romanov, V., Dilmore, R., & Hedges, S. (2006). Design of an adapter for ultrasound transducer under high operating temperatures and pressures in a slurry bubble column reactor. *Chemical Engineering Research and Design, 84*(2), 133-138.

Soong, Y., Harke, F. W., Gamwo, I. K., Schehl, R. R., & Zarochak, M. F. (1997). Hydrodynamic study in a slurry-bubble-column reactor. *Catalysis Today, 35*(4), 427-434. doi: http://dx.doi.org/10.1016/S0920-5861(96)00211-8

Soto, E., Goujon, C., Zenit, R., & Manero, O. (2006). A study of velocity discontinuity for single air bubbles rising in an associative polymer. *Physics of Fluids, 18*(12), -. doi: doi:http://dx.doi.org/10.1063/1.2397011

Stegeman, D., Knop, P., Wijnands, A., & Westerterp, K. (1996). Interfacial area and gas holdup in a bubble column reactor at elevated pressures. *Industrial & Engineering Chemistry Research, 35*(11), 3842-3847.

Stewart, C. W. (1995). Bubble Interaction in Low-Viscosity Liquids. *International Journal of Multiphase Flow, 21*(6), 1037-1046. doi: Doi 10.1016/0301-9322(95)00030-2

Su, Y. F., Wang, Y. F., Zeng, Q. H., Li, J. H., Yu, G. S., Gong, X., & Yu, Z. H. (2008). Influence of liquid properties on flow regime and backmixing in a special bubble column. *Chemical Engineering and Processing, 47*(12), 2296-2302. doi: DOI 10.1016/j.cep.2008.01.006

Suh, I. S., Schumpe, A., Deckwer, W. D., & Kulicke, W. M. (1991). Gas-Liquid Mass-Transfer in the Bubble Column with Viscoelastic Liquid. *Canadian Journal of Chemical Engineering, 69*(2), 506-512.

Sulaymon, A. H., & Mohammed, A. A. (2010). Separation and Hydrodynamic Performance of Air-Kerosene-Water System by Bubble Column. *International Journal of Chemical Reactor Engineering, 8*.

Takeo, U. (1971). Determination of bubble-size distribution in a BWR. *Nucl. Eng. Des, 22*, 252-261.

Terasaka, K., & Shibata, H. (2003). Oxygen transfer in viscous non-Newtonian liquids having yield stress in bubble columns. *Chemical Engineering Science, 58*(23-24), 5331-5337. doi: DOI 10.1016/j.ces.2003.09.011

Terasaka, K., & Tsuge, H. (2003). Gas holdup for slug bubble flow of viscous liquids having a yield stress in bubble columns. *Chemical Engineering Science, 58*(2), 513-517.

Thang, N., & Davis, M. (1979). The structure of bubbly flow through venturis. *International Journal of Multiphase Flow, 5*(1), 17-37.

Thomasi, S. S., Cerri, M. O., & Badino, A. C. (2010). Average shear rate in three pneumatic bioreactors. *Bioprocess and Biosystems Engineering, 33*(8), 979-988.

Ueyama, K., Morooka, S., Koide, K., Kaji, H., & Miyauchi, T. (1980). Behavior of Gas Bubbles in Bubble Columns. *Industrial & Engineering Chemistry Process Design and Development, 19*(4), 592-599. doi: 10.1021/i260076a015

Urseanu, M. I., Guit, R. P. M., Stankiewicz, A., van Kranenburg, G., & Lommen, J. H. G. M. (2003). Influence of operating pressure on the gas hold-up in bubble columns for high viscous media. *Chemical Engineering Science, 58*(3-6), 697-704. doi: Doi 10.1016/S0009-2509(02)00597-3

Vatai, G., & Tekić, M. (1989). Gas hold-up and mass transfer in bubble columns with pseudoplastic liquids. *Chemical Engineering Science, 44*(10), 2402-2407.

Velez-Cordero, J. R., & Zenit, R. (2011). Bubble cluster formation in shear-thinning inelastic bubbly columns. *Journal of Non-Newtonian Fluid Mechanics, 166*(1-2), 32-41. doi: DOI 10.1016/j.jnnfm.2010.10.003

Vial, C., Camarasa, E., Poncin, S., Wild, G., Midoux, N., & Bouillard, J. (2000). Study of hydrodynamic behaviour in bubble columns and external loop airlift reactors through analysis of pressure fluctuations. *Chemical Engineering Science, 55*(15), 2957-2973. doi: Doi 10.1016/S0009-2509(99)00551-5

Vijayan, M., Schlaberg, H., & Wang, M. (2007). Effects of sparger geometry on the mechanism of flow pattern transition in a bubble column. *Chemical Engineering Journal, 130*(2), 171-178.

Waghmare, Y., Rice, R. G., & Knopf, F. C. (2008). Mass transfer in a viscous bubble column with forced oscillations. *Industrial & Engineering Chemistry Research, 47*(15), 5386-5394.

Wallis, G. B. (1969). One-dimensional Two-phase Flow. *McGraw-Hill, New York, NY*.

Wang, T. F., Wang, J. F., & Jin, Y. (2007). Slurry reactors for gas-to-liquid processes: A review. *Industrial & Engineering Chemistry Research, 46*(18), 5824-5847. doi: Doi 10.1021/Ie070330t

Welch, P. D. (1967). The use of a fast Fourier transform for the estimation of power spectra. *IEEE Trans. Audio and Electroacoustics*(AU-15), 70-73.

Wender, I. (1996). Reactions of synthesis gas. *Fuel Processing Technology, 48*(3), 189-297. doi: http://dx.doi.org/10.1016/S0378-3820(96)01048-X

Wild, G., Poncin, S., Li, H. Z., & Olmos, E. (2003). Some Aspects of the Hydrodynamics of Bubble Columns. *International Journal of Chemical Reactor Engineering, 1*.

Wilkinson, P. M., Haringa, H., & Van Dierendonck, L. L. (1994). Mass transfer and bubble size in a bubble column under pressure. *Chemical Engineering Science, 49*(9), 1417-1427. doi: http://dx.doi.org/10.1016/0009-2509(93)E0022-5

Wilkinson, P. M., Spek, A. P., & van Dierendonck, L. L. (1992). Design parameters estimation for scale-up of high-pressure bubble columns. *Aiche Journal, 38*(4), 544-554. doi: 10.1002/aic.690380408

Xu, S., Qu, Y., Chaouki, J., & Guy, C. (2005). Characterization of homogeneity of bubble flows in bubble columns using RPT and fibre optics. *International Journal of Chemical Reactor Engineering, 3*(1).

Xue, J. (2004). *Bubble velocity, size and interfacial area measurements in bubble columns.* (PhD Doctoral dissertation), Washington University, Ann Arbor. ProQuest Dissertations & Theses Full Text database.

Xue, J., Al-Dahhan, M., Dudukovic, M. P., & Mudde, R. F. (2008). Bubble velocity, size, and interfacial area measurements in a bubble column by four-point optical probe. *AIChE J., 54*(2), 350-363. doi: 10.1002/aic.11386

Yang, G., & Fan, L. (2003). Axial liquid mixing in high-pressure bubble columns. *Aiche Journal, 49*(8), 1995-2008.

Yang, G., Luo, X., Lau, R., & Fan, L. (2000). Heat-transfer characteristics in slurry bubble columns at elevated pressures and temperatures. *Industrial & Engineering Chemistry Research, 39*(7), 2568-2577.

Yifeng, S., Yifei, W., Qinghua, Z., Jian-hui, L., Guangsuo, Y., & Zunhong, Y. (2008). Influence of liquid properties on flow regime and backmixing in a special bubble column. *Chemical Engineering and Processing: Process Intensification, 47*(12), 2296-2302.

Yosim, S., & Barclay, K. (1981). *The Chemistry of the Rockgas Process for Coal Gasification.* Paper presented at the Proceedings of the Second International Symposium on Molten Salts, JR Selman and J. Braunstein, Eds.(Pennington, NJ: Electrochemical Society, 1981).

Zahradnik, J., Fialova, M., Ruzicka, M., Drahos, J., Kastanek, F., & Thomas, N. H. (1997). Duality of the gas-liquid flow regimes in bubble column reactors. *Chemical Engineering Science, 52*(21-22), 3811-3826. doi: Doi 10.1016/S0009-2509(97)00226-1

Znad, H., Báleš, V., Markoš, J., & Kawase, Y. (2004). Modeling and simulation of airlift bioreactors. *Biochemical Engineering Journal, 21*(1), 73-81. doi: http://dx.doi.org/10.1016/j.bej.2004.05.005

APPENDIX A – EQUIPMENT USED FOR PERFORMING EXPERIMENTS AND PREPARING THE NON-NEWTONIAN SOLUTIONS

A.1. Photos of the Plexiglass bubble column reactor operating at ambient condition

Figure A-1. Photo of the bubble column reactor operating at ambient condition.

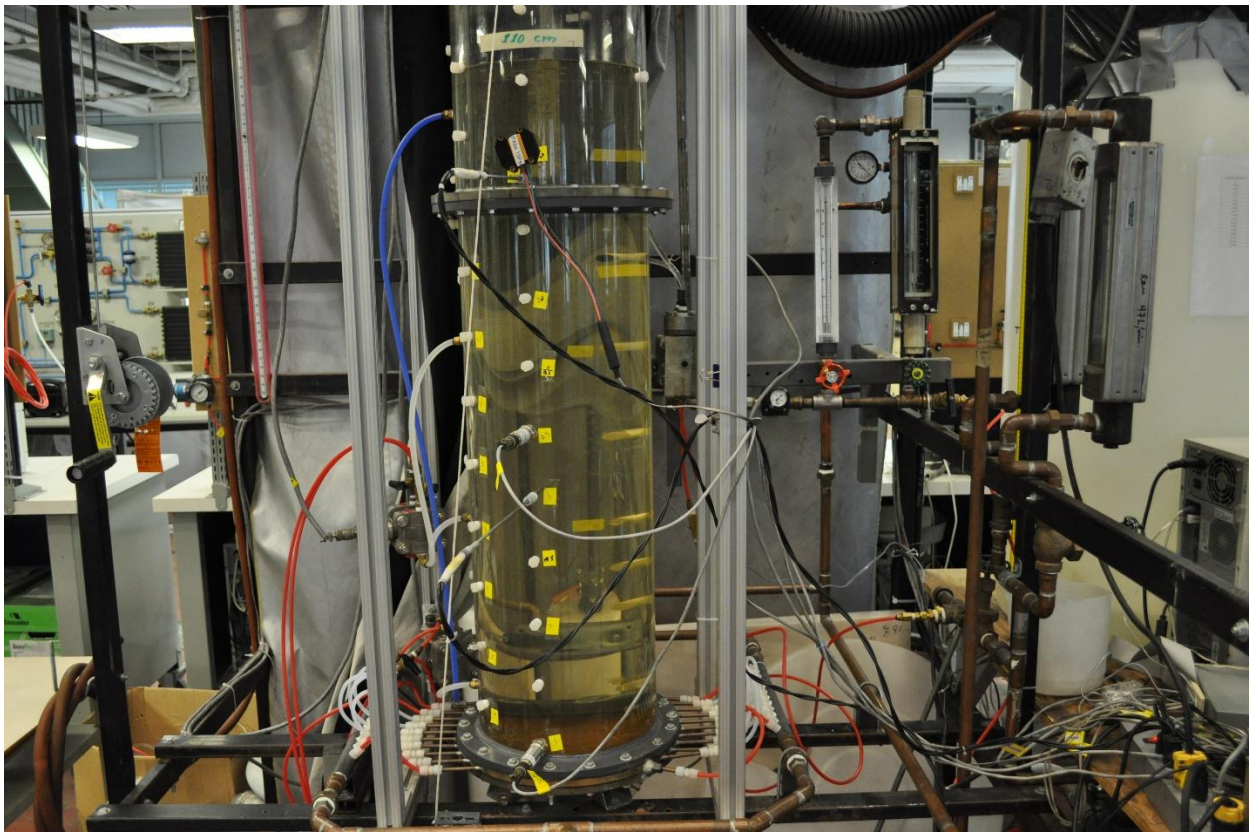

Figure A-2. Photo of measurement technique installed on the bubble column reactor operating at ambient condition.

A.2. Gas/liquid distributor plate in the Plexiglass bubble column reactor

In the Plexiglass bubble column, the liquid phase is fed into the column by a conical wind box, which is located at the bottom of the column. Then it crosses 268 2-mm orifices (4000 orifices m^{-2}) in the perforated plate distributor. The gas phase is fed into 11 horizontal conduits with a diameter of 6.35 mm hollowed out directly in the distributor plate. The gas phase is fed into each side of the conduits and enters the column via 94 1-mm holes. This specifically designed distributor plate provides a uniform distribution for both the gas and liquid phases (in the case of a continuous liquid phase). A schematic of the distributor plate is shown in Figure A-3.

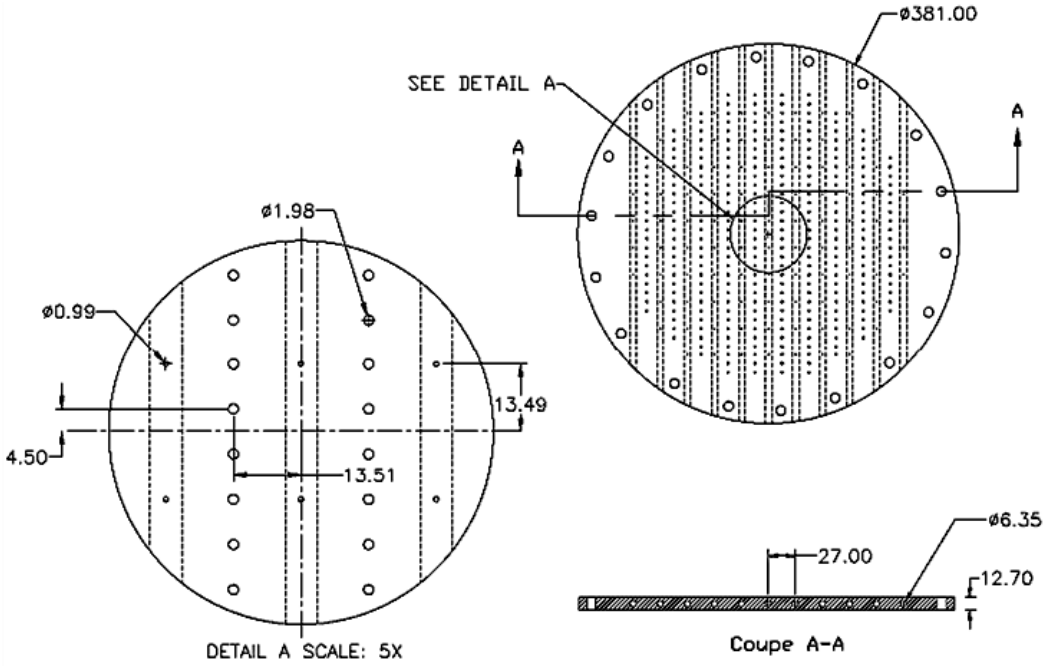

Figure A-3. Schematic of the Distributor plate installed in the Plexiglass bubble column reactor.

A.3. Agitation vessels used for preparing non-Newtonian liquids

In order to prepare the non-Newtonian solutions, two different agitation vessels were used, as shown below.

(a) (b)

Figure A-4. The agitation vessel used for preparing non-Newtonian liquids: (a) side view; (b) top view.

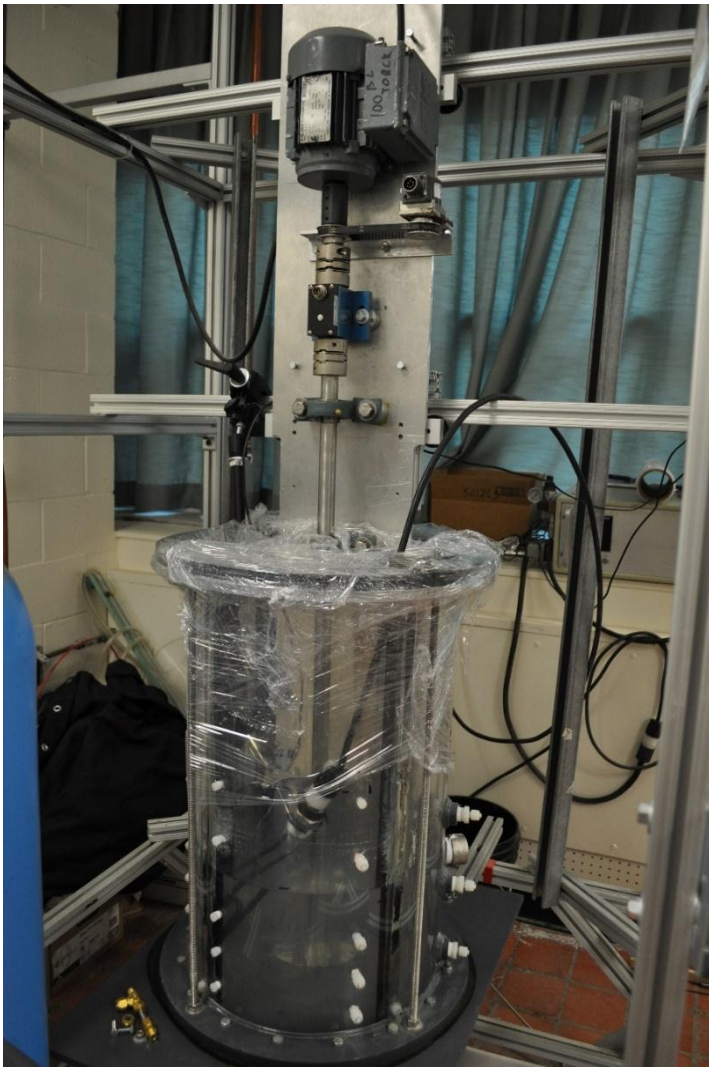

Figure A-5. A photo of the agitation vessel equipped with heating element for dissolving PAA in water.